

ABSTRACT

SH2-containing inositol 5'-phosphatase (SHIP) is an enzyme involved in the PI3K cellular signaling pathway. In response to external stressors, SHIP is recruited to the internal cell membrane of eukaryotic cells to selectively hydrolyze the 5' phosphate group of membrane-bound phosphatidylinositol-3,4,5-trisphosphate (P(3,4,5)P₃) to generate phosphatidylinositol-3,4-bisphosphate (PI(3,4)P₂). This process, among others such as phosphorylation by PI3K and dephosphorylation by PTEN, is an intermediate in the transmission of signals from the cell membrane to the cell nucleus, effectively influencing cellular growth and development. Aberrations in these processes are known to influence abnormal cellular function and are observed in certain disease states such as cancer and insulin resistance. Modulation of the activity of SHIP has therefore been found to be a potential avenue for the treatment of such states. Indeed, the inhibition of SHIP by small molecules discovered by high-throughput screening of the NCI Diversity Set has been shown to induce apoptosis in cancer cells. This dissertation reports new milligram- to gram-scale synthetic routes for quinoline aminoalcohols NSC13480 and NSC30578 that were discovered to be active SHIP inhibitors. Additionally, analogues were made, and all molecules were assayed *in vitro*. Up to 46% inhibition was observed in the isoform SHIP1, while up to 66% inhibition was observed in SHIP2, suggesting that quinolines may be more selective SHIP2 inhibitors. Interestingly, the commercially available anti-malarial drug mefloquine was also shown to inhibit both SHIP1 and SHIP2 almost equally.

Trichloroacetimidates (TCIs) are well-known and typically commercially available reagents in organic synthesis. They are often used for the installation of protecting groups for heteroatom functional groups such as alcohols, used in carbon-carbon forming reactions such as in Schmidt's glycosylations in carbohydrate chemistry, or in Overman's [3,3]-sigmatropic rearrangement of allylic trichloroacetimidates to trichloroacetamides for the stereoselective conversion of chiral alcohols to chiral amines. While these reactions are very typically acid-catalyzed, the reactions of trichloroacetimidates under mild conditions without any added catalysts or promoters is attractive, especially in cases where molecules may be sensitive to the acidic conditions introduced by the typically strong acids used such as BF_3 or TMSOTf. This dissertation reports the development of the catalyst-free esterification reaction of a variety of carboxylic acids using 4-methoxybenzyl trichloroacetimidate. Most carboxylic acids were found to be reactive in dichloromethane at room temperature, including sterically hindered acids secondary- and tertiary- substituted carboxylic acids and Boc-protected amino acids. Additionally, a chiral acid such as Naproxen was successfully esterified without racemization, indicating the mild nature of the reaction conditions.

**SYNTHETIC STUDIES ON QUINOLINE SHIP INHIBITORS AND NEW METHODS
FOR C-O AND C-C BOND FORMATIONS USING TRICHLOROACETIMIDATES**

Christopher M. Russo

B.S., The University of Scranton, 2009

DISSERTATION

Submitted in partial fulfillment of the requirements for the degree of

Doctor of Philosophy in Chemistry

Syracuse University

June 2023

Copyright © Christopher M. Russo 2023

All Rights Reserved

ACKNOWLEDGEMENTS

It is difficult for me to describe what type of journey this has been. Through all the ups and downs, and lefts and rights, my career at Syracuse University has been an incredible learning experience in both chemistry and life in general. Most importantly, I greatly value all the people I have met both in Syracuse and beyond who have played a part in this journey. To these people listed below and any deserving individuals I may have not included, thank you, always.

First and foremost, I'd like to thank my excellent advisor Dr. John Chisholm. I cannot describe in words how much I value everything you have done for me during our time together. Your patience is outstanding, and I am eternally grateful to have had the opportunity to work in your lab and learn from you.

Of course, thank you also to the rest of the professors at Syracuse University, especially my instructors Drs. Michael Sponsler, Mathew Maye, Daniel Clark, Yan-Yueng Luk, and James Kallmerten and my dissertation committee members Drs. James Hougland, Nancy Totah, Davoud Mozhdehi, Xiaoran Hu, and John Tillotson. Your support has been overwhelming. Thank you also to the Syracuse University staff, especially Sally Prash, the best glassblower and landlord I know.

I cannot omit my undergraduate research advisor and first organic chemistry instructor, Dr. Jennifer Tripp. Thank you for introducing me to the world that I love, and for giving me the opportunity to do radiocarbon dating research with you at the University of Scranton. Thank you to the rest of the Scranton chemistry family, too.

Thank you to Dennis Viernes, my senior labmate at Syracuse University. You have been an invaluable resource and great friend in both chemistry and life. Thank you for your encouragement and the fun times we had together. Thank you also to labmates Lydia Choi,

Jigisha Shah, Kyle Howard, Arijit Adhikari, Daniel Wallach, Brian Duffy, Nivedita Mahajani, and Otto Dungan, plus all of the undergrads, especially Katie Armstrong. You all kept it interesting.

Thank you to Dr. William Kerr of SUNY Upstate Medical University and the many members of his lab for the collaborative research opportunity. The experience has been an example to me of how humans can rarely accomplish greatness alone.

Thank you to my many friends and acquaintances. Apart from those already listed, I am especially grateful to Casey Simons for showing me how to enjoy life and for your never-ending encouragement. Thank you to other Syracuse friends, including Jen Elward and Rabeka Alam, and to my Scranton friends, especially Scott Yaninas, Jason Stankiewicz, John Connell, Jon Pipan, and Amanda Applegate for your friendships. Somehow, we survived the gauntlet together.

Thank you to everyone at Villanova University, where I am currently, especially Dr. Matthew O'Reilly for giving me an amazing opportunity to be the best chemist (and sometimes biologist) I can be, plus all my labmates and friends, especially Vincent Fumo, Hannah Kessler, Samantha Brayton, and D. Merle Bernhard. Thank you for helping me feel young again for just a bit longer.

Lastly, thank you to my family. Thank you to my parents Robert Russo Sr. and Karen Russo, née Williams, for your support and for doing the things that parents do. Thank you to my brother, Robert Russo Jr., my sister-in-law Jacqueline "J.J." Russo, née Storer, and my wonderful niece and nephew, Claire and Bobby. Though I may not say it, you all mean the world to me. I could not have done this without you all.

TABLE OF CONTENTS

Abstract	i
Title Page	iii
Acknowledgements	v
Table of Contents	vii
List of Figures	ix
List of Schemes	x
List of Tables	xii
Abbreviations and Acronyms	xiii
Dedication	xvii

Chapter 1. Synthesis and Testing of Quinoline Aminoalcohols for SHIP Inhibition

1.1. Introduction	1
1.1.1. SH2-Containing Inositol Phosphatases	1
1.1.1.2. Mechanism of SHIP1 and SHIP2 catalysis	6
1.1.1.3. Inhibition of SHIP	8
1.1.2. Quinoline SHIP Inhibitors	10
1.2. Results and Discussion	12
1.2.1. Synthesis of NSC13480	12
1.2.2. Synthesis of NSC305787	30
1.2.3. Synthesis of Analogues	34
1.2.4. Biological Testing	38
1.2.5. Docking Quinoline Analogs into the SHIP1 Active Site	40
1.3. Conclusion	41
1.4. Experimental Procedures	43
1.5. ^1H and ^{13}C NMR Spectra	61
1.6. References	97

Chapter 2. Promoter-Free Formation of PMB Esters with 4-Methoxybenzyl-2,2,2-trichloroacetimidate

2.1. Introduction	106
2.2. Results and Discussion	107
2.3. Conclusion	113
2.4. Experimental Procedures	115
2.5. ^1H and ^{13}C NMR Spectra	123
2.6. References	156

Chapter 3. Rhodium-Catalyzed Tandem Alkyne Dimerization/1,4-Addition Reaction

3.1. Introduction	160
3.2. Results and Discussion	161
3.3. Conclusion	170
3.4. Experimental Procedures	171
3.5. ^1H and ^{13}C NMR Spectra	187
3.6. References	244
Curriculum Vitae	247

LIST OF FIGURES

Figure 1.1. Cellular inositol signaling pathways	2
Figure 1.2. Inositol kinase and phosphatase reactions	3
Figure 1.3. Model of SHIP1 and PIP3	5
Figure 1.4. Active site of SHIP1 and PIP3	8
Figure 1.5. Biologically active quinolines and amino-alcohols	11
Figure 1.6. Quinoline and its numbering scheme	12
Figure 1.7. Stereoisomers of NSC13480	13
Figure 1.8. Model of SHIP1 and NSC13480	41
Figure 3.1. General alkyne dimerization-addition reaction	163
Figure 3.2. Enyne HMBC and NOESY correlations	165
Figure 3.3. Alkyne dimerization-addition proposed mechanism	168

LIST OF SCHEMES

Scheme 1.1.	13
Scheme 1.2.	14
Scheme 1.3.	15
Scheme 1.4.	16
Scheme 1.5.	17
Scheme 1.6.	18
Scheme 1.7.	18
Scheme 1.8.	19
Scheme 1.9.	20
Scheme 1.10.	21
Scheme 1.11.	22
Scheme 1.12.	23
Scheme 1.13.	24
Scheme 1.14.	28
Scheme 1.15.	29
Scheme 1.16.	30
Scheme 1.17.	31

Scheme 1.18.	31
Scheme 1.19.	32
Scheme 1.20.	33
Scheme 1.21.	34
Scheme 1.22.	34
Scheme 1.23.	35
Scheme 1.24.	37
Scheme 1.25.	37
Scheme 1.26.	38
Scheme 2.1.	112
Scheme 2.2.	113
Scheme 3.1.	161
Scheme 3.2.	170

LIST OF TABLES

Table 1.1. Alcohol oxidation optimizations	16
Table 1.2. Phosphonate synthesis optimizations	25
Table 1.3. Horner-Wadsworth-Emmons reaction optimizations	27
Table 1.4. Terminal epoxide synthesis optimizations	36
Table 1.5. Biological data for SHIP inhibition	39
Table 2.1. Trichloroacetimidate esterification products	108
Table 2.2. Trichloroacetimidate esterification products	110
Table 3.1. Alkyne dimerization-addition ligand screen	162
Table 3.2. Variation of alkynes in dimerization-addition reactions	164
Table 3.3. Reaction of 2-methyl-3-butyne-2-ol	166
Table 3.4. Variation of electron deficient alkenes in dimerization-addition reactions	167

ABBREVIATIONS AND ACRONYMS

[α]	Specific rotation
3AC	3 α -aminocholestane
Akt	Protein kinase B
Akt1	Protein kinase B 1
Akt2	Protein kinase B 2
AIBN	Azobisisobutyronitrile
AML	Acute myelogenous leukemia
Anal.	Combustion elemental analysis
anhyd	Anhydrous
ATG	Autophagy-related
BAECs	Bovine aortic endothelial cells
bFGF	Basic fibroblast growth factor
BHT	Butylated hydroxytoluene
BM	Bone marrow
BMMC	Bone marrow mast cell
bs	Broad singlet
Btk	Bruton's tyrosine kinase
calcd	Calculated
CD	Crohn's Disease
CF	Cystic fibrosis
CI	Chemical ionization
CLogP	Calculated partition coefficient
cod	1,5-Cyclooctadiene
compd	Compound
concd	Concentrated
COSMIC	College of Science Major Instrumentation
CSA	Camphorsulfonic acid
Cy	Cyclohexyl
δ	Chemical shift in part per million
DCB	1,4-Dichlorobenzene
DCE	1,2-Dichloroethane
DCM	Dichloromethane
DBU	1,8-Diazabicyclo[5.4.0]undec-7-ene
DEPT	Distortionless enhancement by polarization transfer
DIAD	Diisopropyl azodicarboxylate
DIBAL	Diisobutylaluminum hydride
DMAP	4-Dimethyl aminopyridine
dba	Dibenzylideneacetone
DMF	Dimethylformamide
DMP	Dess-Martin periodinane
DMPU	1,3-dimethyl-3,4,5,6-tetrahydro-2(1H)-pyrimidinone
DMSO	Dimethyl sulfoxide
DPM	Diphenyl methyl
EGF	Epidermal growth factor

EGFR	Epidermal growth factor receptor
ERK	Extracellular regulated kinase
ES	Embryonic stem
ESI	Electrospray ionization
FP	Fluorescence polarization
FT	Fourier transform
Gab	Grb2-associated binding
Glut4	Glucose transporter type 4
Grp1	General receptor for phosphoinositides 1
GSK3 β	Glycogen synthase kinase 3 β
GTP	Guanosine triphosphate
GvHD	Graft vs. Host disease
H&E	Hematoxylin and Eosin
HGF	Hepatocyte growth factor
HIV	Human immunodeficiency virus
HMBC	Heteronuclear multiple bond correlation
HRMS	High-resolution mass spectroscopy
HSC	Hematopoietic stem cells
HTS	High-throughput screening
HWE	Horner-Wadsworth-Emmons
IBD	Inflammatory bowel disease
IC50	Half maximal inhibitory concentration
I-1,3,4,5-P4	Inositol-1,3,4,5-tetrakisphosphate
IL-1 β	Interleukin-1 β
IP	Inositol phospholipid
IP4	Inositol-1,2,4,5-tetrakisphosphate
JNK	c-Jun N-terminal kinases
KD	Equilibrium dissociation constant
LAH	Lithium aluminum hydride
LDA	Lithium diisopropylamine
lit.	Literature value
LN	Lymph node
MAP	Mitogen-activated protein
MAPK	Mitogen-activated protein kinases
m-CPBA	meta-Chloroperoxybenzoic acid
MEF	Mouse embryonic fibroblasts
Mes	2,4,6-Trimethylphenyl (mesityl)
MDCK	Madin-Darby canine kidney
MG+	Malachite Green
MIR	Myeloid immunoregulatory
MM	Multiple myeloma
MOM	Methoxymethyl
M	Methylsulfonyl (mesyl)
MS	Molecular sieves
MySCs	Myeloid suppressor cells
NCI	National Cancer Institute

NHK	Nozaki–Hiyama–Kishi
NK	Natural killer
NMO	N–Methylmorpholine N–oxide
NMR	Nuclear Magnetic Resonance
NO	Nitrite
NOESY	Nuclear Overhauser effect spectroscopy
PCC	Pyridinium chlorochromate
PDC	Pyridinium dichlorochromane
PDK1	Phosphatidylinositide kinase 1
PH	Pleckstrin homology
PI3K	Phosphatidylinositol–3–kinase
PI–3,4–P2	Phosphatidylinositol–3,4–bisphosphate
PI–3,4,5–P3	Phosphatidylinositol–3,4,5–trisphosphate
PIPn	Phosphoinositides
Piv	Pivalate
PKB	Protein kinase B
PLC– γ	Phospholipase C– γ
PMB	para-methoxybenzyl
PMP	para–Methoxyphenyl
PPTS	Pyridinium para–toluenesulfonate
PTEN	Phosphatase and tensin homolog
PTH	Parathyroid hormone
p–TsCl	para–Toluenesulfonyl chloride
Ras	Receptor tyrosine kinases
RBC	Red blood cell
rt	Room temperature
SAR	Structure–activity relationship
Shc	Src homology 2–containing
SH2	Src homology 2 containing
SHIP	Src homology 2 domain–containing inositol 5’–phosphatase
SHIP1	Src homology 2 domain–containing inositol 5’–phosphatase 1
SNPs	Single–nucleotide polymorphisms
TBAF	Tetrabutylammonium fluoride
TBS	tert–Butyldimethylsilyl
TBDPS	tert–Butyldiphenylsilyl
TEMPO	2,2,6,6–Tetramethylpiperidin–1–oxyl
TES	Triethylsilyl
TFA	Trifluoroacetic acid
TFAA	Trifluoroacetic anhydride
TFP	Tri–2–furylphosphine
THP	Tetrahydropyran–2–yl
TMEDA	N,N,N,N–Tetramethylethylenediamine
TMS	Tetramethylsilane
THF	Tetrahydrofuran
TIPS	Triisopropyl
TLC	Thin layer chromatography

TMS	Tetramethylsilane
Tf	Trifluoromethanesulfonyl (triflyl)
Ts	para-Toluenesulfonyl (tosyl)
V-ATPases	Vacuolar (H ⁺)-ATPases
Yphos	Tyrosine phosphorylated

DEDICATION

To my family: Mom, Dad, Rob, and countless others past, present, and future.

Through nature's inflexible grace, I'm learning to live.

Chapter 1. Synthesis and Testing of Quinoline Aminoalcohols for SHIP Inhibition

1.1. Introduction

1.1.1. SH2-Containing Inositol Phosphatases

The SH2-containing inositol 5'-phosphatase (SHIP) is an enzyme involved in cellular signaling, specifically playing a role in the PI3K pathway. The PI3K signaling nexus is a major signaling pathway used by eukaryotic cells to transfer information through the plasma membrane to the nucleus to react to changes in their surroundings. Phosphoinositides are key participants in this pathway, with the pattern of phosphorylation present on the inositol acting as a recognition element for protein kinases that initiate signaling. Inositol phosphorylation is tightly regulated by inositol kinases and phosphatases, as the signals controlled by these second messengers influence a host of cellular functions, including apoptosis.¹ Modulation of this signaling has become an active area, as aberrant activation or loss of function is implicated in many diseases and disorders.² Enzymes including PI3K, PTEN, SHIP and INPP4 are known to metabolize phosphatidylinositols (**Figure 1.1** and **Figure 1.2**). PI3K activity has been shown to significantly influence cellular physiology,³ rapidly synthesizing phosphatidylinositol-3,4,5-trisphosphate (PI(3,4,5)P₃) when PI3K is activated⁴ and initiating signaling through Akt.

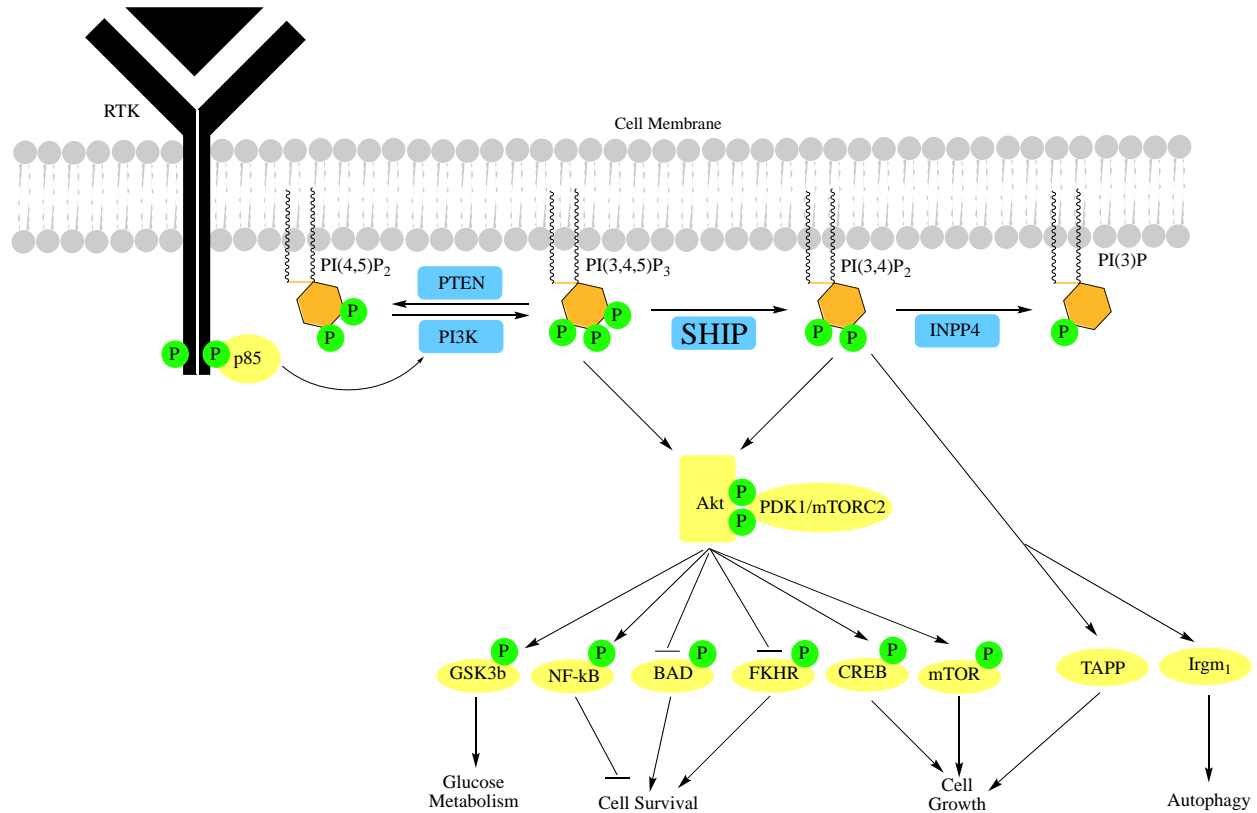


Figure 1.1. Modification of Inositols Mediated by PI3K, PTEN, SHIP and INPP4 and the PI3K Pathway. The formation of PI(3,4,5)P₃ and PI(3,4)P₂ leads to signals which are transmitted to the nucleus through a phosphorylation cascade.

Inositol phosphatases like SHIP influence PI(3,4,5)P₃ levels by controlling the position and rate of phosphate hydrolysis. The primary inositol phosphatases involved in processing PI(3,4,5)P₃ are PTEN (Phosphatase and Tensin Homolog Protein) and SHIP.⁵ Although PTEN and SHIP can both negatively regulate the PI3K pathway, they do so in different ways: PTEN converts PI(3,4,5)P₃ to PI(4,5)P₂ while SHIP converts PI(3,4,5)P₃ to phosphatidylinositol-3,4-bisphosphate (PI(3,4)P₂).^{5a} By decreasing the concentration of PI(3,4,5)P₃, PTEN and SHIP both influence the PI3K pathway's downstream effector cascades; however, SHIP may have dual roles in PI3K signaling, as its product (PI(3,4)P₂) also leads to activation of downstream

effectors like Akt and Irgm1.⁶ This Akt activating role is especially relevant in malignant cells,^{2k,7} therefore SHIP can both negatively and positively influence many aspects of cellular pathology.

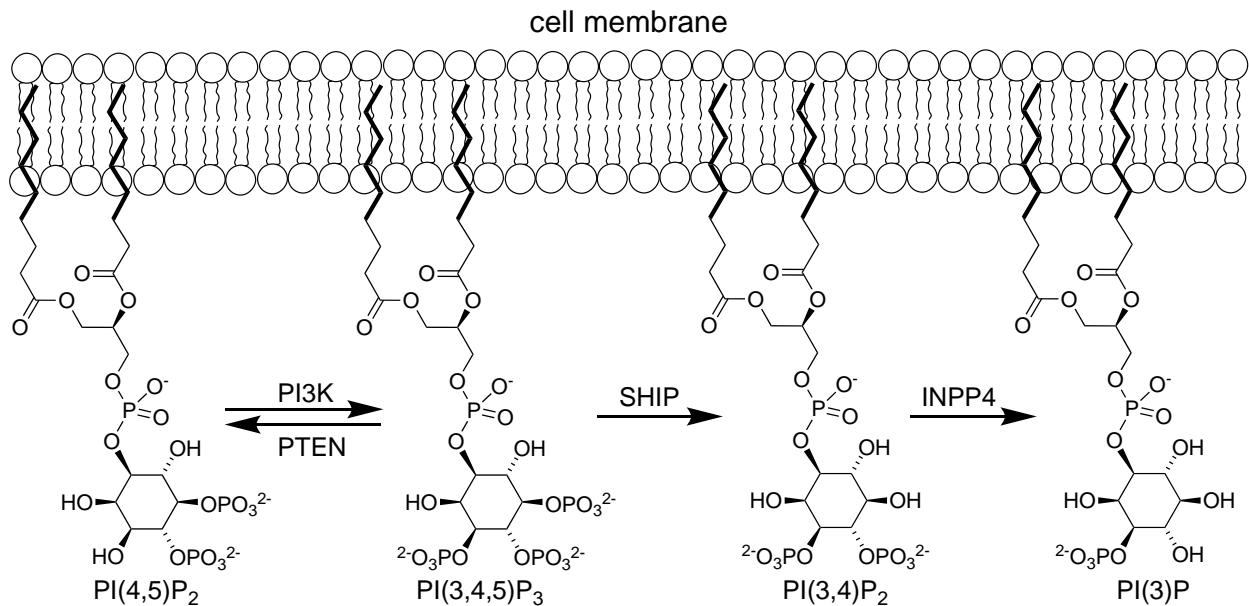


Figure 1.2. Modification of Inositols Mediated by PI3K, PTEN, SHIP and INPP4 and the PI3K Pathway. The phosphorylation of inositols intercalated in the cell membrane is controlled by inositol kinase and phosphatase enzymes.

Two major isoforms of SHIP are associated with the PI3K pathway: SHIP1 and SHIP2. While these enzymes share a high level of homology,⁸ SHIP1 and SHIP2 differ considerably in their tissue distribution. Expression of SHIP1 is primarily confined to cells of hematopoietic and myeloid lineage,⁹ but this phosphatase is also expressed by osteoblasts and mesenchymal stem cells.^{21,9} SHIP2 is more ubiquitously expressed across many other cell and tissue types.¹⁰ Furthermore, the binding kinetics of the enzyme SH2 domains vary significantly.¹¹ SHIP1 plays a key role in regulation of the immune system,^{8,12} while SHIP2 has been reported to act as a negative regulator of the insulin-signaling pathway, which can influence insulin sensitivity.¹³ Differences in tissue distribution, specificity of recruitment and kinetic differences between the

two enzymes are likely responsible for the dissimilar roles observed *in vivo* between SHIP1 and SHIP2.

Recently, there have been several x-ray structural studies on the phosphatase domain of SHIP1 and SHIP2. While the entire enzyme has resisted crystallization, a fragment of the enzyme containing the phosphatase domain and a nearby regulatory domain (the C2 domain) was crystallized for both SHIP1 and SHIP2. These studies, coupled with x-ray crystal studies on similar phosphatase enzymes and mutagenesis studies, allow for a model of the SHIP active site to be constructed. Structural information about SHIP1 has now become more abundant, with groups reporting x-ray crystal structures of the phosphatase domain of SHIP1.¹⁴ At first, these structures focused on the SHIP2 phosphatase domain,¹⁵ but more recently these structures include both the catalytically active phosphatase domain attached to the neighboring C2 domain for SHIP2¹⁶ and SHIP1.¹⁴ The inclusion of the C2 domain is important, as this section of the enzyme includes the site where PI(3,4)P₂ and agonists have been shown to interact with the enzyme to enhance its phosphatase activity.¹⁷ These structures allow for a direct comparison of the similarity of the enzymes in a three dimensional matrix. SHIP1 and SHIP2 have been reported to be ~60% similar in amino acid sequence, and therefore are predicted to have similar structures. The x-ray structural data are consistent with this prediction. For example, the two crystal structures containing the phosphatase and C2 domains (5OKM¹⁶ and 6IBD^{14a}) show high structural similarity (RMSD = 0.641 Å (2369 to 2369 atoms) (**Figure 1.3**). Most of the key elements (β -sheets and α -helical substructures) occupy overlapping regions in the two structures. Some differences are seen in the flexible loop regions, especially in the P4-interactive motif (P4IM) loop region. The active site of the phosphatase domain is very similar, with most secondary and tertiary structures demonstrating high homology between SHIP1 and SHIP2.

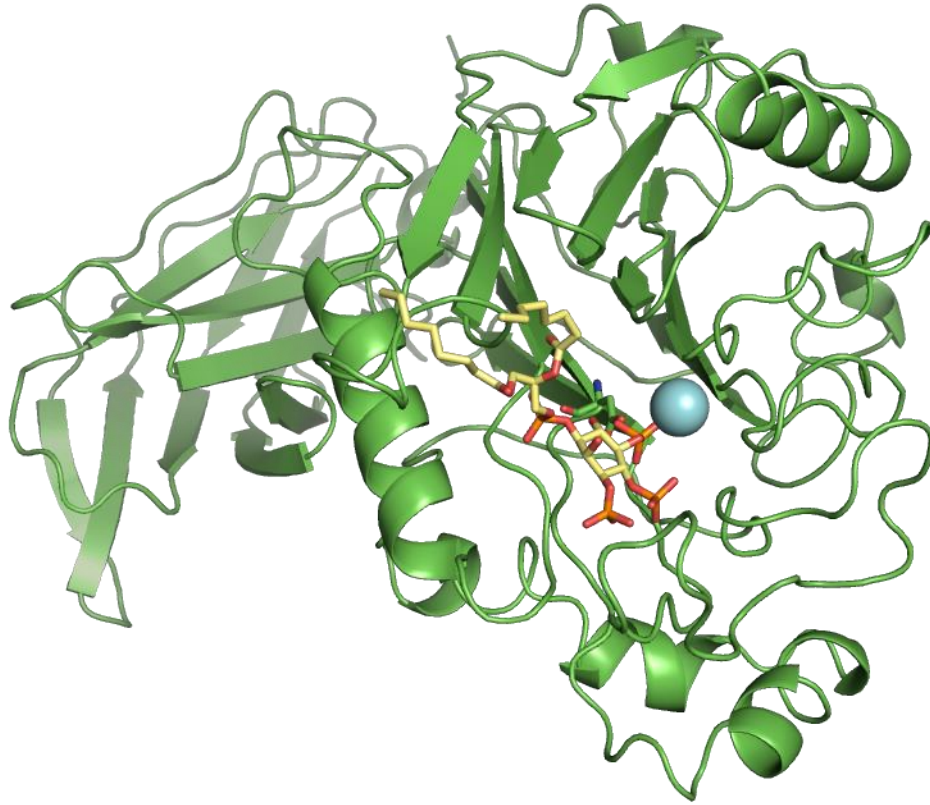


Figure 1.3. Model of SHIP1 phosphatase domain and PIP3. Structure of SHIP1 (in green, 6IBD) aligned with a model of PI(3,4,5)P₃ constructed as described by Lietha,¹⁶ where coordinates for the inositol and metal ion are taken from PDB: 3MTC.¹⁸

While the phosphate binding site of the phosphatase domain of SHIP1 and SHIP2 are very similar, some other areas of the enzyme show significant differences. The region closest to the inositol binding site that is most different is the P4IM flexible loop region which interacts with the 3' and 4' phosphate.¹⁵ Potter and co-workers describe molecular dynamics studies where this loop can rest in an open conformation or a closed conformation, which has significantly more interactions with the 3' and 4' phosphate of PI(3,4,5)P₃.¹⁵ In the overlapping structures, both conformations have been captured, although given the flexibility of the loop the conformations should probably be considered a snapshot of a mobile section of the protein.

Mui and co-workers have reported the identification of the site on the C2 domain of SHIP1 where PI(3,4)P₂ and SHIP1 agonists bind to accelerate the phosphatase reaction.¹⁹ The identification of this site should accelerate the development of SHIP1 agonists, which also may exhibit antitumor properties.¹⁷ Investigations by Leitha and co-workers into the mechanism of allosteric communication between the C2 domain and the phosphatase domain in SHIP2 using molecular dynamics simulations and amino acid mutagenesis implicated conformational changes in three loop regions as leading to the acceleration of the phosphatase activity.¹⁶ Overall this study delineated changes in protein dynamics and active site stabilization rather than large conformational changes as the main causes of the increase in SHIP2 phosphatase activity. The high overall sequence identity that SHIP1 shares with SHIP2 (~50%) suggests that the mechanism of allosteric acceleration may be similar between the enzymes.

1.1.1.2. Mechanism of SHIP1 and SHIP2 catalysis

The mechanism of the catalytic phosphate hydrolysis of PI(3,4,5)P₃ by SHIP has been intensively investigated. The first mechanism for the catalysis by 5'-inositol phosphatases like SHIP was proposed by Mitchell and co-workers, who used the homology between the inositol phosphatases and AP endonucleases to guide their studies.²⁰ This work identified six conserved motifs in the 5-phosphatase family and, using site-directed mutagenesis, validated that these conserved motifs are critical for catalytic activity. These residues included a glutamic acid residue which is important for binding of a Mg²⁺ ion in the phosphatase active site. This metal ion serves as a Lewis acid to activate the 5'-phosphate for hydrolysis. Several asparagines and a histidine were also highly conserved, with these sidechains being utilized to bind to the phosphates on the inositol. A key aspartic acid (D587 SHIP1, D607 SHIP2) was identified as

being involved in the hydrolysis of the phosphate, which directs addition of a water molecule to the 5'-phosphate as proposed in the mechanism of AP endonuclease.²¹ The addition of the water molecule to the phosphate then leads to a transient pentavalent phosphate intermediate, which then proceeds to the observed products of inositol and free phosphate. Phosphatases may hydrolyze phosphates through associative or dissociative mechanisms,²² but an associative mechanism is supported by both ¹⁸O labeling²³ and molecular dynamics simulations²⁴ for AP endonucleases. Given the strong sequence similarity between the inositol phosphatases and the AP endonuclease, it is very likely that the mechanisms proceed through similar pathways. Still, questions remained about the number of metal ions in the transition state, the movement of the metal ion during phosphate cleavage and the orientation of the inositol in the active site.²⁵

The reported crystal structures of SHIP2^{15-16,18} have led to a greater understanding of the number of metal ions in the active site, the specific residues that are interact with the substrate, and the orientation of the inositol during the hydrolysis of the 5'-phosphate. The mechanism that emerges is summarized in **Figure 1.4** below using the SHIP2 residues.²⁶ After binding in the active site, a magnesium ion directed by a nearby glutamate coordinates to the 5'-phosphate, activating the phosphate to nucleophilic attack. The inositol is held in place by interactions between a number of other residues and the phosphates on the inositol ring. Overall, the PIP3 binding site is quite polar, with many basic and acidic residues. A key aspartic acid residue (Asp607 in SHIP2, Asp587 in SHIP1) then directs a water molecule to interact with the 5' phosphate, facilitating the hydrolysis. The protonation of the magnesium salt of the inositol has not been studied in detail, but several polar sidechains (like the nearby Glu473) may facilitate a proton transfer to liberate the PI(3,4)P₂ product of the enzyme.

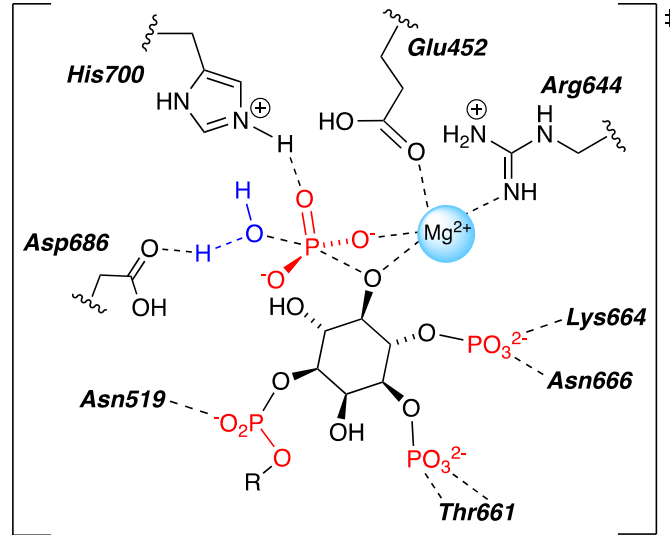


Figure 1.4. Catalysis of the cleavage of the 5'-phosphate of PI(3,4,5)P₃ by SHIP1 (PDB:6IBD)

1.1.1.3. Inhibition of SHIP

SHIP1, SHIP2 and PTEN are typically viewed as opposing the activity of the PI3K/Akt signaling axis that promotes survival in cancer cells and tumors. However, there is emerging evidence that SHIP1 and SHIP2 may actually facilitate, rather than suppress tumor cell survival like PTEN.^{2k,7,27} Consistent with this view, the enzymatic activities of SHIP1 and SHIP2 are quite distinct from that of PTEN which reverses the PI3K reaction to generate PI(4,5)P₂ from PI(3,4,5)P₃, while the 5' poly-phosphatase activity of SHIP1/2 converts PI(3,4,5)P₃ to PI(3,4)P₂. This distinction is crucial as it enables SHIP1/2 and PTEN to have distinctly different effects on Akt signaling. In fact, the PH domain of Akt binds with greater affinity to the SHIP1/2 product PI(3,4)P₂ leading to more potent activation of Akt than the direct product of PI3K, PI(3,4,5)P₃.²⁸ Thus SHIP1, which is expressed by most blood cell malignancies, could actually promote growth and survival of cancer cells. Consistent with this hypothesis, PI(3,4)P₂ levels are increased in leukemia cells²⁹ and increased levels of PI(3,4)P₂ in INPP4A and INPP4B knockout mice promote cell transformation and tumorigenicity.³⁰ Thus, via generation of PI(3,4)P₂, SHIP1/2

could in some contexts amplify survival or proliferative signals in neoplastic cells by providing additional docking sites at the plasma membrane for recruitment and activation of PH-domain containing kinases such as Akt.³¹ Consistent with this hypothesis, we recently found that a SHIP1 selective inhibitor, 3- α -aminocholestane (3AC), reduces Akt activation and promotes apoptosis of human blood cell cancers that express SHIP1.^{2k,7} We further confirmed a role for PI(3,4)P₂ in cancer signaling by showing that introduction of exogenous PI(3,4)P₂ into leukemia cells protects them from SHIP1 inhibition in a dose-responsive fashion.⁷ Thus, SHIP1 inhibitors can now be considered as potential therapeutics to decrease the growth and survival of certain hematologic malignancies like multiple myeloma (MM). There may also be applications for SHIP1/2 inhibitors in non-hematologic cancers as SHIP2 expression is increased in breast cancer and promotes survival signals from EGF-R in these tumors.^{27b,27c} Another potential role for SHIP1 in promoting survival of cancer cells was revealed by our recent demonstration that SHIP1 sets a threshold for extrinsic cell death mediated by Fas/Caspase 8 in mucosal T cells and human T cell leukemia.³²

SHIP inhibitors may also be useful for the treatment of Alzheimer's disease. Genome wide association studies (GWAS) have identified single nucleotide polymorphisms (SNP)s in the INPP5D (SHIP1) gene linked to Alzheimer disease risk, including the rs35349669 (rs669) SNP which is strongly associated with Alzheimer's disease.³³ In cohorts totaling ~74,000 individuals, the rs669T minor allele was robustly associated with AD risk (odds ratio, 1.08, population attributable fraction of 4.6%) with these patients exhibiting increased *INPP5D* gene expression in peripheral blood.³⁴ A second study found that an AD-associated SNP in the INPP5D locus in a Japanese cohort was also associated with increased SHIP1 mRNA expression.³⁵ SHIP is present in microglia, and may play a role in limiting signaling that controls microglia function in reduce

amyloidosis, remove dead or dying neurons and perhaps even NFTs. Depending upon local or systemic signals these microglia may either promote inflammatory processes that might be detrimental in AD or homeostatic functions that could be beneficial.³⁶ Recent studies with pan-SHIP1/2 inhibitors have shown that treatment of BV2 microglia cells with these compounds leads to a significant increase in lysosomal content of these cells with the pan SHIP inhibitor K161.³⁷ An increase in lysosomal content may provide microglia with an enhanced phagocytosis ability, which may facilitate the degradation of dead neurons and/or A β peptides.³⁷ Further experiments showed one compound (K161) significantly increased phagocytosis of dead neurons in these cells. Behavioral studies are now being conducted in Alzheimer's mice to determine if this inhibitor can slow Alzheimer's progression.

1.1.2. Quinoline SHIP Inhibitors

To discover potential SHIP inhibitors, a high-throughput screen was performed by collaborators in the Kerr lab of SUNY Upstate Medical University. Through these efforts, several molecules were found in the NCI Diversity set that showed significant SHIP inhibition.^{2k,7} These can be divided into three classes: aminosteroids, tryptamines, and quinolines. The quinoline SHIP inhibitors NSC13480 and NSC305787 were found to be effective at killing breast cancer cells *in vitro*. These effects correlated with the molecules' observed abilities to inhibit SHIP2, which has been shown to play a role in the development of immunological defects. Since these discoveries were made, we were tasked to produce multi-milligram to multi-gram high-quality samples of the inhibitors in order to further understand the role that SHIP plays in normal cell growth and in cancer suppression or other immunological pathologies. Additionally, structural analogues were desired to investigate the potential of more

water-soluble or more active inhibitors. Thus, we began a synthetic study of the quinoline SHIP inhibitors NSC13480 and NSC305787.

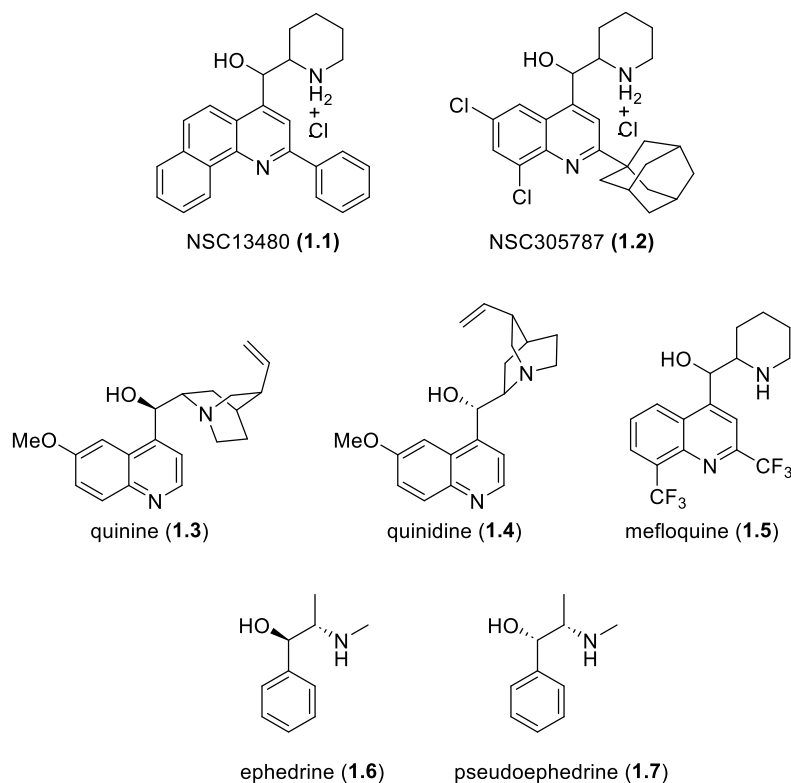


Figure 1.5. Biologically active quinoline and amino-alcohol based molecules, including SHIP inhibitors NSC13480 and NSC305787, natural-products quinine and quinidine, synthetic antimalarial mefloquine, and central nervous system stimulants ephedrine and pseudoephedrine.

NSC13480's structure has a few main functional groups or pharmacophores. The molecule is foremost a quinoline. With the positions enumerated in **Figure 1.6** as a template, NSC13480 is substituted with a phenyl ring at its 2-position and another fused at its 7- and 8-positions. Additionally, a piperidyl-methanol moiety is attached at the 4-position to form a 1,2-aminoalcohol configuration, where both the oxygen- and nitrogen-substituted carbons are stereogenic. This specific quinoline-aminoalcohol configuration with a 6-membered piperidine is notoriously found in the natural products quinine (**1.3**) and quinidine (**1.4**), as well as the related

anti-malarial drug mefloquine (**1.5**). The more generic aryl-1,2-aminoalcohol relationship is also found in active pharmaceuticals such as ephedrine (**1.6**) and pseudoephedrine (**1.7**).

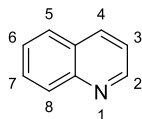


Figure 1.6. Quinoline numbering template. Nitrogen is considered the first position and each perimeter carbon is numbered sequentially from there.

1.2. Results and Discussion

1.2.1. Synthesis of NSC13480

Initially, the stereochemistry of the aminoalcohol portion of NSC13480 and NSC305787 was not known, as the structure from the library did not specify the stereochemistry and their original syntheses were not obviously stereoselective. As seen in **Figure 1.7**, up to 4 stereoisomers are possible. Preliminary NMR analysis of a NSC13480 sample from the NCI appeared to show a single diastereomer. Since this sample did not rotate plane-polarized light, the assumption was made that the sample was provided as a racemic mixture. Given the SHIP inhibitory activity of these molecules, we undertook a synthesis of these systems to verify the relative stereochemistry of molecules. Based on the anti-aminoalcohol relationship seen in similar molecules such as mefloquine, it was assumed that NSC13480 and NSC305787 contained the same relative stereochemistry, and structures **1.1a** and/or **1.1b** became the desired synthetic targets. Given that the literature syntheses of these molecules did not form the aminoalcohol portion of the molecule in a stereocontrolled manner and were presented with near kilogram-scale procedures, efforts were directed towards developing a new route which could selectively provide the desired compound on a more practical milligram to gram scale.

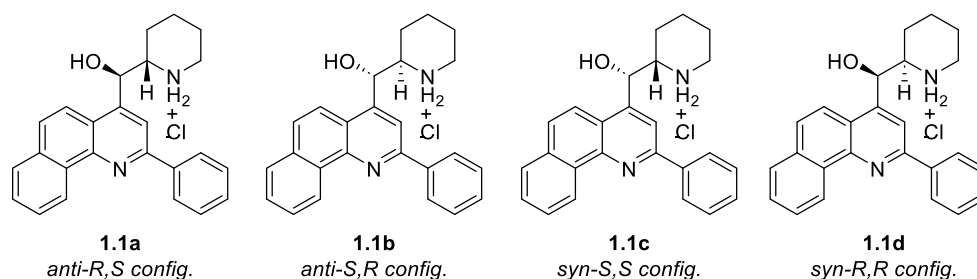
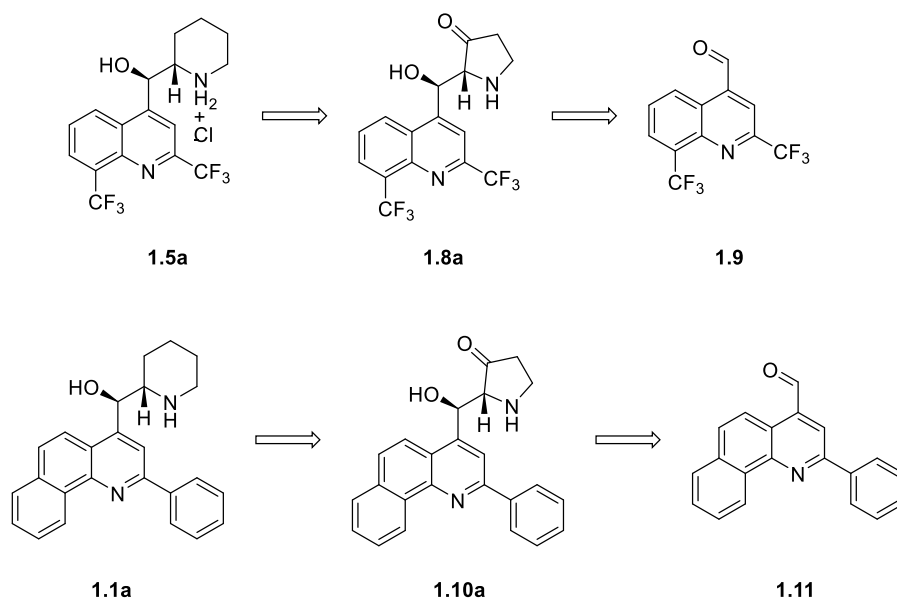


Figure 1.7. Four stereoisomers of NSC13480.

Using Mefloquine as a model, we attempted to follow a procedure for its synthesis as a guide for the synthesis of our own quinoline aminoalcohols. In this synthesis, the corresponding 2,8-bis(trifluoromethyl)quinoline-4-carbaldehyde was reacted in a proline-catalyzed aldol reaction to generate both stereocenters of Mefloquine in one step. The resulting product was converted to its final target via a Beckmann Rearrangement and borane reduction. We assumed that this sequence could be adapted to synthesize a single enantiomer of NSC13480.

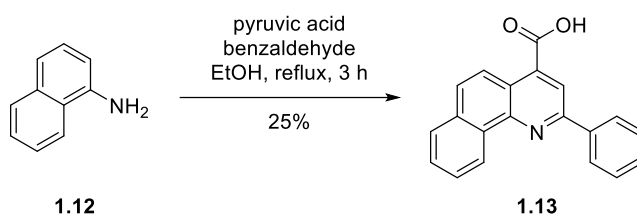
Scheme 1.1.



The original synthesis of NSC13480 employed a Doebner Condensation, which condenses an aniline and an aldehyde with pyruvic acid to synthesize a quinoline substituted with the aldehyde's group at the quinoline 2-position and a carboxylic acid at the quinoline 4-

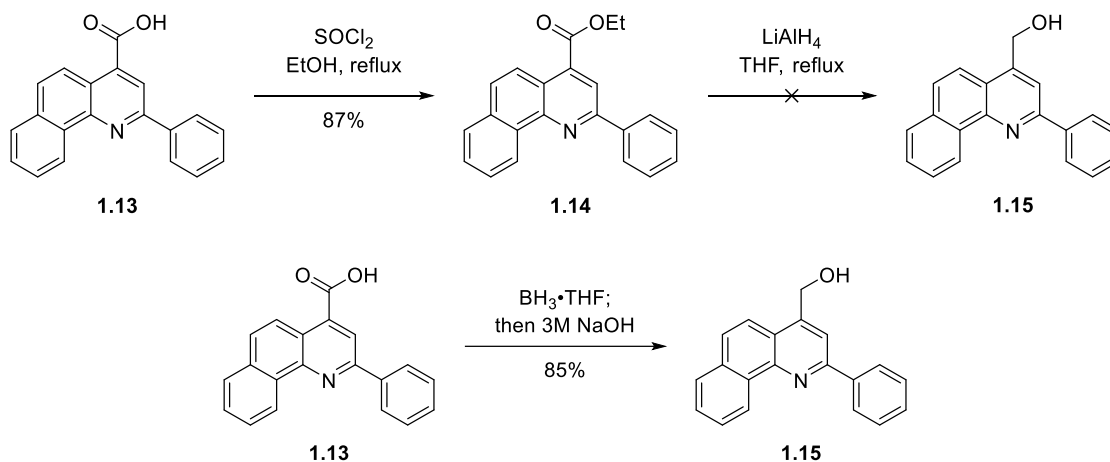
position. Adapting this synthesis, 1-naphthylamine **1.12** was condensed with benzaldehyde and pyruvic acid to provide carboxylic acid **1.13**. The reaction is inherently low-yielding; yields of 20-30% are typical, but the procedure is simple: The components are refluxed in ethanol for 3 hours, cooled to room temperature, and the precipitate is filtered and washed to provide a high-purity product. The reaction can also be scaled with consistency, from 14 mmol to 175 mmol, which allowed us to produce anywhere from 1 to 15 g in a single operation.

Scheme 1.2.

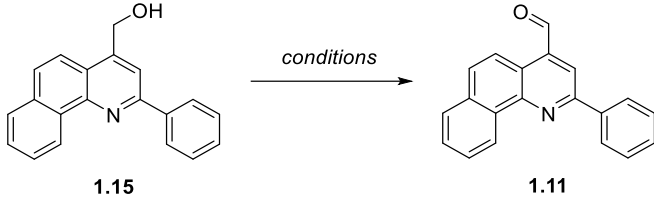


Converting carboxylic acids to aldehydes is a well-known functional group conversion. There are methods for directly reducing a carboxylic acid to an aldehyde; however, a two-step procedure of reduction followed by the oxidation of alcohols is better known and reliable. Overall, the conversion becomes a two-step, but still straightforward route. We first attempted such a reduction via the carboxylic ethyl ester **1.14**, which was obtained in high yield using a classical Fisher esterification mediated by thionyl chloride. Unfortunately, attempts to reduce this ester with lithium aluminum hydride to alcohol **1.15** resulted in apparent decomposition of the starting material. On the other hand, reduction of the carboxylic acid directly to alcohol **1.15** using Brown's borane procedure worked well.

Scheme 1.3.



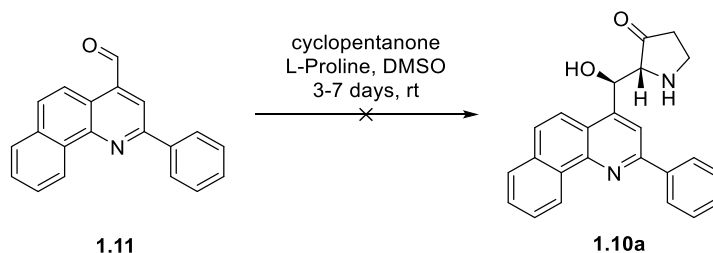
With a reliable method for synthesizing alcohol **1.15**, we began to explore the multitude of reliable methods for oxidizing an alcohol to an aldehyde (see **Table 1.1**). A quick literature search returned similar systems that were oxidized using an Albright-Goldman reaction, that is, with a mixture of acetic anhydride and DMSO. Application of this reaction, though convenient, produced only 49% of the desired aldehyde, with the remaining material being a mixture of the starting alcohol **1.15** and the methylthiomethyl ether of the same alcohol as a result of a competing Pummerer rearrangement. With the Parikh-Doering reaction, which uses DMSO, sulfur trioxide (as $\text{SO}_3 \cdot \text{pyr}$), and triethylamine, aldehyde **1.11** was obtained in only 36% yield. Manganese dioxide was also tried, but an even lower yield of 20% was obtained. Following the poor results of these three oxidation procedures, pyridinium chlorochromate (PCC) was used. This reagent was found to efficiently and fully oxidize alcohol **1.15**. The addition of silica gel to the reaction aided the work-up procedure, which consisted of direct silica gel chromatography of the reaction mixture to provide aldehyde **1.11** in good yield and purity. At this point, we had a reliable, easy-to-reproduce, three-step route for synthesizing ample quantities aldehyde **1.11**. What followed were several attempts to convert this aldehyde into isomers of NSC13480.

Table 1.1.

Chemical reaction showing the conversion of compound **1.15** (a benzimidazole derivative with a hydroxymethyl group) to compound **1.11** (a benzimidazole derivative with an aldehyde group) under various conditions.

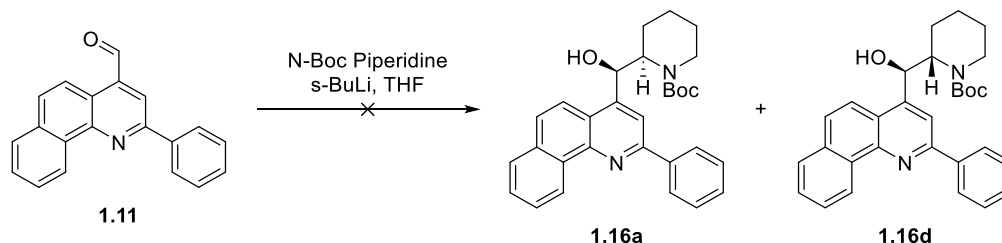
entry	conditions	Yield (%)
1	Ac ₂ O, DMSO	49
2	SO ₃ ·Pyr, Et ₃ N, DMSO	36
3	MnO ₂ , CHCl ₃	20
4	PCC, SiO ₂ , DCM	68

The first attempt to synthesize target **1.1a** was with the previously mentioned proline-catalyzed aldol reaction. This reaction was attractive due to its advertised efficiency in the synthesis of Mefloquine: two stereocenters were set using innocuous and inexpensive reagents. To synthesize Mefloquine, the reported procedure involved stirring the respective aldehyde with cyclopentanone and *L*-proline for 3 days in DMSO. They obtained a 69% yield of a separable mixture of *syn*-aldol product (71% e.e.) and 9% *anti*-aldol product (74% e.e.); the *syn*-aldol product was used to make the *anti*-Mefloquine isomer with 95% e.e. Unfortunately, applying this method to our aldehyde **1.11** for 3, 4, or 7 days resulted in mixtures of inseparable, unidentifiable products. The long, three-day reaction time coupled with the extensive labor and/or technology that would be required to isolate the product lead us to abandon this route.

Scheme 1.4.

At this point, other routes to the target utilizing the same aldehyde were considered. In the *L*-proline catalyzed Mefloquine synthesis, a nucleophile is added to an aldehyde, and another three to four steps lead to the final product. We were curious to know whether we could add a nucleophile to the aldehyde and arrive at our final product in fewer steps. A literature search proved it possible to add Boc-protected piperidines and pyrrolidines directly to aromatic aldehydes using *s*-BuLi to generate a carbanion adjacent to the nitrogen. In the case of pyrrolidines, asymmetric deprotonation is possible using chiral diamines such as Sparteine and its analogues. For the few times that we tried adding N-Boc-piperidine to aldehyde **1.11**, we did obtain products; however, we were unable to fully identify their structures and we were unable to convert either of them to any desired NSC13480 precursor.

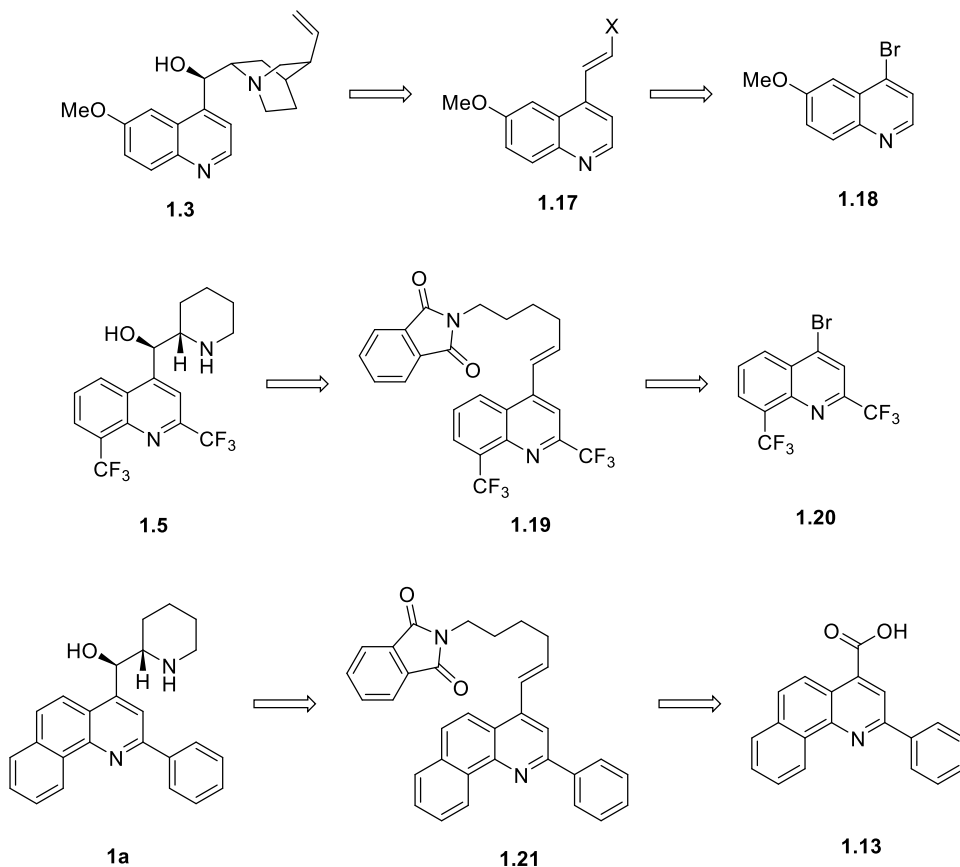
Scheme 1.5.



The attempted proline-catalyzed aldol reaction and direct nucleophilic addition of piperidine both relate to the same retrosynthetic disconnection. Since these routes were problematic, we switched focus towards a different disconnection at the 4-position of the quinoline. Such a strategy has been used previously: Jacobsen used a Suzuki coupling in the synthesis of quinine and quinidine, while Adams and Barlin independently used a Heck reaction in the synthesis of Mefloquine analogues. Both procedures were used to join the aromatic carbon of their quinoline to the section that would eventually become aliphatic aminoalcohols. With this in mind, we sought to synthesize the corresponding olefin using reactions of this type, as seen below. Due to the ease with which carboxylic acid **1.13** was made, we were not quick to abandon

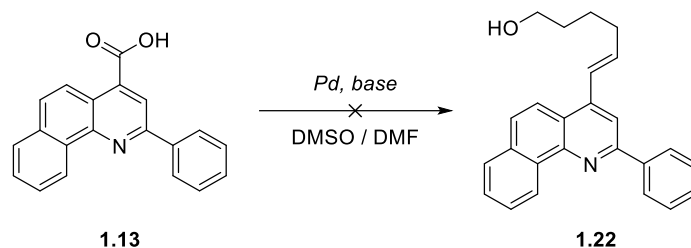
it as a starting point for reaching this olefin. As such, decarboxylative Heck and Hunsdiecker reactions were investigated.

Scheme 1.6.



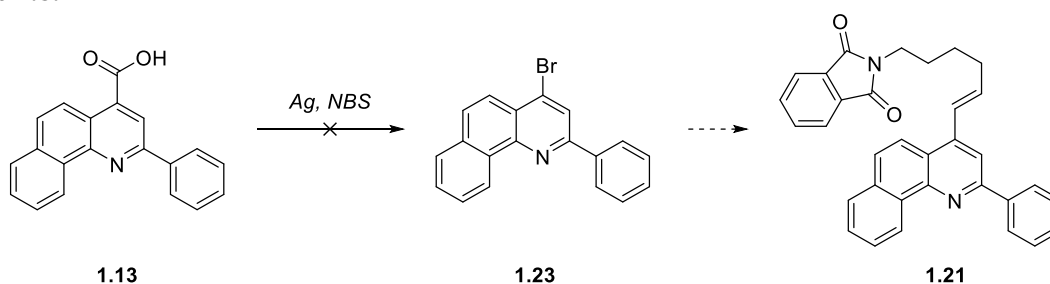
Decarboxylative Heck reactions are known, but only for a few select reactants; the reaction has yet to develop into something widely applicable. Never the less, a few experiments to decarboxylate and couple acid **1.13** to hex-1-ene-6-ol were attempted. A variety of palladium sources [palladium(II) acetate, palladium(II) trifluoroacetate], bases [silver(I) carbonate, copper(II) fluoride, potassium carbonate] and solvents [DMSO, DMF] were screened, but no desired product was observed in any reaction.

Scheme 1.7.



The Hunsdiecker reaction is a known method for converting carboxylic acids to halides, and the halides of quinolines are known to undergo transition metal catalyzed coupling reactions. Unfortunately, a procedure using N-bromosuccinimide and triethyl amine failed to convert acid **1.13** into bromide **1.23**. More traditional methods are known, but we had little interest in using the stoichiometric amounts of silver or lead that these procedures required. This would have been prohibitively expensive and toxic on the scales we required here at the early stages of the synthesis of isomers of NSC13480.

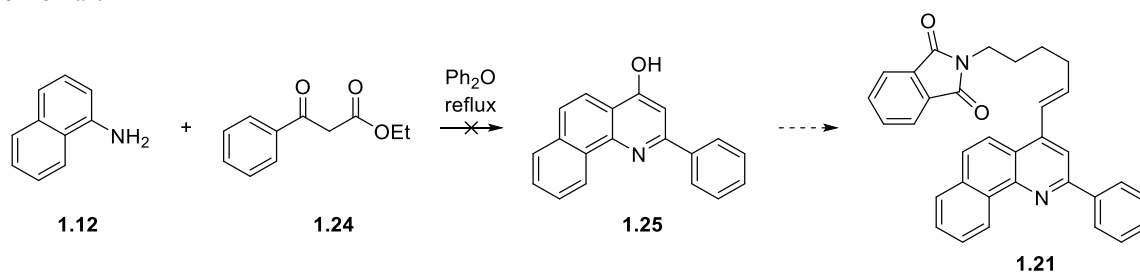
Scheme 1.8.



Instead of using carboxylic acid **1.13** to access a Heck product such as olefin **1.21**, we decided to start our synthesis of NSC13480 isomers from scratch using a Conrad-Limpach Synthesis. Instead of producing a quinoline with a *carboxylic acid* at the 4-position as in the Doebner Condensation, the Conrad-Limpach reaction generates a quinoline with a *hydroxyl group* at the 4-position. This phenolic compound would be more amenable to substitution at the 4-position, as the hydroxyl group is easily converted into a traditional leaving group; either a halide or a sulfonate. Unfortunately, the Conrad-Limpach synthesis is not as simple in operation as the Dobner condensation described earlier. Instead of a one-step neutral reaction in refluxing

ethanol, two-steps are required: an acid catalyzed condensation in toluene followed by a thermally promoted cyclization in which diphenyl ether is used. The higher boiling temperature of diphenyl ether (258 °C) and the fact that diphenyl ether is a solid at room temperature makes it a difficult-to-use solvent. Additionally, the reactants used in the Conrad-Limpach synthesis are the same as those used in the Knorr Quinoline synthesis. The two reactions compete with each other, and often times special conditions are required to favor one over the other. Despite the five times the reaction was attempted, ethyl benzoyl acetate and 1-naphthylamine failed to condense to produce any observable desired product according to known procedures.

Scheme 1.9.



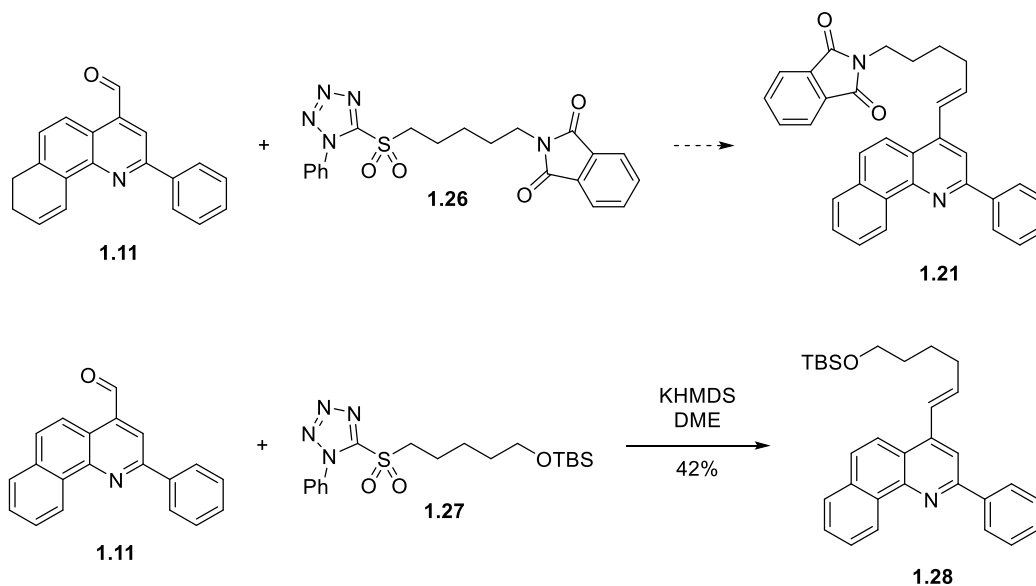
Being unable to access a halide or pseudohalide at the quinoline 4 position, a synthesis that used quinoline carboxylic acid **1.13** as a starting point was reconsidered. In examples described earlier for the synthesis of quinine and Mefloquine, despite the different procedures and reagents used in their respective coupling reactions, each synthesis involved the epoxidation of an *E* or *trans* disubstituted double bond. Since we already were able to easily produce aldehyde **1.11**, we investigated some methods to convert this aldehyde into the desired olefin **1.21**.

The Julia olefination and Wittig reaction (and their relatives) are classical reactions for the synthesis of olefins. Both involve the addition of a carbanion to a carbonyl followed by elimination to generate a double bond. While the stereochemical outcome of the Wittig reaction depends on the stability of the carbanion, the outcome of the Julia olefination depends more on

the reaction conditions used. A classical Wittig reaction of aldehyde **1.11** would generate an undesired *cis* olefin. We therefore decided to use the Julia olefination, which could achieve the desired *trans* stereochemistry regardless of the coupling partners used.

In order to produce olefin **1.21** using a Julia-Kocienski olefination, two compounds were required: aldehyde **1.11**, which is already easily made, and phthalimide protected sulfone **1.26**. Since neither the synthesis nor use of this sulfone was known in the literature, we felt it would be beneficial to first synthesize and use known TBS protected model **1.27**, as the behavior of the silyl ether was known and expected to be better than that of the phthalimide group. Thus, our goal was to make sulfone **1.27**.

Scheme 1.10.

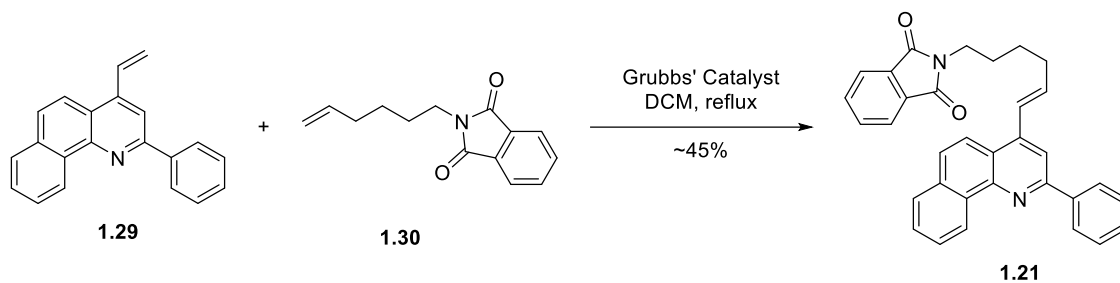


Sulfone **27** was synthesized according to known methods: monoprotection of pentan-1,5-diol, Mitsunobu substitution of the remaining alcohol with 5-phenyl-1H-tetrazole, and oxidation of the sulfide to a sulfone with *m*-chloroperchloric acid. Yields were modest, but enough compound was obtained to test the Julia-Kocienski olefination. The first attempt failed to produce any product, possibly due to water contamination. The second attempt successfully

generated olefin in 42% yield with an acceptable *E:Z* ratio of 9:1 determined by ^1H NMR. The third attempted failed to produce any product. Additionally, attempts to make the phthalamide substituted sulfone **1.26** in as many steps as TBS protected sulfone **1.27** failed; a more lengthy sequence involving an alcohol protection and deprotection would have to be used. Because the Julia-Kocienski route was low-yielding, had only modest *E:Z* selectivity, and required cryogenic temperatures, we considered the other methods of synthesizing olefin **1.21**, such as an olefin metathesis or a Horner Wadsworth Emmons reaction.

The next reaction that we evaluated was an olefin metathesis catalyzed by Grubb's ruthenium catalyst(s). The reaction would not generate the phosphine oxide waste of the Wittig reaction or require the cryogenic conditions of the Julia-Kocienski olefination. Although an additional step is required to convert aldehyde **1.6** to vinyl quinoline **1.29**, only one step is required to generate the coupling partner **1.30**, compared to three to five steps for the synthesis of Julia coupling partner sulfones **1.26** or **1.27**. This metathesis route was thought to be a more rapid method to achieve our goal, even though it employed an expensive ruthenium based catalyst.

Scheme 1.11.



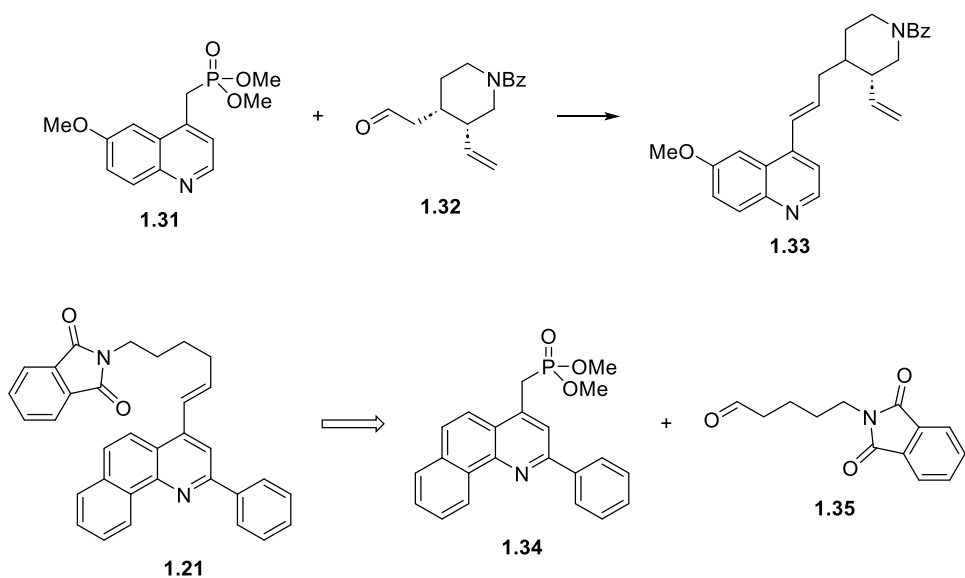
Conveniently, hex-5-en-1-ol is commercial available and inexpensive. This compound was converted to phthalimide substituted olefin **1.30** in 91% yield in one step using Mitsunobu conditions. Styrene **1.29**, on the other hand, could not be made in one step from a commercial available starting material, but it could be made in one step from the relatively easily accessible

aldehyde **1.11**. Thus, aldehyde **1.11** was subjected to different methylenation procedures. Methyl triphenylphosphine never provided more than 44% yield, but 5-(methylsulfonyl)-1-phenyl-1*H*-tetrazole provided vinyl quinoline **1.29** in 91% yield. Both coupling partners were easily synthesized in high yield, showing that perhaps olefin metathesis could be a more convenient method for synthesizing trans-olefin **1.21**.

The metathesis reaction was attempted using Generation II Grubbs' Catalyst (GII). Refluxing 1.0 equivalent of vinyl quinoline **1.29** with 3.0 equivalents of phthalimide substituted olefin **1.30** and 5 mol% GII in dichloromethane for 1 day produced desired olefin **1.21** in 27% yield. Extending the reaction time to 3 days reaction produced variable results, with yields ranging from 30% to 60%. Additionally, purification of the product was complicated, as each reaction also generated significant quantities of dimerized olefin **1.30**, a consequence of having to use olefin **1.30** in excess. Multiple purifications by silica gel chromatography were required to obtain acceptably pure product; additional purifications would have been required to produce analytically pure product. Olefin metathesis, though inherently useful, proved to be more of a burden than expected and was abandoned as a method for generating our olefin.

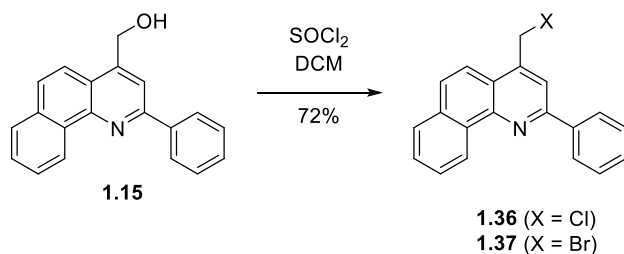
While both the Julia-Kocienski and metathesis routes were successful in producing a *trans* olefin, but they were not efficient enough to reliably provide our desired olefin **1.21** in high yields and purity. Based on the research of Kobayashi, we decided to try a third method: The Horner-Wadsworth Emmons reaction. In their synthesis of quinine, they coupled a quinolyl phosphonate with an aliphatic aldehyde. We thought that a similar sequence could be introduced into our synthesis of isomers of NSC13480.

Scheme 1.12.



Benzylic phosphonates are traditionally made via the Arbuzov reaction from a benzylic halide. In the event the benzylic halide is not immediately available, it can be conveniently made from a benzylic alcohol. This is exactly the sort of functional group we had already made with ease: quinoline alcohol **1.15** is made from quinoline carboxylic **1.13** via borane reduction. Thus, to convert this to a phosphonate, it was first treated with thionyl chloride to produce the intermediate benzyl chloride **1.36** in moderate to high yield. Like the two reactions prior, the procedure was adaptable enough to produce a wide range of yields, from a 100 mg to 15 g. Bromide **1.37** could also be made in acceptable yield by treating alcohol **1.15** with phosphorus tribromide.

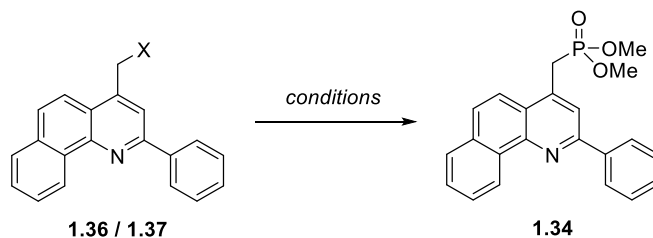
Scheme 1.13.



The next step to complete prior to the olefination step was a classical Arbuzov reaction in which a phosphonate is made by displacing a halide with a symmetrical phosphite. As seen in

Table 1.2, high concentrations of phosphite were necessary for a successful reaction and usage of a bromide did not appear to have any significant improvement over the usage of a chloride. The most convenient and most efficient conditions were found to be refluxing 1 mmol chloride **1.36** in 2 mL phosphite and 3 mL toluene for 2 days.

Table 1.2.



entry	X	mmol P(OMe) ₃ per mmol X	mL P(OMe) ₃ per mmol X	mL toluene per mmol X	Time (d)	Yield (%)
1	Cl	2.0	0.25	100	1	0
2	Cl	40.0	5.0	0	1	62
3	Br	10.0	1.0	0	1	81
4	Cl	8.5	1.0	2.0	1	0
5	Cl	16.9	2.0	3.0	2	85
6	Br	16.9	2.0	3.0	2	52

With a suitable method for synthesizing phosphonate **1.34** from carboxylic acid **1.13** in three steps, synthesis of the phthalimide substituted coupling partner aldehyde **1.35** was engaged. Conveniently, and unlike the sulfone **1.26** required for the Julia olefination, the aldehyde required for the Horner Wadsworth Emmons reaction is well-known in the literature, having been synthesized in two steps from the commercially available and inexpensive 5-amino-pentan-1-ol by a straight-forward condensation and oxidation. The condensation was successful in our hands at all scales attempted. Yields as high as 98% were achieved in a single reaction producing 28 g of material in a single operation.

The oxidation to the aldehyde was less amenable to scale-up, as the aldehyde was discovered to be air-sensitive. Still, some 1 to 2 g could be made at a time using PCC as the

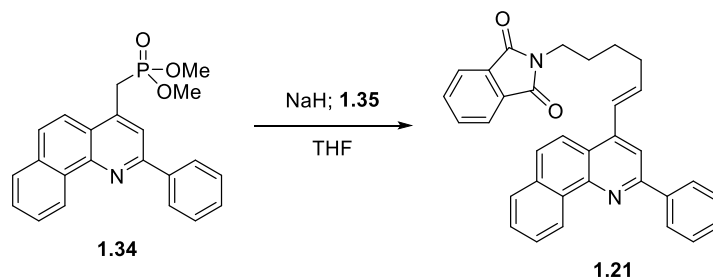
oxidant, as suggested by literature procedures. This method was convenient at first, but for larger scale syntheses of NSC13480, excessive chromium waste would become an issue. Rather than use PCC or a DMSO-based oxidation, we considered a more attractive TEMPO-based oxidation instead which did not generate chromium byproducts or the malodorous dimethyl sulfide. Using 1 mol% TEMPO with inexpensive trichloroisocyanuric acid as a stoichiometric oxidant, aldehyde **1.35** could be synthesized rapidly in high yield. In 30 minutes, upwards of 5 g of pure aldehyde could be produced without a need for purification beyond filtration and aqueous two-phase extraction.

Carboxylic acid **1.13** is relatively easily converted to phosphonate **1.34** in good yield over three steps; four if including the step to synthesize the carboxylic acid itself. Each of these steps can be performed on multi-gram scales, in part thanks to the ease with which carboxylic acid **1.13** is purified: A simple filtration allows for the generation of many grams that can be carried forward through the additional three steps. Likewise, aldehyde **1.35** can be synthesized in large scale in only two steps from very inexpensive, non-toxic starting materials. With easy access to both coupling partners, a successful Horner Wadsworth Emmons reaction would allow for formation of the entire carbon skeleton of NSC13480.

Following the procedure of Kobayashi, the Horner Wadsworth Emmons reaction was attempted using equal ratios of phosphonate to aldehyde, with sodium hydride as the base and THF as the solvent. As seen in **Table 1.3**, the first attempt resulted in 77% yield of olefin **1.21**; however, a repetition of the reaction resulted in only 16% yield. Thinking that perhaps the quantity of base was an issue, six reactions were attempted with an increased amount of sodium hydride. Of these six reactions, two produced no product, while four produced yields of 62 to 85%. Clearly, there was some aspect of the reaction that caused it to either work well or not at

all. In entry 9, it was discovered that the reaction success was dependent upon the presence of water. Presumably, under anhydrous conditions, deprotonation of aldehyde **1.35** lead to an irreversible, dead-end formation of its enolate, while the addition of water made this deprotonation reversible, which allowed the olefination to proceed. This theory is supported by the fact that for experiments where the reaction appeared to not progress, the slow, dropwise addition of water promoted the rapid formation of the desired olefin. Unfortunately, this water-addition method could not be reproduced reliably, as vastly different yields were obtained between entries 9, 10, and 11. The HWE reaction using sodium hydride, though sometimes successful, was too unpredictable for our purposes, thus optimizations were sought.

Table 1.3.



entry	mmol Phophonate	equiv. Aldehyde	equiv. NaH	Yield (%)
1	0.66	1.0	1.2	77
2	0.64	1.0	1.2	16
3	1.00	1.0	5.0	0
4	1.00	1.0	5.0	62
5	1.80	1.0	4.0	73
6	5.31	1.0	3.0	85
7	5.78	1.0	3.0	85
8	9.47	1.0	3.0	0
9	1.41	1.2	1.1	61
10	11.0	1.2	1.1	30
11	10.3	1.2	1.2	48

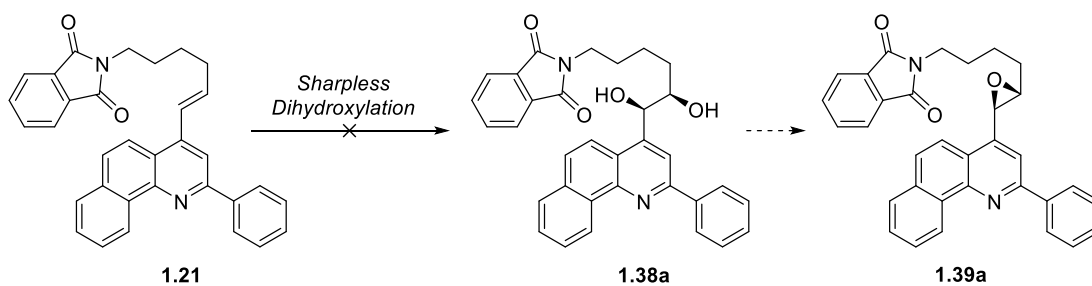
Because sodium hydride was unreliable, different bases were considered for the Horner Wadsworth Emmons reaction. Hydroxides and alkoxides might have proven beneficial compared

to the results encountered with the sodium hydride quench, as the combination of water and the hydride generates sodium hydroxide; however, we sought to keep the reaction anhydrous if possible. Thus, we investigated modifications which use milder amine bases and metal halide salts as activators. In 1984, Masamune and Roush reported that sodium hydride and potassium *tert*-butoxide caused similar enolization problems on an aliphatic aldehyde, but amines such as DIPEA or DBU, when paired with lithium chloride, promoted only the olefination reaction. Thus, we used the combination of DBU and LiCl to couple phosphonate **1.34** and aldehyde **1.35**. These conditions proved to be far more reliable, as they provided consistent yields between 70 and 80% with high *E* selectivity: only trace amounts of the *Z* isomer were detected.

After completing the synthesis of olefin **1.21**, we were now prepared to revisit stereoselective transformations that would allow us to separately synthesize multiple isomers of NSC13480 that we originally sought in the *L*-proline aldol route. In multiple published methods for the asymmetric synthesis of similar quinolines, the *anti*-relationship between the alcohol and amine is accessed with the stereospecific opening of an enantiopure *trans*-epoxide. From our *trans*-olefin, we hoped to use similar stereoselective epoxidation methods.

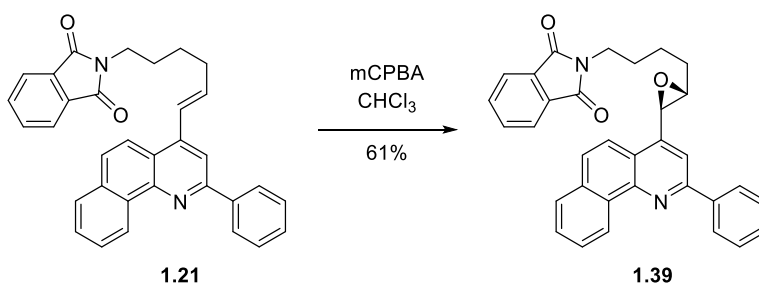
One such method starts with a Sharpless dihydroxylation, followed by conversion of the resulting diol to an epoxide. This method was used in the synthesis of quinine and quinidine. Unfortunately, enantiopure diol **1.38a** could not be reliably made from olefin **1.21** in our hands using the standard published procedure. In a control experiment, stilbene was easily converted to stilbene oxide using the same method, which lead us to suspect that olefin **1.21** was an inherently poor substrate for this method. Low solubility or the partial cleavage of the phthalamide group may have been contributing factors.

Scheme 1.14.



Apart from the desire to synthesize separated enantiomers, we originally avoided a racemic synthesis due to the unpredictable behavior of the quinoline nitrogen when exposed to *m*CPBA, a standard asymmetric electrophilic oxidizing agent. In one report, *m*CPBA undesirably oxidized an unhindered the nitrogen to the corresponding *N*-oxide, while in another report, this did not occur for a more hindered nitrogen. Following the limited success of our asymmetric routes, we concluded that it would be more practical to finish a synthesis of a racemic mixture of *anti* NSC13480 isomers. Thus, olefin **1.21** was treated with *m*CPBA; approximately 3 equivalents were required to achieve full conversion of olefin **1.21** to racemic epoxide **1.39a**. Conveniently, the hindered quinoline nitrogen did not oxidize, a fact supported by elemental combustion analysis.

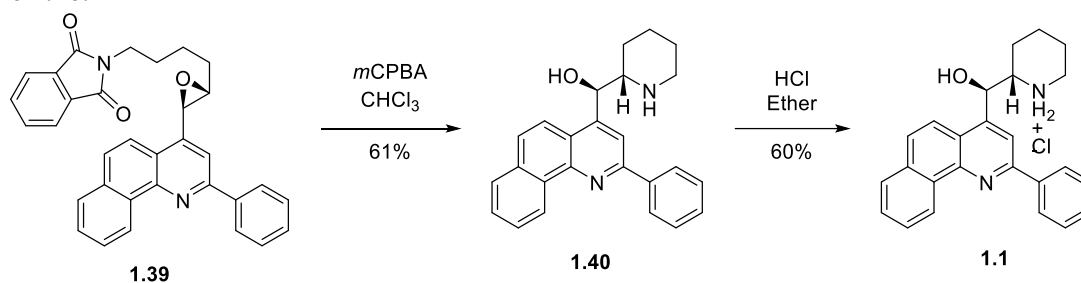
Scheme 1.15.



After finding that an electrophilic epoxidation procedure worked well, we were hopeful that the final two steps would be just as successful. Indeed, treating racemic epoxide **1.39** with an excess of hydrazine, as in a classical Gabriel Synthesis, cleaved the phthalimide protecting group to reveal the primary amine. This amine was not isolated, though, as it spontaneously reacted

intramolecularly with the epoxide to produce a piperidine ring and adjacent alcohol of compound racemic **1.40**. Consistent with S_N2 -epoxide opening, a single diastereomer, albeit a mixture of enantiomers was obtained.

Scheme 1.16.



As mentioned previously, the relative stereochemistry of the NCI sample was unknown to us; however, we did have an 1H NMR of this sample. To compare this sample with our own, we isolated amine **1.35** as its hydrochloride salt, and its 1H NMR was shown to be identical to the original NCI sample, confirming that we had correctly predicted its relative stereochemistry. Thus, we had completed a new synthesis for NSC13480, which was shown to be a mixture of *anti*-isomers. This verified that the relative stereochemistry of the aminoalcohol was identical to that which was tested by the Kerr group.

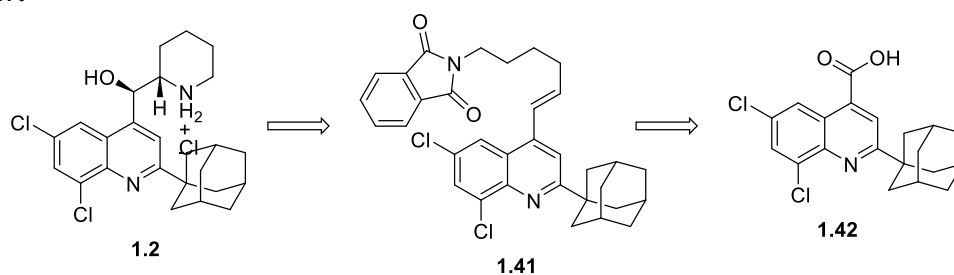
1.2.2. Synthesis of NSC305787

After a successful synthesis of NSC13480 was finished, we turned our attention towards the similar NSC305787. Much like NSC13480, NSC305787 is a substituted quinoline. The piperidinyl-methanol moiety at the 4-position is the same, but at the 2-position, there is a bulky adamantyl group, and at the 6- and 8- positions, there is a chlorine each. Also, like NSC13480,

there is a published synthesis of NSC305787, though its stereoselectivity was ambiguous and the scale and involved high-pressure hydrogenation, which we could not achieve in our laboratory.

Since the two molecules are similar, our experience in synthesizing NSC13480 allowed us to develop a new synthesis for NSC305787 in a much more rapid and streamlined fashion. We did not attempt deviate from our already working methods except in the early stage construction of the quinoline core. Thus, the retrosynthetic plan for NSC305878 was designed based on the successful reactions used to make NSC13480.

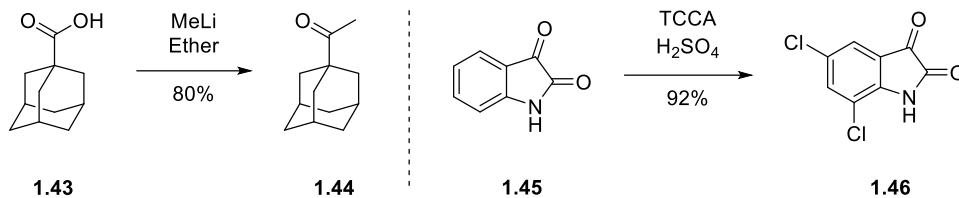
Scheme 1.17.



In the original synthesis of NSC305787, carboxylic acid **1.42** was synthesized using a Pfitzinger reaction. This reaction is different from the Doebner condensation in that it condenses a substituted isatin with a ketone rather than an aniline with an aryl aldehyde and pyruvic acid. While the success of the Pfitzinger reaction is limited by bulky groups such as the adamantyl group, it tends to provide better results than the corresponding Doebner reaction, especially when an alkyl group is needed at the 2-position of the desired quinoline and when the corresponding isatin and ketone are readily available. In the case of carboxylic acid **1.42**, 5,7-dichloroisatin and adamantyl methyl ketone were required. Both were synthesized according to published procedures. Adamantyl methyl ketone was made in high yield by adding methyl lithium to adamantyl carboxylic acid. Dichlorination of isatin with trichloroisocyanuric acid provided 5,7-dichloroisatin in good yield. On large scales, this process resulted in an incredibly exothermic

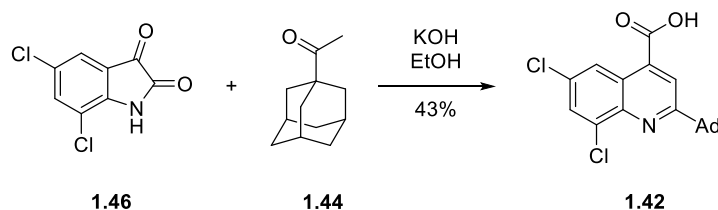
reaction. Thus, as a modification to an already published procedure, this reaction was started at -78 °C and was allowed to warm slowly to room temperature and stir for 3 days.

Scheme 1.18.



Refluxing isatin **1.46** with 1.1 equivalents of ketone **1.44** in ethanol for 1 to 3 days consistently provided a typical 22% yield of **1.42** after recrystallization, with complete consumption of the starting isatin, but with approximately 50% starting ketone **1.44** recovered in each case. To compensate, the less expensive isatin was used in a two-fold excess compared to the more expensive ketone. Under these modified conditions, the desired product was provided in 40% yield after recrystallization, with complete consumption of both starting materials observed.

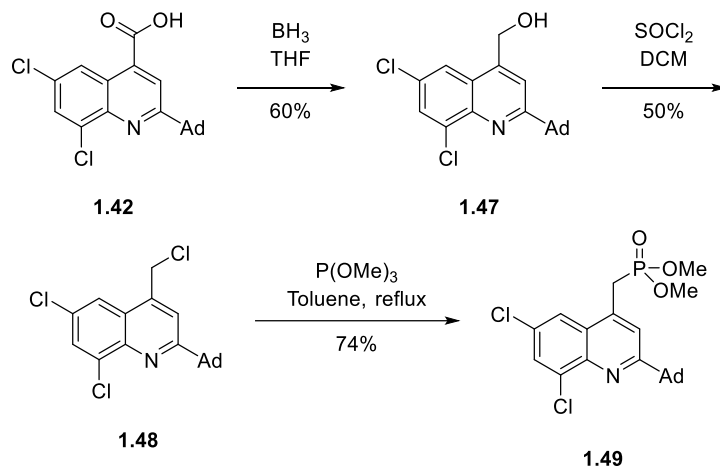
Scheme 1.19.



As with NSC13480, reduction of carboxylic acid **1.42** to alcohol **1.47** was optimally performed with borane-tetrahydrofuran complex. The conversion to chloride **1.48** was unexpectedly difficult. Thionyl chloride at room temperature, though successful in the synthesis of NSC13780, gave inconsistent results. Attempts to use thionyl chloride with pyridine, oxalyl chloride, oxalyl chloride with DMF, or methane sulfonyl chloride, all gave complicated mixtures or low yields of the desired chloride. Appel conditions pairing triphenyl phosphine with carbon tetrachloride, hexachloroethylene, or trichloroisocyanuric acid also all provided inconsistent

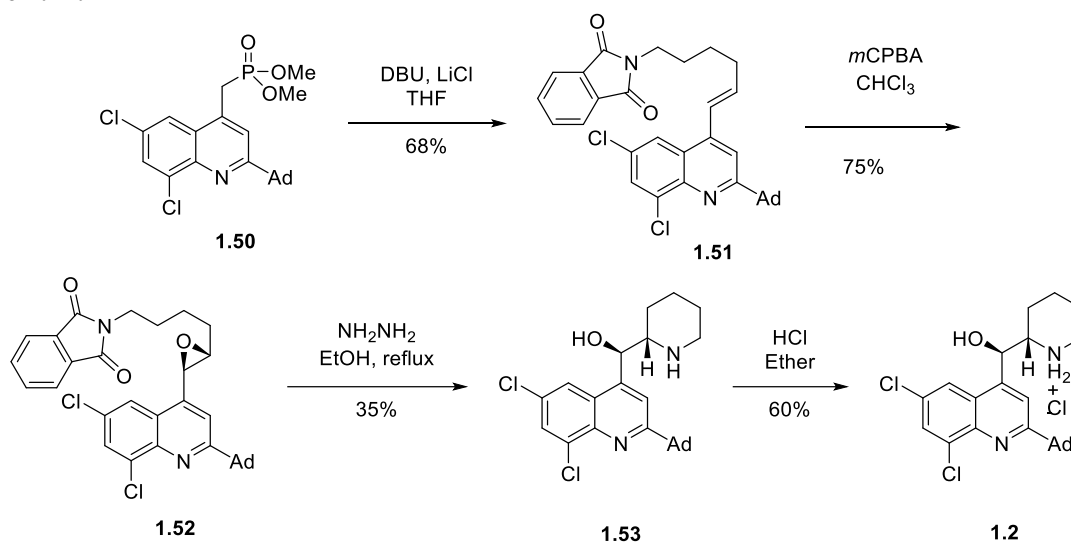
yields and purities. Only thionyl chloride at 0°C for 1 hour gave a consistent 50% yield. Longer reaction times or higher temperatures lead to significant amounts of an unidentified side-product.

Scheme 1.20.



The Arbuzov reaction provided phosphonate **1.49** in moderate yield. Likewise, the same HWE olefination using DBU/LiCl, epoxidation with *m*CPBA, cyclization, and acidification steps followed to synthesize NSC305787 in good yield. Like with NSC13480, ¹H NMRs of the NSC sample and the material we synthesized were compared, and the two samples were deemed equivalent, proving that NSC305787 also was a racemic mixture of *anti* isomers. The success of this second synthesis showed that our route towards piperidinylmethanol substituted quinolines is not limited to only one target. Its success on two different occasions suggests that it may be broadly applicable to many molecules of this type, which will be useful in the synthesis of analogs.

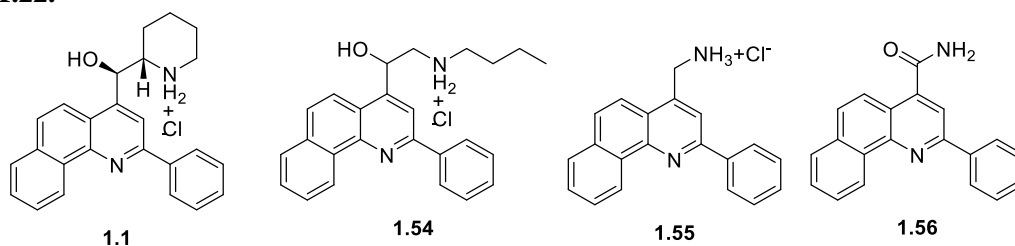
Scheme 1.21.



1.2.3. Synthesis of Analogues

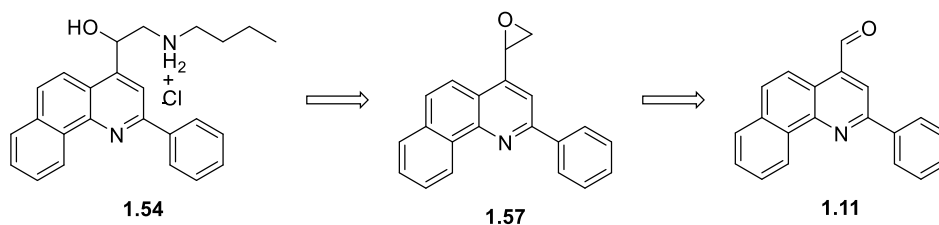
After we had developed new, scalable syntheses of NSC13480 and NSC305787, we turned our focus on the synthesis of analogues of these molecules in order to determine a relationship between the structure of the quinolines and their SHIP inhibition activity. Ideally, we would develop a molecule that was as active as or more active than the parent molecules, but with fewer steps and in higher yield. Considering that constructing the stereogenic piperidinylmethanol portion of the molecules takes considerable effort, we were interested in learning whether this moiety was necessary for SHIP inhibition. Some analogues of NSC13480 were designed and synthesized, all of which would be made from the same starting compound, carboxylic acid **1.13**, and contain the same polyaromatic substructure.

Scheme 1.22.

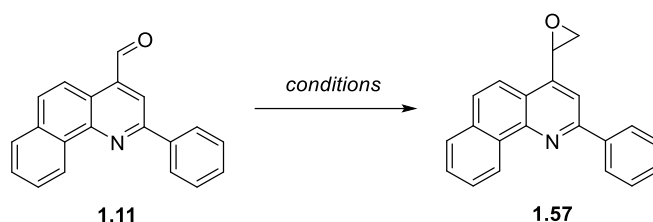


In analogue **1.54**, the cyclic piperidine of **1.1** is replaced by a straight-chain butyl amine, but the number of carbons and placement of heteroatoms remains the same. Two recently published reports of Mefloquine analogues inspired us to make this molecule from epoxide **1.57**, synthesized from aldehyde **1.11**, for which we already had a working route. Two known methods of converting an aldehyde to epoxide were available: (1) Direct methylenation using a sulfonium or sulfoxonium ylide or (2) Electrophilic epoxidation of vinyl quinoline **1.29**, which we also had synthesized previously.

Scheme 1.23.

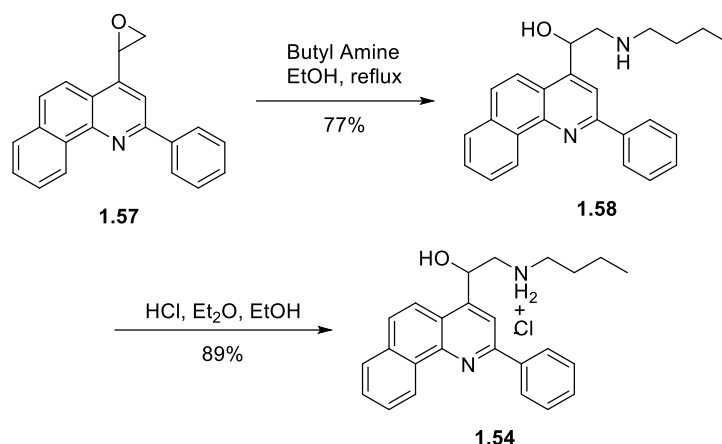


While electrophilic epoxidation of olefin **1.29** did produce product, the reaction was not efficient: With *m*CPBA 38% yield was obtained. These reactions provided enough material to carry the synthesis forwards, but we were interested in developing a more efficient route towards epoxide **1.57**. The results are summarized in **Table 1.4** below.

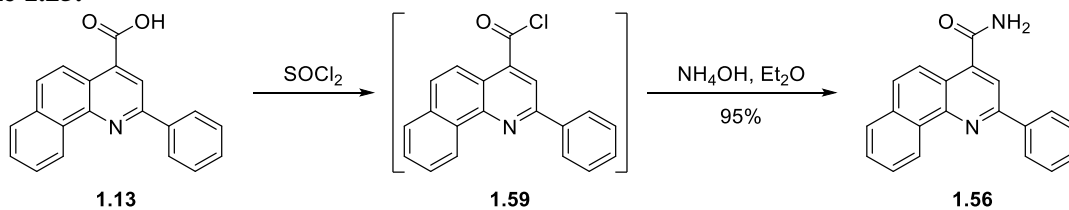
Table 1.4.

Entry	Reagent (equiv.)	Base (equiv.)	Solvent	Time	Yield (%)
1	(Me ₃ SO) ⁺ I ⁻ (1.2)	NaH (1.2)	THF	1 d	0
2	(Me ₃ SO) ⁺ I ⁻ (0.9)	NaH (0.9)	THF	4 h	0
3	(Me ₃ SO) ⁺ I ⁻ (1.0)	DBU (1.0)	THF	2 h	0
4	(Me ₃ SO) ⁺ I ⁻ (0.9)	NaHMDS (0.9)	THF	1 d	0
5	(Me ₃ S) ⁺ I ⁻ (1.0)	NaH (1.0)	THF	1 d	21
6	(Me ₃ S) ⁺ I ⁻ (1.0)	DBU (1.0)	THF	1 d	0
7	(Me ₃ S) ⁺ I ⁻ (1.5)	NaOH (70)	DCM/H ₂ O	1 d	81

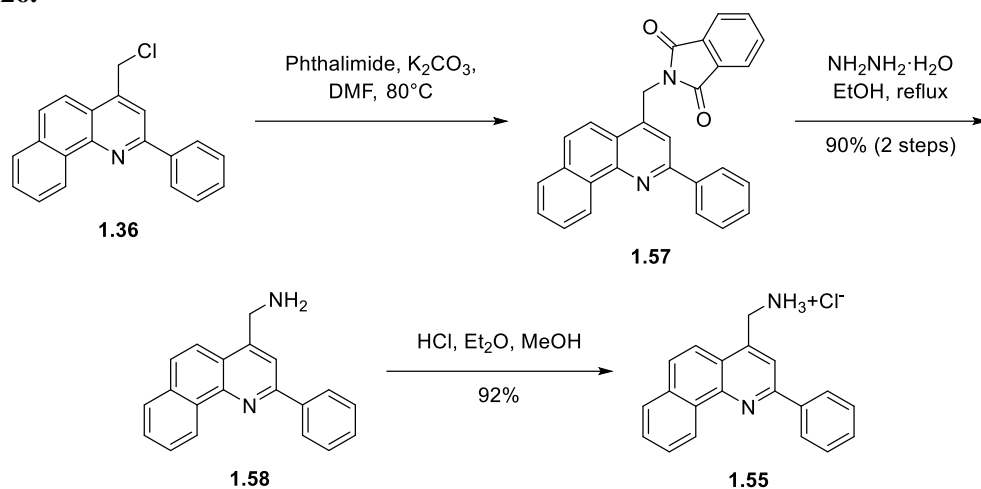
Reacting aldehyde **1.11** with trimethylsulfoxonium iodide and sodium hydride resulted in consumption of the aldehyde, but no epoxide was observed. Using less than 1 equivalent of reagents in a shorter reaction time provided the same results, as did switching to either DBU or NaHMDS. Trimethylsulfonium iodide provided better results. In THF with NaH, 21% yield of epoxide **1.57** was obtained. Using DBU provided no reaction. Only with a two-phase solvent system did we obtain epoxide **1.57** in high yield. Nucleophilic opening of this epoxide with butyl amine provided amine **1.58**, which was isolated as hydrochloride salt **1.54**. This analogue was made in 5 linear steps from carboxylic acid **1.13**; less than the 7 steps required for the parent compound.

Scheme 1.24.

Two other analogues synthesized, primary amine hydrochloride **1.55** and primary amide **1.56**, both retain a polar functionality at the quinoline's 4-position, but with reduced complexity relative to both NSC13480 and butyl amine hydrochloride **1.54**. Amide **1.56** was made by sequentially treating carboxylic acid **1.13** with thionyl chloride and ammonium hydroxide. The intermediate acyl chloride **1.59** was not isolated, thus making this essentially a 1 step sequence from carboxylic acid **1.13**. Treatment of amide **1.15** with lithium aluminum hydride or borane failed to provide any desirable reduction products, so analogue **1.55** was made via Gabriel synthesis from chloride **1.36**; 5 steps from carboxylic acid **1.13**.

Scheme 1.25.

Scheme 1.26.



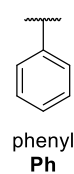
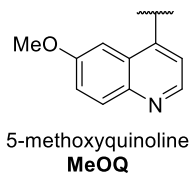
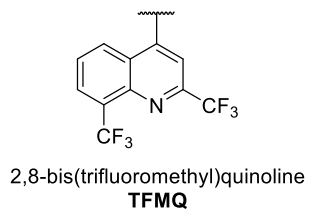
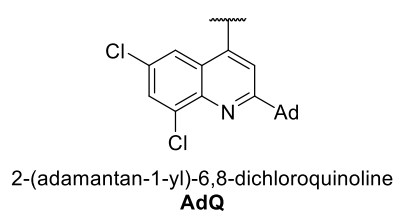
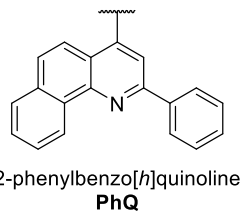
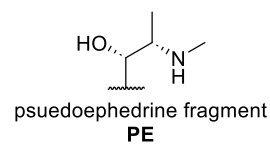
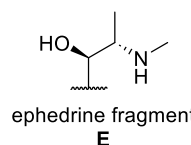
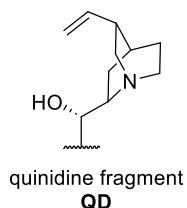
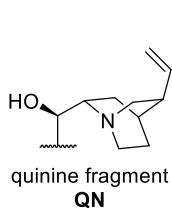
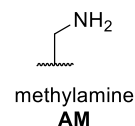
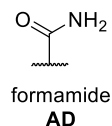
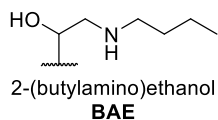
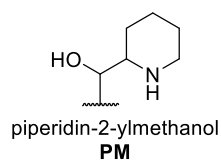
1.2.4. Biological Testing

Following the synthesis of NSC13480 and NSC305787, the two compounds, their analogues, and some commercially available aminoalcohols were submitted to SUNY Upstate University for SHIP inhibition testing using a malachite green assay. Activity values are measures of enzyme activity in the presence of an inhibitor relative to enzyme activity in the absence of an inhibitor. Enzyme activity is determined by measuring the amount of phosphate produced over a constant time.

The molecules tested have two major pharmacophores A and B that were considered in structure-activity relationship determinations. For example, parent compound NSC13480's pharmacophore A is the piperidinylmethanol moiety while its pharmacophore B is the quinoline and its remaining substituents.

Table 1.5.

Entry	A	B	K#	Compound	% inhibition (SHIP1)	% inhibition (SHIP2)
1	PM	PhQ	K101	1.1	38%	17%
2	PM	AdQ	K102	1.2	38%	66%
3	PM	TFMQ	K121	1.5	46%	56%
4	BAE	PhQ	K184	1.54	37%	63%
5	AD	PhQ	K135	1.56	-10%	25%
6	AM	PhQ	K136	1.55	41%	66%
7	QN	MeOQ	K120	1.3	-17%	9%
8	QD	MeOQ	K171	1.4	19%	5%
9	E	Ph	K202	1.6	4%	-7%
10	PE	Ph	K203	1.7	-3%	1%



Considering SHIP1, compounds that contain constant aminoalcohol structures and varying quinoline substituents (K101, K102 and K121) showed comparably inhibition ability, suggesting that a variety of quinoline substitutions are tolerated. The aminoalcohol and butyl-aminoalcohol compound K184 showed comparable inhibition to K101, suggesting that the piperidine structure is not strictly required. The simpler primary amine K136 was also as active as the parent compounds, while amide K135 did not inhibit SHIP1, suggesting that the 2-position can be greatly simplified, but likely requires an amine functionality. Commercially available quinine (K120), quinidine (K171), ephedrine (K202), and pseudoephedrine (K203) were relatively ineffective at inhibiting SHIP1.

Considering SHIP2, K101 showed minimal inhibition, while K102 and Mefloquine (K121) showed strong inhibition of the enzyme. Trends in the inhibition of SHIP2 by the remaining compounds were similar to those observed in SHIP1 inhibition: Butyl-aminoalcohol K184 and primary amine K136 were comparable to K102. Amide K135 was ineffective compared to K102, though showed some inhibition. Quinine (K120), quinidine (K171), ephedrine (K202), and pseudoephedrine (K203) were relatively ineffective at inhibiting SHIP2. These quinolines generally appear to be better at inhibiting SHIP2, with K101 being an obvious exception. The discrepancy between the inhibition ability of K101 and its analogues is not clear.

1.2.5. Docking Quinoline Analogs into the SHIP1 Active Site

Attempts were made to gain a better understanding of how the quinoline analogs were binding to the enzyme. While we have no direct evidence that the quinolines bind to the active site of SHIP (the enzyme kinetics needed to prove this are still ongoing), other lipophilic amines like the aminosteroids have been shown to be competitive inhibitors (unpublished results). We

therefore performed a docking simulation utilizing Autodock Vina and the reported x-ray structure of SHIP1 (PDB: 6XY7), this structure was chosen as it has the metal ion as part of the structure) to attempt to ascertain the binding mode of the quinoline to the active site. Three possible binding poses of **1.55** and their relative energies are shown below in Figure 1.8. Interestingly, similar poses were found both with and without the metal ion present, which may indicate that the quinoline is binding in the same manner regardless of the presence of a metal ion. In the future we hope to utilize these docking studies to design new more potent SHIP inhibitors.

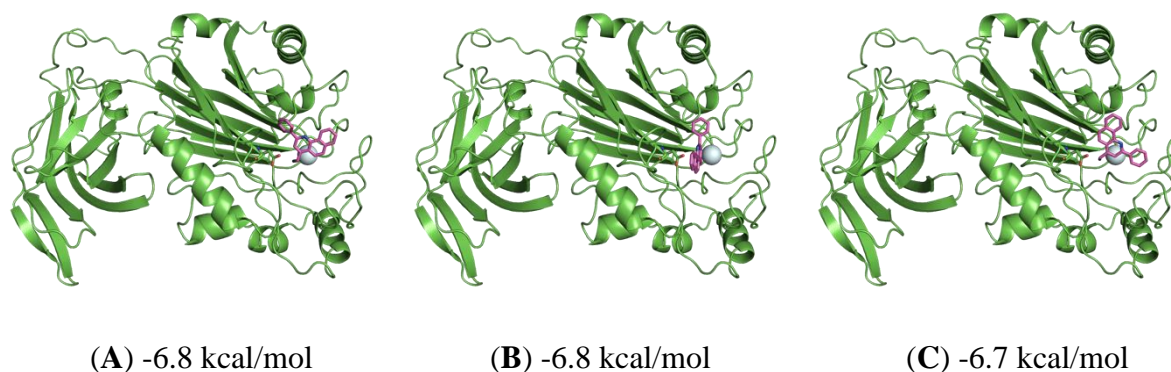
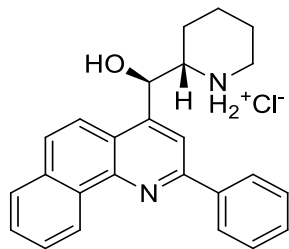


Figure 1.8. Docking pose of the quinoline 1 in the SHIP1 active site

1.3. Conclusion

In summary, new synthetic routes to quinoline-based SHIP inhibitors NSC13480 and NSC305787 have been developed which do not require special equipment for their synthesis. These routes provide the products in a diastereoselective manner. The parent quinolines, several intermediates and similar commercially available compounds have been tested for activity against SHIP1 and SHIP2. In addition to the activity demonstrated by the parent compounds, mefloquine hydrochloride proved to be active as a SHIP inhibitor at high concentrations. The SHIP1/2 activity of mefloquine may explain the reports of the antitumor activity of the molecule,

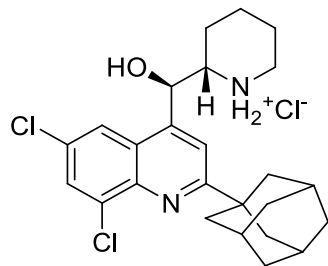
as the concentration seen for SHIP inhibition is similar to the concentration observed for cancer cell killing.²⁰ Quinine and quinidine were not active in the assay, and neither were ephedrine or pseudoephedrine. A brief structure activity study showed that both the quinoline core and a pendant amine at the 4-position of the quinoline were required for significant SHIP1/2 inhibition, but the alcohol and the piperidine ring were not critical components for this activity. Future studies exploring the structure-activity relationships in these systems are underway and will be reported in due course.



2-(hydroxy(2-phenylbenzo[*h*]quinolin-4-yl)methyl)piperidin-1-ium chloride (1.1).

Amine **1.40** (1.37 g, 3.72 mmol) was suspended in diethyl ether and anhydrous hydrogen chloride (2M in diethyl ether, 4.0 mL, 8.0 mmol) was added. The resulting precipitate was collected by vacuum filtration, suspended in ethanol, and filtered again to provide 900 mg (60%) amine hydrochloride salt X as a white solid.

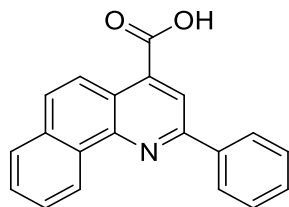
1.1. mp= 258 °C (dec.); IR (solid) 3280, 2936, 2854, 2710, 1589, 1377, 1106, 832, 698 cm⁻¹; ¹H NMR (300 MHz, DMSO-*d*₆) δ 9.65 (d, *J* = 12.8 Hz, 1H), 9.43-9.37 (m, 1H), 8.39 (d, *J* = 10.4 Hz, 3H), 8.32 (s, 1H), 8.24 (d, *J* = 9.6 Hz, 1H), 8.10-8.06 (m, 1H), 8.03 (d, *J* = 12.8, 1H), 7.84-7.75 (m, 2H), 7.65-7.58 (m, 2H), 7.57-7.50 (m, 1H), 6.60 (d, *J* = 4.2 Hz, 1H), 5.90 (s, 1H), 3.52-3.39 (m, 1H), 3.09-2.94 (m, 1H), 1.79-1.52 (m, 4H), 1.37-1.19 (m, 2H). ¹³C NMR (75 MHz, DMSO-*d*₆) 153.8, 147.3, 145.2, 138.7, 132.9, 131.0, 129.5, 128.9, 128.4, 127.8, 127.6, 127.1, 126.9, 124.3, 121.7, 120.9, 116.3, 67.5, 58.7, 44.0, 21.6, 21.1, 20.8; Anal. Calcd for C₂₅H₂₅ClN₂O: C, 74.15; H, 6.22; N, 6.92. Found: C, 73.11; H, 6.37; N, 6.90.



2-((2-(adamantan-1-yl)-6,8-dichloroquinolin-4-yl)(hydroxy)methyl)piperidin-1-ium chloride (1.2).

Amine **1.52** (678 mg, 1.52 mmol) was suspended in diethyl ether and anhydrous hydrogen chloride (2M in diethyl ether, 1.6 mL, 3.2 mmol) was added. The resulting precipitate was collected by vacuum filtration, re-suspended in a minimal amount of diethyl ether with a minimal amount of ethanol added and filtered again to provide 440 mg (60%) amine hydrochloride salt **1.2** as a white solid.

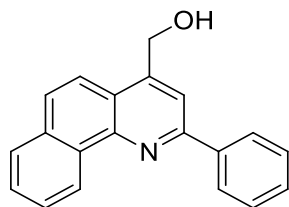
1.2. mp = 202°C (dec.); IR (film) 3271, 2904, 2847, 1595, 1451, 1130 cm⁻¹; ¹H NMR (300 MHz, DMSO-*d*₆) δ 10.15 (d, *J* = 9.8 Hz, 1H), 8.52 (d, *J* = 2.1 Hz, 1H), 8.46-8.35 (m, 1H), 8.05 (d, *J* = 2.1 Hz, 1H), 7.85 (s, 1H), 6.57 (d, *J* = 4.5 Hz, 1H), 5.85 (s, 1H), 3.31-3.20 (m, 2H), 2.94 (q, *J* = 11.5 Hz, 1H), 2.12 (br s, 3H), 2.06 (br s, 6H), 1.78 (br s, 6H), 1.72-1.53 (m, 4H), 1.33-1.12 (m, 2H). ¹³C NMR (100 MHz, DMSO-*d*₆) δ 168.8, 149.1, 141.6, 134.5, 129.3, 128.9, 126.1, 122.4, 117.7, 72.3, 61.1, 46.4, 41.2, 41.1, 36.2, 28.1, 26.2, 25.8, 23.9. Anal. Calcd for C₂₅H₃₁Cl₃N₂O: C, 62.31; H, 6.48; N, 5.81. Found: C, 60.40; H, 6.39; N, 5.83.



2-phenylbenzo[*h*]quinoline-4-carboxylic acid (1.13).

1-Naphthylamine (25.0 g, 175 mmol) was dissolved in 100 mL of ethanol. Benzaldehyde (17.8 mL, 18.6 g, 175 mmol) and pyruvic acid (12.2 mL, 15.4 g, 175 mmol) were added sequentially to the 1-naphthylamine solution at room temperature. The reaction was refluxed open to air for 3 h. After cooling to rt, the mixture was vacuum filtered. The resulting solid was thoroughly washed with ethanol and dried under vacuum to yield 14.0 g (27%) of **1.13** as a yellow solid.

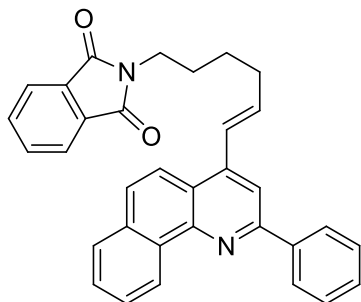
1.13. mp = 294-297 °C; TLC R_f = 0.11 (20% ethyl acetate / 80% hexanes); IR (solid) 3061, 1704, 2623, 1256, 868, 742, 687 cm^{-1} . ^1H NMR (300 MHz, $\text{DMSO-}d_6$) δ 9.42-9.39 (m, 1H), 8.58 (s, 1H), 8.54 (d, J = 9.3 Hz, 1H), 8.48-8.44 (m, 2H), 8.11-8.04 (m, 2H), 7.87-7.79 (m, 2H), 7.66-7.53 (m, 3H); ^{13}C NMR (75 MHz, $\text{DMSO-}d_6$) δ 167.9, 154.4, 146.3, 138.1, 138.0, 133.1, 130.8, 129.9, 129.1, 128.9, 128.7, 128.0, 127.5, 127.2, 124.5, 122.3, 121.9, 118.9. Anal. Calcd for $\text{C}_{20}\text{H}_{13}\text{NO}_2$: C, 80.25; H, 4.38; N, 4.68; O, 10.69. Found: C, 80.04; H, 4.39; N, 4.96.



(2-phenylbenzo[h]quinolin-4-yl)methanol (1.15).

Carboxylic acid **1.13** (5.00 g, 16.7 mmol) was suspended in 17 mL anhydrous THF under argon. After cooling the mixture to 0 °C, borane-tetrahydrofuran complex (1M in THF, 34.0 mL, 34.0 mmol) was slowly added to the well-stirred mixture. After hydrogen gas evolution ceased, the reaction was stirred at rt for 6 h. The mixture was cooled to 0 °C and aqueous NaOH (3 M, 17 mL) was slowly added. The mixture was stirred at rt for 12 h, concentrated under vacuum, and extracted with ethyl acetate. The combined organic extracts were dried with MgSO₄, filtered, and evaporated to an oil which was titrated with methanol. The remaining solvent was removed under vacuum to yield X g (80%) of **1.15** as a white solid.

1.15. mp = 140-144 °C; TLC R_f = 0.32 (20% ethyl acetate / 80% hexanes); IR (solid) 3343, 3061, 2899, 1591, 1377, 1020, 756, 693 cm⁻¹. ¹H NMR (300 MHz, DMSO-*d*₆) δ 9.41-9.38 (m, 1H), 8.44-8.40 (m, 2H), 8.32 (s, 1H), 8.03-8.07 (m, 1H), 8.00-7.94 (m, 2H), 7.83-7.74 (m, 2H), 7.65-7.59 (m, 2H), 7.56-7.50 (m, 1H), 5.72 (t, J = 5.5 Hz, 1H), 5.16 (d, J = 5.5 Hz, 2H); ¹³C NMR (75 MHz, DMSO-*d*₆) δ 154.4, 149.0, 145.0, 139.1, 133.2, 131.3, 129.5, 129.0, 128.3, 128.0, 127.13, 127.09, 127.05, 124.4, 122.5, 121.1, 116.0. Anal. Calcd. for C₂₀H₁₅NO: C, 84.19; H, 5.30; N, 4.91. Found: C, 84.06; H, 4.97; N, 5.09.

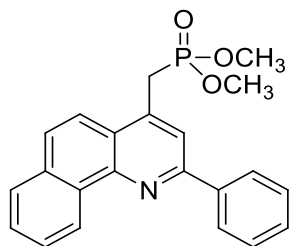


(E)-2-(6-(2-phenylbenzo[h]quinolin-4-yl)hex-5-en-1-yl)isoindoline-1,3-dione (1.21).

Phosphonate **1.34** (377 mg, 1.00 mmol) and lithium chloride (63 mg, 1.50 mmol) were combined in a flask under argon and 5 mL of anhydrous THF was added followed by DBU (228 mg, 224 μL , 1.50 mmol). Aldehyde **1.35** (347 mg, 1.50 mmol) was dissolved in 5 mL anhydrous THF under argon. The aldehyde solution was transferred to the stirred phosphonate solution dropwise at rt. After stirring for 24 hours, the reaction was diluted with water and extracted with ethyl acetate. The combined organic extracts were dried with MgSO_4 , filtered, and concentrated under vacuum. Purification by silica gel chromatography (20% ethyl acetate / 80% hexanes) provided 330 mg (68%) of olefin **1.21** as a yellow solid.

1.21. mp = 135-144 $^{\circ}\text{C}$; TLC R_f = 0.67 (30% ethyl acetate / 70% hexanes); IR (solid) 3059, 2934, 2872, 1705, 1581, 1398, 1368, 1036, 721 cm^{-1} ; ^1H NMR (300 MHz, CDCl_3) δ 9.52-9.50 (m, 1H), 8.37-8.35 (m, 2H), 8.02 (s, 1H), 8.00 (d, J = 9.2 Hz, 1H), 7.9 (d, J = 7.8 Hz, 1H), 7.86-7.82 (m, 2H), 7.80 (d, J = 9.1 Hz, 1H), 7.76-7.67 (m, 4H), 7.59-7.54 (m, 2H), 7.50-7.46 (m, 1H), 7.19 (d, J = 15.7 Hz, 1H), 6.53 (dt, J = 15.7, 6.9 Hz, 1H), 3.79 (t, J = 7.3 Hz, 2H), 2.47 (q, J = 7.1 Hz, 2H), 1.85 (p, J = 7.5 Hz, 2H), 1.67 (p, J = 7.6 Hz, 2H).

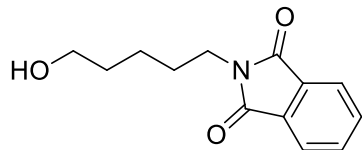
^{13}C NMR (75 MHz, CDCl_3) δ 168.6, 155.1, 146.6, 144.0, 140.1, 137.1, 134.0, 133.7, 132.21, 132.19, 129.2, 128.9, 128.1, 127.7, 127.6, 127.1, 126.9, 126.1, 125.3, 123.3, 122.9, 121.2, 115.6, 37.9, 33.1, 28.3, 26.4. Anal Calcd for $\text{C}_{33}\text{H}_{26}\text{N}_2\text{O}_2$: C, 82.13; H, 5.43; N, 5.81; O, 6.63. Found: C, 82.44; H, 5.13; N, 5.84.



Dimethyl ((2-phenylbenzo[*h*]quinolin-4-yl)methyl)phosphonate (1.34).

Chloride **1.36** (1.97 g, 6.50 mmol) and trimethyl phosphite (13.7 g, 13.0 mL, 110 mmol) were combined in a flask with 6.5 mL toluene. The mixture was refluxed for 3 d. After cooling to room temperature, the mixture was concentrated under vacuum to a brown oil which was triturated with diethyl ether. The resulting precipitate was vacuum filtered and washed with cold diethyl ether to yield 2.12 g (87%) of phosphonate **1.34** as a white solid.

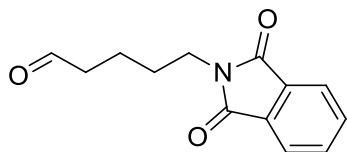
1.34. mp = 136-137 °C; TLC R_f = 0.43 (20% acetone / 80% dichloromethane); IR (solid) 3061, 2953, 2851, 1587, 1252, 1053, 804 cm^{-1} ; ^1H NMR (300 MHz, CDCl_3) δ 9.54-9.51 (m, 1H), 8.37-8.34 (m, 2H), 8.02-7.84 (m, 4H), 7.79-7.68 (m, 2H), 7.60-7.54 (m, 2H), 7.52-7.46 (m, 1H), 3.75 (d, J = 22.5 Hz, 2H), 3.66 (d, J = 10.8 Hz, 6H); ^{13}C NMR (75 MHz, CDCl_3) δ 155.03, 154.99, 146.9, 146.8, 139.6, 138.5, 138.4, 133.7, 132.3, 129.5, 129.0, 128.5, 127.8, 127.6, 127.2, 125.4, 124.3, 124.2, 121.23, 121.21. Anal Calcd for $\text{C}_{22}\text{H}_{20}\text{NO}_3\text{P}$: C, 70.02; H, 5.34; N, 3.71. Found C, 69.69; H, 5.42; N, 3.88.



2-(5-hydroxypentyl)isoindoline-1,3-dione (1.35a).

5-Amino-1-pentanol (18.7 g, 181 mmol) and phthalic anhydride (26.8 g, 181 mmol) were heated in 181 mL toluene under Dean-Stark conditions for 24 hours. The mixture was cooled to room temperature, transferred to a separatory funnel using ethyl acetate, washed once with brine, dried with sodium sulfate, and concentrated under vacuum to provide 39.2 g (93%) alcohol **1.35a** as a white solid.

1.35a. mp = 43-48 °C; TLC R_f = 0.29 (60% ethyl acetate / 40% hexanes); ^1H NMR (300 MHz, CDCl_3) δ 7.87-7.80 (m, 2H), 7.74-7.67 (m, 2H), 3.70 (t, J = 7.1 Hz, 2H), 3.64 (t, J = 6.3 Hz, 2H), 1.77-1.56 (m, 4H), 1.48-1.36 (m, 2H).

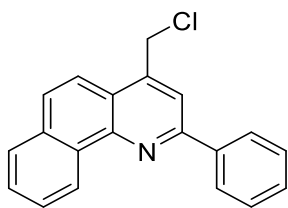


5-(1,3-dioxoisoindolin-2-yl)pentanal (1.35).

Alcohol **1.35a** (932 mg, 4.00 mmol) was dissolved in 13 mL anhydrous dichloromethane at 0°C under argon and trichloroisocyanuric acid (974 mg, 4.20 mmol) and TEMPO (6 mg, 0.04 mmol) were added. The mixture was stirred at room temperature for 20 minutes, filtered through celite,

washed with saturated sodium bicarbonate, 1M HCl, and brine, dried with sodium sulfate, and concentrated under vacuum to provide 850 mg (92%) aldehyde **1.35** as a yellow oil.

1.35. TLC $R_f = 0.70$ (100% diethyl ether); ^1H NMR (300 MHz, CDCl_3) δ 9.76 (t, $J = 1.6$ Hz, 1H), 7.88-7.81 (m, 2H), 7.75-7.68 (m, 2H), 3.71 (t, $J = 6.8$ Hz, 2H), 2.51 (td, $J = 7.4, 1.5$ Hz, 2H), 1.80-1.61 (m, 4H).

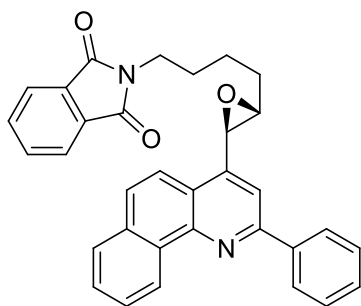


4-(chloromethyl)-2-phenylbenzo[h]quinoline (1.36).

Alcohol **1.15** (13.5 g, 47.4 mmol) was dissolved in 95 mL anhydrous dichloromethane. Neat thionyl chloride (4.82 mL, 7.90 g, 66.4 mmol) was slowly added to the solution at rt. The reaction was stirred at rt for 18 h and then carefully quenched with saturated aqueous NaHCO_3 . The reaction was diluted with an equal volume of water and vigorously stirred until all solids dissolved. The organic layer was isolated, washed with brine, dried with Na_2SO_4 , filtered, and evaporated under vacuum to yield 10.4 g (72%) chloride **1.36** as a tan solid.

1.36. mp = 145-153 °C; TLC $R_f = 0.80$ (20% ethyl acetate / 80% hexanes); IR (solid) 3062, 2942, 1588, 1053, 752, 689 cm^{-1} ; ^1H NMR (400 MHz, CDCl_3) δ 9.53-9.50 (m, 1H), 8.36-8.34 (m, 2H), 8.06 (s, 1H), 7.99 (d, $J = 8.7$ Hz, 1H), 7.95-7.88 (m, 2H), 7.79-7.70 (m, 2H), 7.60-7.55 (m, 2H), 7.52-7.48 (m, 1H), 5.10 (s, 2H); ^{13}C NMR (100 MHz, CDCl_3) δ 155.4, 146.8, 142.5,

139.4, 133.7, 132.2, 129.6, 129.0, 128.6, 128.3, 127.9, 127.6, 127.3, 125.3, 123.0, 120.4, 119.1, 43.1. Anal. Calcd. for C₂₀H₁₄ClN: C, 79.07; H, 4.65; Cl, 11.67; N, 4.61. Found: C, 78.96; H, 4.50; N 4.83.

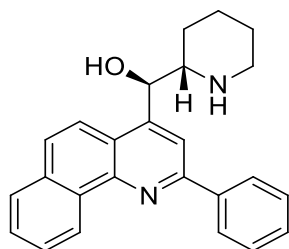


2-(4-(3-(2-phenylbenzo[*h*]quinolin-4-yl)oxiran-2-yl)butyl)isoindoline-1,3-dione (1.39).

Olefin **1.21** (4.76 g, 9.86 mmol) was dissolved in 62 mL CHCl₃. To this was added 3-chloroperbenzoic acid (approx. 70%, 5.11 g, approx. 29.6 mmol). The mixture was refluxed for 18 h. When complete, excess peracid was consumed by vigorously stirring the reaction with 10% aq. Na₂SO₃. The mixture was poured into sat. aq. NaHCO₃ and extracted with dichloromethane. The combined organics were washed once with brine, dried with Na₂SO₄, and concentrated under vacuum. The crude solid was triturated with methanol to provide 3.00 g of epoxide **1.39** (61%) as a tan solid.

1.39. mp = 55-69°C; TLC *R_f* = 0.61 (30% ethyl acetate / 70% hexanes); IR (solid) 3059, 2933, 2858, 1710, 1590, 1466, 720 cm⁻¹; ¹H NMR (400 MHz, CDCl₃) δ 9.51 (dd, *J* = 7.9, 0.8 Hz, 1H), 8.37-8.34 (m, 2H), 7.95 (s, 1H), 7.93-7.89 (m, 2H), 7.88-7.83 (m, 2H), 7.80 (d, *J* = 9.0 Hz, 1H), 7.78-7.69 (m, 4H), 7.58-7.52 (m, 2H), 7.50-7.45 (m, 1H), 4.36 (d, *J* = 1.9 Hz, 1H), 3.78 (t, *J* = 7.2 Hz, 2H), 3.04-3.01 (m, 1H), 2.07-1.98 (m, 1H), 1.95-1.80 (m, 3H), 1.75-1.62 (m, 2H). ¹³C

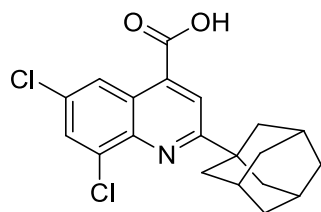
NMR (100 MHz, CDCl₃) δ 168.6, 155.6, 146.0, 143.9, 139.7, 134.1, 133.6, 132.2, 132.2, 129.5, 128.9, 128.3, 127.8, 127.6, 127.2, 125.3, 123.3, 123.1, 120.0, 114.1, 62.8, 55.9, 37.7, 32.0, 28.6, 23.4. Anal Calcd for C₃₃H₂₆N₂O₃: C, 79.50; H, 5.26; N, 5.62; O, 9.63. Found: C, 79.50; H, 5.26; N, 5.62.



(2-phenylbenzo[*h*]quinolin-4-yl)(piperidin-2-yl)methanol (1.40).

Epoxide **1.39** (3.00 g, 6.00 mmol) was dissolved in 30 mL ethanol and 30 mL THF. Hydrazine hydrate (600 μ L, 12.4 mmol) was added and the mixture was refluxed for 2 hours. Purification by silica gel chromatography (90% dichloromethane / 9% methanol / 1% NH₄OH) provided crude product as a brown solid. This was suspended in a minimal amount of methanol and filtered to provide 1.37 g amine **1.40** (62%) as a tan solid.

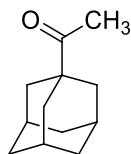
1.40. mp = 175 °C; TLC R_f = 0.20 (90% dichloromethane / 9% methanol / 1% NH₄OH); IR (solid) 3286, 3060, 2932, 2851, 2744, 1590, 1443, 1382, 1107, 1048, 885, 700 cm⁻¹. ¹H NMR (300 MHz, DMSO-*d*₆) δ 9.41-9.36 (m, 1H), 8.38 (d, J = 7.5 Hz, 2H), 8.28 (s, 1H), 8.15 (d, J = 9.3 Hz, 1H), 8.05-8.00 (m, 1H), 7.93 (d, J = 9.3 Hz, 1H), 7.81-7.72 (m, 2H), 7.64-7.56 (m, 2H), 7.55-7.48 (m, 1H), 5.71 (br s, 1H), 5.32 (br s, 1H), 2.95-2.83 (m, 2H), 2.48-2.38 (m, 1H), 1.73-1.64 (m, 1H), 1.58-1.49 (m, 1H), 1.46-1.38 (m, 1H), 1.32-1.10 (m, 3H). ¹³C NMR (100 MHz, DMSO-*d*₆) δ 153.8, 150.3, 145.3, 139.0, 133.0, 131.3, 129.4, 129.0, 128.3, 127.8, 127.0, 126.9, 124.5, 122.8, 121.6, 116.9, 72.2, 61.4, 46.5, 26.7, 26.0, 24.1. Anal Calcd for C₂₅H₂₄N₂O: C, 81.49; H, 6.57; N, 7.60; O, 4.34. Found: C, 81.16; H, 6.24; N, 7.83.



2-(adamantan-1-yl)-6,8-dichloroquinoline-4-carboxylic acid (1.42).

Dichloroisatin **1.45** (33.8 g, 157 mmol, 2.0 equiv), ketone **1.44** (14.0 g, 78.7 mmol, 1.0 equiv), and potassium hydroxide (28.6 g, 501 mmol, 6.4 mmol) were combined with 78 mL ethanol and 26 mL H₂O and heated to reflux for 48 hours. The mixture was concentrated under vacuum to a brown paste and taken up in H₂O and diethyl ether. The organic layer was discarded and the aqueous layer was washed once more with diethyl ether. The aqueous layer was acidified (pH 4 to 5) by the dropwise addition of concentrated HCl. The resulting precipitate was isolated by vacuum filtration and recrystallized from ethanol to provide 12.7 g (43%) of carboxylic acid **1.42** as a tan solid.

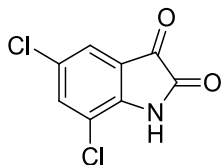
1.42. mp = 152-157°C; TLC R_f = 0.15 (30% ethyl acetate / 70% hexanes); IR (solid) 3462, 2902, 2848, 2651, 1703, 1591, 1268, 1193 cm⁻¹; ¹H NMR (300 MHz, DMSO-*d*₆) δ 8.71 (s, 1H), 8.16-8.12 (m, 2H), 2.11 (br s, 3H), 2.68 (br s, 6H), 1.79 (br s, 6H). ¹³C NMR (100 MHz, DMSO-*d*₆) 169.4, 166.9, 142.2, 136.1, 134.5, 131.1, 129.7, 124.6, 123.6, 120.8, 40.9, 36.0, 28.0. Anal Calcd for C₂₀H₁₉Cl₂NO₂: C, 63.84; H, 5.09; N, 3.72. Found: C, 64.18; H, 5.03; N, 3.87.



1-(adamantan-1-yl)ethanone (1.44).

1-Adamantanecarboxylic acid (7.20 g, 40.0 mmol) was dissolved in 40 mL diethyl ether under argon. The mixture was maintained at approximately -5°C with a salt-ice bath while methyl lithium (1.6M in diethyl ether, 52.5 mL, 84.0 mmol) was added dropwise with vigorous stirring. After complete addition, the cooling bath was removed and the slurry was allowed to stir for one hour at room temperature. The reaction was quenched and diluted by the addition of water and extracted with diethyl ether. The combined organic extracts were dried with MgSO_4 , filtered, concentrated under vacuum, and purified by silica gel chromatography (10% ethyl acetate / 90% hexanes) to yield 5.70 g (80%) of ketone **1.44** as a white solid.

1.44. mp = $52\text{-}54^{\circ}\text{C}$; TLC R_f = 0.43 (10% ethyl acetate / 90% hexanes); ^1H NMR (300 MHz, CDCl_3) δ 2.09 (s, 3H), 2.04 (br s, 3H), 1.82-1.64 (m, 12H).

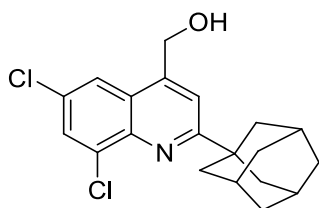


5,7-dichloroindoline-2,3-dione (1.46).

Isatin (14.7 g, 100 mmol) and trichloroisocyanuric acid (23.2 g, 100 mmol) were combined in a flask and cooled to -78°C with a dry ice-acetone bath. Concentrated sulfuric acid (75 mL) was

added dropwise to the mixture via addition funnel. The mixture was allowed to slowly warm to room temperature. After stirring for 3 days, the mixture was poured over ice and stirred until all ice had melted. The precipitate was collected by vacuum filtration and washed twice with water. The orange-red solid was then washed with acetone until only a white solid (isocyanuric acid) remained. The filtrate was concentrated under vacuum to yield 19.8 g (92%) of dichloroisatin **1.46** as an orange-red solid.

1.46. mp = 211-217 °C; TLC R_f = 0.65 (50% ethyl acetate / 50% hexanes); ^1H NMR (300 MHz, DMSO- d_6) δ 11.59 (br s, 1H), 7.85 (d, J = 2.0 Hz, 1H), 7.57 (d, J = 2.0 Hz, 1H).

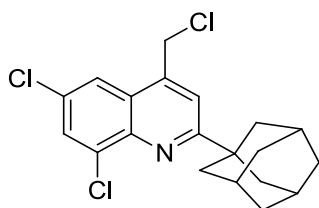


2-(adamantan-1-yl)-6,8-dichloroquinolin-4-ylmethanol (1.47).

Carboxylic acid **1.42** (3.48 g, 9.26 mmol) was dissolved in 10 mL anhydrous THF under argon. After cooling the mixture to 0°C, borane-tetrahydrofuran complex (1 M in THF, 18.5 mL, 18.5 mmol) was slowly added to the mixture. After hydrogen gas evolution ceased, the cooling bath was removed and the mixture was allowed to stir at room temperature overnight. The mixture was again cooled to 0°C and quenched with 20 mL 3M NaOH. The cooling bath was removed and after stirring at room temperature for 6 hours, the mixture was extracted with diethyl ether. The combined organic extracts were dried with MgSO_4 , filtered, concentrated under vacuum,

and purified by silica gel chromatography (30% ethyl acetate / 70% hexanes) to yield 2.00 g (60%) of alcohol **1.47** as a beige solid.

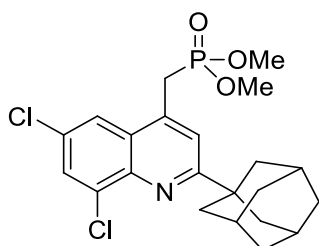
1.47. mp = 190-198°C; TLC R_f = 0.56 (30% ethyl acetate / 70% hexanes); IR (solid) 3278, 2899, 2845, 1596, 1448, 1081, 1060 cm^{-1} ; ^1H NMR (300 MHz, CDCl_3) δ 7.83 (d, J = 2.3 Hz, 1H), 7.77 (d, J = 2.2 Hz, 1H), 7.68 (s, 1H), 5.13 (dd, J = 5.7, 0.9 Hz, 2H), 2.16 (br s, 3H), 2.13 (br s, 6H), 1.91, (t, J = 5.8 Hz, 1H), 1.83 (br s, 6H); ^{13}C NMR (75 MHz, CDCl_3) δ 170.1, 145.1, 142.5, 135.9, 130.9, 129.7, 126.0, 121.1, 117.0, 62.3, 41.9, 40.6, 37.0, 28.9. Anal. Calcd. for $\text{C}_{20}\text{H}_{21}\text{Cl}_2\text{NO}$: C, 66.30; H, 5.84; N, 3.87. Found: C, 66.44; H, 5.59; N, 3.69.



2-(adamantan-1-yl)-6,8-dichloro-4-(chloromethyl)quinoline (1.47).

Alcohol **1.46** (8.36 g, 23.1 mmol) was dissolved in dichloromethane (250 mL). Thionyl chloride (2.52 mL 34.66 mmol) was then added. The mixture was stirred at room temperature for 1 h and then quenched with sat. aq. NaHCO_3 . The organic layer was separated and the aqueous layer was extracted with dichloromethane. The combined organic extracts were dried over sodium sulfate, filtered, concentrated under vacuum, and purified by silica gel chromatography (1% ether / 99% hexanes) to provide 4.40 g (50%) of chloride **1.47** as a white solid.

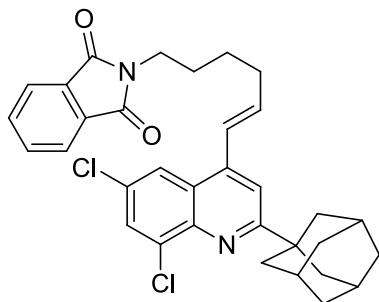
1.47. mp = 155-158°C; TLC R_f = 0.34 (100% hexanes); IR (solid) 2900, 2847, 1672, 1597, 1450, 721 cm^{-1} ; ^1H NMR (300 MHz, CDCl_3) δ 7.94 (d, J = 2.2 Hz, 1H), 7.80 (d, J = 2.4 Hz, 1H), 7.58 (s, 1H), 4.91 (s, 2H), 2.17 (br s, 3H), 2.12 (br s, 6H), 1.83 (br s, 6H); ^{13}C NMR (75 MHz, CDCl_3) δ 170.0, 142.9, 141.5, 136.2, 131.4, 130.1, 126.1, 121.3, 119.9, 42.8, 41.8, 40.6, 36.9 28.8. Anal. Calcd. for $\text{C}_{20}\text{H}_{20}\text{Cl}_3\text{N}$: C, 63.09; H, 5.29; N, 3.68. Found: C, 63.28; H, 5.63; N, 3.57.



Dimethyl ((2-(adamantan-1-yl)-6,8-dichloroquinolin-4-yl)methyl)phosphonate (1.48).

Chloride **1.47** (1.20 g, 3.15 mmol) and trimethyl phosphite (6.27 mL, 53.2 mmol) were combined in a flask with 3.5 mL toluene. The mixture was refluxed for 3 days, concentrated under vacuum, and purified by silica gel chromatography (40% ethyl acetate / 60% hexanes) to provide 1.06 g (74%) phosphonate **1.48** as a white solid.

1.48. mp = 152-153°C; TLC R_f = 0.33 (60% ethyl acetate / 40% hexanes); IR (solid) 2952, 2902, 2847, 1772, 1711, 1594, 1398, 1239, 1075, 1031, 856, 830 cm^{-1} ; ^1H NMR (300 MHz, CDCl_3) δ 7.91 (d, J = 2.1 Hz, 1H), 7.78 (d, 2.1Hz, 1H), 7.54 (d, J = 3.6 Hz, 1H), 3.66 (d, J = 11.1 Hz, 6H), 3.55 (d, J = 22.5 Hz, 2H), 2.16 (br s, 3H), 2.11 (br s, 6H), 1.82 (br s, 6H); ^{13}C NMR (75 MHz, CDCl_3) δ 169.42, 169.37, 142.9, 142.8, 137.5, 137.4, 135.9, 131.0, 129.8, 127.4, 127.3, 122.01, 121.99, 121.8, 121.7, 53.4, 53.3, 41.8, 40.4, 36.9, 31.1, 29.2, 28.84. Anal. Calcd. for $\text{C}_{22}\text{H}_{26}\text{Cl}_2\text{NO}_3\text{P}$: C, 58.16; H, 5.77; N, 3.08. Found: C, 57.97; H, 5.57; N, 2.94.

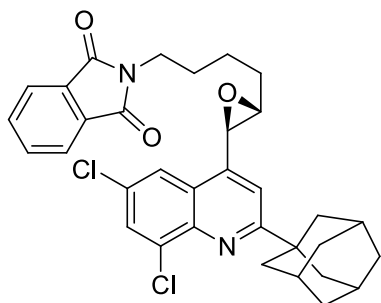


2-((*E*)-6-(2-(adamantan-1-yl)-6,8-dichloroquinolin-4-yl)hex-5-en-1-yl)isoindoline-1,3-dione (1.50).

Phosphonate **1.49** (454 mg, 1.00 mmol) and lithium chloride (63 mg, 1.50 mmol) were combined in a flask under argon and 5 mL of anhydrous THF was added followed by DBU (152 mg, 149 μ L, 1.00 mmol). Aldehyde **1.35** (347 mg, 1.50 mmol) was dissolved in 5 mL anhydrous THF under argon. The aldehyde solution was transferred to the stirred phosphonate solution dropwise at rt. After stirring for 24 hours, the reaction was diluted with H₂O and extracted with ethyl acetate. The combined organic extracts were dried with MgSO₄, filtered, and concentrated under vacuum. Purification by silica gel chromatography (10 % ethyl acetate / 90% hexanes) provided 402 mg of olefin **1.50** (68 %) as a white foam.

1.50. mp = 63-69 °C; TLC R_f = 0.29 (5% ethyl acetate / 95% hexanes); IR (film) 2903, 2848, 1771, 1712, 1396, 719 cm⁻¹; ¹H NMR (300 MHz, CDCl₃) δ 7.92 (d, J = 2,1 Hz, 1H), 7.86-7.83 (m, 2H), 7.74-7.69 (m, 3H), 7.53 (s, 1H), 6.95 (d, 15.6 Hz, 1H), 6.40 (dt, J = 6.9, 15.6 Hz, 1H), 3.77 (t, J = 6.9 Hz, 2H), 2.42 (q, J = 6.9 Hz, 2H), 2.19-2.10 (m, 9H), 1.86-1.76 (m, 8H), 1.68-1.56 (m, 2H). ¹³C NMR (75 MHz, CDCl₃) δ 169.7, 168.6, 143.1, 142.8, 137.8, 135.6, 134.1, 132.2, 130.3, 129.5, 126.4, 125.4, 123.4, 121.8, 115.8, 41.9, 40.4, 37.8, 37.0, 33.1, 28.9, 28.3,

26.4. Anal Calcd for C₃₃H₃₂Cl₂N₂O₂: C, 70.84; H, 5.76; N, 5.01. Found: C, 70.57; H, 5.90; N, 5.03.

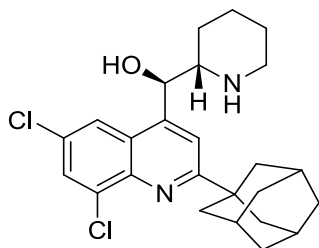


2-(4-(3-(2-(adamantan-1-yl)-6,8-dichloroquinolin-4-yl)oxiran-2-yl)butyl)isoindoline-1,3-dione (1.51).

Olefin **1.50** (3.27 g, 5.84 mmol) and *m*-chloroperbenzoic acid (approx. 70%, 3.03 g, approx. 17.5 mmol) were dissolved in 34 mL chloroform. The mixture was refluxed for 15 hours. After cooling to rt, the reaction was quenched with 10% aqueous Na₂SO₃, diluted with dichloromethane, washed with saturated sodium bicarbonate, and brine. The organic layer was dried with sodium sulfate, filtered, concentrated under vacuum and purified by silica gel chromatography (10% ethyl acetate / 90% hexanes) to provide 2.52 g (75%) epoxide **1.51** as a white foam.

1.50. TLC R_f = 0.26 (30% ethyl acetate / 70% hexanes); IR (solid) 2904, 2849, 1772, 1713, 1596, 1397, 720 cm⁻¹. ¹H NMR (300 MHz, CDCl₃) δ 7.87-7.83 (m, 3H), 7.77 (d, J = 2.1 Hz, 1H), 7.74-7.70 (m, 2H), 7.48 (s, 1H), 4.14 (d, J = 1.8 Hz, 1H), 3.76 (t, J = 7.1 Hz, 2H), 2.93-2.88 (m, 1H), 2.14 (br s, 3H), 2.10-1.96 (m, 8H), 1.88-1.76 (m, 8H), 1.70-1.58 (m, 2H); ¹³C NMR (75 MHz, CDCl₃) δ 170.3, 168.6, 142.9, 142.2, 136.1, 134.1, 132.2, 131.0, 129.7, 126.4, 123.4, 120.6,

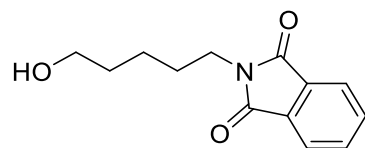
114.9, 62.9, 55.5, 41.8, 40.6, 37.7, 36.9, 35.7, 32.0, 29.9, 28.9. Anal Calcd for C₃₃H₃₂Cl₂N₂O₃: C, 68.87; H, 5.60; N, 4.87. Found: C, 68.98; H, 4.92; N, 5.84.



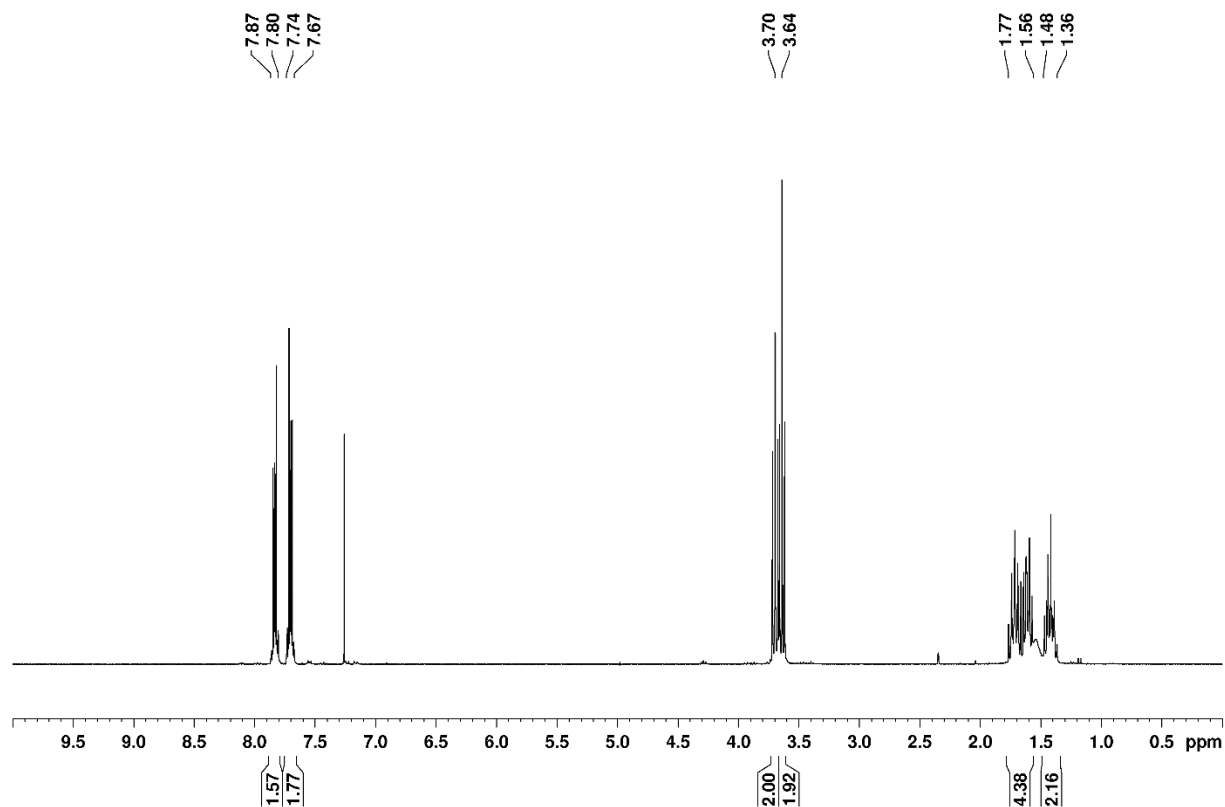
(2-(adamantan-1-yl)-6,8-dichloroquinolin-4-yl)(piperidin-2-yl)methanol (1.52).

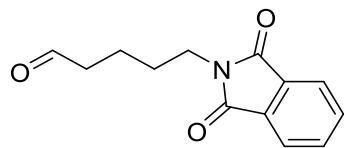
Epoxide **1.51** (2.50 g, 4.34 mmol) was dissolved in 15 mL ethanol. Hydrazine hydrate (632 μ L, 13.0 mmol) was added and the mixture was refluxed for 3 hours. The mixture was concentrated under vacuum and purified by silica gel chromatography (90% dichloromethane / 9% methanol / 1% NH₄OH) to provide 678 mg of amine **1.52** (35%) as a beige solid.

1.52. mp = 180 °C (dec.); TLC R_f = 0.29 (90% dichloromethane / 9% methanol / 1% NH₄OH); IR (solid) 3309, 3068, 2906, 2849, 2675, 1597, 1482, 1309, 1116, 869 cm⁻¹. ¹H NMR (300 MHz, DMSO-*d*₆) δ 8.25 (d, J = 2.1 Hz, 1H), 7.99 (d, J = 2.1, 1H), 7.78 (s, 1H), 5.66 (s, 1H), 5.08 (s, 1H), 2.88 (d, J = 14.4 Hz, 1H), 2.71-2.63 (m, 1H), 2.44-2.30 (m, 1H), 2.11 (br s, 3H), 2.05 (br s, 6H), 1.78 (br s, 6H), 1.73-1.64 (m, 1H), 1.48-1.38 (m, 2H), 1.28-1.11 (m, 3H). ¹³C NMR (100 MHz, DMSO-*d*₆) δ 168.8, 146.4, 141.6, 134.6, 130.4, 129.4, 125.2, 121.9, 117.5, 67.6, 58.4, 44.1, 41.1, 39.8, 36.2, 28.0, 21.7, 21.0, 20.7. Anal Calcd for C₂₅H₃₀Cl₂N₂O: C, 67.41; H, 6.79; N, 6.29. Found: C, 67.55; H, 6.96; N, 6.26.

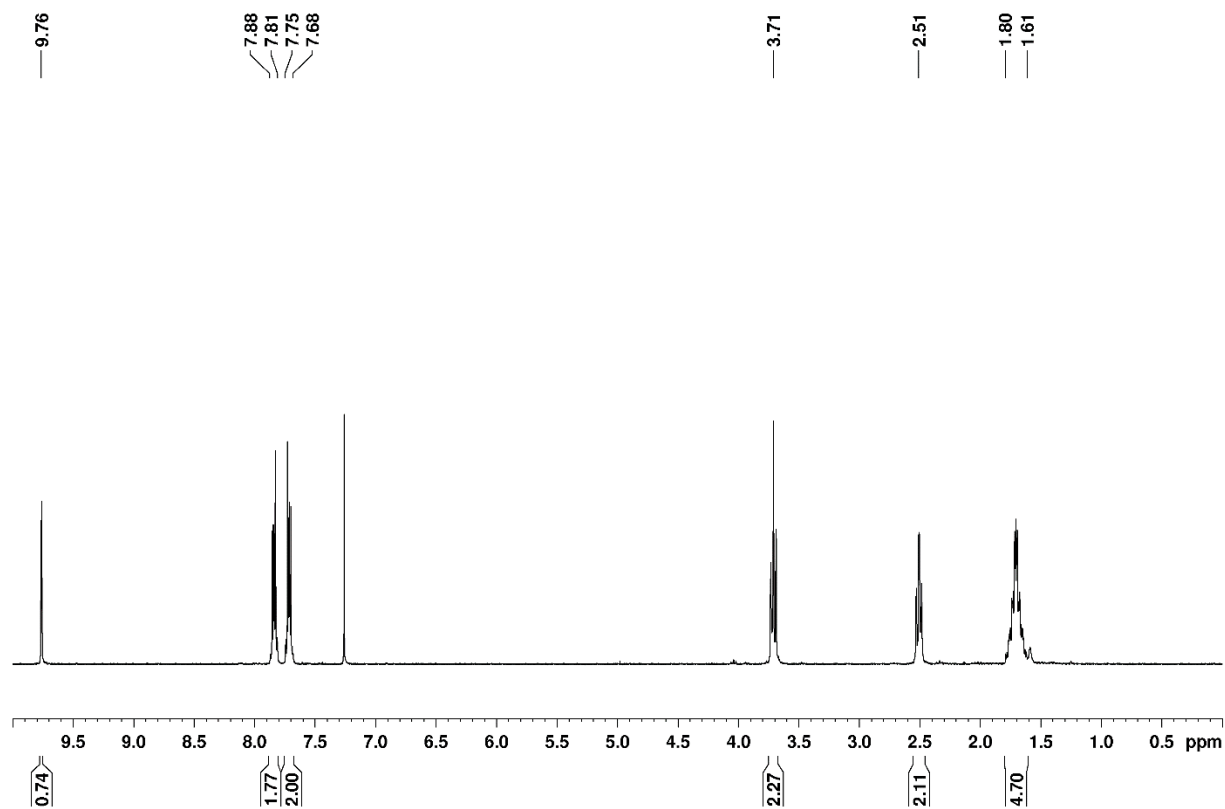


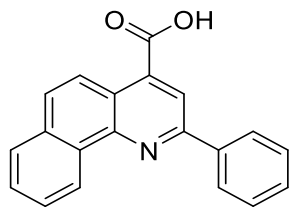
1.35a



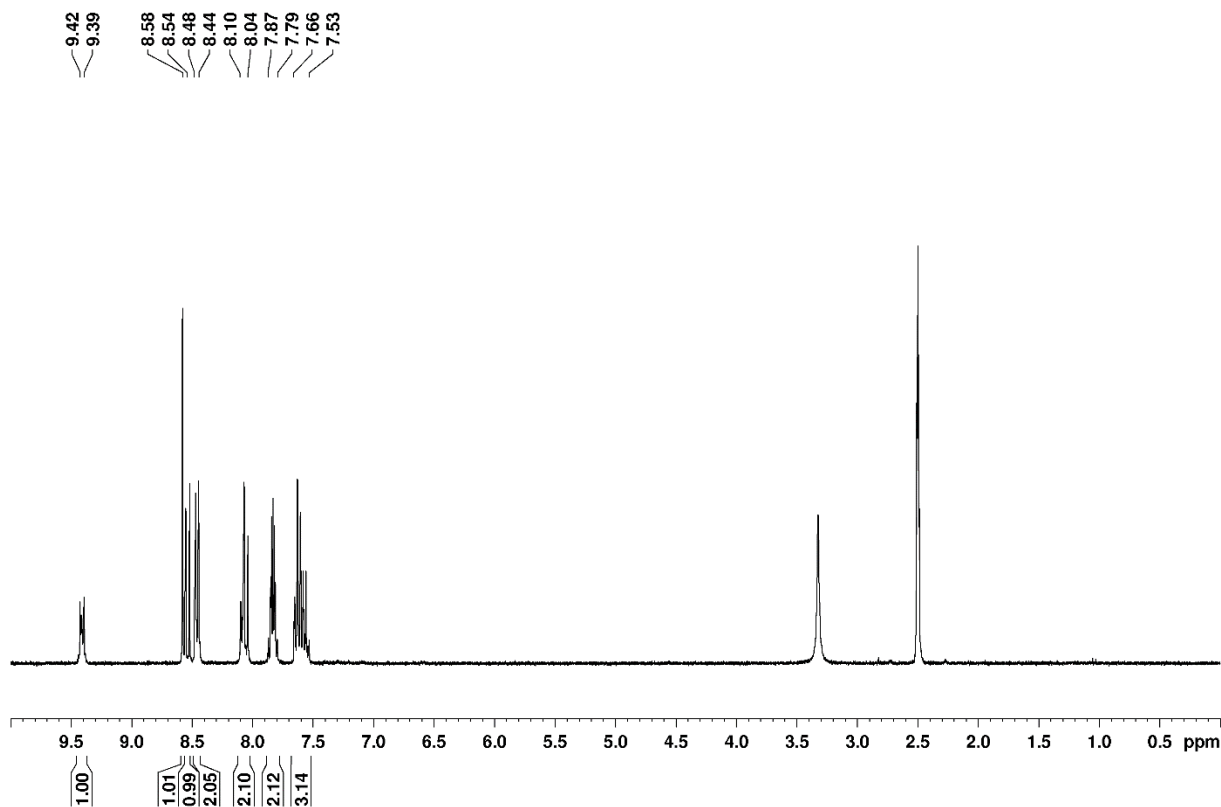


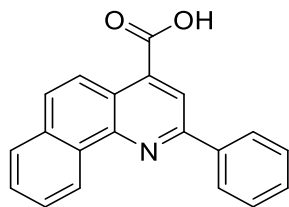
1.35



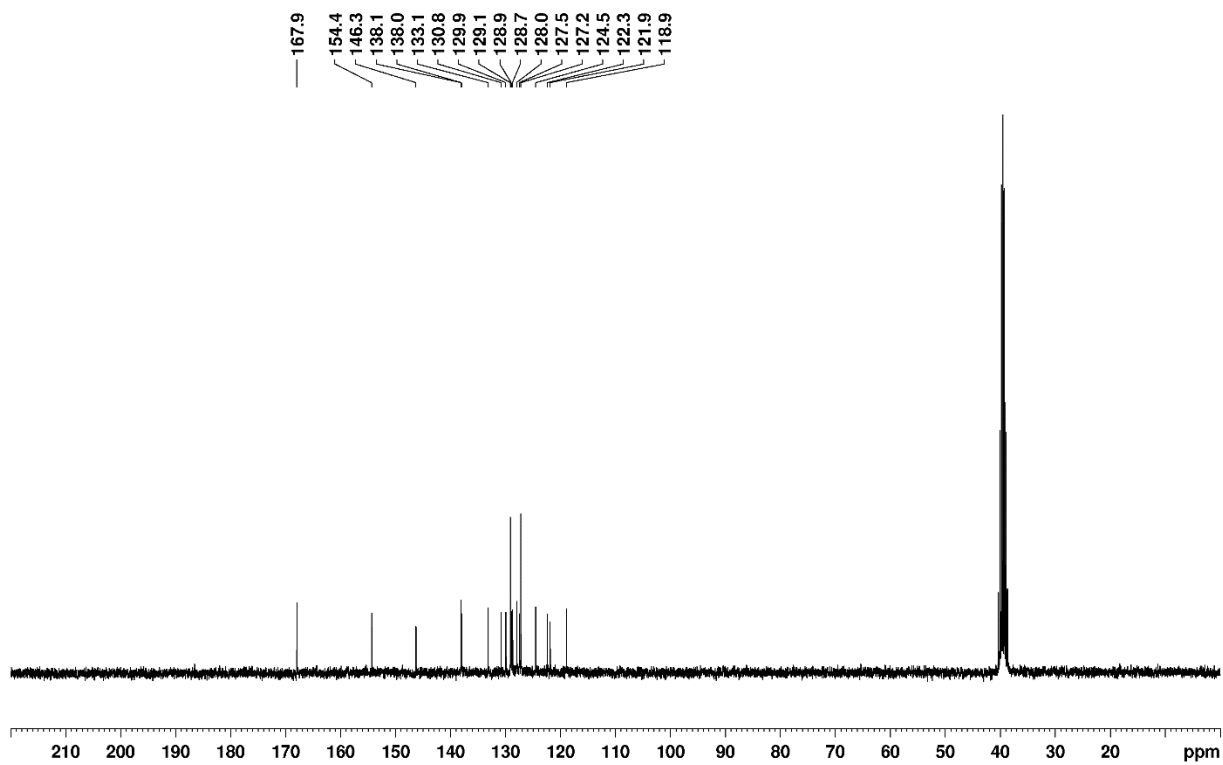


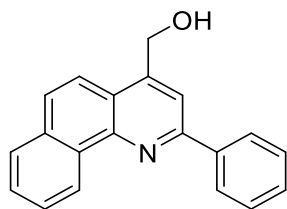
1.13



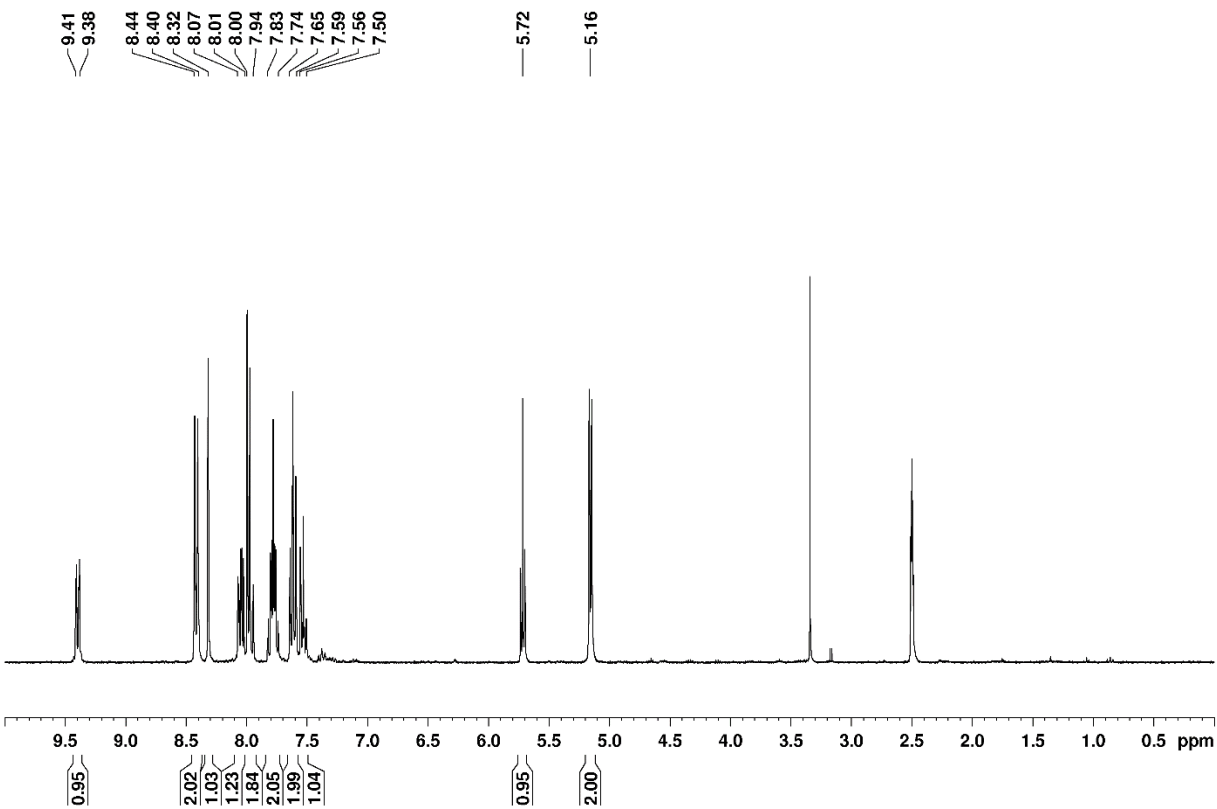


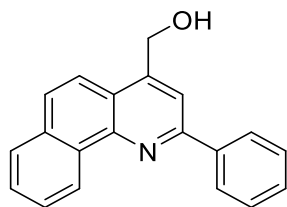
1.13



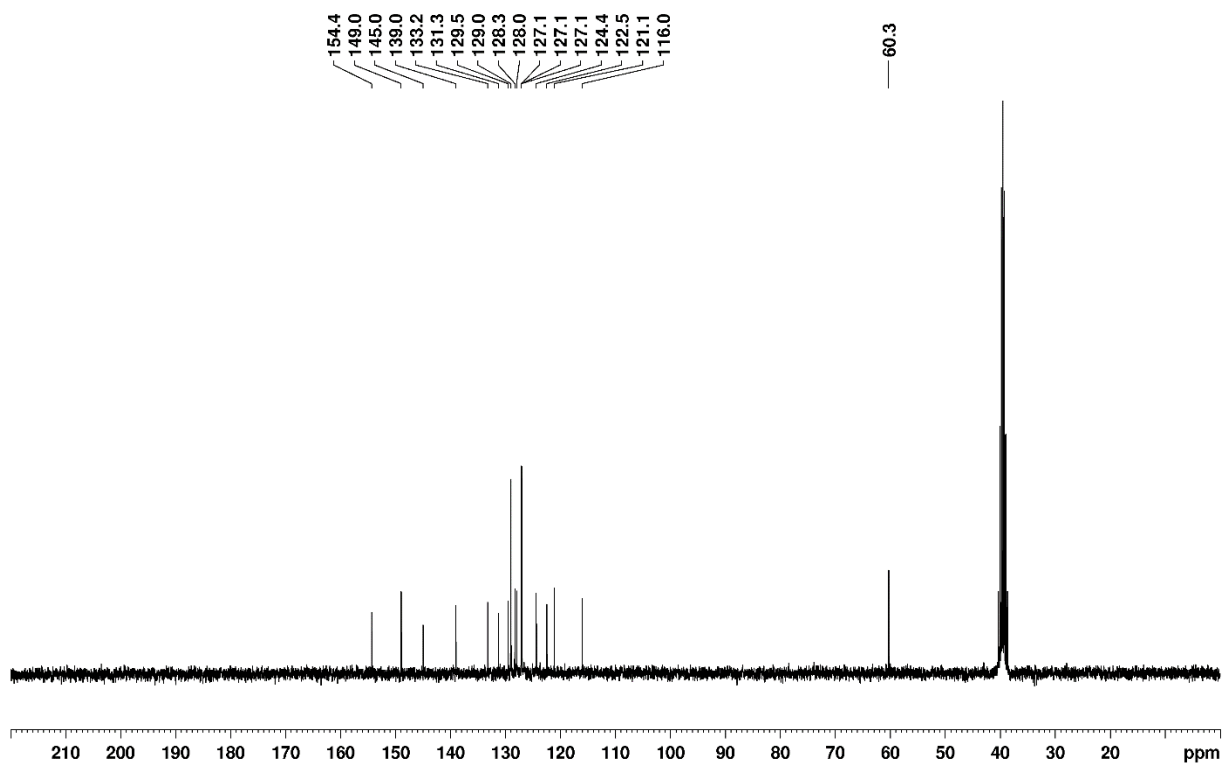


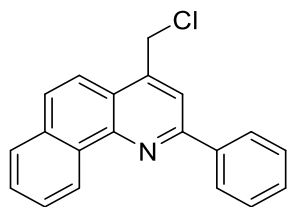
1.15



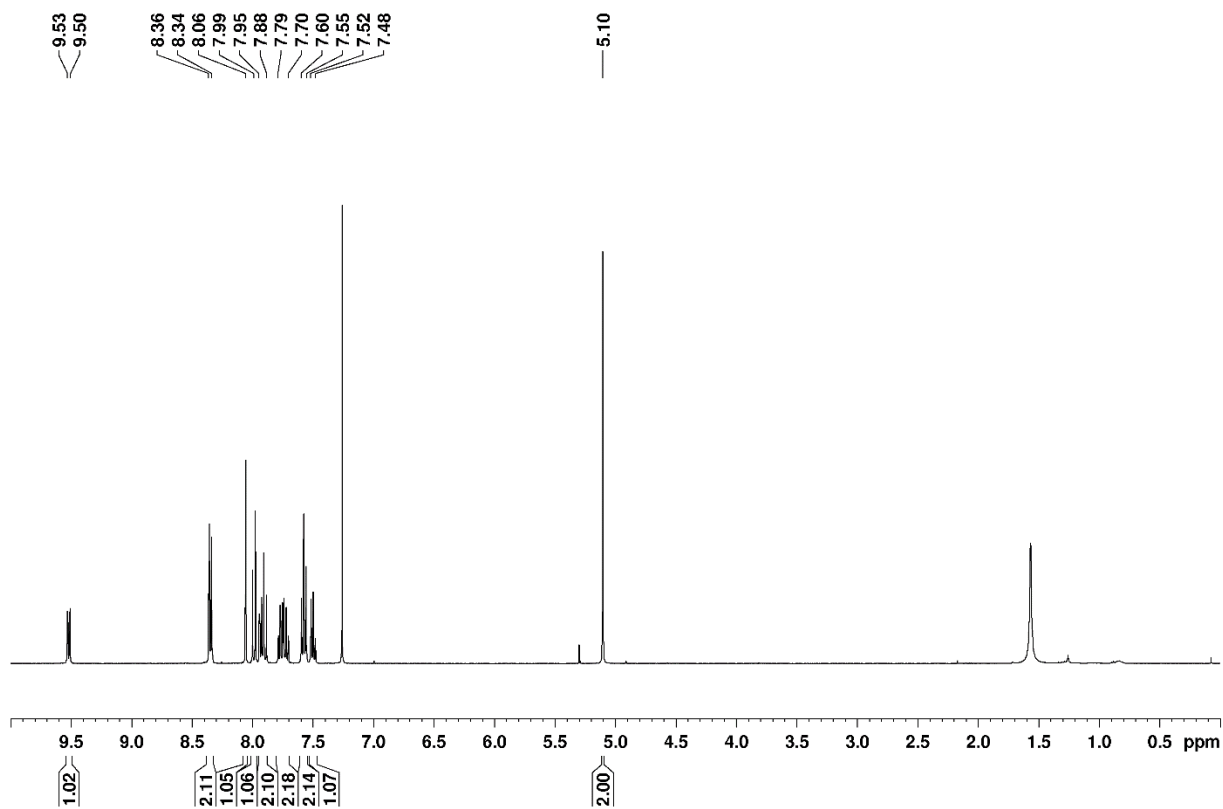


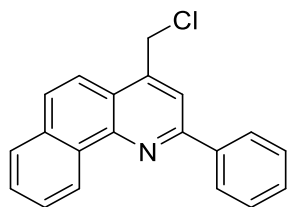
1.15



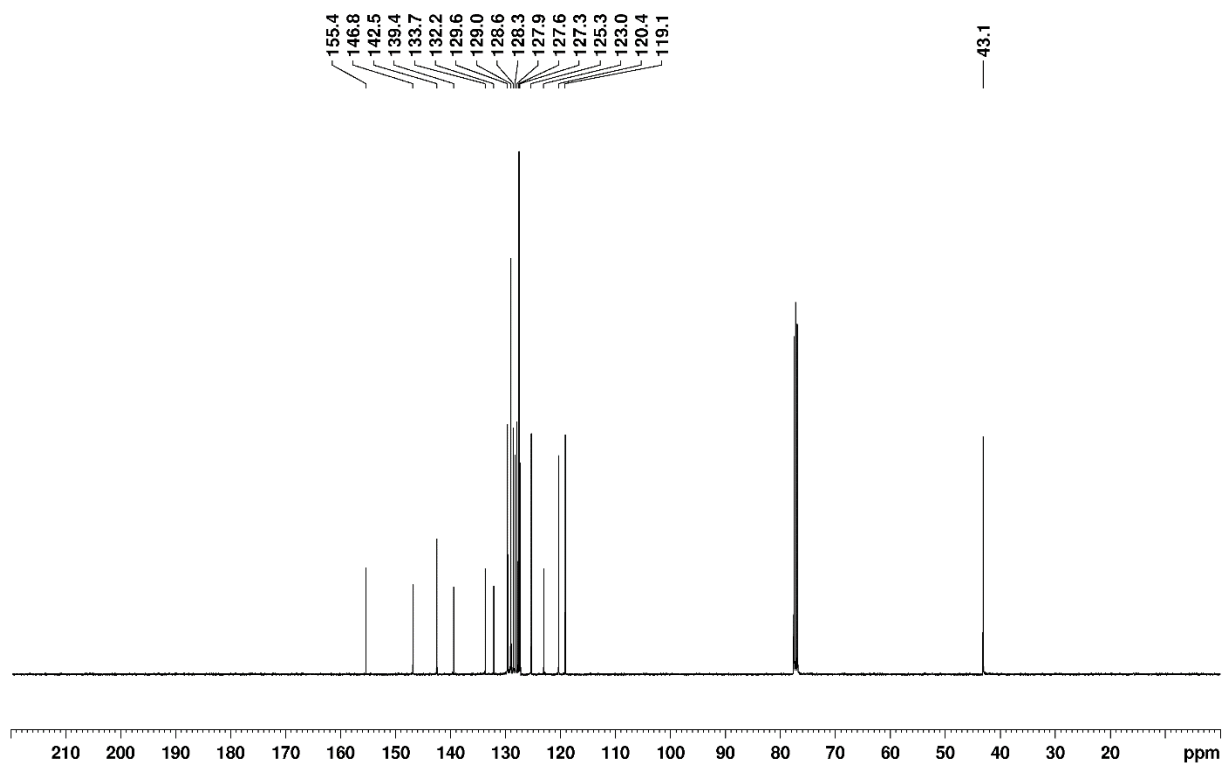


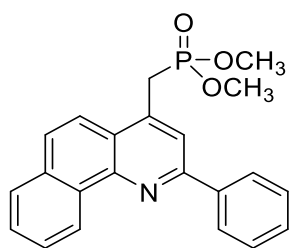
1.36



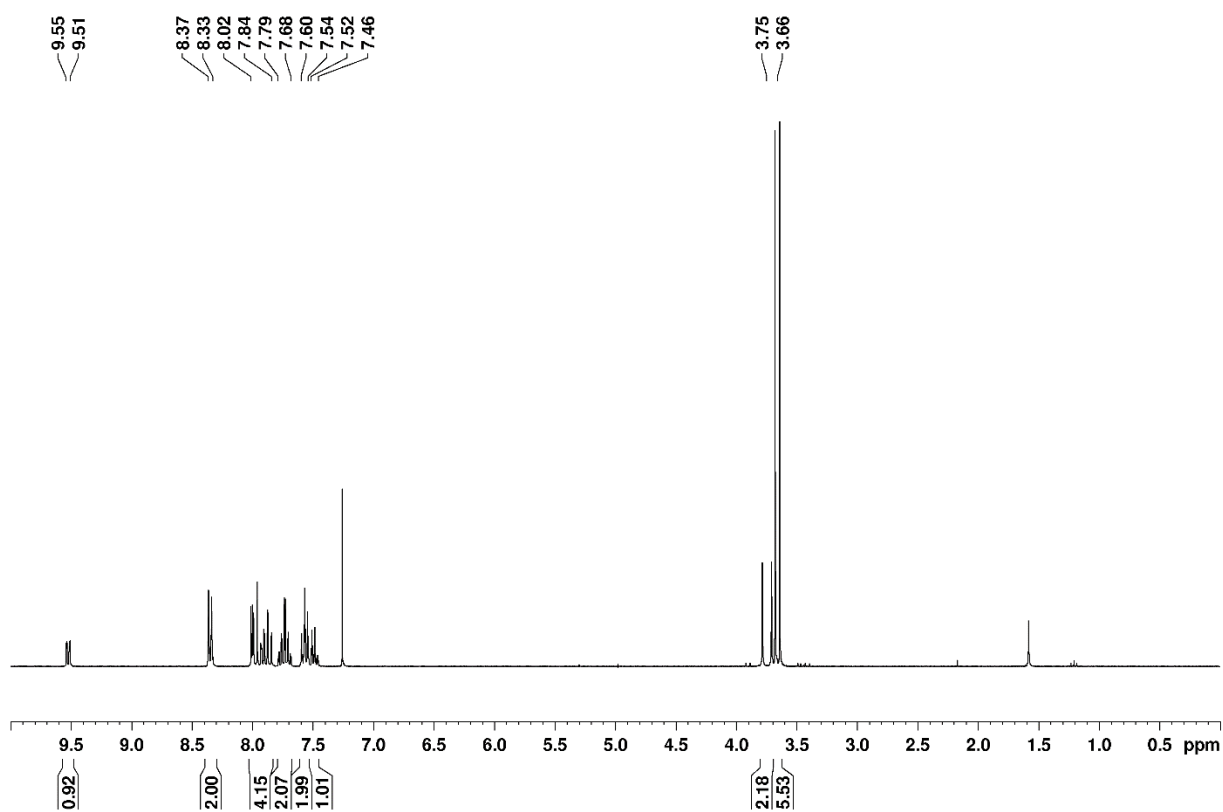


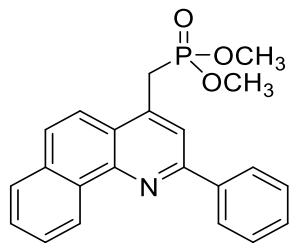
1.36



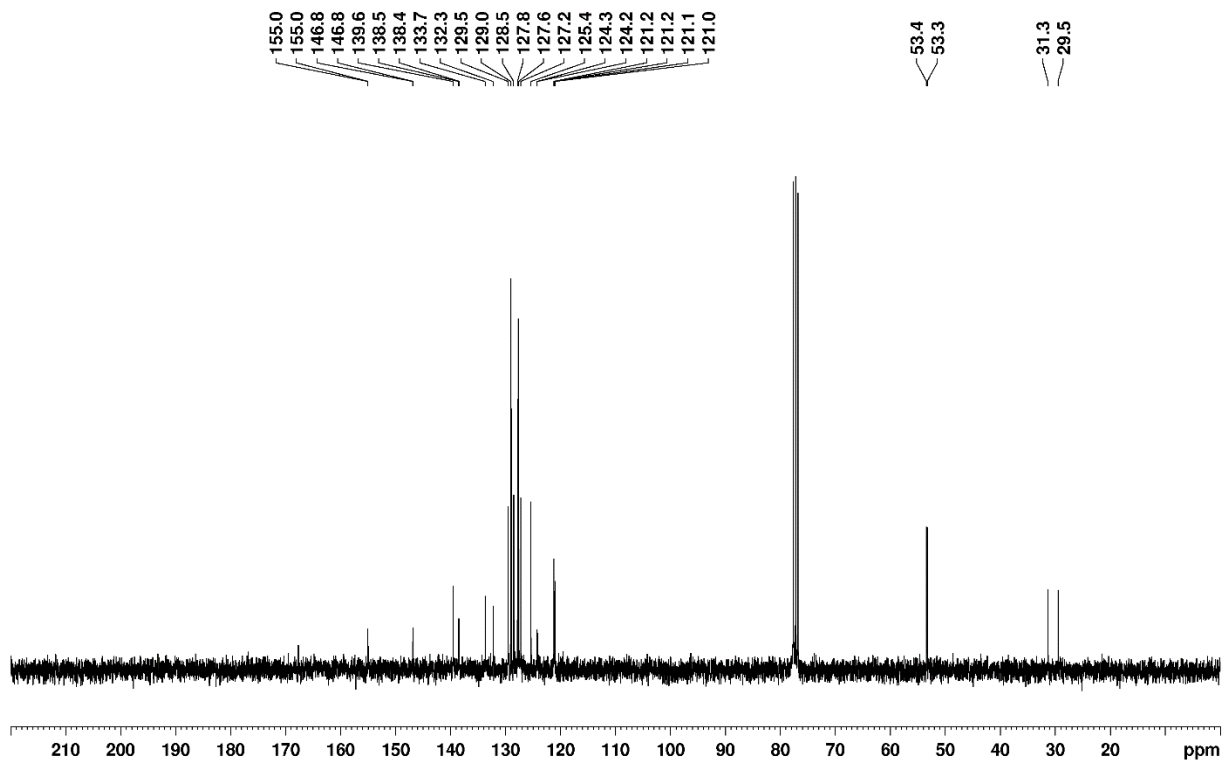


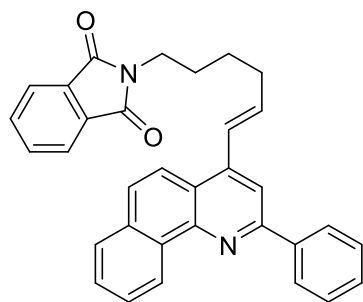
1.34



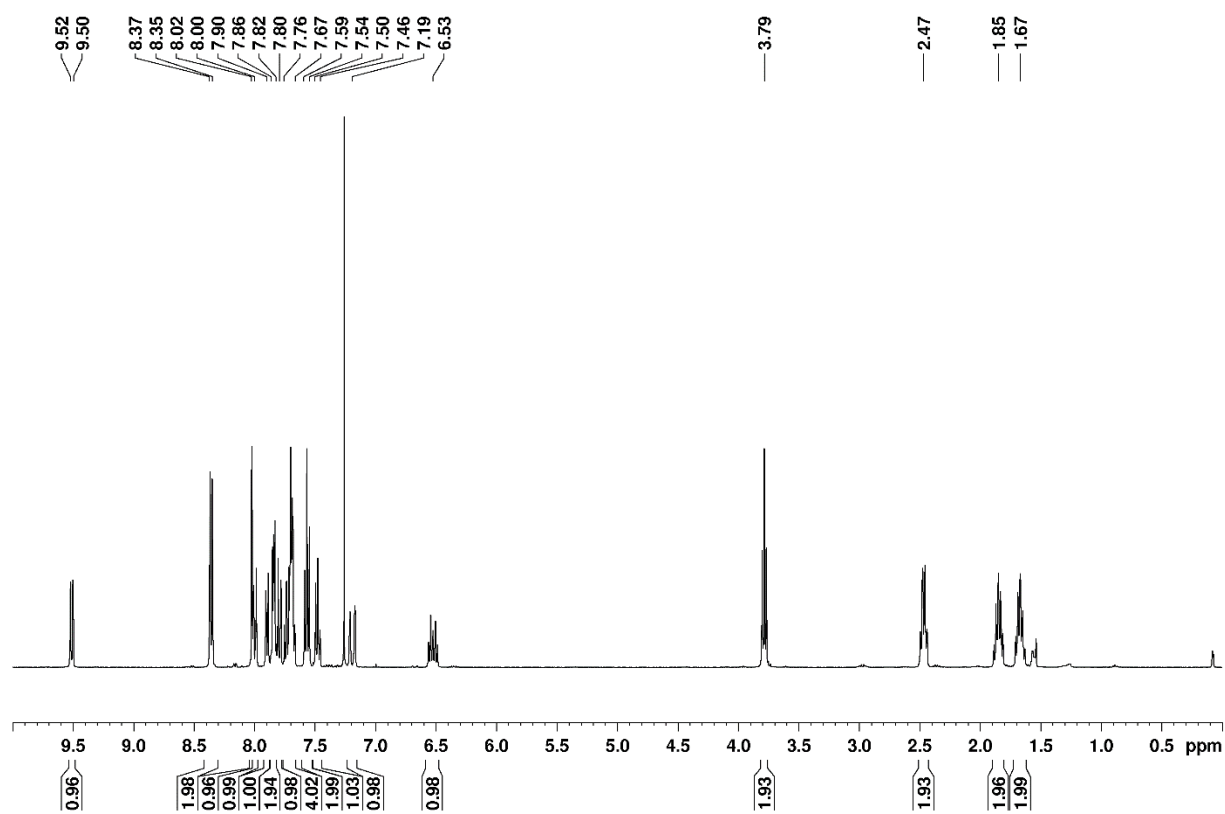


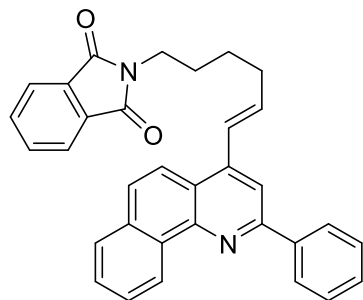
1.34



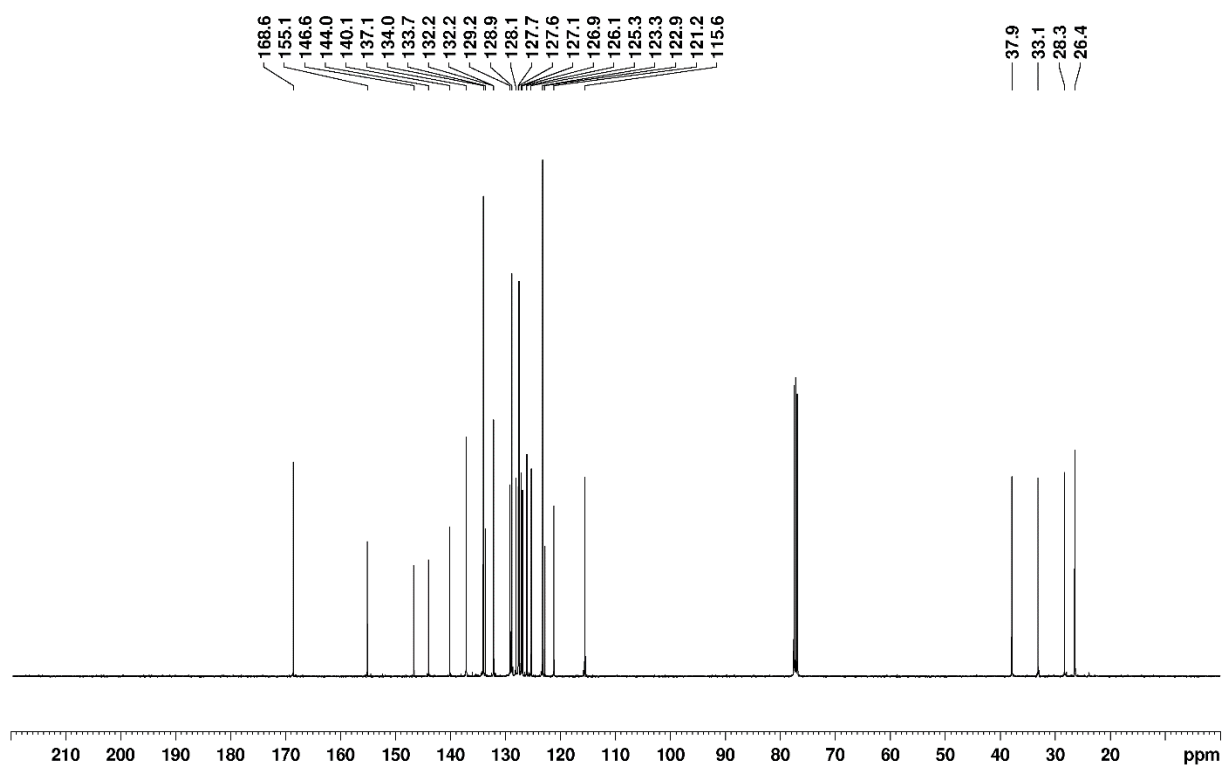


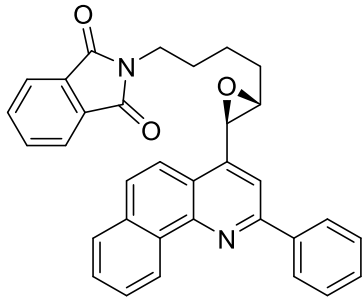
1.21



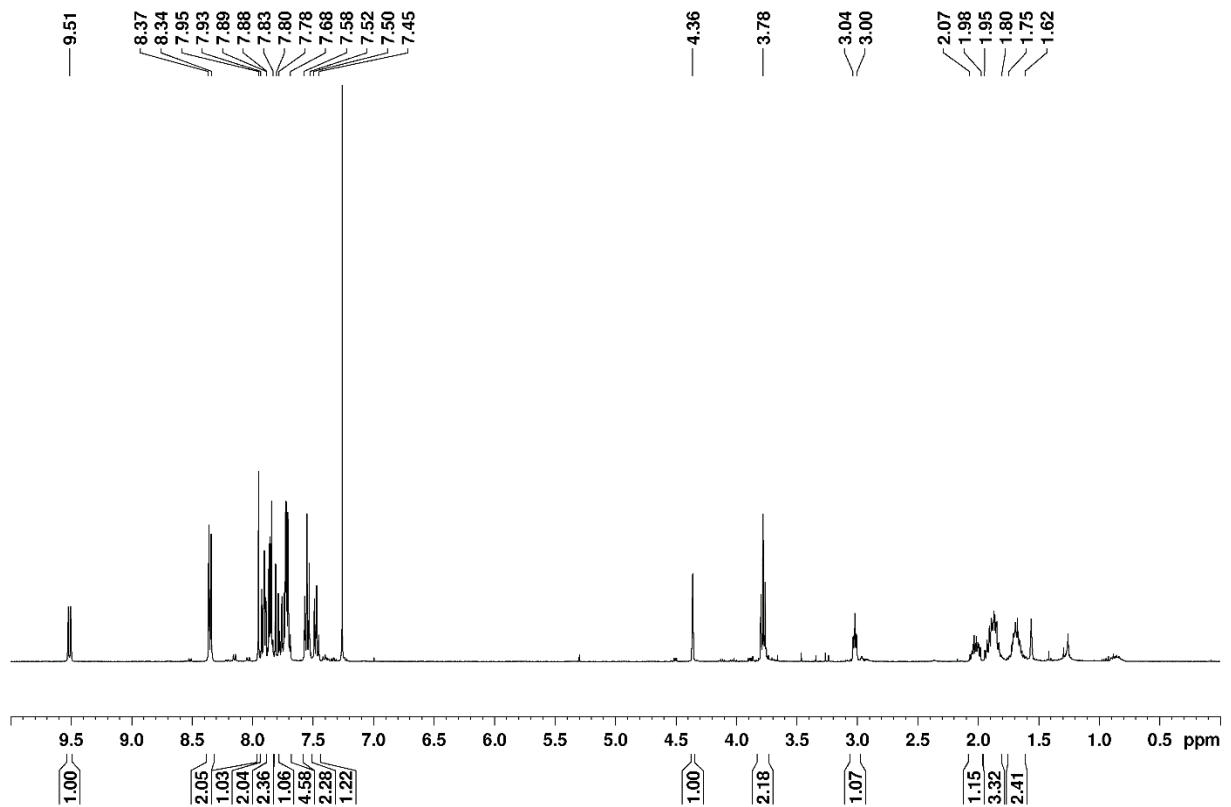


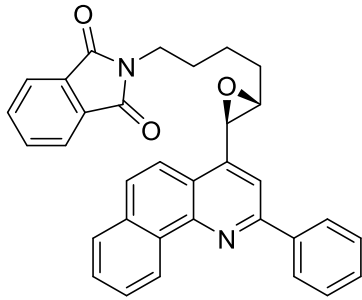
1.21



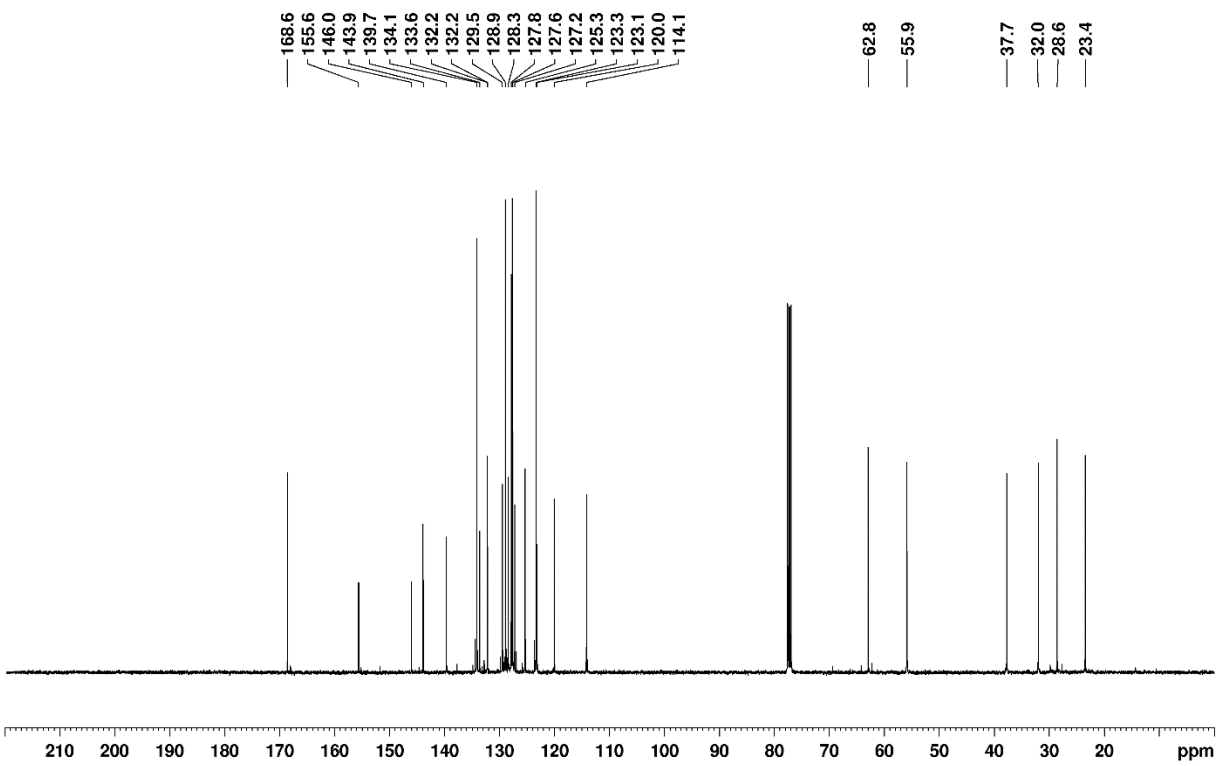


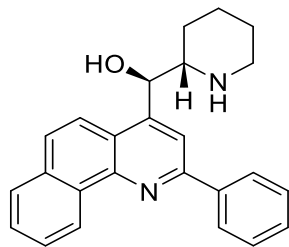
1.39



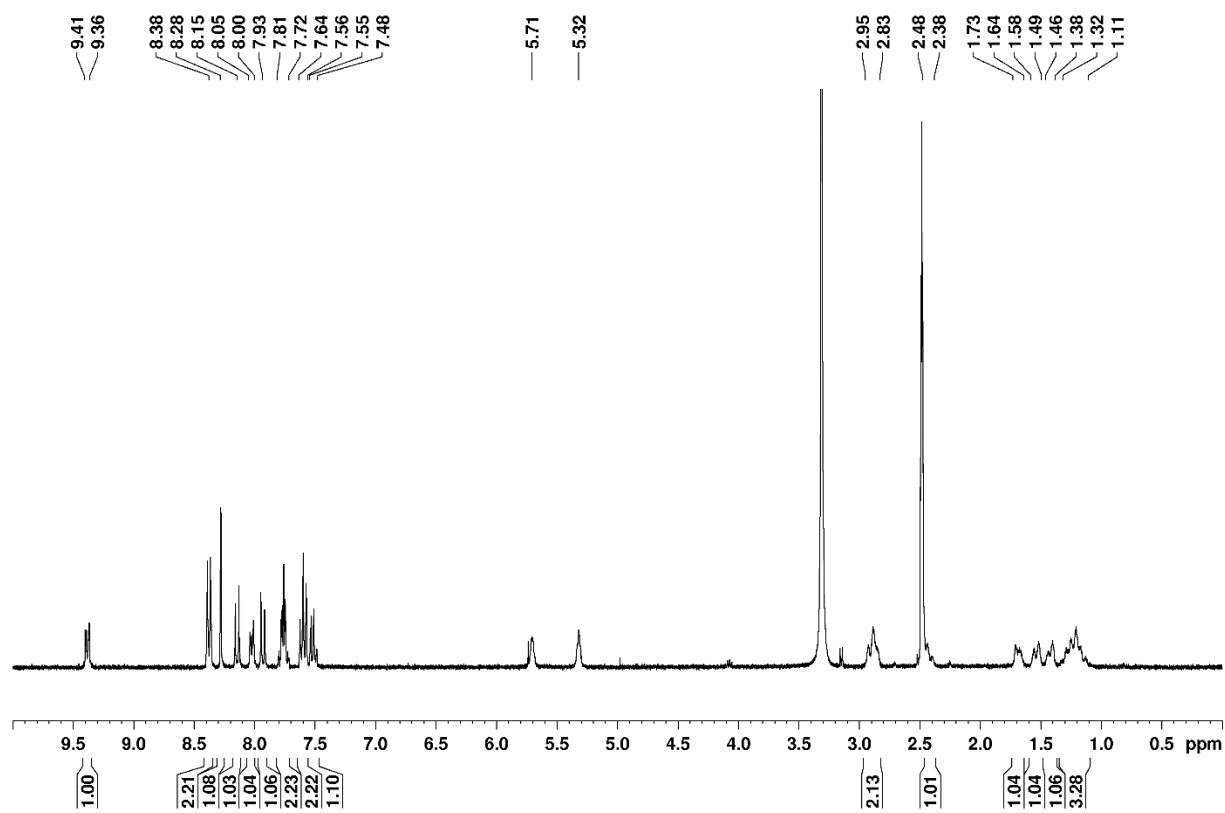


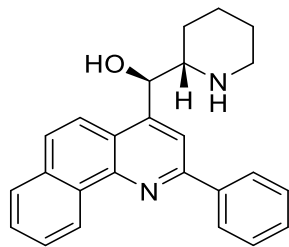
1.39



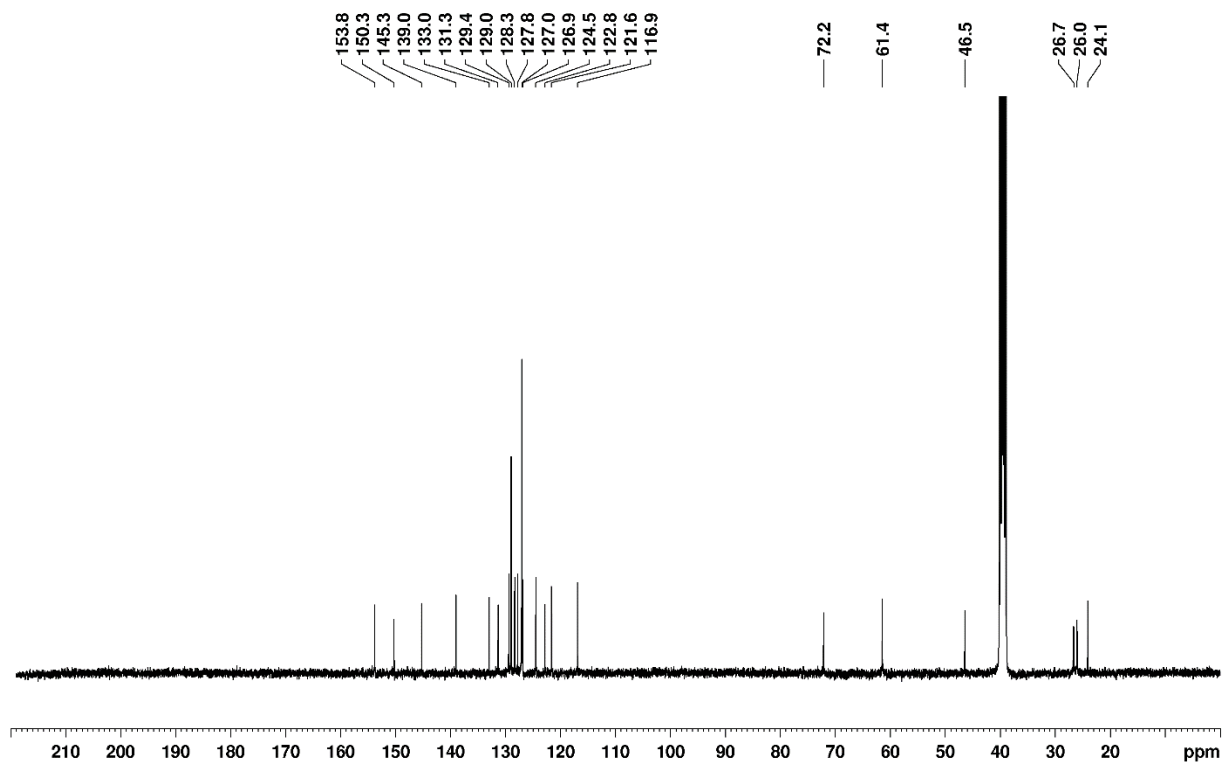


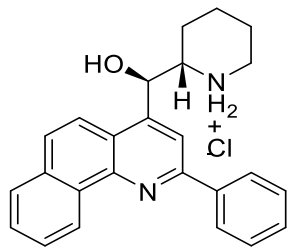
1.40



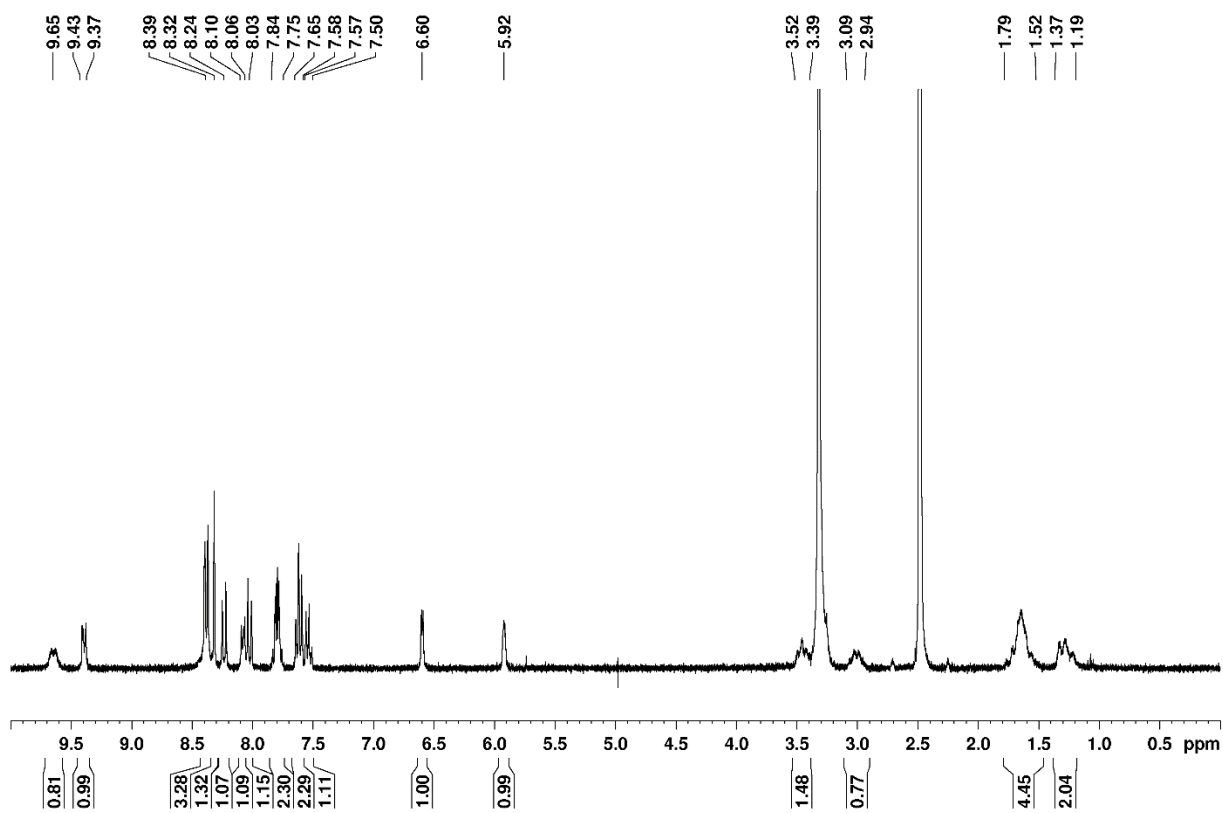


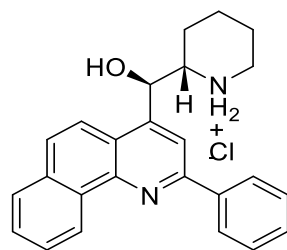
1.40



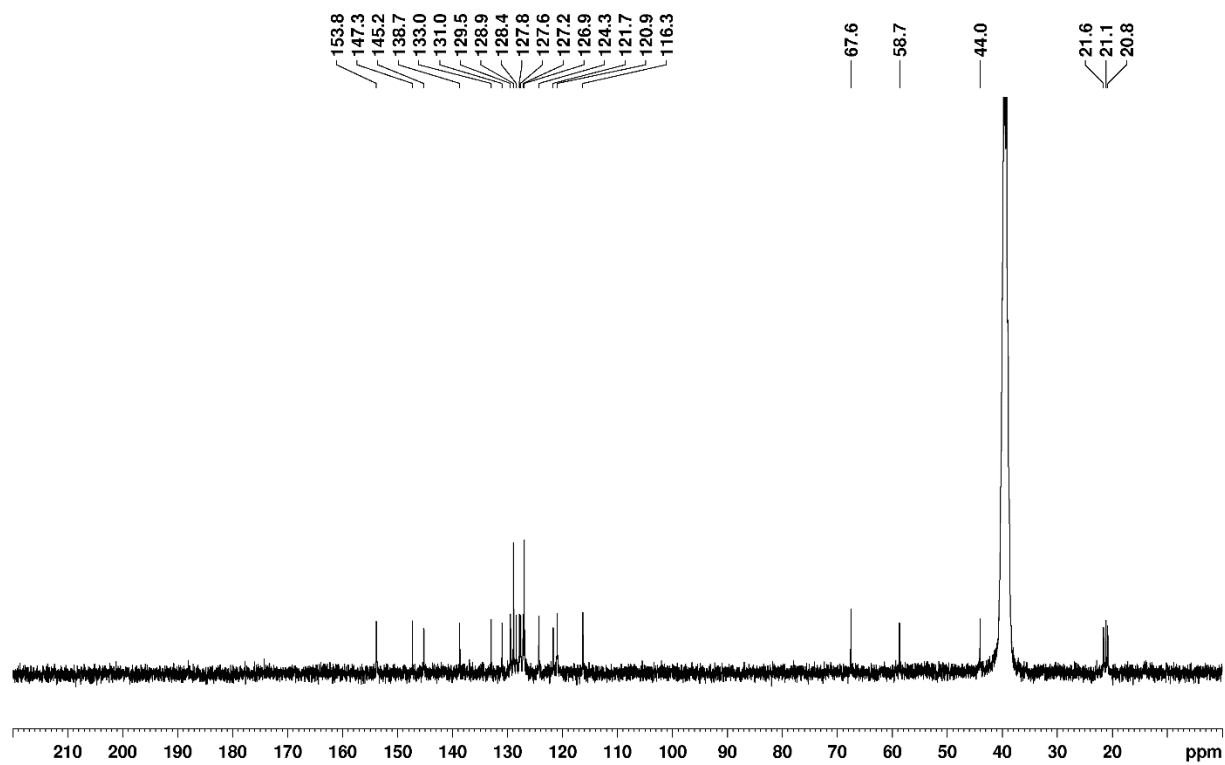


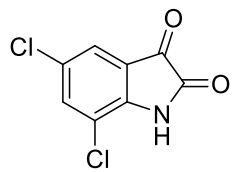
1



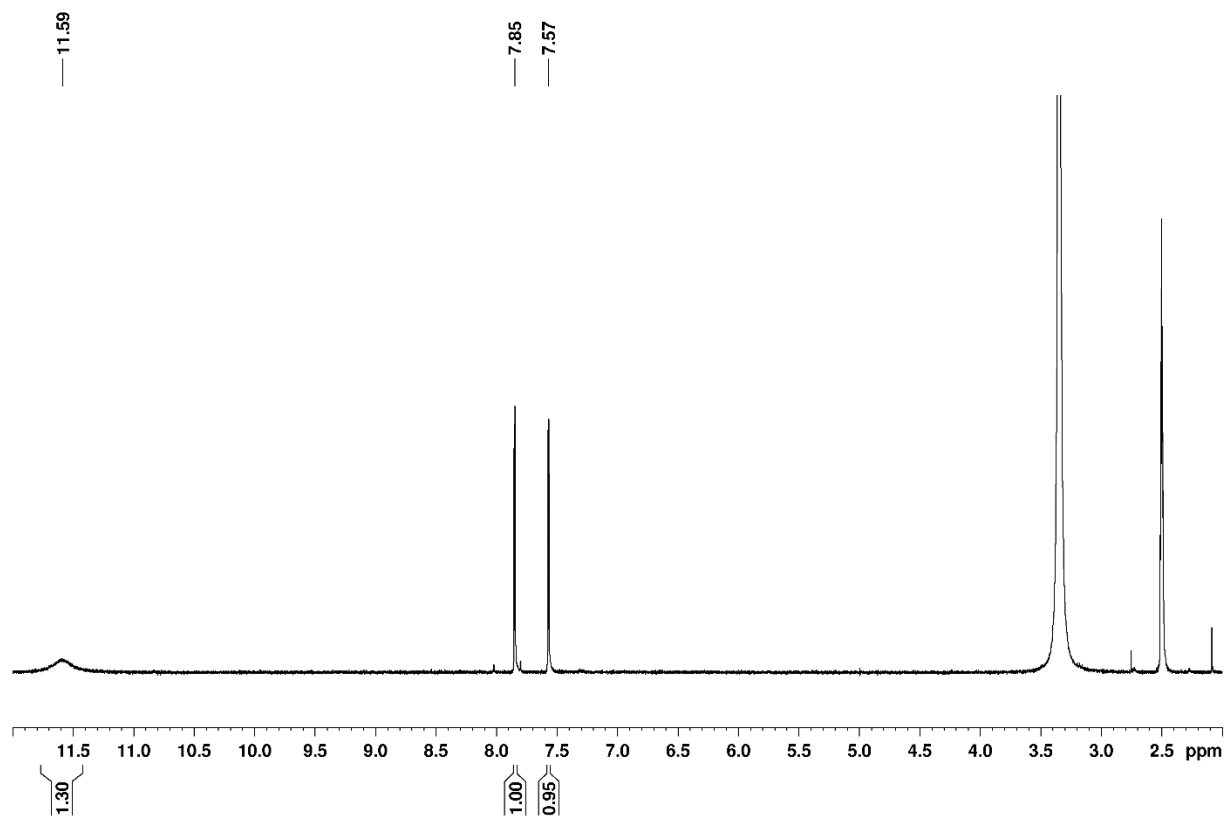


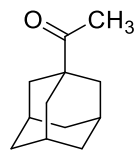
1.1



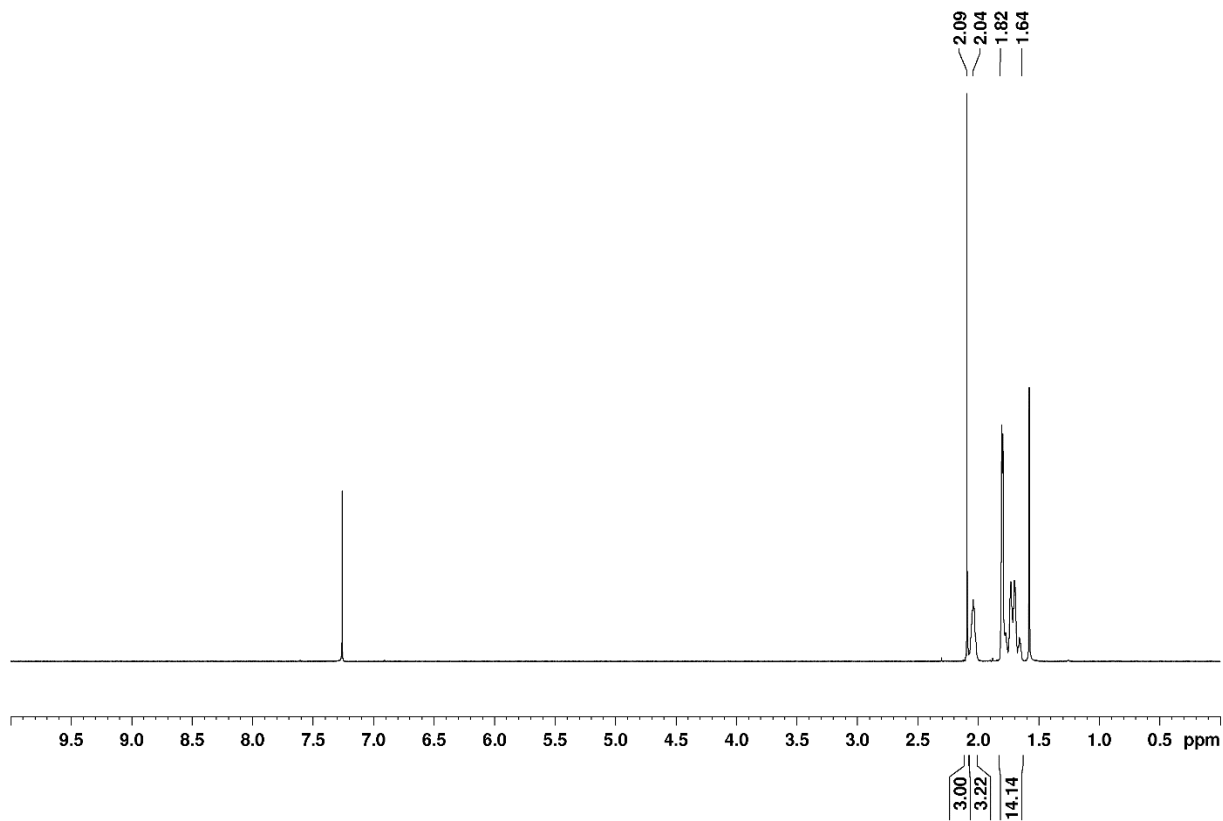


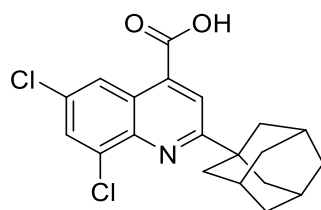
1.46



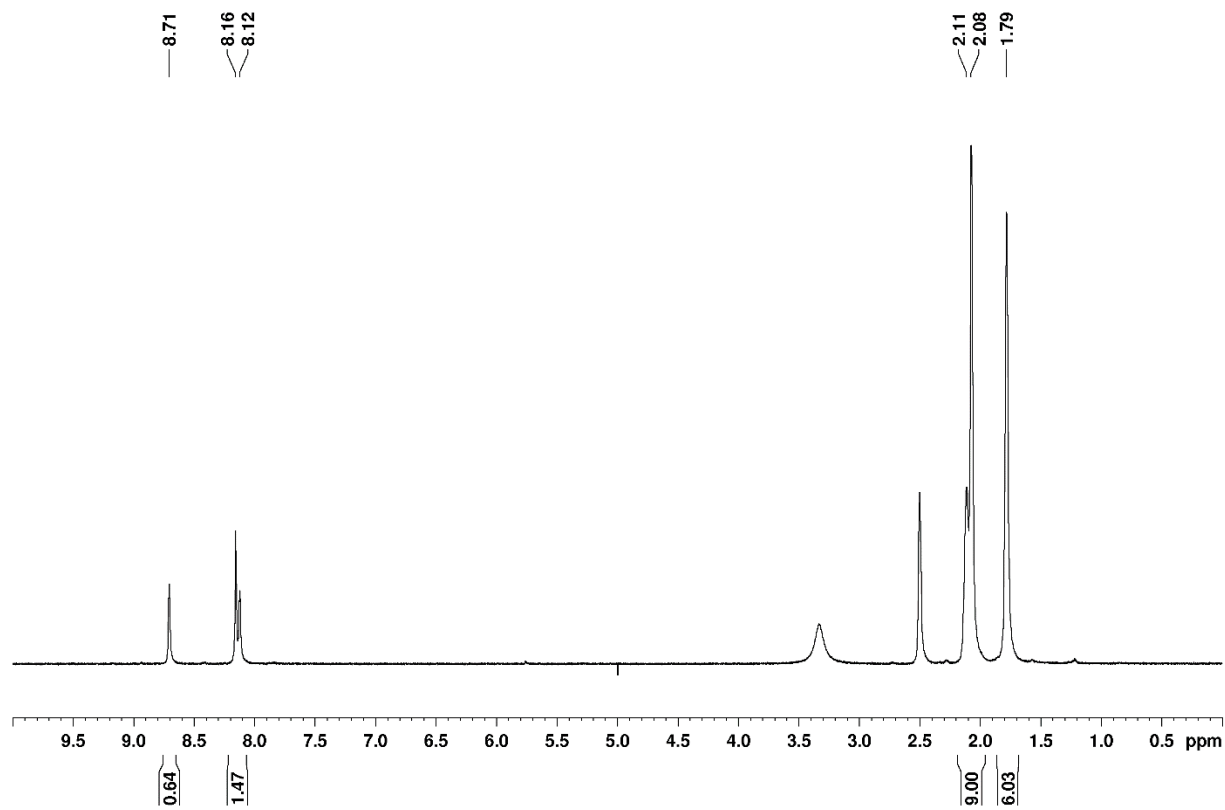


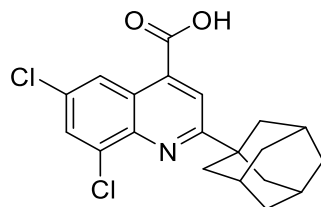
1.44



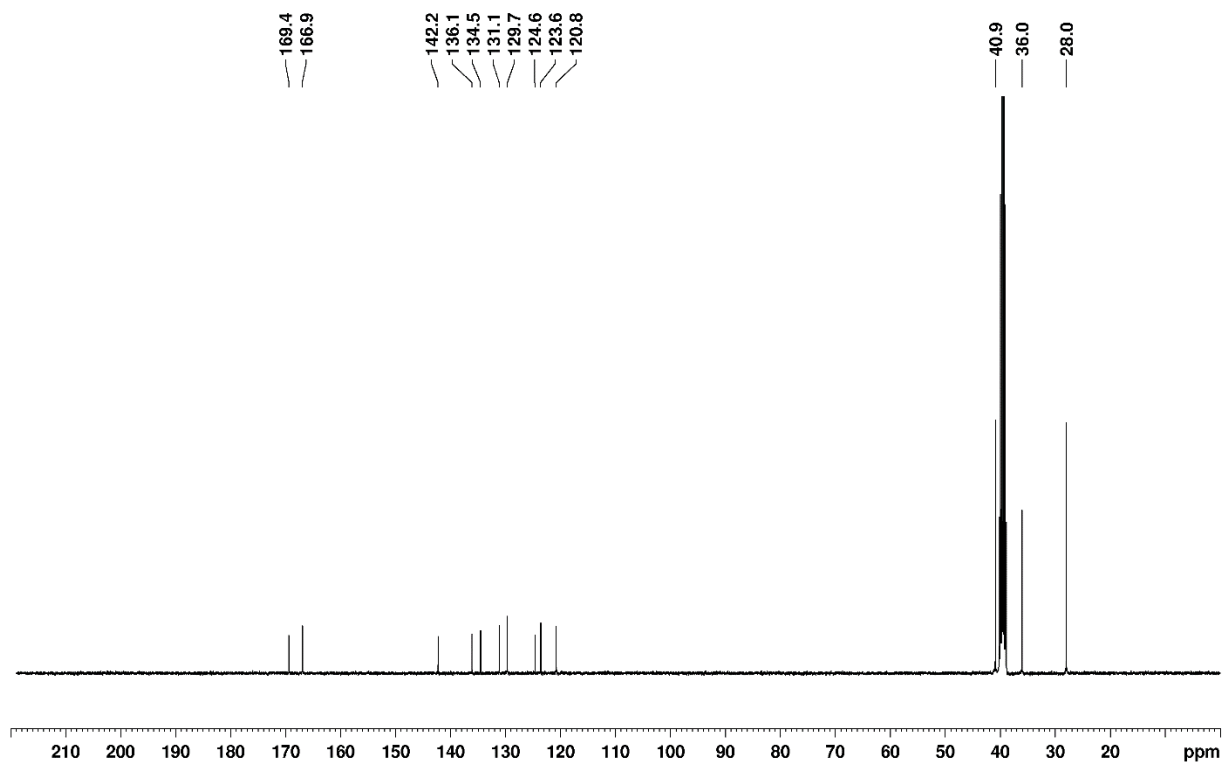


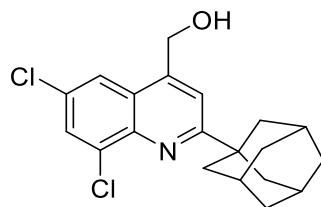
1.42



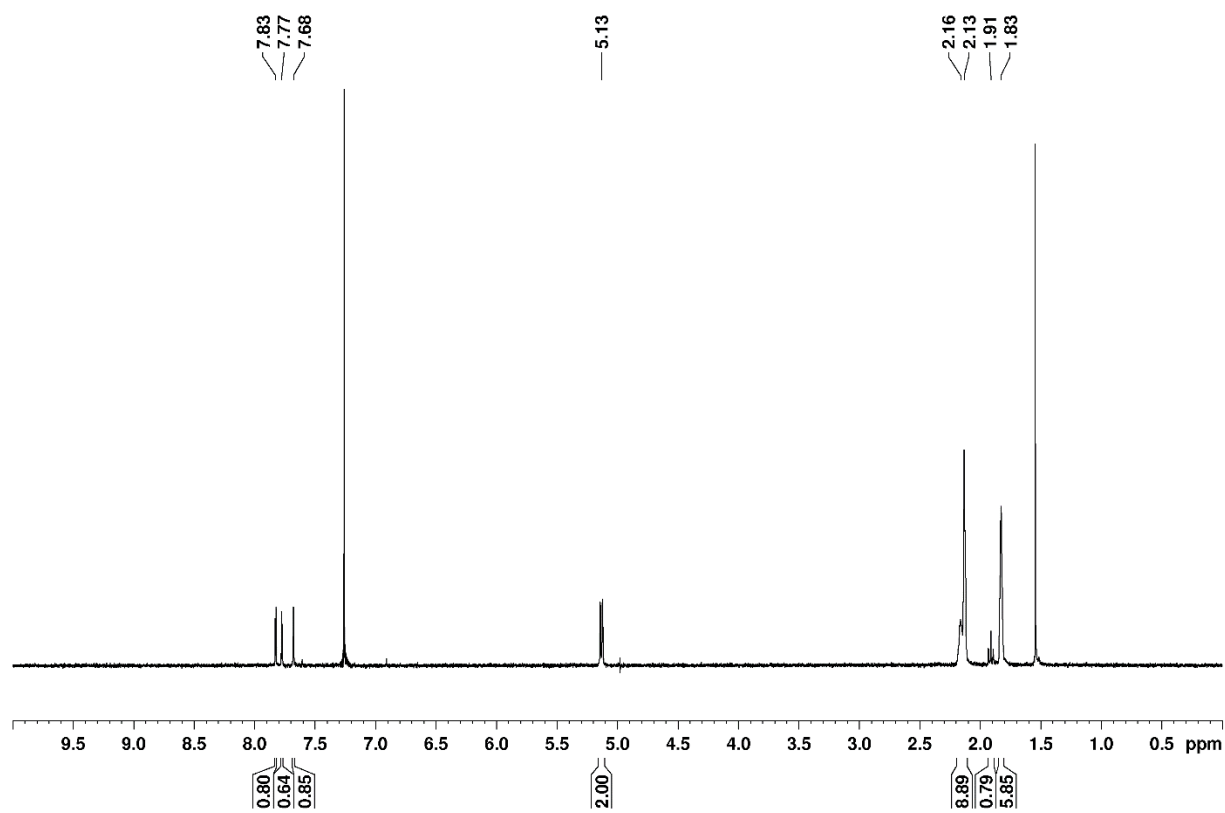


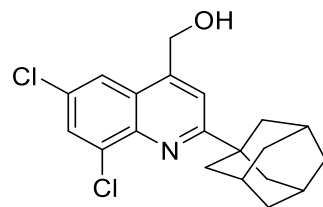
1.46



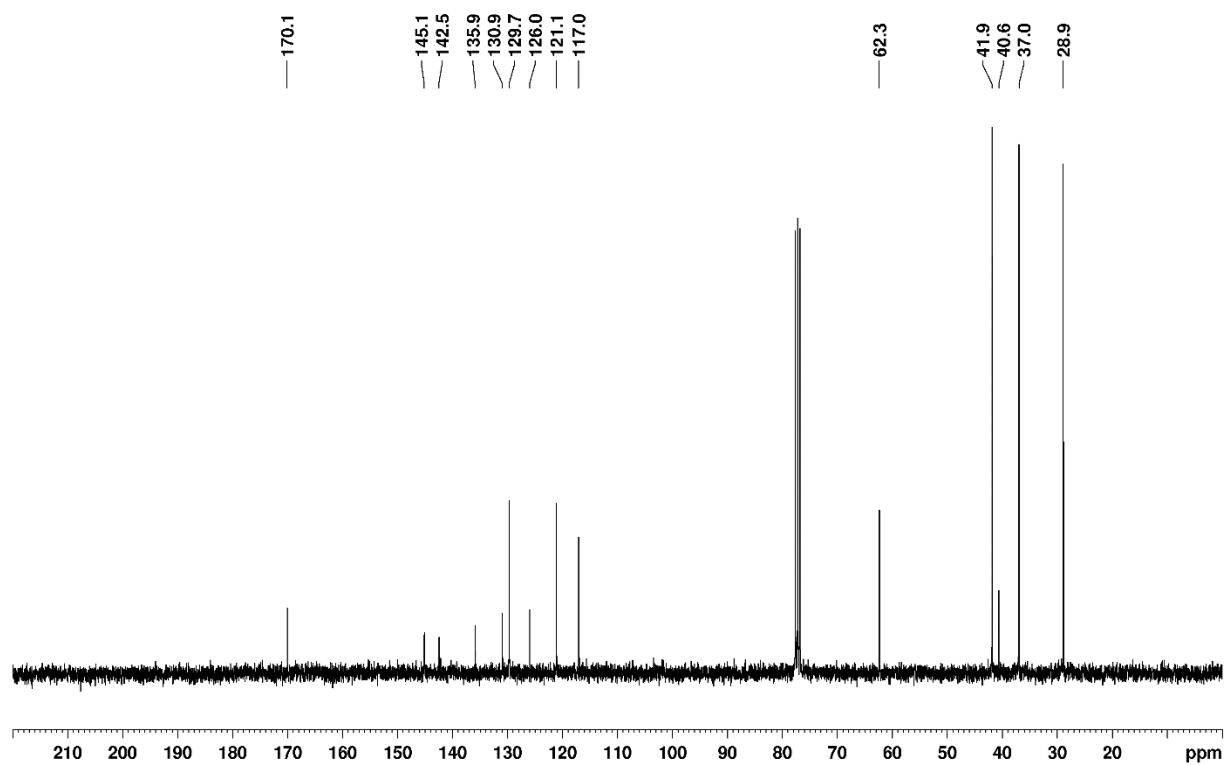


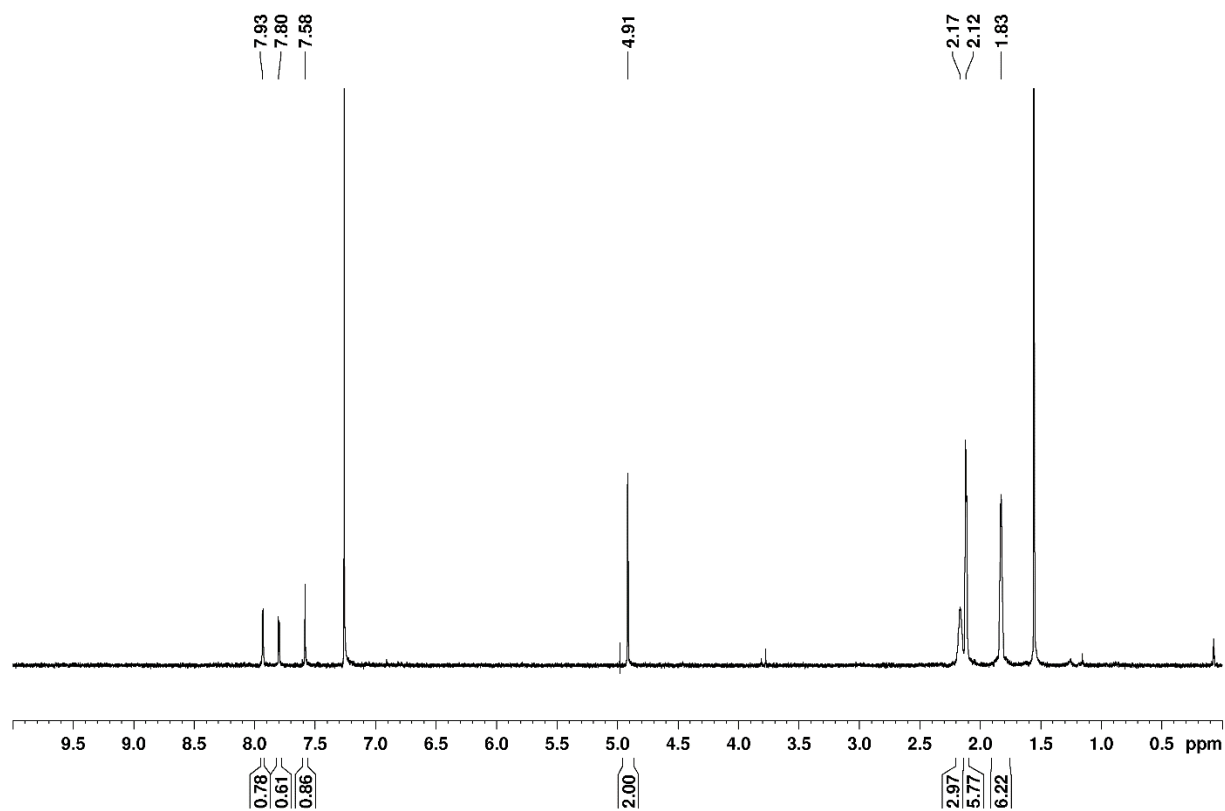
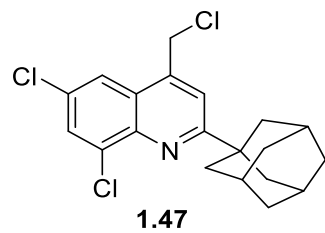
1.47

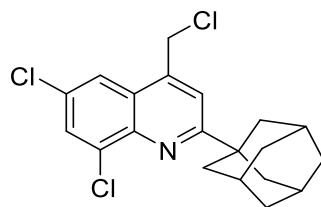




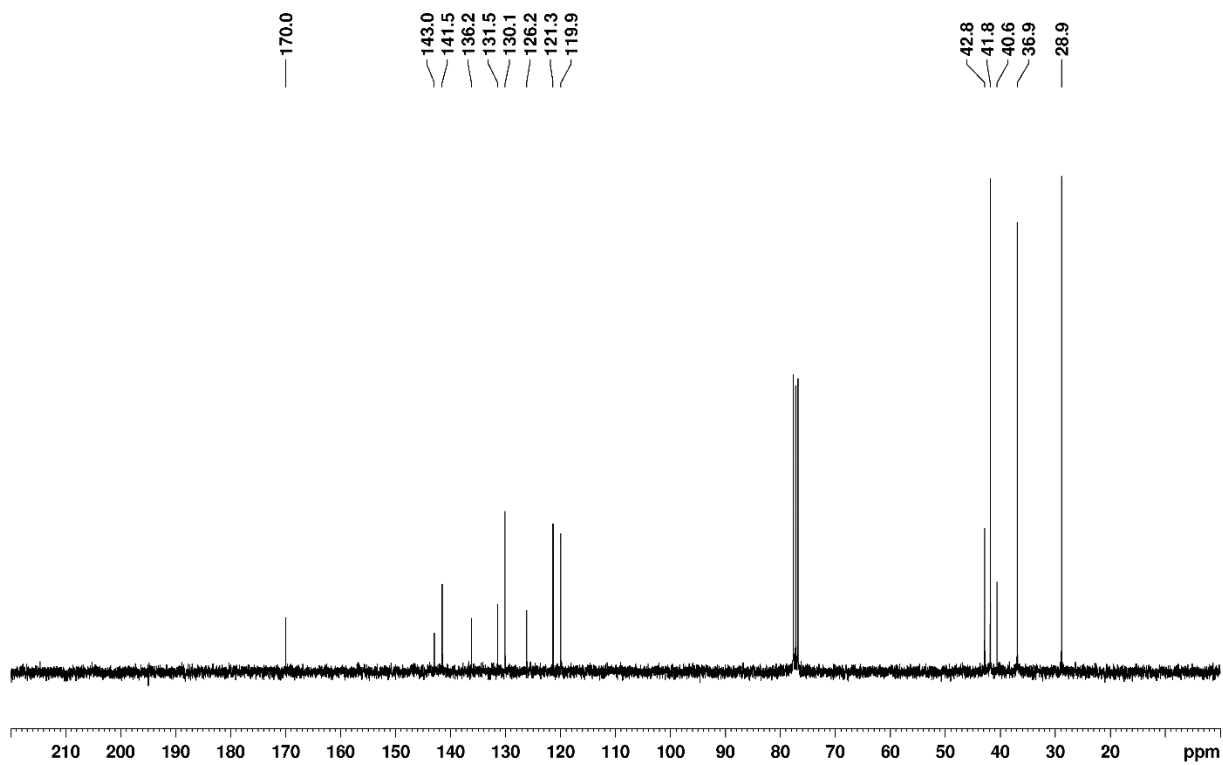
1.47

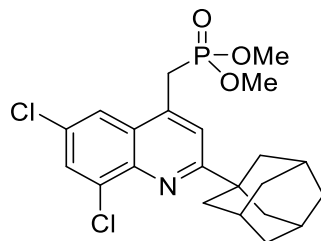




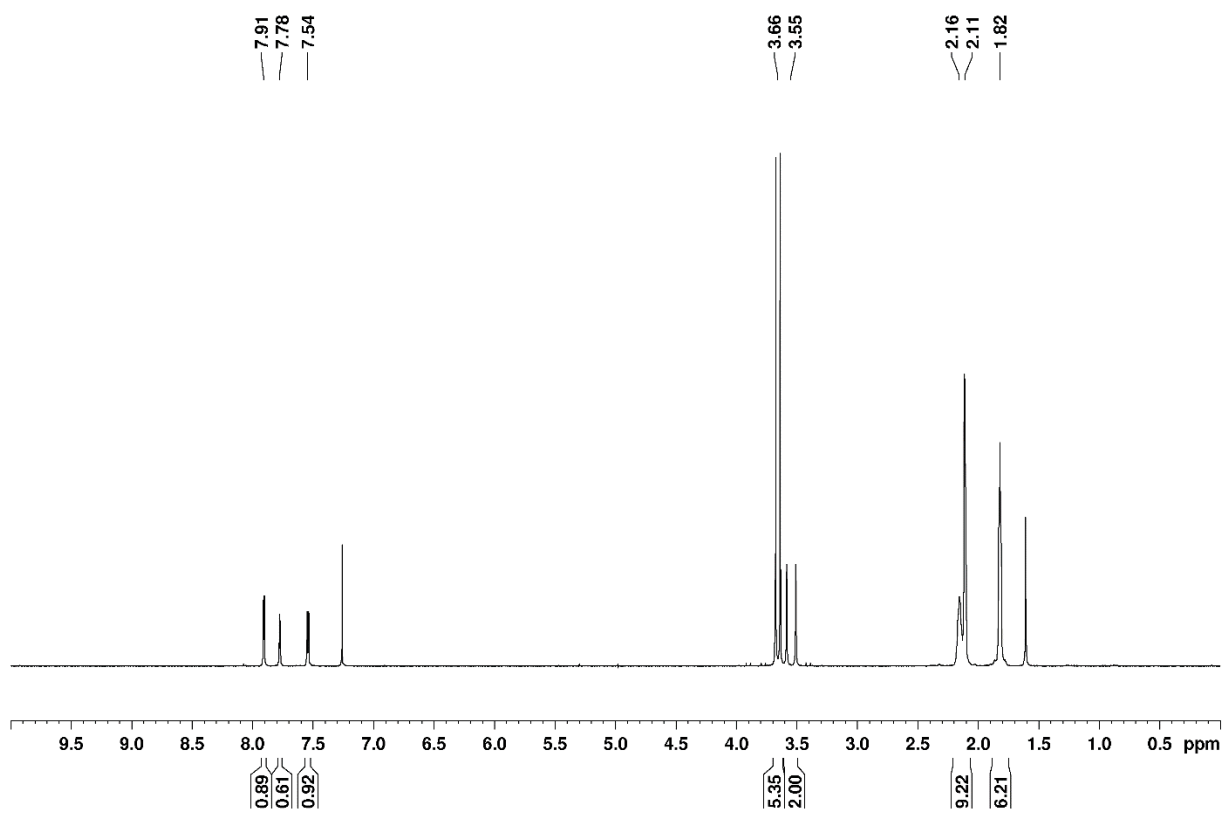


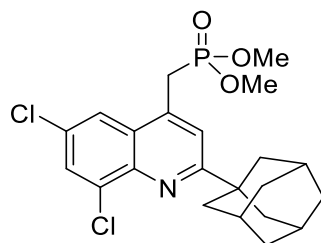
1.48



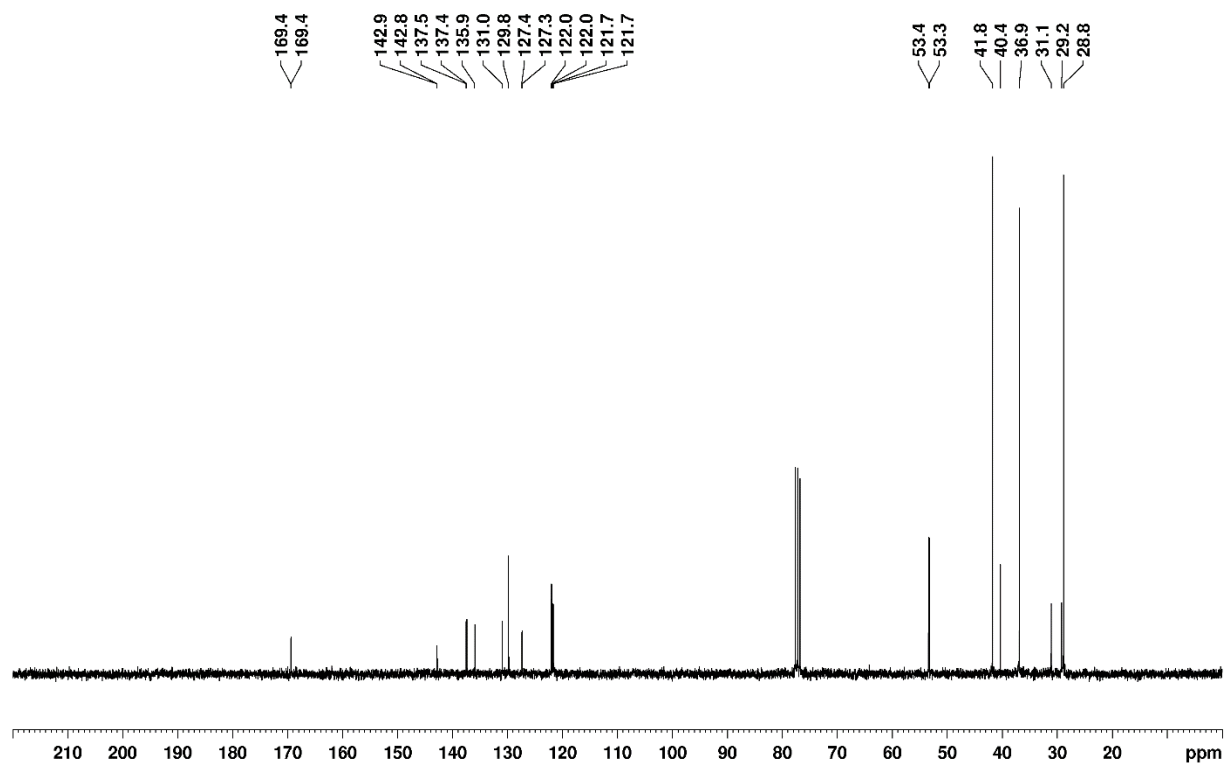


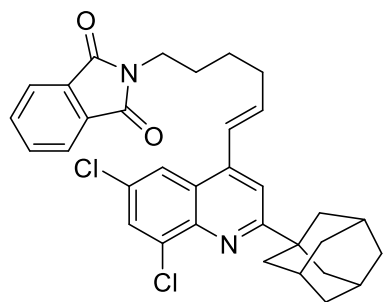
1.48



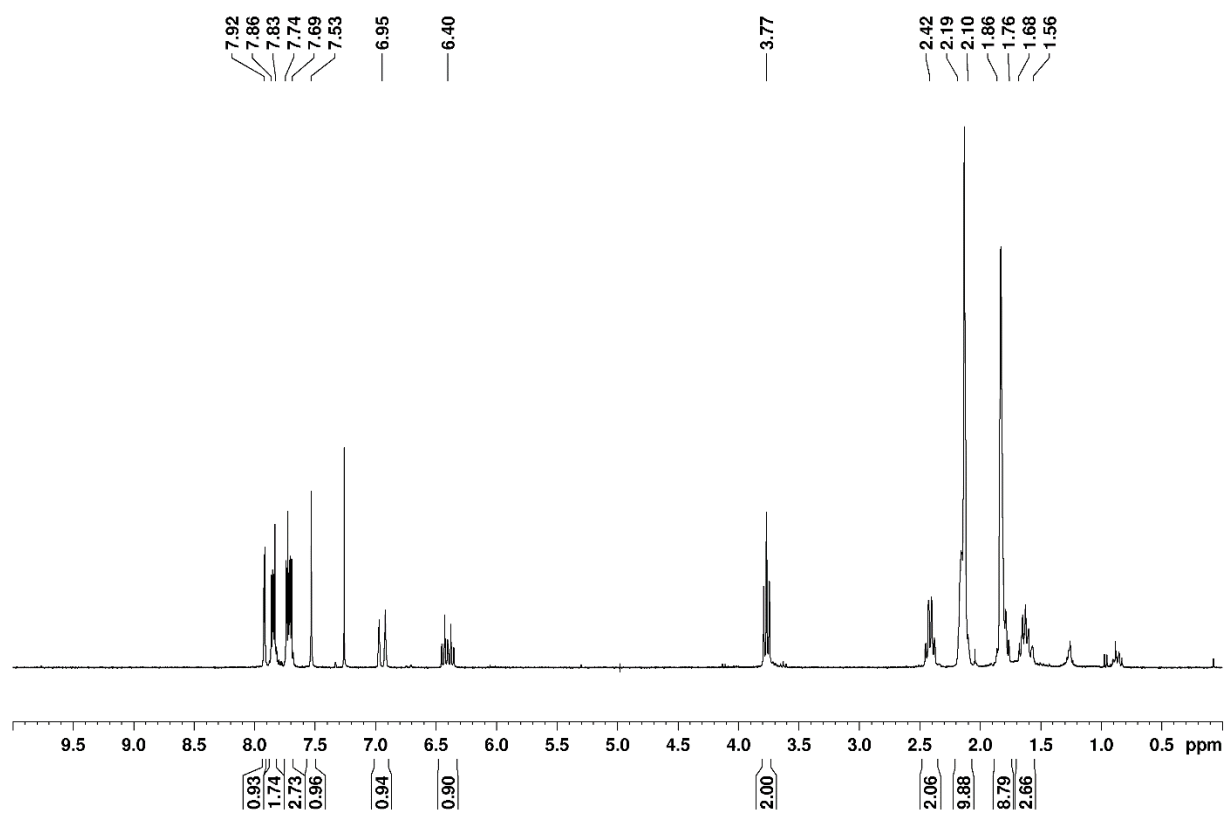


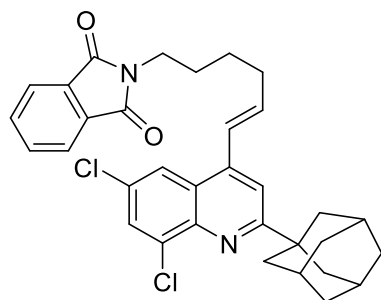
1.49



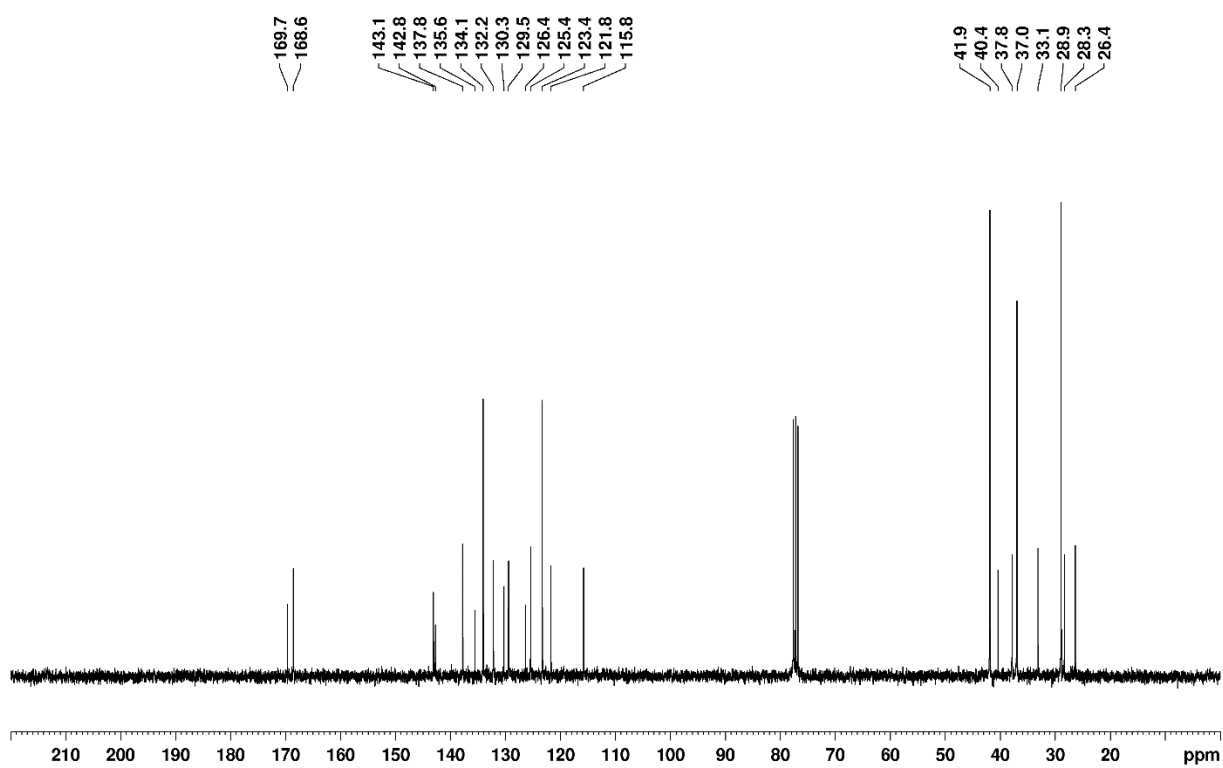


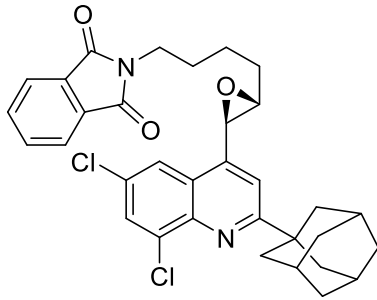
1.50



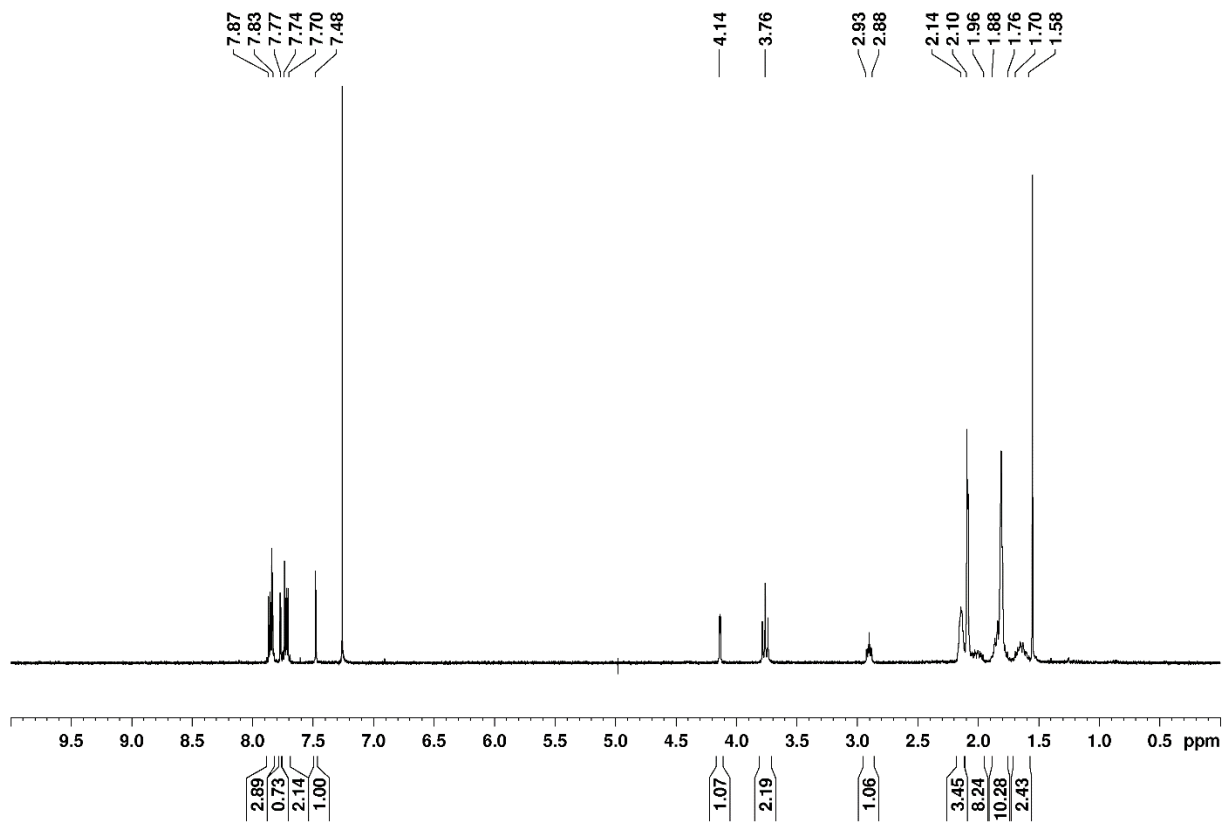


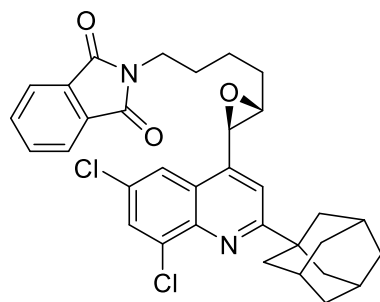
1.51



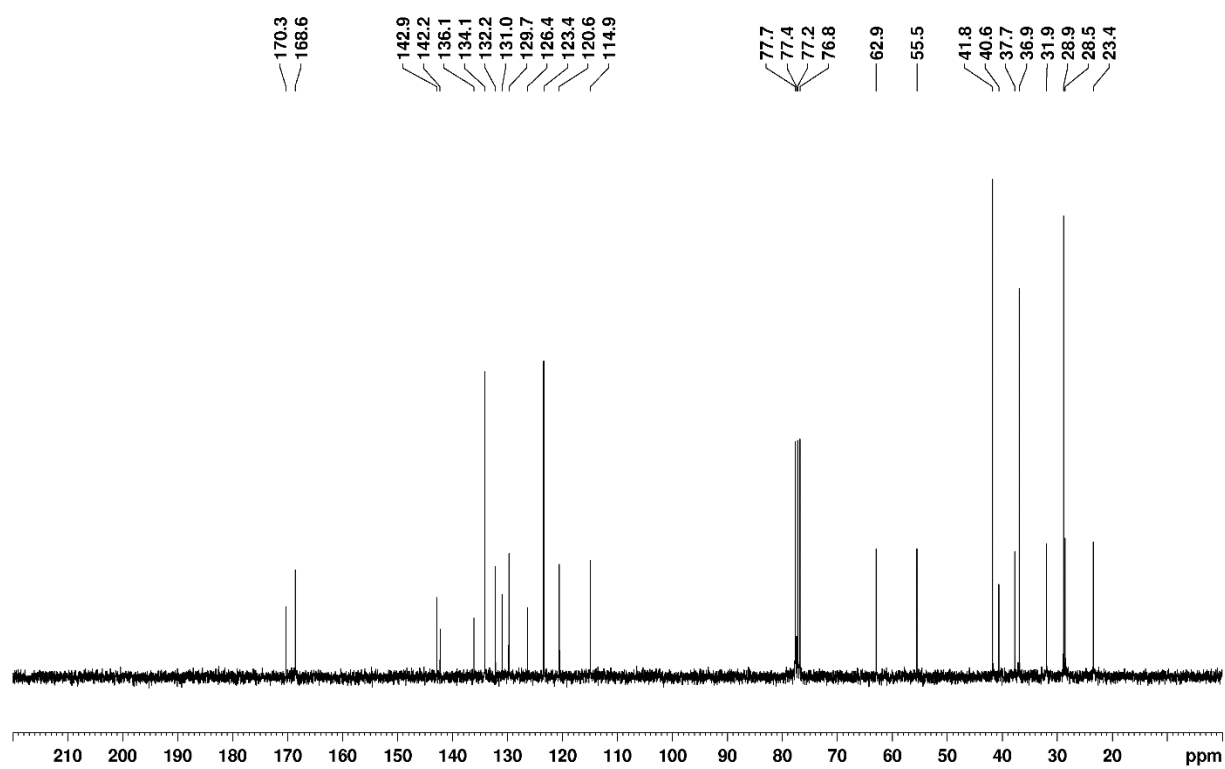


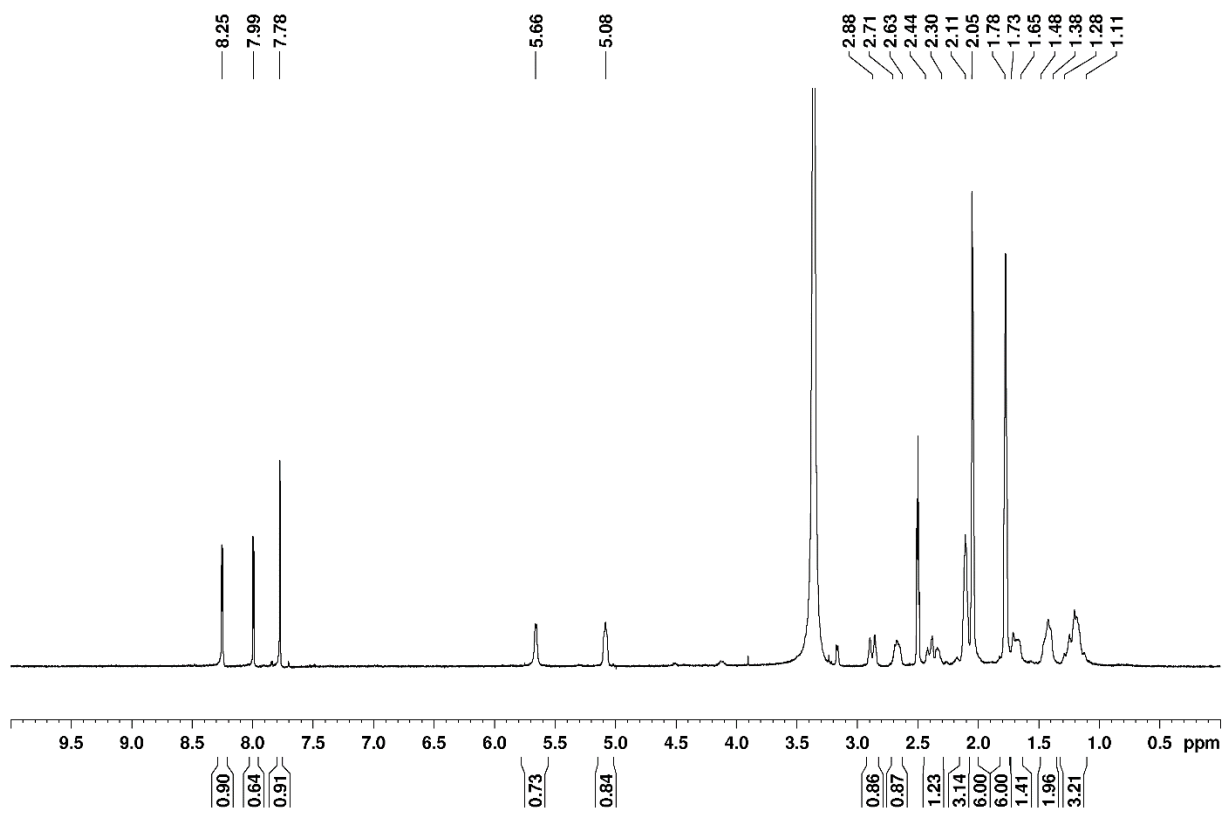
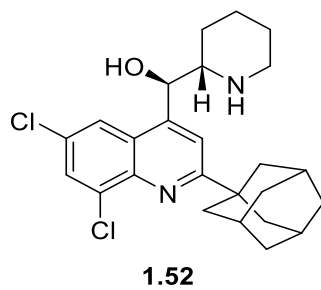
1.51

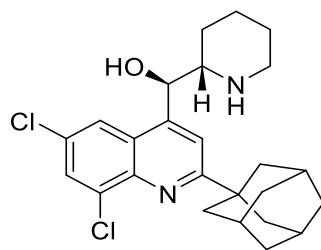




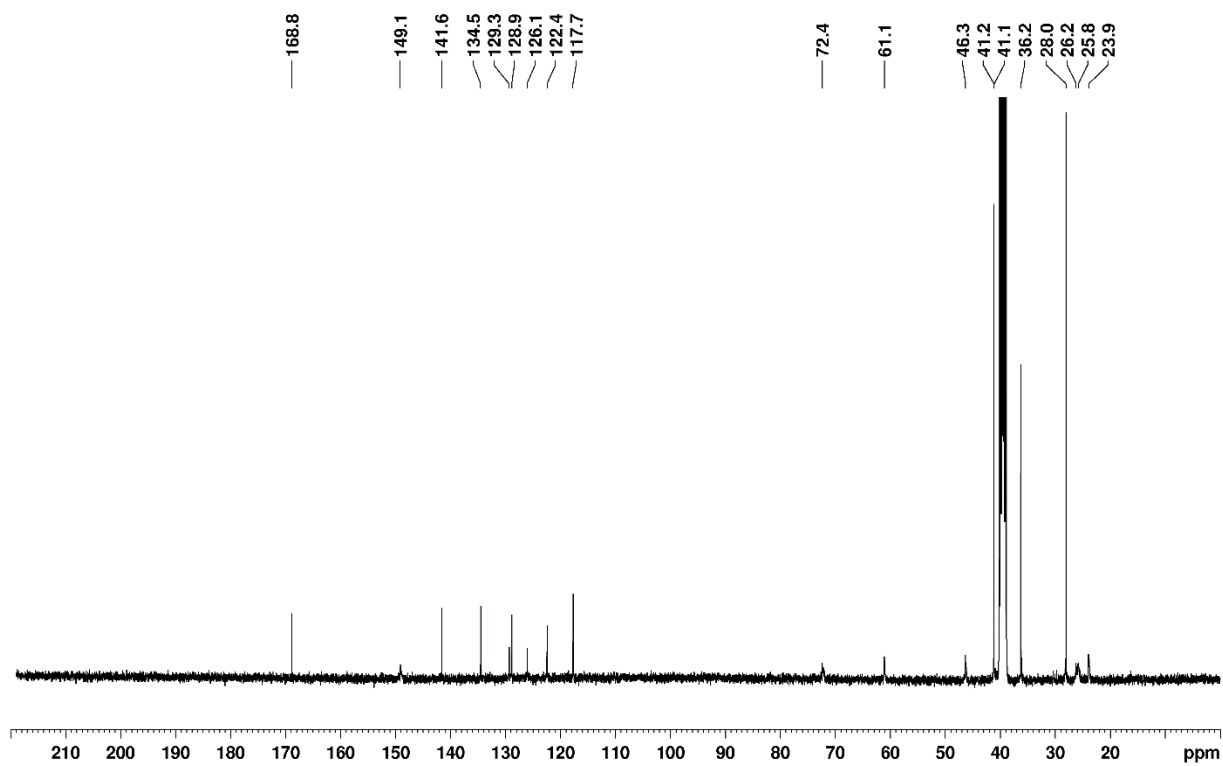
1.52

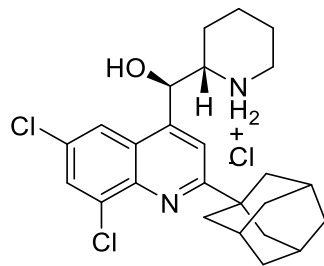




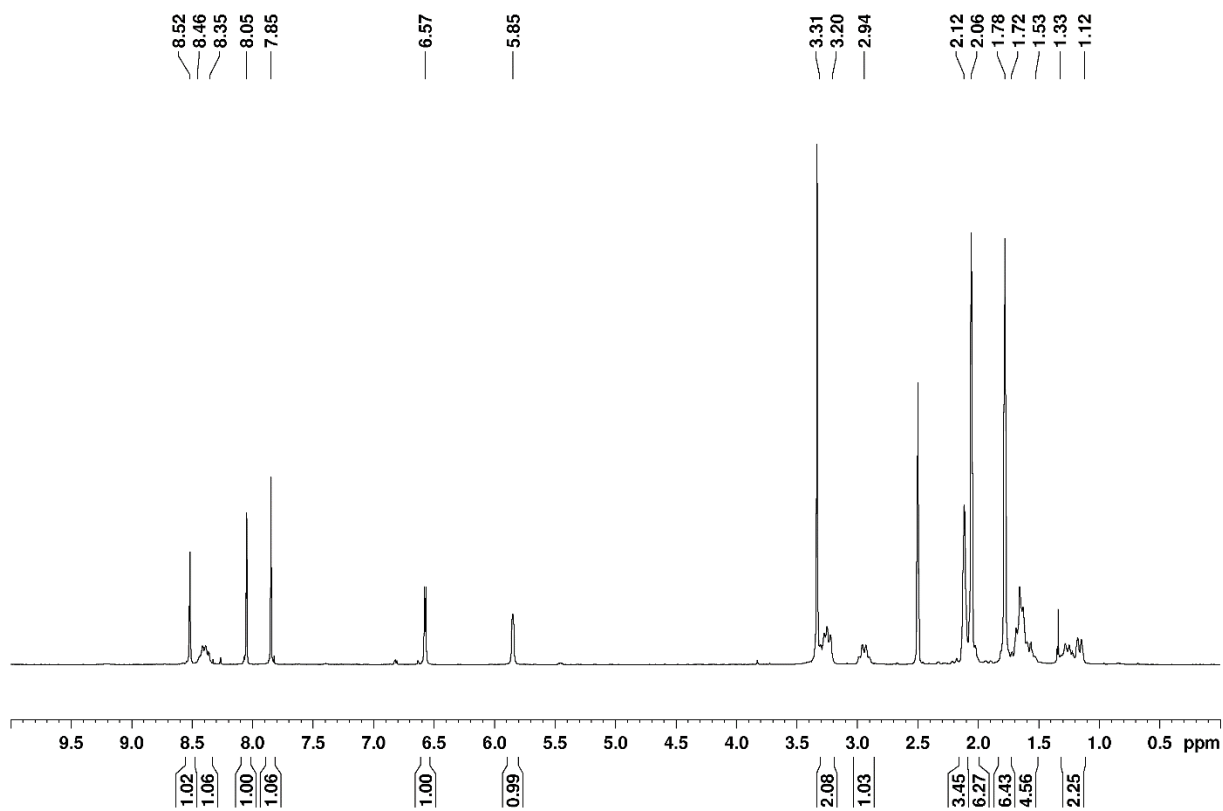


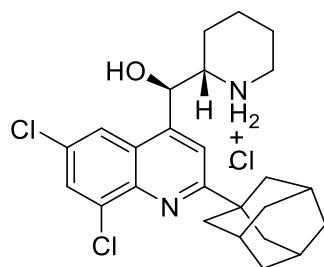
1.53



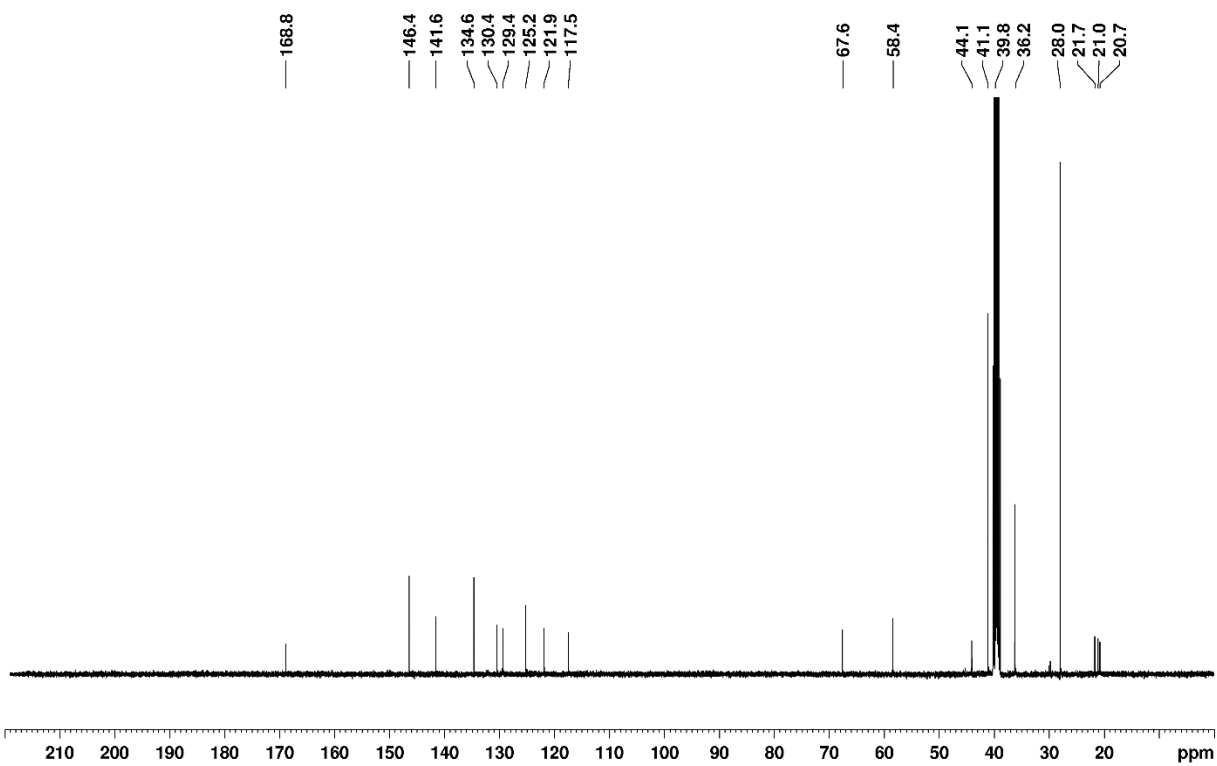


1.2





1.2



1.6. References

- (1) (a) Zhang, X.; Majerus, P. W. Phosphatidylinositol signaling reactions. *Semin. Cell Dev. Biol.* **1998**, *9*, 153. (b) Catimel, B.; Yin, M.-X.; Schieber, C.; Condron, M.; Patsiouras, H.; Catimel, J.; Robinson, D. E. J. E.; Wong, L. S.-M.; Nice, E. C.; Holmes, A. B.; Burgess, A. W. PI(3,4,5)P₃ Interactome. *J. Proteome Res.* **2009**, *8*, 3712.
- (2) (a) Ooms, L. M.; Horan, K. A.; Rahman, P.; Seaton, G.; Gurung, R.; Kethesparan, D. S.; Mitchell, C. A. The role of the inositol polyphosphate 5-phosphatases in cellular function and human disease. *Biochem. J.* **2009**, *419*, 29. (b) Dyson, J. M.; Fedele, C. G.; Davies, E. M.; Becanovic, J.; Mitchell, C. A. Phosphoinositide phosphatases: just as important as the kinases. *Subcell. Biochem.* **2012**, *58*, 215. (c) Bunney, T. D.; Katan, M. Phosphoinositide signalling in cancer: beyond PI3K and PTEN. *Nat.Rev.Cancer* **2010**, *10*, 342. (d) Edimo, W. s. E.; Janssens, V.; Waelkens, E.; Erneux, C. Reversible Ser/Thr SHIP phosphorylation: A new paradigm in phosphoinositide signalling? Targeting of SHIP1/2 phosphatases may be controlled by phosphorylation on Ser and Thr residues. *BioEssays* **2012**, *34*, 634. (e) Liu, P.; Cheng, H.; Roberts, T. M.; Zhao, J. J. Targeting the phosphoinositide 3-kinase pathway in cancer. *Nat. Rev. Drug Discov.* **2009**, *8*, 627. (f) Foster, J. G.; Blunt, M. D.; Carter, E.; Ward, S. G. Inhibition of PI3K signaling spurs new therapeutic opportunities in inflammatory/autoimmune diseases and hematological malignancies. *Pharmacol. Rev.* **2012**, *64*, 1027. (g) Blunt, M. D.; Ward, S. G. Pharmacological targeting of phosphoinositide lipid kinases and phosphatases in the immune system: success, disappointment, and new opportunities. *Front. Immunol.* **2012**, *3*, Article 226. (h) Suwa, A.; Kurama, T.; Shimokawa, T. SHIP2 and its involvement in various diseases. *Expert Opin. Ther. Targets* **2010**, *14*, 727. (i) Hamilton, M. J.; Ho, V. W.; Kuroda, E.;

Ruschmann, J.; Antignano, F.; Lam, V.; Krystal, G. Role of SHIP in cancer. *Exp. Hematol.* **2011**, *39*, 2. (j) Fernandes, S.; Iyer, S.; Kerr, W. G. Role of SHIP1 in cancer and mucosal inflammation. *Ann. N. Y. Acad. Sci.* **2013**, *1280*, 6. (k) Fuhler, G. M.; Brooks, R.; Toms, B.; Iyer, S.; Gengo, E. A.; Park, M. Y.; Gumbleton, M.; Viernes, D. R.; Chisholm, J. D.; Kerr, W. G. Therapeutic potential of SH2 domain-containing inositol-5'-phosphatase 1 (SHIP1) and SHIP2 inhibition in cancer. *Mol. Med.* **2012**, *18*, 65. (l) Iyer, S.; Margulies, B. S.; Kerr, W. G. Role of SHIP1 in bone biology. *Ann. N. Y. Acad. Sci.* **2013**, *1280*, 11.

(3) Cantley, L. C. The phosphoinositide-3-kinase pathway. *Science* **2002**, *296*, 1655.

(4) Marion, F.; Williams, D. E.; Patrick, B. O.; Hollander, I.; Mallon, R.; Kim, S. C.; Roll, D. M.; Feldberg, L.; Van Soest, R.; Andersen, R. J. Liphagal, a Selective Inhibitor of PI3 Kinase a Isolated from the Sponge Aka coralliphaga: Structure Elucidation and Biomimetic Synthesis. *Org. Lett.* **2006**, *8*, 321.

(5) (a) Leslie, N. R.; Biondi, R. M.; Alessi, D. R. Phosphoinositide-regulated kinases and phosphoinositide phosphatases. *Chem. Rev.* **2001**, *101*, 2365. (b) Krystal, G. Lipid phosphatases in the immune system. *Semin. Immunol.* **2000**, *12*, 397.

(6) Sewell, G. W.; Marks, D. J.; Segal, A. W. The immunopathogenesis of Crohn's disease: a three-stage model. *Curr. Opin. Immunol.* **2009**, *21*, 506.

(7) Brooks, R.; Fuhler, G. M.; Iyer, S.; Smith, M. J.; Park, M. Y.; Paraiso, K. H.; Engelman, R. W.; Kerr, W. G. SHIP1 Inhibition Increases Immunoregulatory Capacity and Triggers Apoptosis of Hematopoietic Cancer Cells. *J. Immunol.* **2010**, *184*, 3582.

(8) (a) Krystal, G.; Damen, J. E.; Helgason, C. D.; Huber, M.; Hughes, M. R.; Kalesnikoff, J.; Lam, V.; Rosten, P.; Ware, M. D.; Yew, S.; Humphries, R. K. Ships ahoy. *Int. J. Biochem. Cell Biol.* **1999**, *31*, 1007. (b) Erneux, C.; Govaerts, C.; Communi, D.; Pesesse, X. The diversity and

possible functions of the inositol polyphosphate 5-phosphatases. *Biochim. Biophys. Acta* **1998**, *1436*, 185.

(9) Hazen, A. L.; Smith, M. J.; Despons, C.; Winter, O.; Moser, K.; Kerr, W. G. SHIP is required for a functional hematopoietic stem cell niche. *Blood* **2009**, *113*, 2924.

(10) Pesesse, X.; Deleu, S.; De Smedt, F.; Drayer, L.; Erneux, C. Identification of a second SH2-domain-containing protein closely related to the phosphatidylinositol polyphosphate 5-phosphatase SHIP. *Biochem. Biophys. Res. Co.* **1997**, *239*, 697.

(11) Zhang, Y.; Wavreille, A. S.; Kunys, A. R.; Pei, D. The SH2 domains of inositol polyphosphate 5-phosphatases SHIP1 and SHIP2 have similar ligand specificity but different binding kinetics. *Biochemistry* **2009**, *48*, 11075.

(12) Helgason, C. D.; Damen, J. E.; Rosten, P.; Grewal, R.; Sorensen, P.; Chappel, S. M.; Borowski, A.; Jirik, F.; Krystal, G.; Humphries, R. K. Targeted disruption of SHIP leads to hemopoietic perturbations, lung pathology, and a shortened life span. *Genes Dev.* **1998**, *12*, 1610.

(13) (a) Clement, S.; Krause, U.; Desmedt, F.; Tanti, J. F.; Behrends, J.; Pesesse, X.; Sasaki, T.; Penninger, J.; Doherty, M.; Malaisse, W.; Dumont, J. E.; Le Marchand-Brustel, Y.; Erneux, C.; Hue, L.; Schurmans, S. The lipid phosphatase SHIP2 controls insulin sensitivity. *Nature* **2001**, *409*, 92. (b) Sleeman, M. W.; Wortley, K. E.; Lai, K. M.; Gowen, L. C.; Kintner, J.; Kline, W. O.; Garcia, K.; Stitt, T. N.; Yancopoulos, G. D.; Wiegand, S. J.; Glass, D. J. Absence of the lipid phosphatase SHIP2 confers resistance to dietary obesity. *Nat. Med.* **2005**, *11*, 199.

(14) (a) Bradshaw, W. J.; Williams, E. P.; Fernandez-Cid, A.; Burgess-Brown, N.; von Delft, F.; Arrowsmith, C. H.; Edwards, A.; Bountra, C.; Gileadi, O. The Phosphatase and C2 domains of Human SHIP1 DOI:10.2210/pdb6IBD/pdb. **2019**, PDB ID: 6IBD. (b) Gardill, B. R.; Cheung, S.

T.; Mui, A. L.; Van Petegem, F. Crystal Structure of a SHIP1 surface entropy reduction mutant. *PDB ID : 6DLG* **2019**, DOI: 10.2210/pdb6DLG/pdb.

(15) Mills, S. J.; Persson, C.; Cozier, G.; Thomas, M. P.; Tresaugues, L.; Erneux, C.; Riley, A. M.; Nordlund, P.; Potter, B. V. L. A Synthetic Polyphosphoinositide Headgroup Surrogate in Complex with SHIP2 Provides a Rationale for Drug Discovery. *ACS Chem. Biol.* **2012**, *7*, 822.

(16) Le Coq, J.; Camacho-Artacho, M.; Velazquez, J. V.; Santiveri, C. M.; Gallego, L. H.; Campos-Olivas, R.; Dolker, N.; Lietha, D. Structural basis for interdomain communication in SHIP2 providing high phosphatase activity. *eLife* **2017**, *6*, e26640/1.

(17) Ong, C. J.; Ming-Lum, A.; Nodwell, M.; Ghanipour, A.; Yang, L.; Williams, D. E.; Kim, J.; Demirjian, L.; Qasimi, P.; Ruschmann, J.; Cao, L. P.; Ma, K.; Chung, S. W.; Duronio, V.; Anderson, R. J.; Krystal, G.; Mui, A. L. Small-molecule agonists of SHIP1 inhibit the phosphoinositide 3-kinase pathway in hematopoietic cells. *Blood* **2007**, *110*, 1942.

(18) Tresaugues, L.; Silvander, C.; Flodin, S.; Welin, M.; Nyman, T.; Graeslund, S.; Hammarstroem, M.; Berglund, H.; Nordlund, P. Structural Basis for Phosphoinositide Substrate Recognition, Catalysis, and Membrane Interactions in Human Inositol Polyphosphate 5-Phosphatases. *Structure* **2014**, *22*, 744.

(19) Chamberlain, T. C.; Cheung, S. T.; Yoon, J. S. J.; Ming-Lum, A.; Gardill, B. R.; Shakibakho, S.; Dzananovic, E.; Ban, F.; Samiea, A.; Jawanda, K.; Priatel, J.; Krystal, G.; Ong, C. J.; Cherkasov, A.; Andersen, R. J.; McKenna, S. A.; Petegem, F. V.; Mui, A. L.-F. Interleukin-10 and Small Molecule SHIP1 Allosteric Regulators Trigger Anti-Inflammatory Effects Through SHIP1/STAT3 Complexes. *bioRxiv* **2020**.

(20) (a) Whisstock, J. C.; Romero, S.; Gurung, R.; Nandurkar, H.; Ooms, L. M.; Bottomley, S. P.; Mitchell, C. A. The inositol polyphosphate 5-phosphatases and the apurinic/aprimidinic base

excision repair endonucleases share a common mechanism for catalysis. *J. Biol. Chem.* **2000**, 275, 37055. (b) Whisstock, J. C.; Wiradjaja, F.; Waters, J. E.; Gurung, R. The structure and function of catalytic domains within inositol polyphosphate 5-phosphatases. *IUBMB Life* **2002**, 53, 15.

(21) Mol, C. D.; Izumi, T.; Mitra, S.; Tainer, J. A. DNA-bound structures and mutants reveal abasic DNA binding by APE1 DNA repair and coordination. *Nature* **2000**, 403, 451.

(22) Hengge, A. C. Mechanistic studies on enzyme-catalyzed phosphoryl transfer. *Adv. Phys. Org. Chem.* **2005**, 40, 49.

(23) (a) Mundle, S. T.; Delaney, J. C.; Essigmann, J. M.; Strauss, P. R. Enzymatic Mechanism of Human Apurinic/Apyrimidinic Endonuclease against a THF AP Site Model Substrate. *Biochemistry* **2009**, 48, 19. (b) Tsutakawa, S. E.; Shin, D. S.; Mol, C. D.; Izumi, T.; Arvai, A. S.; Mantha, A. K.; Szczesny, B.; Ivanov, I. N.; Hosfield, D. J.; Maiti, B.; Pique, M. E.; Frankel, K. A.; Hitomi, K.; Cunningham, R. P.; Mitra, S.; Tainer, J. A. Conserved Structural Chemistry for Incision Activity in Structurally Non-homologous Apurinic/Apyrimidinic Endonuclease APE1 and Endonuclease IV DNA Repair Enzymes. *J. Biol. Chem.* **2013**, 288, 8445.

(24) Aboelnga, M. M.; Wetmore, S. D. Unveiling a Single-Metal-Mediated Phosphodiester Bond Cleavage Mechanism for Nucleic Acids: A Multiscale Computational Investigation of a Human DNA Repair Enzyme. *J. Am. Chem. Soc.* **2019**, 141, 8646.

(25) Braun, W.; Schein, C. H. Membrane Interaction and Functional Plasticity of Inositol Polyphosphate 5-Phosphatases. *Structure* **2014**, 22, 664.

(26) Mills, S. J.; Silvander, C.; Cozier, G.; Tresaugues, L.; Nordlund, P.; Potter, B. V. L. Crystal Structures of Type-II Inositol Polyphosphate 5-Phosphatase INPP5B with Synthetic Inositol

Polyphosphate Surrogates Reveal New Mechanistic Insights for the Inositol 5-Phosphatase Family. *Biochemistry* **2016**, *55*, 1384.

(27) (a) Prasad, N. K.; Decker, S. J. SH2-containing 5'-inositol phosphatase, SHIP2, regulates cytoskeleton organization and ligand-dependent down-regulation of the epidermal growth factor receptor. *J Biol Chem* **2005**, *280*, 13129. (b) Prasad, N. K.; Tandon, M.; Badve, S.; Snyder, P. W.; Nakshatri, H. Phosphoinositol phosphatase SHIP2 promotes cancer development and metastasis coupled with alterations in EGF receptor turnover. *Carcinogenesis* **2008**, *29*, 25.

(c) Prasad, N. K. SHIP2 phosphoinositol phosphatase positively regulates EGFR-Akt pathway, CXCR4 expression, and cell migration in MDA-MB-231 breast cancer cells. *Int J Oncol* **2009**, *34*, 97. (d) Blunt, M. D.; Ward, S. G. Targeting PI3K isoforms and SHIP in the immune system: new therapeutics for inflammation and leukemia. *Curr. Opin. Pharmacol.* **2012**,

12, 444.

(28) Franke, T. F.; Kaplan, D. R.; Cantley, L. C.; Toker, A. Direct regulation of the Akt proto-oncogene product by phosphatidylinositol-3,4-bisphosphate. *Science* **1997**, *275*, 665.

(29) Jain, S. K.; Susa, M.; Keeler, M. L.; Carlesso, N.; Druker, B.; Varticovski, L. PI 3-kinase activation in BCR/abl-transformed hematopoietic cells does not require interaction of p85 SH2 domains with p210 BCR/abl. *Blood* **1996**, *88*, 1542.

(30) (a) Gewinner, C.; Wang, Z. C.; Richardson, A.; Teruya-Feldstein, J.; Etemadmoghadam, D.; Bowtell, D.; Barretina, J.; Lin, W. M.; Rameh, L.; Salmena, L.; Pandolfi, P. P.; Cantley, L. C. Evidence that inositol polyphosphate 4-phosphatase type II is a tumor suppressor that inhibits PI3K signaling. *Cancer Cell* **2009**, *16*, 115. (b) Ivetac, I.; Gurung, R.; Hakim, S.; Horan, K. A.; Sheffield, D. A.; Binge, L. C.; Majerus, P. W.; Tiganis, T.; Mitchell, C. A. Regulation of

PI(3)K/Akt signalling and cellular transformation by inositol polyphosphate 4-phosphatase-1.

EMBO Rep **2009**, *10*, 487.

(31) Kerr, W. G. Inhibitor and Activator: Dual Functions for SHIP in Immunity and Cancer. *Ann. N.Y. Acad. Sci* **2011**, *1217*, 1.

(32) Park, M. Y.; Srivastava, N.; Sudan, R.; Viernes, D. R.; Chisholm, J. D.; Engelman, R. W.; Kerr, W. G. Impaired T-cell survival promotes mucosal inflammatory disease in SHIP1-deficient mice. *Mucosal Immunol* **2014**, *7*, 1429.

(33) (a) Ruiz, A.; Heilmann, S.; Becker, T.; Hernandez, I.; Wagner, H.; Thelen, M.; Mauleon, A.; Rosende-Roca, M.; Bellenguez, C.; Bis, J. C.; Harold, D.; Gerrish, A.; Sims, R.; Sotolongo-Grau, O.; Espinosa, A.; Alegret, M.; Arrieta, J. L.; Lacour, A.; Leber, M.; Becker, J.; Lafuente, A.; Ruiz, S.; Vargas, L.; Rodriguez, O.; Ortega, G.; Dominguez, M. A.; Igap; Mayeux, R.; Haines, J. L.; Pericak-Vance, M. A.; Farrer, L. A.; Schellenberg, G. D.; Chouraki, V.; Launer, L. J.; van Duijn, C.; Seshadri, S.; Antunez, C.; Breteler, M. M.; Serrano-Rios, M.; Jessen, F.; Tarraga, L.; Nothen, M. M.; Maier, W.; Boada, M.; Ramirez, A. Follow-up of loci from the International Genomics of Alzheimer's Disease Project identifies TRIP4 as a novel susceptibility gene. *Transl Psychiatry* **2014**, *4*, e358. (b) Zhang, M.; Schmitt-Ulms, G.; Sato, C.; Xi, Z.;

Zhang, Y.; Zhou, Y.; St George-Hyslop, P.; Rogaeva, E. Drug Repositioning for Alzheimer's Disease Based on Systematic 'omics' Data Mining. *PLoS One* **2016**, *11*, e0168812.

(34) Lambert, J. C.; Ibrahim-Verbaas, C. A.; Harold, D.; Naj, A. C.; Sims, R.; Bellenguez, C.; Jun, G.; Destefano, A. L.; Bis, J. C.; Beecham, G. W.; Grenier-Boley, B.; Russo, G.; Thornton-Wells, T. A.; Jones, N.; Smith, A. V.; Chouraki, V.; Thomas, C.; Ikram, M. A.; Zelenika, D.; Vardarajan, B. N.; Kamatani, Y.; Lin, C. F.; Gerrish, A.; Schmidt, H.; Kunkle, B.; Dunstan, M. L.; Ruiz, A.; Bihoreau, M. T.; Choi, S. H.; Reitz, C.; Pasquier, F.; Hollingworth, P.; Ramirez, A.;

Hanon, O.; Fitzpatrick, A. L.; Buxbaum, J. D.; Campion, D.; Crane, P. K.; Baldwin, C.; Becker, T.; Gudnason, V.; Cruchaga, C.; Craig, D.; Amin, N.; Berr, C.; Lopez, O. L.; De Jager, P. L.; Deramecourt, V.; Johnston, J. A.; Evans, D.; Lovestone, S.; Letenneur, L.; Moron, F. J.; Rubinsztein, D. C.; Eiriksdottir, G.; Sleegers, K.; Goate, A. M.; Fievet, N.; Huentelman, M. J.; Gill, M.; Brown, K.; Kamboh, M. I.; Keller, L.; Barberger-Gateau, P.; McGuinness, B.; Larson, E. B.; Green, R.; Myers, A. J.; Dufouil, C.; Todd, S.; Wallon, D.; Love, S.; Rogaeva, E.; Gallacher, J.; St George-Hyslop, P.; Clarimon, J.; Lleo, A.; Bayer, A.; Tsuang, D. W.; Yu, L.; Tsolaki, M.; Bossu, P.; Spalletta, G.; Proitsi, P.; Collinge, J.; Sorbi, S.; Sanchez-Garcia, F.; Fox, N. C.; Hardy, J.; Naranjo, M. C.; Bosco, P.; Clarke, R.; Brayne, C.; Galimberti, D.; Mancuso, M.; Matthews, F.; European Alzheimer's Disease, I.; Genetic; Environmental Risk in Alzheimer's, D.; Alzheimer's Disease Genetic, C.; Cohorts for, H.; Aging Research in Genomic, E.; Moebus, S.; Mecocci, P.; Del Zompo, M.; Maier, W.; Hampel, H.; Pilotto, A.; Bullido, M.; Panza, F.; Caffarra, P.; Nacmias, B.; Gilbert, J. R.; Mayhaus, M.; Lannfelt, L.; Hakonarson, H.; Pichler, S.; Carrasquillo, M. M.; Ingelsson, M.; Beekly, D.; Alvarez, V.; Zou, F.; Valladares, O.; Younkin, S. G.; Coto, E.; Hamilton-Nelson, K. L.; Gu, W.; Razquin, C.; Pastor, P.; Mateo, I.; Owen, M. J.; Faber, K. M.; Jonsson, P. V.; Combarros, O.; O'Donovan, M. C.; Cantwell, L. B.; Soininen, H.; Blacker, D.; Mead, S.; Mosley, T. H., Jr.; Bennett, D. A.; Harris, T. B.; Fratiglioni, L.; Holmes, C.; de Bruijn, R. F.; Passmore, P.; Montine, T. J.; Bettens, K.; Rotter, J. I.; Brice, A.; Morgan, K.; Foroud, T. M.; Kukull, W. A.; Hannequin, D.; Powell, J. F.; Nalls, M. A.; Ritchie, K.; Lunetta, K. L.; Kauwe, J. S.; Boerwinkle, E.; Riemenschneider, M.; Boada, M.; Hiltunen, M.; Martin, E. R.; Schmidt, R.; Rujescu, D.; Wang, L. S.; Dartigues, J. F.; Mayeux, R.; Tzourio, C.; Hofman, A.; Nothen, M. M.; Graff, C.; Psaty, B. M.; Jones, L.; Haines, J. L.; Holmans, P. A.; Lathrop, M.; Pericak-Vance, M. A.; Launer, L. J.; Farrer, L. A.; van Duijn, C. M.; Van

Broeckhoven, C.; Moskvina, V.; Seshadri, S.; Williams, J.; Schellenberg, G. D.; Amouyel, P. Meta-analysis of 74,046 individuals identifies 11 new susceptibility loci for Alzheimer's disease. *Nat Genet* **2013**, *45*, 1452.

(35) Yoshino, Y.; Yamazaki, K.; Ozaki, Y.; Sao, T.; Yoshida, T.; Mori, T.; Mori, Y.; Ochi, S.; Iga, J. I.; Ueno, S. I. INPP5D mRNA Expression and Cognitive Decline in Japanese Alzheimer's Disease Subjects. *J Alzheimers Dis* **2017**, *58*, 687.

(36) (a) Wendeln, A. C.; Degenhardt, K.; Kaurani, L.; Gertig, M.; Ulas, T.; Jain, G.; Wagner, J.; Hasler, L. M.; Wild, K.; Skodras, A.; Blank, T.; Staszewski, O.; Datta, M.; Centeno, T. P.; Capece, V.; Islam, M. R.; Kerimoglu, C.; Staufenbiel, M.; Schultze, J. L.; Beyer, M.; Prinz, M.; Jucker, M.; Fischer, A.; Neher, J. J. Innate immune memory in the brain shapes neurological disease hallmarks. *Nature* **2018**, *556*, 332. (b) Keren-Shaul, H.; Spinrad, A.; Weiner, A.; Matcovitch-Natan, O.; Dvir-Szternfeld, R.; Ulland, T. K.; David, E.; Baruch, K.; Lara-Astaiso, D.; Toth, B.; Itzkovitz, S.; Colonna, M.; Schwartz, M.; Amit, I. A Unique Microglia Type Associated with Restricting Development of Alzheimer's Disease. *Cell* **2017**, *169*, 1276.

(37) Pedicone, C.; Fernandes, S.; Dungan, O. M.; Dormann, S. M.; Viernes, D. R.; Adhikari, A. A.; Choi, L. B.; De Jong, E. P.; Chisholm, J. D.; Kerr, W. G. Pan-SHIP1/2 inhibitors promote microglia effector functions essential for CNS homeostasis. *J. Cell. Sci.* **2019**, jcs.238030.

Chapter 2. Promoter-Free Formation of PMB Esters with 4-Methoxybenzyl-2,2,2-trichloroacetimidate

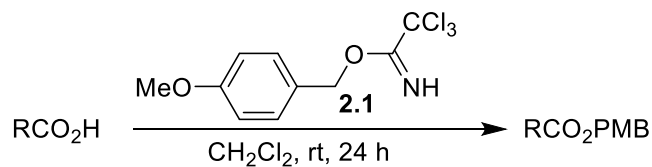
2.1. Introduction

4-Methoxybenzyl (PMB) esters are common protecting groups for carboxylates.¹⁻³ These esters are useful as they can be removed by treatment with Brønsted acids,^{4, 5} Lewis acids,⁶⁻⁸ or hydrogenation,^{9, 10} which nicely complements other esters that are typically removed via basic hydrolysis. The flexibility in the removal of PMB esters explains their increasingly common role in the synthesis of many complex molecules.¹¹⁻¹⁶ While the formation of 4-methoxybenzyl esters in simple molecules is usually achieved by alkylation reactions with 4-methoxybenzyl chloride, these conditions typically employ a strong base or acylation catalysts such as DMAP, which can limit the scope of these transformations in complex systems, as sensitive functionality often does not tolerate these conditions. To broaden the scope of the esterification with regard to base sensitive substrates some alternative methods have been developed,^{17, 18} but there remains a need for new methods of PMB ester formation that are compatible with polyfunctional complex molecules and occur under mild conditions. Additionally, it would be beneficial if these reactions are based on inexpensive starting materials. Recently Hayashi reported a single example using 4-methoxybenzyl-2,2,2-trichloroacetimidate (**2.1**) to form a PMB ester without the need for a promoter or catalyst.^{4, 5} This intriguing reaction seemed to indicate that 4-methoxybenzyl-2,2,2-trichloroacetimidate **2.1** may be well suited for the direct introduction of PMB esters. This reagent could serve as a precursor for the PMB ester protecting group since it is commercially available or easily synthesized from trichloroacetonitrile and 4-methoxybenzyl alcohol.¹⁹ An investigation into the generality of this ester formation was therefore initiated.

2.2. Results and Discussion

Initially we adopted the conditions of Hayashi,^{4,5} where dichloromethane was used as the solvent at 0 °C with two equivalents of the trichloroacetimidate. No advantage was found in performing the reaction at low temperature, so the use of an ice bath was abandoned. Some of the esterifications were sluggish, so a reaction time of 24 h was adopted to ensure complete conversion of the starting materials. Under these conditions benzoic acid was esterified in 89% yield after purification by silica column chromatography (**Table 2.1**, entry 1). Other benzoic acids possessing electron poor and electron rich substituents were also esterified in good yield under these conditions (**Table 2.1**, entries 2-4). Alkenes and alkynes were well tolerated (**Table 2.1**, entries 5 and 6) under these reaction conditions. 2-Picolinic acid also formed the PMB ester (**Table 2.1**, entry 7), demonstrating that heterocycles with basic functionality also participate in the esterification reaction.

Table 2.1. Esterifications of Aryl Carboxylic Acids with 4-Methoxybenzyl-2,2,2-trichloroacetimidate

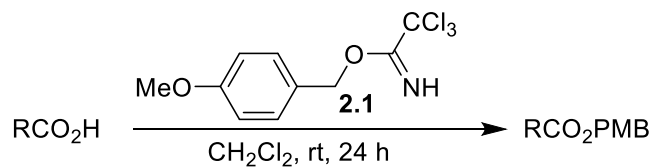


Entry	Ester Product	Yield (%)
1		89
2		85
3		80
4		92
5		94
6		99
7		89

^aReaction was allowed to proceed for 48 h

Alkyl substituted carboxylic acids also proved to be excellent substrates for the esterification reaction (**Table 2.2**). The yield of the esterification showed some dependence on the steric bulk of the group next to the carboxylic acid (**Table 2.2**, entries 1-4), with the yield decreasing slightly with increasing branching next to the carboxylic acid. In one particularly hindered case (entry 9) the reaction also required 48 h to proceed to high conversion. Still, the hindered ester 10 was formed in a synthetically useful 82% yield. The yields with hindered carboxylic acids were significantly higher than those obtained with more hindered imidates like the diphenylmethyl trichloroacetimidate,²⁰ likely for steric reasons. Some efforts were also made to investigate the functional group tolerance of the reaction. Highly electrophilic groups (like the bromide in 12) were quite compatible, providing the ester products in excellent yields. Esterification of vinylacetic acid provided ester **2.13** in 83% yield under the mild reaction conditions, with no detectable isomerization of the β,γ -unsaturated alkene to the more stable α,β position as determined by the analysis of the crude ¹H NMR of the reaction mixture. Other imidate esterifications have shown trace amounts of isomerization in this system,²⁰ and while the reason for the lack of isomerization with imidate **2.1** is unclear, this result indicates that PMB imidate **2.1** should be used in similar systems where isomerization is undesired. The presence of a free alcohol and a carbamate N-H bond were also well tolerated, as shown in entries 7 and 8. With the success of the esterification of N-Boc phenylalanine attempts were made to esterify unprotected phenylalanine, but this returned only the starting amino acid and unreacted imidate, likely due to the limited solubility of the zwitterionic amino acid in dichloromethane.

Table 2.2. Esterifications of Aliphatic Carboxylic Acids with 4-Methoxybenzyl-2,2,2-trichloroacetimidate



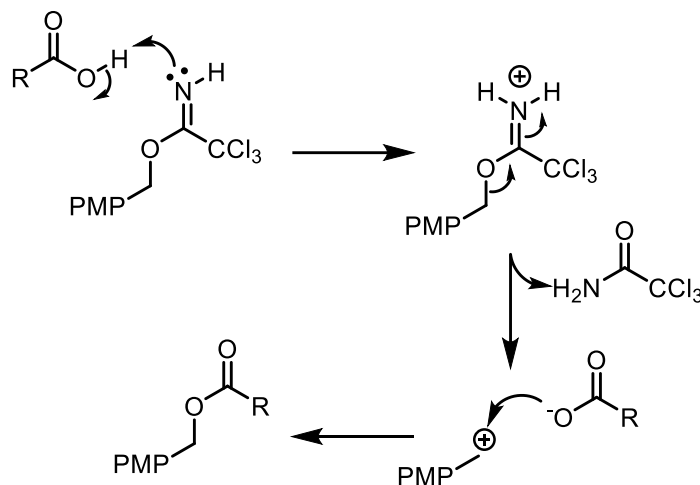
Entry	Ester Product	Yield (%)
1		89
2		86
3		82 ^a
4		78
5		93
6		83
7		79
8		91

^aReaction proceeded for 48 h.

A search of the literature revealed that in most cases esterification reactions with trichloroacetimidates require the presence of a Brønsted or Lewis acid.^{21, 22} Some imidates appear to be reactive enough to form esters without a promoter or catalyst, however. With 2-phenylisopropyl trichloroacetimidate,^{23, 24} glycosyl imidates^{25, 26} and diphenylmethyl 2,2,2-trichloroacetimidate²⁰ ester formation has been reported to occur spontaneously. Schmidt also observed similar reactivity with glycosyl trichloroacetimidates and phosphoric acids leading to the corresponding phosphate esters.^{27, 28} These results indicate that, at least in cases where the corresponding cation is highly stabilized, imidates can be employed to form esters without the need for a catalyst or promoter under mild reaction conditions.

Given that ester formation only occurs in cases where the corresponding cation is especially stabilized, an S_N1 type reaction pathway is implicated in the formation of these esters (Scheme 2.1). The carboxylic acid itself may act as a promoter in this esterification by protonating the basic imidate nitrogen. This would explain the unreactive nature of phenylalanine, as the amino acid exists as a zwitterion with a significantly higher pK_a than a typical carboxylic acid. After activation the protonated imidate can then ionize to form the 4-methoxybenzyl cation, which is then trapped by the carboxylate nucleophile to form the ester. To test the hypothesis of self-promotion, the esterification reaction was attempted with benzoic acid in the presence of two equivalents of triethylamine. No ester formation was observed, leading to the conclusion that activation of the imidate by protonation with the carboxylic acid appears to be a necessary component of the reaction. The successful esterification with 2-picolinic acid in **Table 2.1** (entry 15) can be rationalized by the greater acidity of the pyridinium as opposed to the ammonium formed with triethylamine.

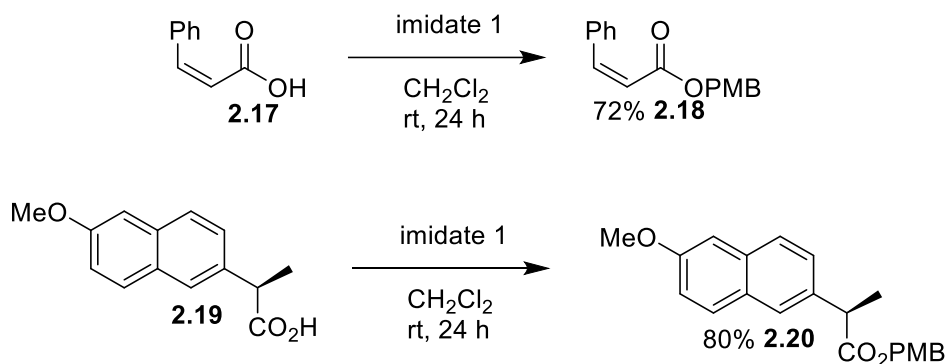
Scheme 2.1. Proposed Mechanism of the Esterification



In order to investigate the effectiveness of these esterification conditions on sensitive substrates some further studies were undertaken (**Scheme 2.2**). First the esterification was performed with the 92:8 cis:trans mixture of α,β -unsaturated ester **2.17**, which was produced by Lindlar reduction of the corresponding alkyne.²⁹ Similar systems are highly prone to isomerization under basic conditions or with common esterification catalysts such as DMAP.³⁰⁻³² Treatment of acid **2.17** with two equivalents of imidate **2.1** gave the corresponding ester in 72% yield after chromatography. No isomerization to the more stable *trans* isomer was detected in the ¹H NMR of the purified product, which showed an unchanged 92:8 ratio of products. This is the first example of the use of an imidate to alkylate a *Z*- In summary, a mild method for protecting carboxylic acids in high yields as their corresponding PMB esters using the commercially available 4-methoxybenzyl-2,2,2-trichloroacetimidate has been explored. The methodology is noteworthy as, unlike with many other imidates,^{20,21} it does not require addition of Brønsted or Lewis acids to form the PMB ester. The transformation is also highly selective for the carboxylic acid functional group, with unprotected alcohols and carbamates being unreactive. These esterification conditions have been shown to be compatible with sensitive systems such as α -

chiral carboxylic acids and cis- α,β -unsaturated carboxylic acids, which form esters without racemization or isomerization, respectively. This method may be of value for the protection of complex polyfunctional substrates, which may decompose under more common esterification conditions. -unsaturated carboxylic acid as a substrate, presenting a straightforward route to access these structures from the corresponding carboxylic acid without isomerization. Next, a chiral carboxylic acid bearing an α -stereocenter was esterified with imidate **2.1**. Chiral naproxen **2.19** was chosen as a challenging substrate for this transformation, as the stereocenter is both benzylic and next to the carboxylic acid, which should allow for facile racemization. Treatment of (*R*)-naproxen with imidate **2.1** provided the PMB ester **2.20** in 80% yield with no detectable racemization of the product as determined by chiral HPLC analysis (the product was compared to racemic material prepared by heating the chiral ester with DBU in toluene). These experiments highlight the effectiveness of these reaction conditions with regard to base sensitive substrates.

Scheme 2.2. Esterification of Sensitive Substrates

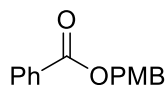


2.3. Conclusion

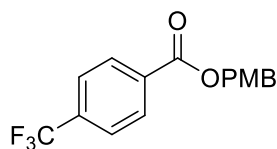
In summary, a mild method for protecting carboxylic acids in high yields as their corresponding PMB esters using the commercially available 4-methoxybenzyl-2,2,2-

trichloroacetimidate has been explored. The methodology is significant, as unlike with many other imidate-based esterification,^{21,22} it does not require addition of a Brønsted or Lewis acid promoter or catalyst to form the PMB ester. The transformation is also selective for the carboxylic acid functional group, with unprotected alcohols and carbamate nitrogens being unreactive. These esterification conditions are compatible with sensitive systems such as α -chiral carboxylic acids and *cis*- α,β -unsaturated carboxylic acids, which form esters without racemization or isomerization, respectively. This method may be of value for the protection of complex polyfunctional substrates, which often decompose under more common esterification conditions.

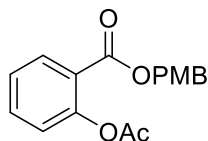
General conditions for esterification using 4-methoxybenzyl-2,2,2-trichloroacetimidate: The carboxylic acid (1.50 mmol) was dissolved in anhydrous CH₂Cl₂ (6 mL, to provide a 0.25M solution). 4-Methoxybenzyl-2,2,2-trichloroacetimidate (430 mg, 3.00 mmol, 2.0 equiv) was then added. After 24 h TLC indicated that all of the starting material had been consumed. The reaction mixture was taken up in ethyl acetate and washed with sodium bicarbonate (sat. aq., 3x). The organic layer was dried (Na₂SO₄), filtered and concentrated. The residue was adsorbed on silica gel and purified by silica gel chromatography to provide the corresponding PMB ester.



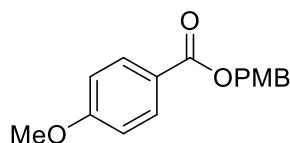
4-Methoxybenzylbenzoate (2.2).¹⁸ Colorless oil (530 mg, 89%): TLC R_f = 0.57 (20:80 ethyl acetate:hexanes); ¹H NMR (300 MHz, CDCl₃) δ 8.10-8.03 (m, 2H), 7.59-7.51 (m, 1H), 7.47-7.36 (m, 4H), 6.92 (d, J = 8.8 Hz, 2H), 5.31 (s, 2H), 3.82 (s, 3H); ¹³C NMR (75 MHz, CDCl₃) δ 166.7, 159.9, 133.2, 130.5, 130.3, 129.9, 128.5, 128.4, 114.2, 66.7, 55.5.



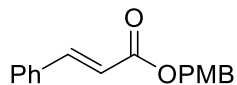
4-Methoxybenzyl-4-(trifluoromethyl)benzoate (2.3). White solid (415 mg, 85%): TLC R_f = 0.47 (15:85 ethyl acetate:hexanes); mp = 48-49 °C; IR (film) 3051, 3014, 2961, 2914, 2841, 1721 cm⁻¹; ¹H NMR (300 MHz, CDCl₃) δ 8.16 (d, J = 8.1 Hz, 2H), 7.69 (d, J = 8.1 Hz, 2H), 7.40 (d, J = 8.7 Hz, 2H), 6.93 (d, J = 8.7 Hz, 2H), 5.33 (s, 2H), 3.82 (s, 3H); ¹³C NMR (75 MHz, CDCl₃) δ 165.4, 160.0, 135.2 (q, J = 33 Hz), 130.4, 129.2, 127.8, 125.5 (q, J = 277 Hz), 125.4, 118.5, 114.2, 67.3, 55.5; Anal calcd for C₁₆H₁₃F₃O₃; C, 61.94, H, 4.22. Found C, 61.94, H, 4.24.



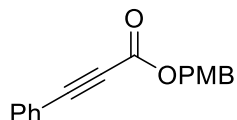
4-Methoxybenzyl-2-acetoxybenzoate (2.4). Colorless oil (534 mg, 80%): TLC R_f = 0.69 (25:75 ethyl acetate:hexanes); IR (neat) 2957, 2837, 1769, 1720, 1610, 1515, 1248 1195 cm^{-1} ; ^1H NMR (300 MHz, CDCl_3) δ 8.04 (d, J = 1.7 Hz, 1H), 7.54 (t, J = 9.0 Hz, 1H), 7.38-7.29 (m, 3H), 7.09 (d, J = 9.0 Hz, 1H), 6.92 (d, J = 8.7 Hz, 2H), 5.24 (s, 2H), 3.81 (s, 3H), 2.13 (s, 3H); ^{13}C NMR (75 MHz, CDCl_3) δ 169.8, 164.6, 159.9, 150.7, 133.2, 132.1, 130.5, 127.7, 126.1, 123.9, 123.5, 114.3, 67.0, 55.4, 20.8. Anal calcd for $\text{C}_{17}\text{H}_{16}\text{O}_5$: C, 67.99; H, 5.37. Found: C, 67.60; H, 5.17.



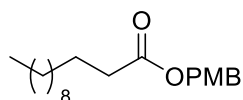
4-Methoxybenzyl-4-methoxybenzoate (2.5).³⁴ Colorless oil (788 mg, 92%): TLC R_f = 0.56 (15:85 ethyl acetate:hexanes); ^1H NMR (300 MHz, CDCl_3) δ 8.03 (d, J = 8.0 Hz, 2H), 7.39 (d, J = 8.5 Hz, 2H), 6.99-6.88 (m, 4H), 5.27 (s, 2H), 3.87 (s, 3H), 3.84 (s, 3H); ^{13}C NMR (75 MHz, CDCl_3) δ 166.5, 163.6, 159.8, 131.9, 130.2, 128.7, 122.9, 114.2, 113.8, 66.5, 55.6, 55.5.



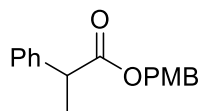
4-Methoxybenzylcinnamate (2.6).³⁴ White solid (508 mg, 94%): TLC R_f = 0.64 (20:80 ethyl acetate:hexanes); mp = 61-63 $^\circ\text{C}$; ^1H NMR (300 MHz, CDCl_3) δ 7.71 (d, J = 16.2 Hz, 1H), 7.55-7.48 (m, 2H), 7.41-7.33 (m, 5H), 6.92 (d, J = 8.8 Hz, 2H), 6.47 (d, J = 16.2 Hz, 1H), 5.19 (s, 2H), 3.82 (s, 3H); ^{13}C NMR (75 MHz CDCl_3) δ 167.0, 159.8, 145.1, 134.5, 130.4, 130.3, 129.0, 128.3, 128.2, 118.1, 114.1, 66.3, 55.4.



4-Methoxybenzyl-3-phenylpropiolate (2.7). White solid (545 mg, 99%): TLC R_f = 0.84 (10:90 ethyl acetate:hexanes); IR (neat) 2956, 2837, 2257, 1694, 1514, 1235 cm^{-1} ; mp = 141-146°C; ^1H NMR (300 MHz, CDCl_3) δ 7.50 (d, 2H, J = 9.0 Hz), 7.37-7.26 (m, 5H), 6.81 (d, 2H, J = 9.0 Hz), 5.13 (s, 2H), 3.73 (s, 3H); ^{13}C NMR (75 MHz CDCl_3) δ 160.2, 154.2, 133.2, 130.9, 130.8, 128.8, 127.3, 119.2, 114.3, 86.7, 80.9, 67.8, 55.5; Anal calcd for $\text{C}_{17}\text{H}_{14}\text{O}_3$: C, 76.68; H, 5.30. Found: C, 76.60; H, 5.27.

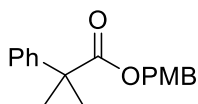


4-Methoxybenzyl dodecanoate (2.8). Colorless oil (954 mg, 89%): TLC R_f = 0.91 (10:90 ethyl acetate:hexanes); IR (neat) 2956, 2837, 1694, 1514, 1235, 900 cm^{-1} ; ^1H NMR (300 MHz, CDCl_3) δ 7.22 (d, J = 9.0 Hz, 2H), 6.81 (d, J = 9.0 Hz, 2H), 4.97 (s, 2H), 3.79 (s, 3H), 2.25 (t, J = 9.0 Hz, 3H), 1.61-1.53 (m, 2H), 1.30-1.10 (m, 17H), 0.81 (t, 3H, J = 6.0 Hz, 3H); ^{13}C NMR (75 MHz CDCl_3) δ 169.9, 160.8, 130.4, 127.6, 114.2, 67.6, 55.5, 35.2, 32.1, 29.8, 29.7, 29.6, 29.1, 27.5, 22.9, 14.4; Anal calcd for $\text{C}_{20}\text{H}_{32}\text{O}_3$: C, 74.96; H, 10.06. Found: C, 74.96; H, 10.25.

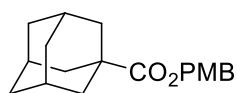


(±)-4-Methoxybenzyl-2-phenylpropionate (2.9). Colorless oil (464 mg, 86%): TLC R_f = 0.51 (20:80 ethyl acetate:hexanes); IR (neat) 2956, 2837, 1734, 1514, 1235 cm^{-1} ; ^1H NMR (300 MHz, CDCl_3) δ 7.31-7.22 (m, 5H), 7.20 (d, J = 9.0 Hz, 2H), 6.82 (d, J = 9.0 Hz, 2H), 5.04 (q, J = 6.0

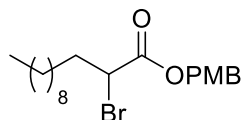
Hz, 2H), 3.79-3.76 (m, 1H), 3.71 (s, 3H), 1.50 (d, $J = 6.0$ Hz, 3H); ^{13}C NMR (75 MHz CDCl_3) δ 173.8, 160.0, 138.5, 130.2, 128.8, 128.7, 127.3, 126.9, 114.2, 73.2, 67.8, 55.5; Anal calcd for $\text{C}_{17}\text{H}_{18}\text{O}_3$: C, 75.53; H, 6.71. Found: C, 75.41; H, 6.65.



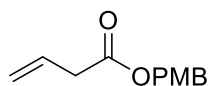
4-Methoxybenzyl-2-methyl-2-phenyl-propanoate (2.10). White solid (250 mg, 82%): mp = 53-54 °C. TLC $R_f = 0.52$ (10:90 ethyl acetate:hexanes). IR (solid) 3024, 2988, 2972, 2939, 2839, 1894, 1725, 1613, 1582, 1442, 1315, 1178, 1028 cm^{-1} . ^1H NMR (CDCl_3 , 300 MHz) δ 7.30 (d, $J = 4.4$ Hz, 4H), 7.26-7.20 (m, 1H), 7.15 (d, $J = 8.9$ Hz, 2H), 6.82 (d, $J = 8.9$ Hz, 2H), 5.04 (s, 2H), 3.80 (s, 3H), 1.58 (s, 6H). ^{13}C NMR (CDCl_3 , 75 MHz) δ 176.6, 159.5, 144.7, 129.7, 128.5, 128.4, 126.8, 113.9, 125.8, 66.4, 55.3, 46.7, 26.6. Anal. calcd for $\text{C}_{18}\text{H}_{20}\text{O}_3$: C, 76.03; H, 7.09. Found: C, 76.39; H, 7.07.



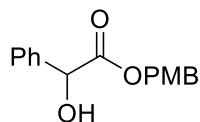
4-Methoxybenzyladamantane carboxylate (2.11).³⁴ Colorless oil (520 mg, 78%): TLC $R_f = 0.65$ (25:75 ethyl acetate:hexanes); IR (neat) 2999, 2906, 2851, 1724, 1514, 1229 cm^{-1} ; ^1H NMR (300 MHz, CDCl_3) δ 7.27 (d, $J = 8.6$ Hz, 2H), 6.88 (d, $J = 8.7$ Hz, 2H), 5.03 (s, 2H), 3.81 (s, 3H), 2.00-1.71 (m, 15H); ^{13}C NMR (75 MHz CDCl_3) δ 177.6, 159.4, 129.5, 113.8, 65.6, 55.3, 38.8, 36.5, 27.9.



4-Methoxybenzyl-2-bromododecanoate (2.12). Yellow oil (407 mg, 93%): TLC $R_f = 0.65$ (25:75 ethyl acetate:hexanes); IR (neat) 3001, 2906, 2851, 1724, 1514, 1229 cm^{-1} ; ^1H NMR (300 MHz, CDCl_3) δ 7.25 (d, $J = 9.0$ Hz, 2H), 6.82 (d, $J = 9.0$ Hz, 2H), 5.07 (s, 2H), 4.15 (t, 1H), 3.73 (s, 3H), 1.98-1.91 (m, 2H), 1.30-1.10 (m, 16H), 0.82 (t, $J = 6.0$ Hz, 3H); ^{13}C NMR (75 MHz CDCl_3) δ 170.0, 160.8, 130.4, 127.6, 114.2, 67.6, 55.5, 46.4, 35.2, 32.1, 29.8, 29.7, 29.6, 29.1, 27.5, 22.9, 14.6; Anal calcd for $\text{C}_{20}\text{H}_{31}\text{BrO}_3$: C, 60.16; H, 7.82. Found: C, 60.01; H, 7.52.

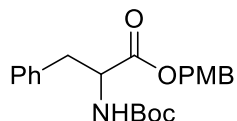


4-Methoxybenzyl-but-3-enoate (2.13).³⁵ Colorless oil (389 mg, 93 % yield): $R_f = 0.50$ (5:95 ethyl acetate:hexanes); ^1H NMR (300 MHz, CDCl_3) δ 7.23 (d, $J = 9.0$ Hz, 2H), 6.81 (d, $J = 9.0$ Hz, 2H), 5.92-5.82 (m, 1H), 5.13-5.11 (m, 1H), 5.08-5.03 (m, 1H), 5.00 (s, 2H), 3.72 (s, 3H), 3.06-3.03 (m, 2H); ^{13}C NMR (75 MHz CDCl_3) δ 171.6, 159.9, 130.5, 130.4, 128.2, 118.8, 114.2, 66.5, 55.5, 39.4.

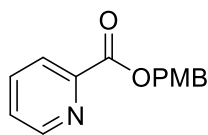


(±)-4-Methoxybenzyl-2-hydroxy-2-phenylacetate (2.14).¹⁸ Colorless oil (495 mg, 79%): TLC $R_f = 0.65$ (30:70 ethyl acetate:hexanes). ^1H NMR (300 MHz, CDCl_3) δ 7.35-7.25 (m, 5H), 7.09 (d, $J = 9.0$ Hz, 2H), 6.78 (d, $J = 9.0$ Hz, 2H), 5.11- 4.96 (m, 3H), 3.71 (s, 3H), 3.57 (d, $J = 6.0$ Hz, 1H); ^{13}C NMR (75 MHz CDCl_3) δ 173.8, 160.0, 138.5, 130.2, 128.8, 128.7, 127.3, 126.9,

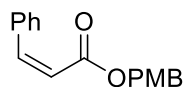
114.2, 73.2, 67.8, 55.5.



(±)-4-Methoxybenzyl-2-[(tert-butoxycarbonyl)amino]phenylpropionate (2.15).³⁶ Colorless oil (342 mg, 89%): TLC R_f = 0.61 (30:70 ethyl acetate:hexanes); ^1H NMR (300 MHz, CDCl_3) δ 7.20-7.11 (m, 5H), 6.99-6.87 (m, 2H), 6.75 (d, J = 9.0 Hz, 2H), 5.03-4.97 (m, 3H), 4.60-4.45 (m, 1H), 3.73 (s, 3H), 3.11-2.90 (m, 2H), 1.35 (s, 9H); ^{13}C NMR (75 MHz CDCl_3) δ 173.5, 160.1, 155.5, 138.6, 132.3, 130.3, 129.5, 127.8, 127.5, 114.6, 80.2, 67.1, 55.5, 54.0, 39.1, 28.5.

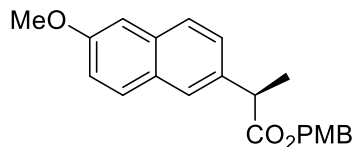


4-Methoxybenzylpicolinate (2.16) Yellow oil (516 mg, 83%): TLC R_f = 0.30 (50:50 ethyl acetate:hexanes); IR (film) 3057, 3005, 2957, 2837, 1717 cm^{-1} ; ^1H NMR (300 MHz, CDCl_3) δ 8.76 (d, J = 7.2 Hz, 1H), 8.12 (d, J = 8.7 Hz, 1H), 7.85-7.79 (m, 1H), 7.48-7.42 (m, 3H), 6.90 (d, J = 8.7 Hz, 2H), 5.40 (s, 2H), 3.81 (s, 3H); ^{13}C NMR (75 MHz, CDCl_3) δ 165.2, 159.8, 150.0, 148.2, 137.0, 130.6, 127.9, 127.0, 125.3, 114.0, 67.4, 55.3; Anal calcd for $\text{C}_{14}\text{H}_{13}\text{NO}_3$: C, 69.12; H, 5.39; N, 5.76. Found C, 69.52; H, 5.65; N, 5.73.



(Z)-4-Methoxybenzyl-3-phenylacrylate (2.18). Colorless oil (130 mg, 72%): TLC R_f = 0.80 (30:70 ethyl acetate:hexanes); IR (thin film) 3002, 2990, 1738, 1623, 1550, 1229, 1090, 710 cm^{-1}

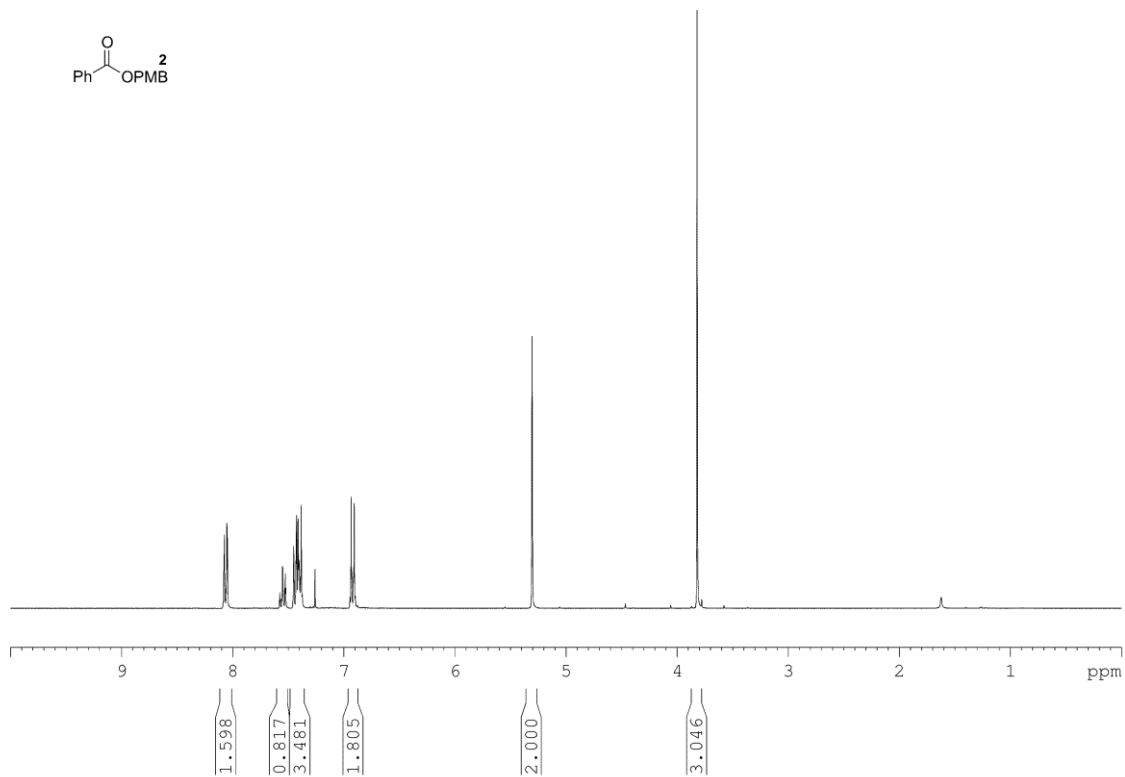
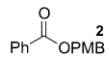
¹H NMR (300 MHz, CDCl₃) δ 7.52-7.47 (m, 2H), 7.32-7.29 (m, 3H), 7.26 (d, *J* = 6.0 Hz, 2H), 7.19-7.17 (m, 3H), 5.90 (d, *J* = 9.4 Hz, 1H), 5.24 (s, 2H), 3.72 (s, 3H); ¹³C NMR (75 MHz CDCl₃) δ 166.6, 159.2, 145.2, 134.0, 129.9, 129.0, 128.9, 128.5, 128.2, 115.7, 113.4, 66.9, 56.2; Anal calcd for C₁₇H₁₆O₃: C, 76.10; H, 6.10. Found: C, 76.01; H, 5.86.

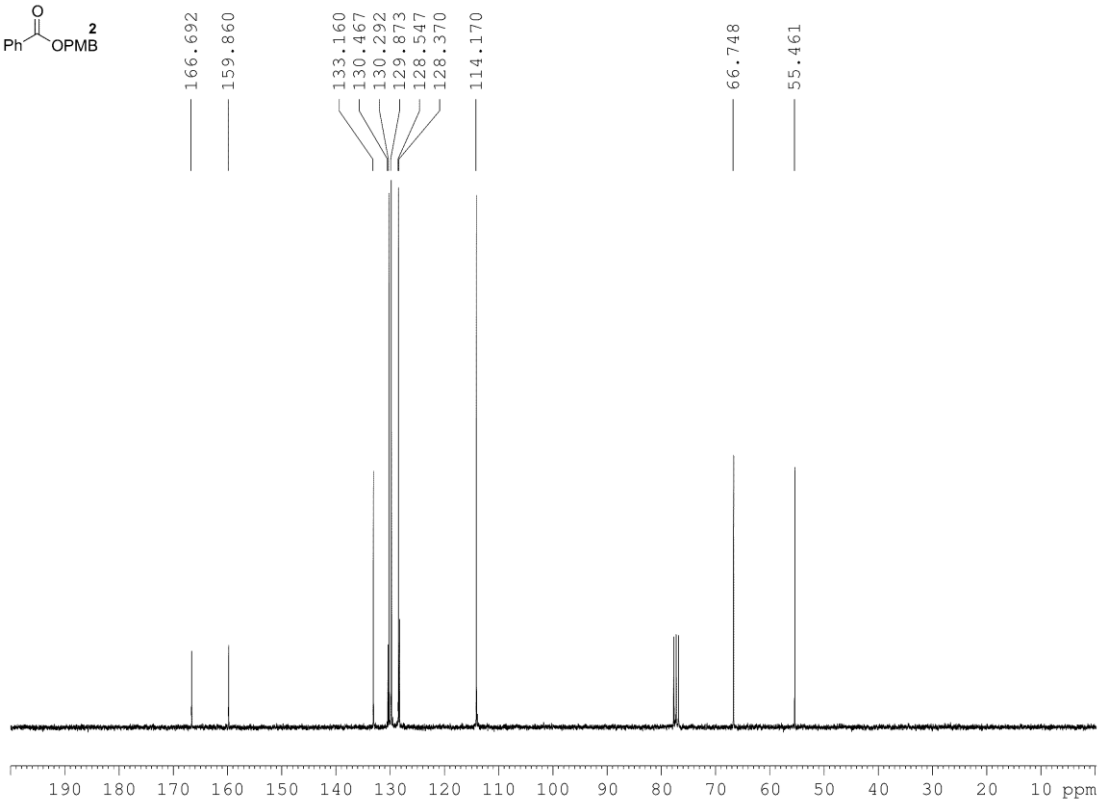
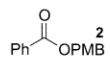


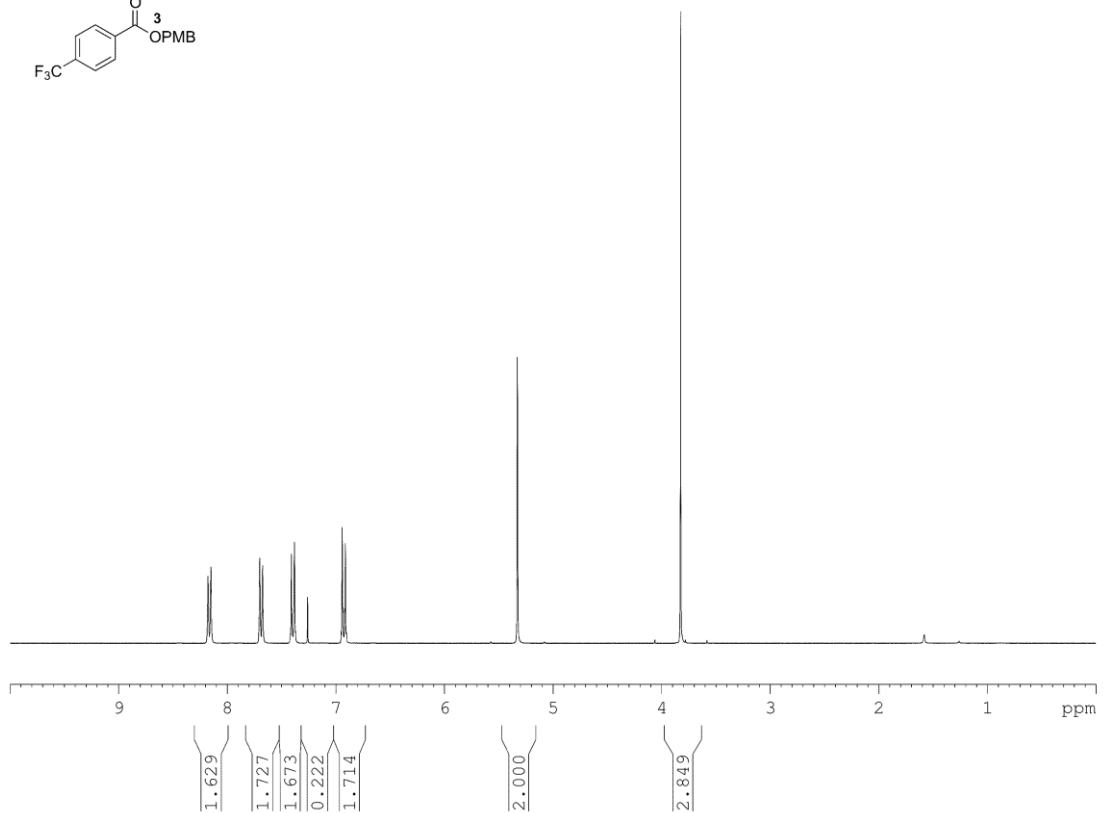
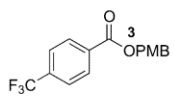
(R)-4-Methoxybenzyl-2-(6-methoxynaphthalen-2-yl)propanoate (2.20). White solid (426 mg, 80%); [α]_D²² = -9.9 (*c* = 0.9 in CH₂Cl₂); mp = 120-122 °C. TLC *R*_f = 0.71 (30:70 ethyl acetate:hexanes); IR (thin film) 3006, 2890, 1748, 1635, 1550, 1289, 1090, 780 cm⁻¹; ¹H NMR (300 MHz, CDCl₃) δ 7.63-7.55 (m, 3H), 7.31 (dd, *J* = 8.5, 1.8 Hz, 1H), 7.13-7.05 (m, 4H), 6.75 (d, *J* = 6.0 Hz, 2H) 4.98 (ab q, *J* = 12.0 Hz, 2H), 3.91 (s, 3H), 3.79 (q, *J* = 7.0 Hz, 1H), 3.69 (s, 3H), 1.49 (d, *J* = 6.6 Hz, 3H); ¹³C NMR (75 MHz CDCl₃) δ 174.8, 159.9, 157.8, 135.9, 133.9, 130.1, 129.5, 129.1, 128.4, 127.3, 126.5, 126.2, 119.2, 114.1, 105.8, 66.6, 55.55, 55.49, 45.7, 18.8; Anal calcd for C₂₂H₂₂O₄: C, 75.41; H, 6.33. Found: C, 75.44; H, 6.33.

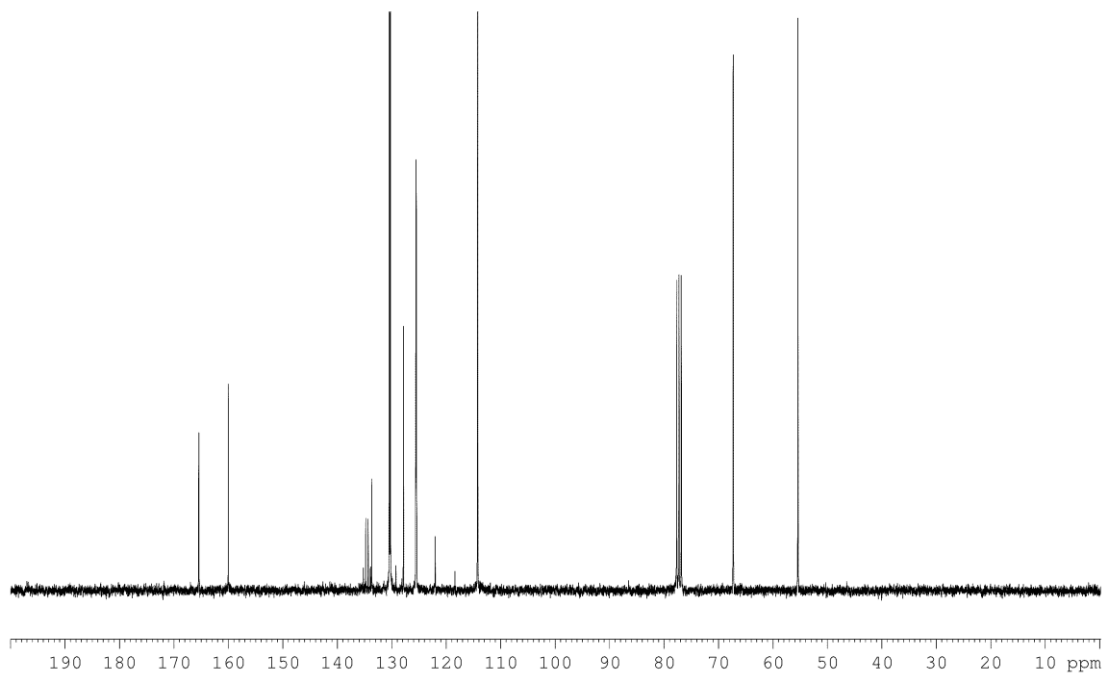
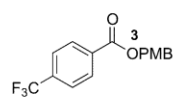
Racemization of Ester 2.20. (-)-Ester **2.20** (0.14 mmol, 50 mg) was dissolved in 2 mL of THF. DBU was added (0.14 mmol, 22μL) and the reaction mixture was warmed to 40 °C for 12 h. The reaction mixture was then cooled to room temp, taken up in ethyl acetate, washed with 1M HCl (3x), dried (Na₂SO₄), filtered and concentrated. The residue was adsorbed on silica gel and purified by silica gel chromatography using 30:70 ethyl acetate:hexanes to provide 48 mg (96%) of (±)-4-methoxybenzyl-2-(6-methoxy-2-naphthyl)propanoate **20**. The enantiomeric ratio was

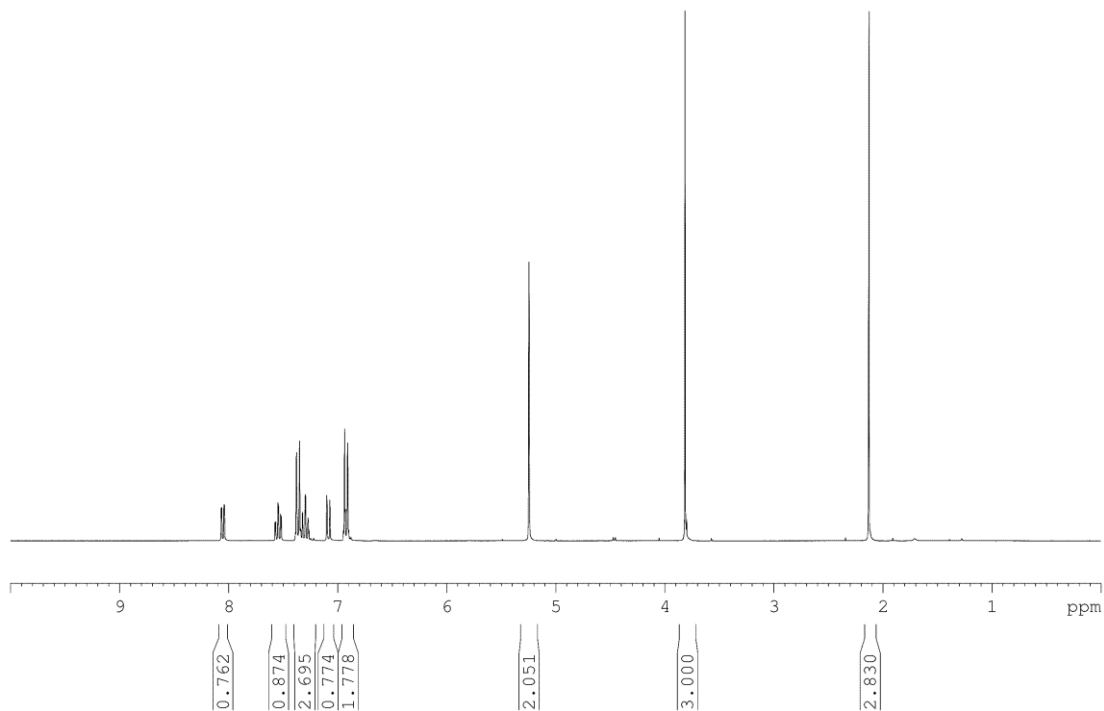
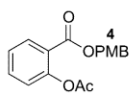
determined by HPLC using a chiral column (OD-H), n-hexane:*i*-PrOH = 90:10, 1 mL/min; (*R*)-enantiomer $t_R = 15.3$ min, (*S*)-enantiomer $t_R = 17.9$ min.

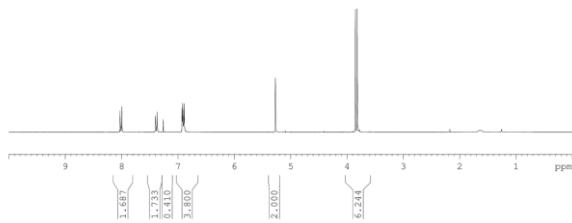
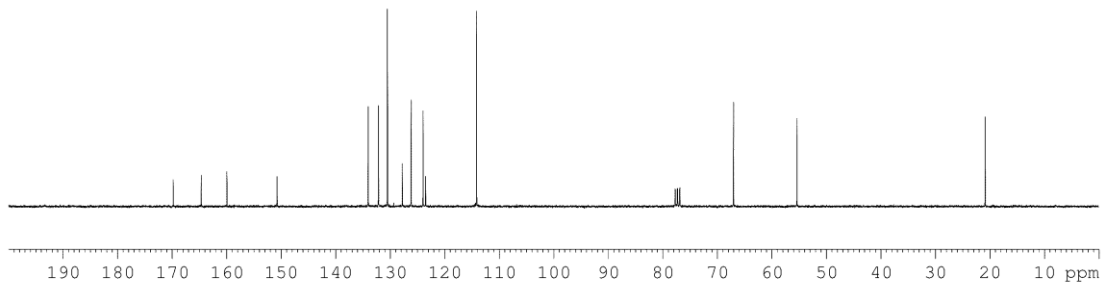
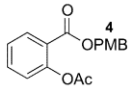


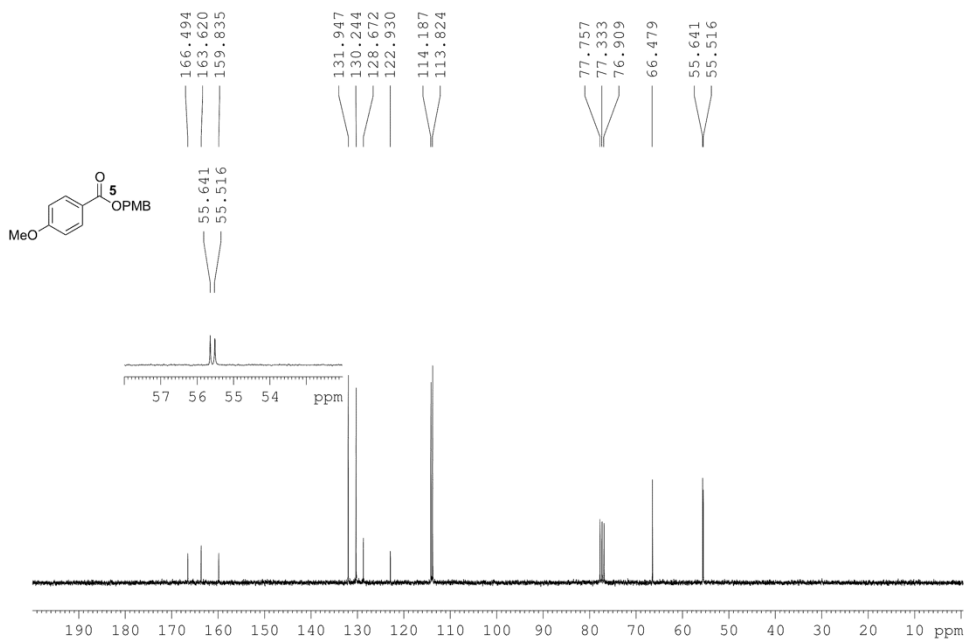


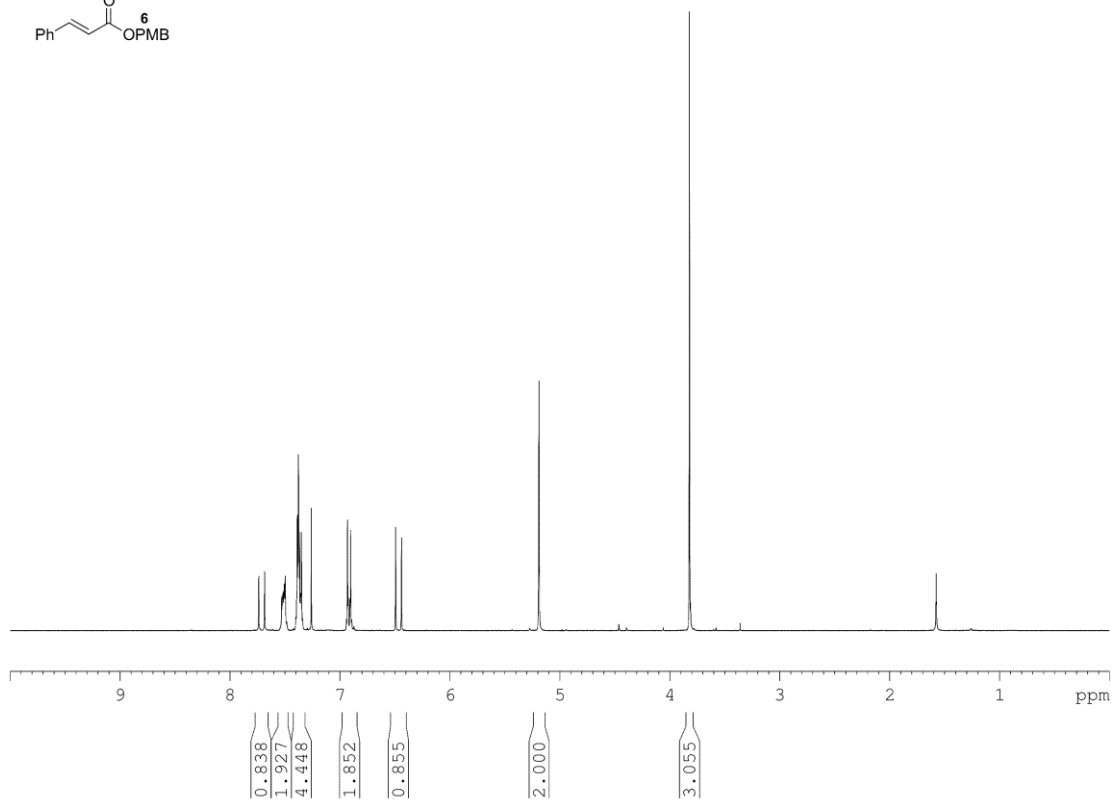
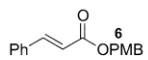


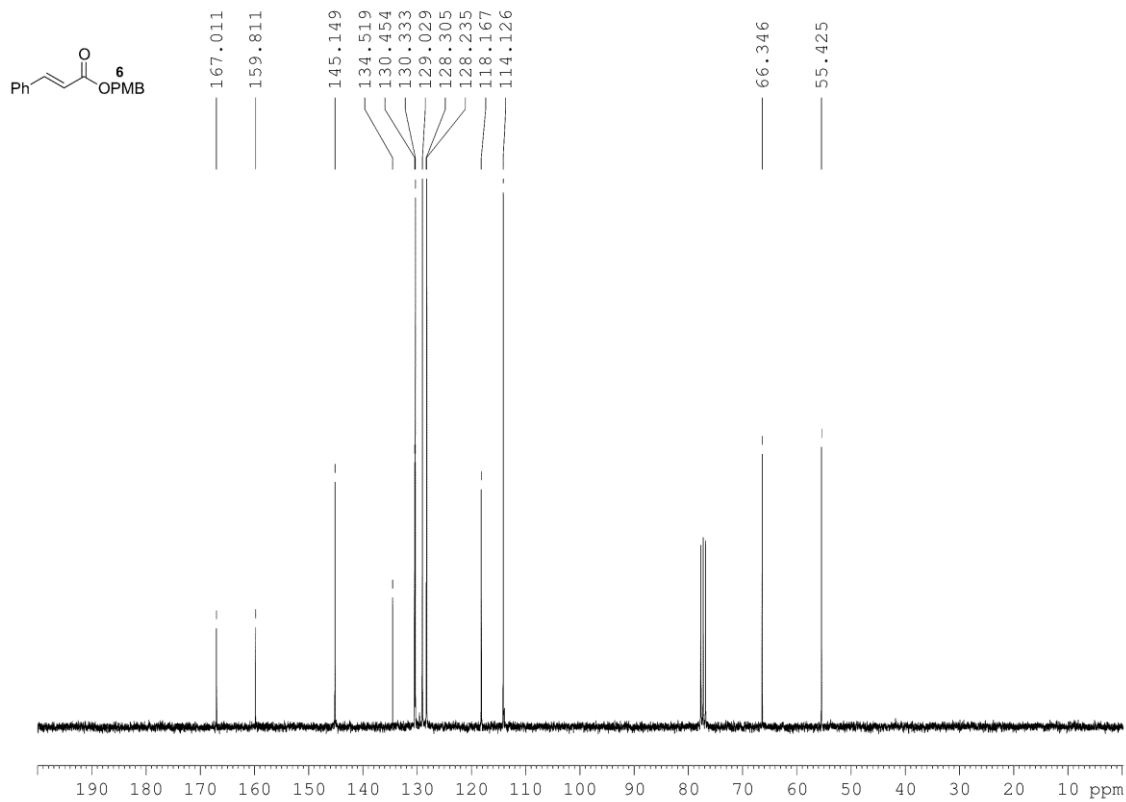


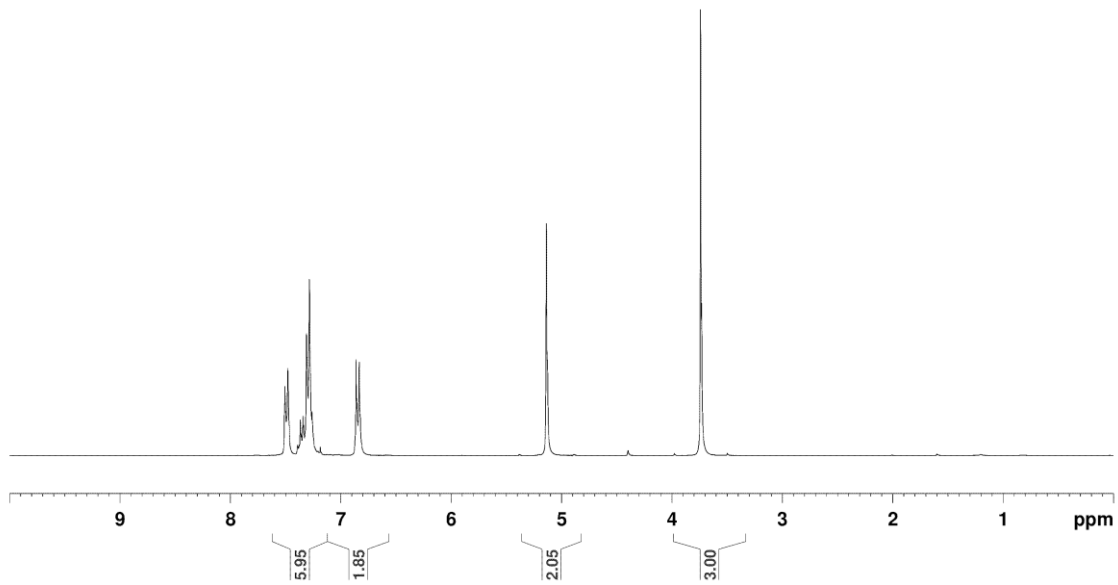
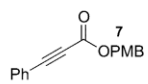


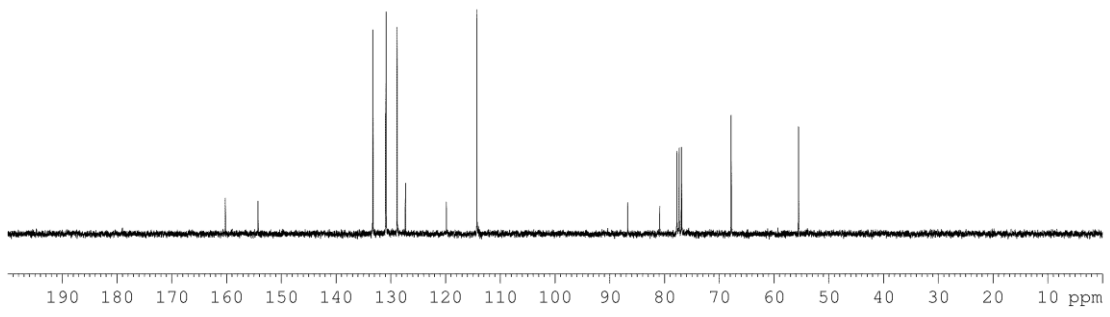
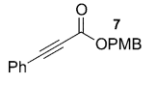


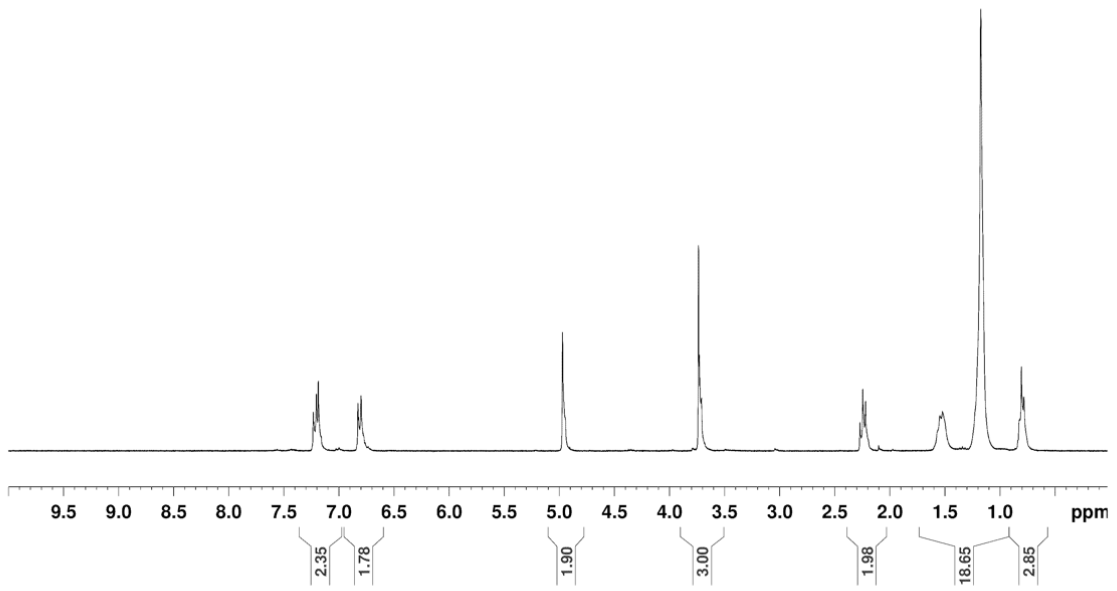
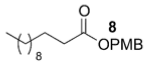


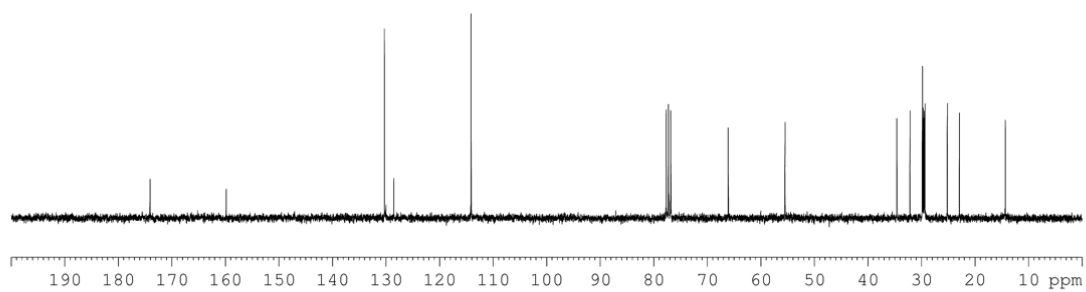
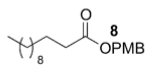


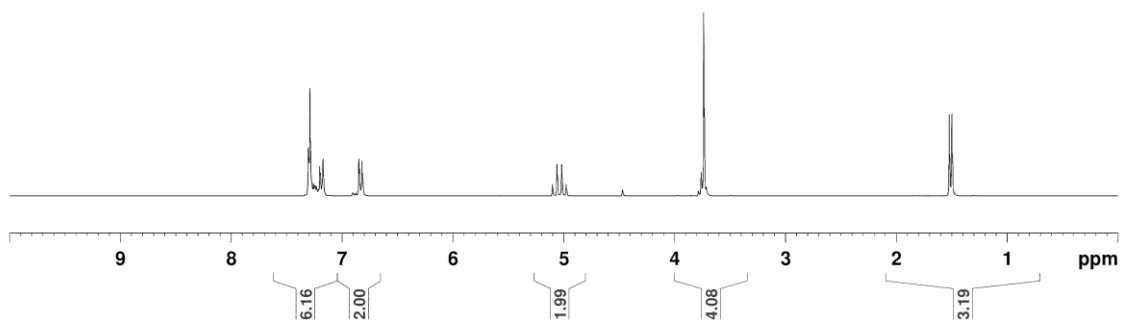
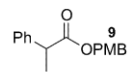


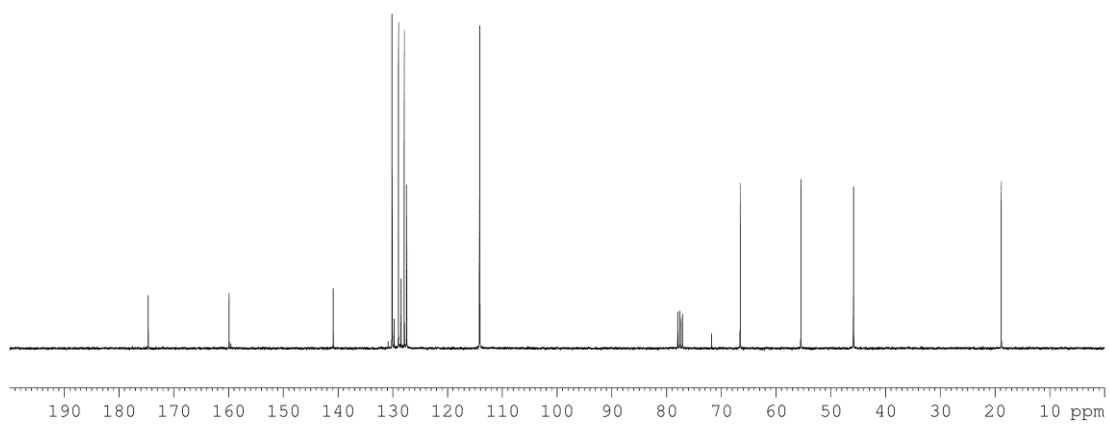
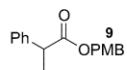


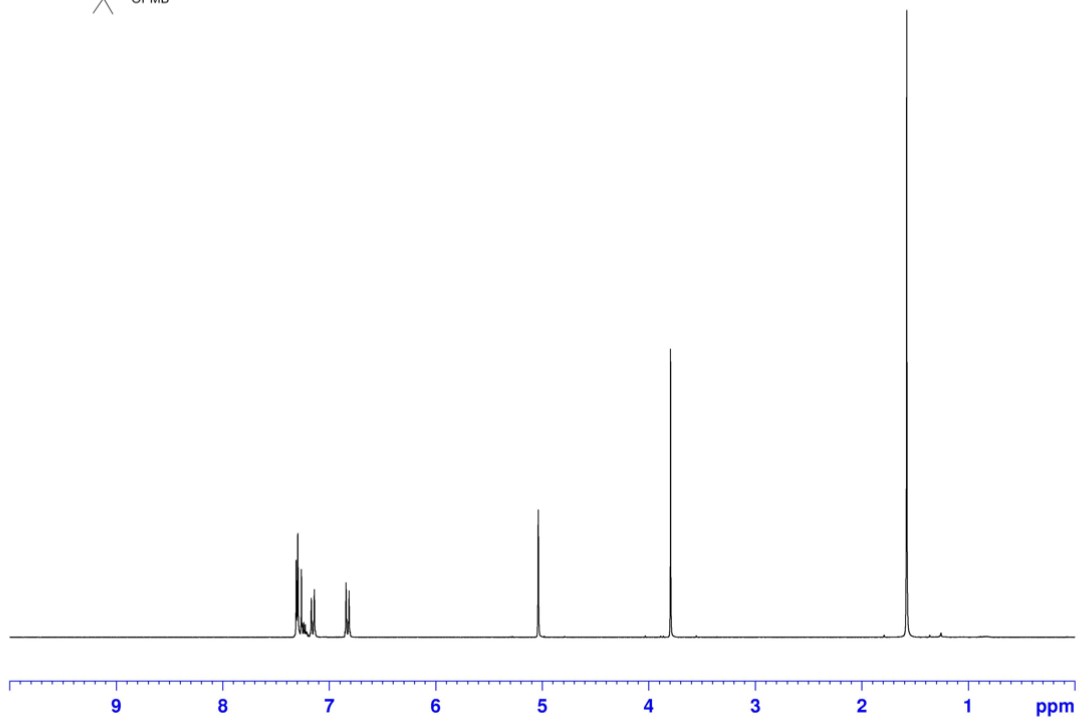
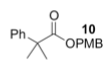


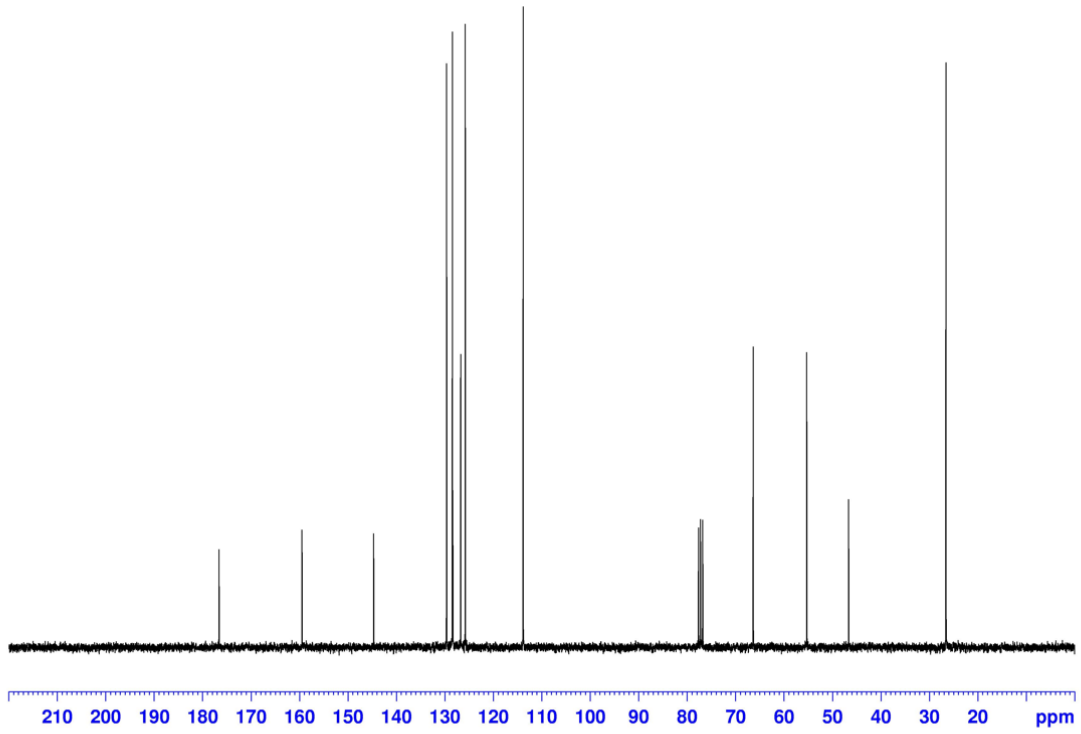
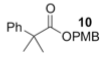


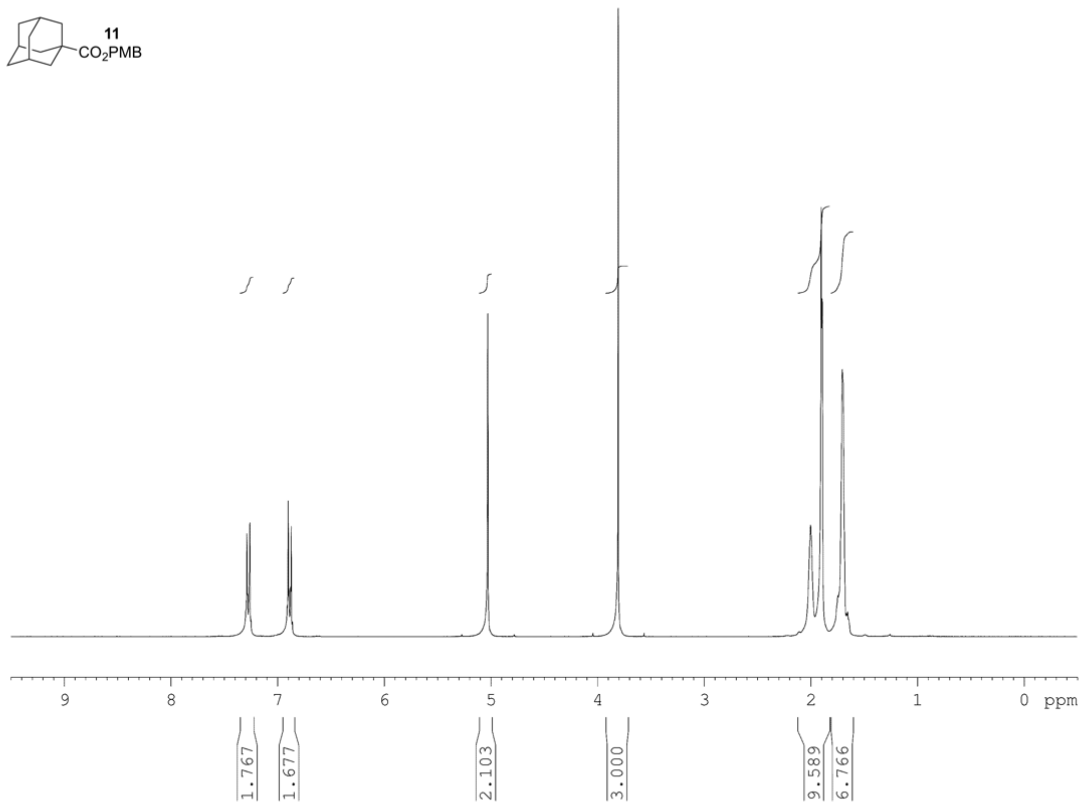
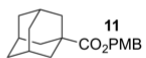


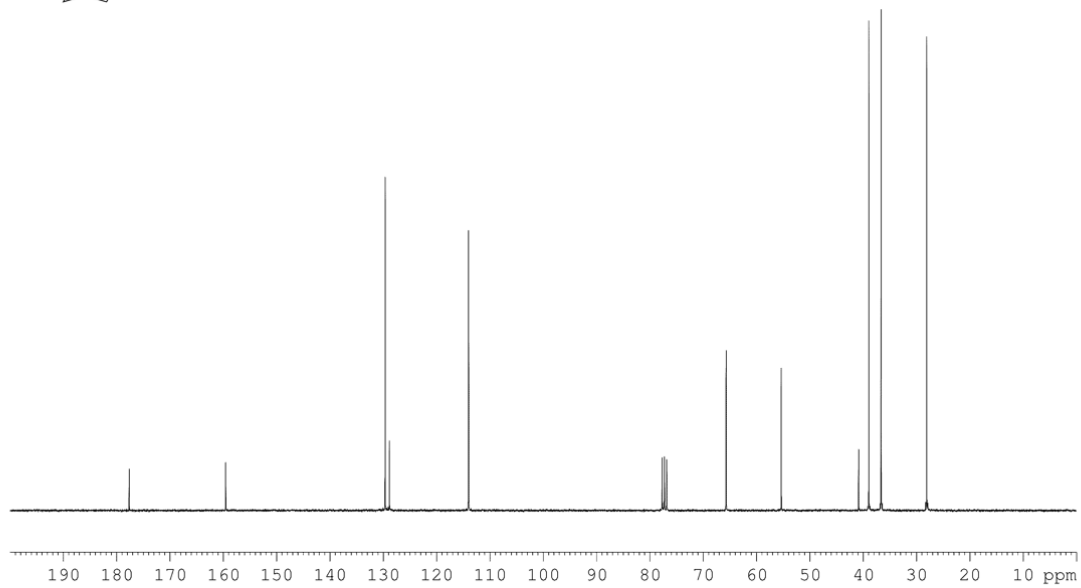
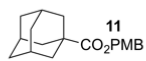


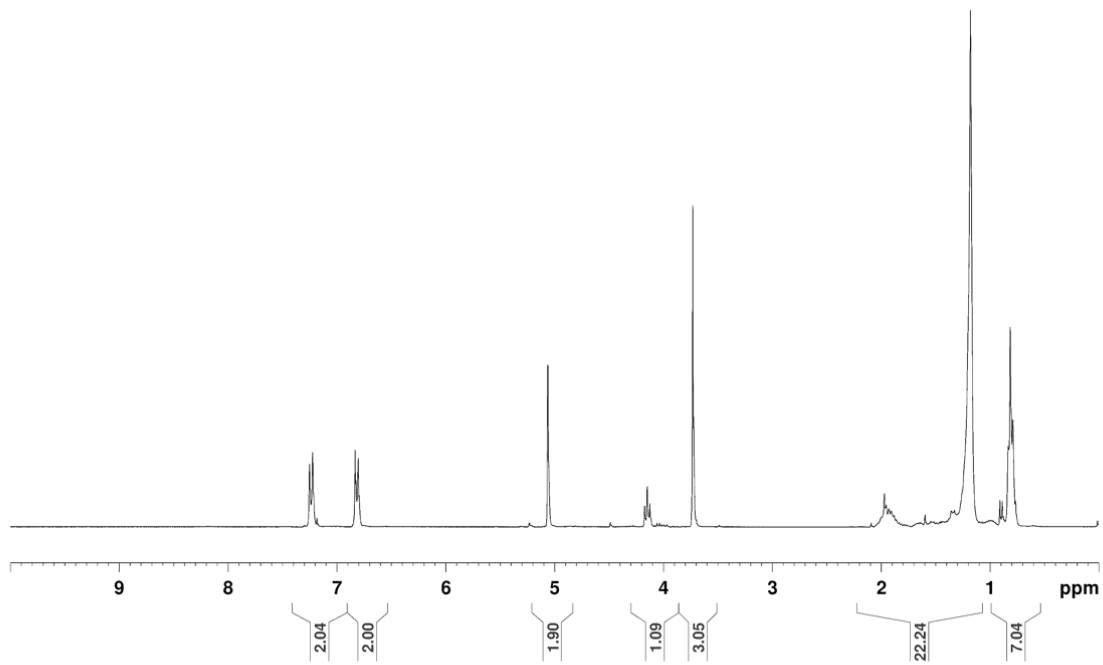
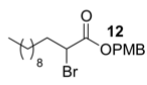


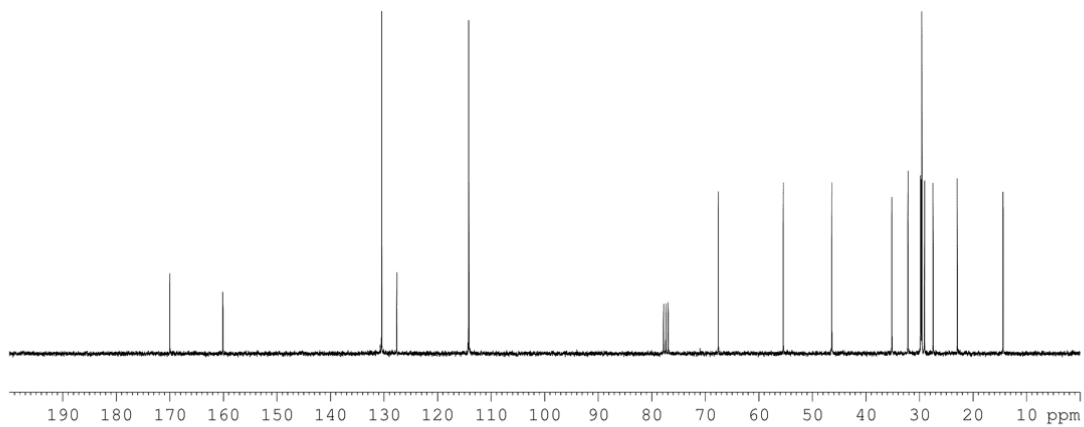
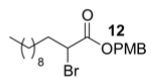


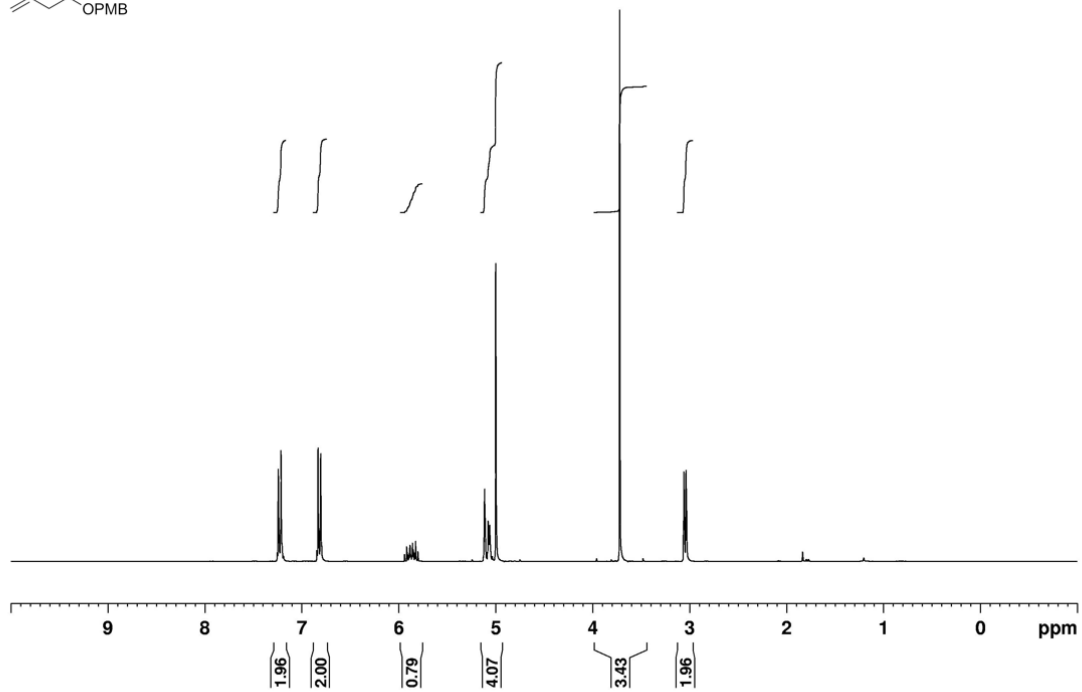
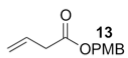


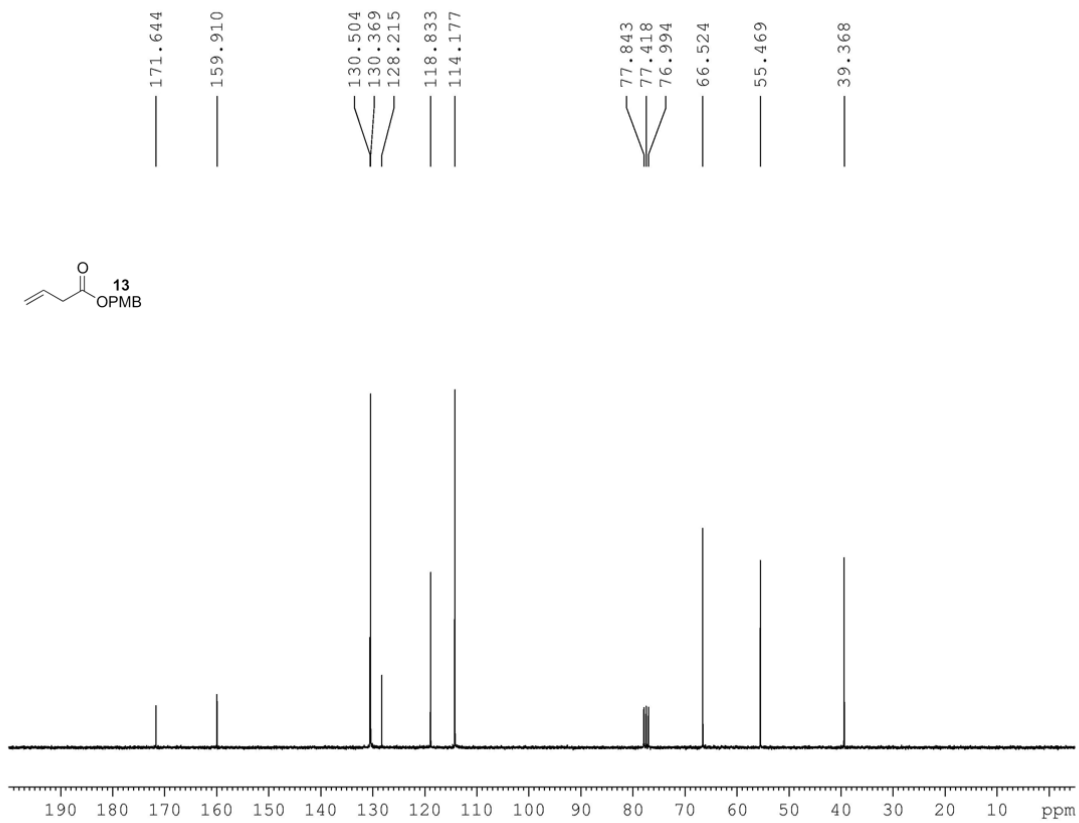


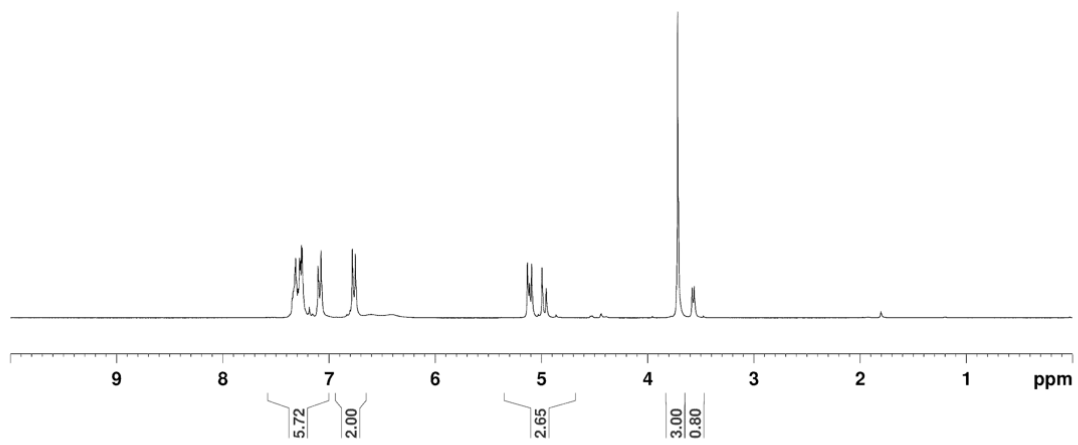
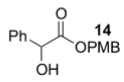


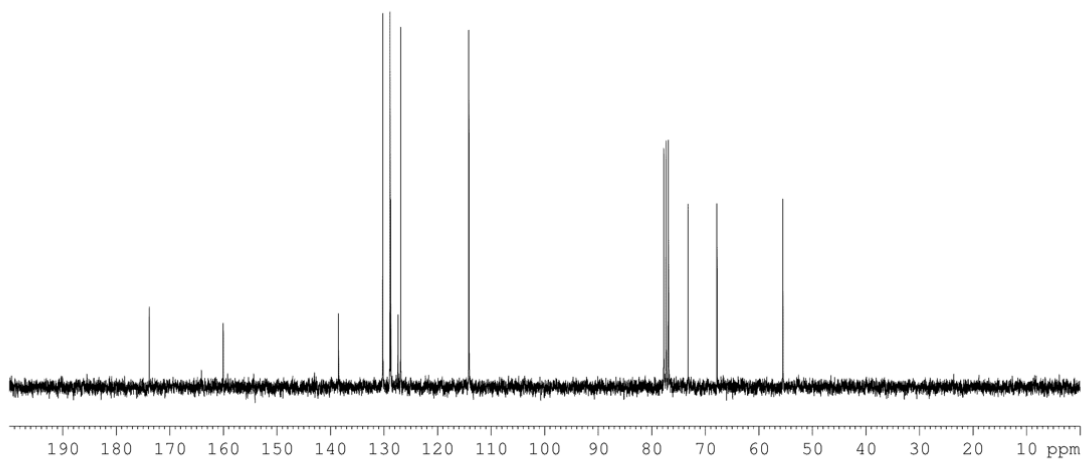
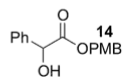


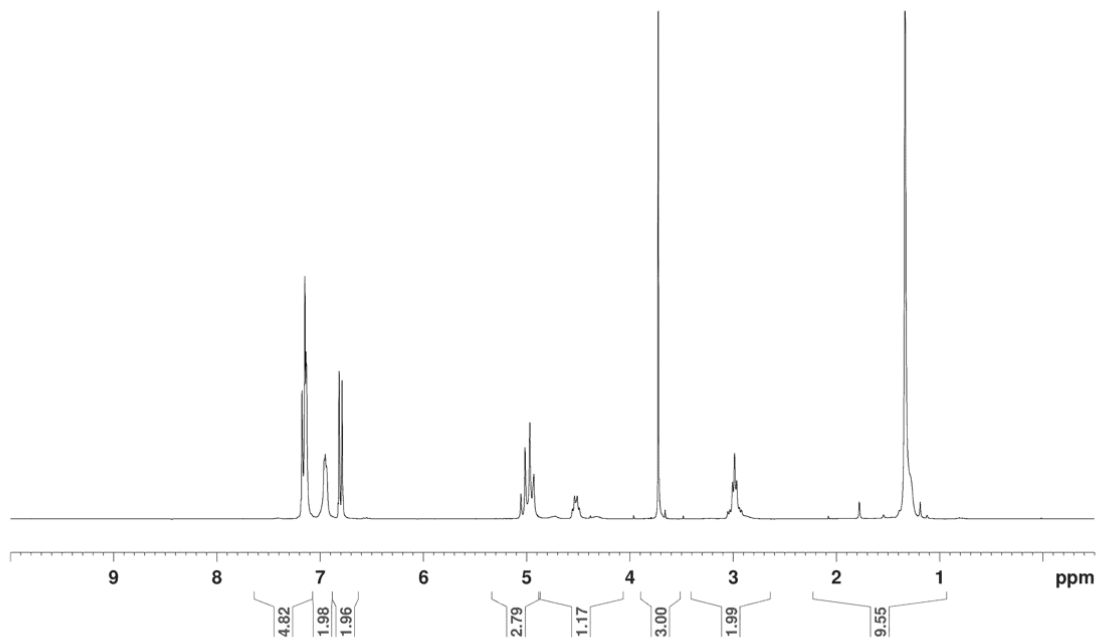
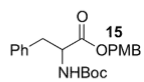


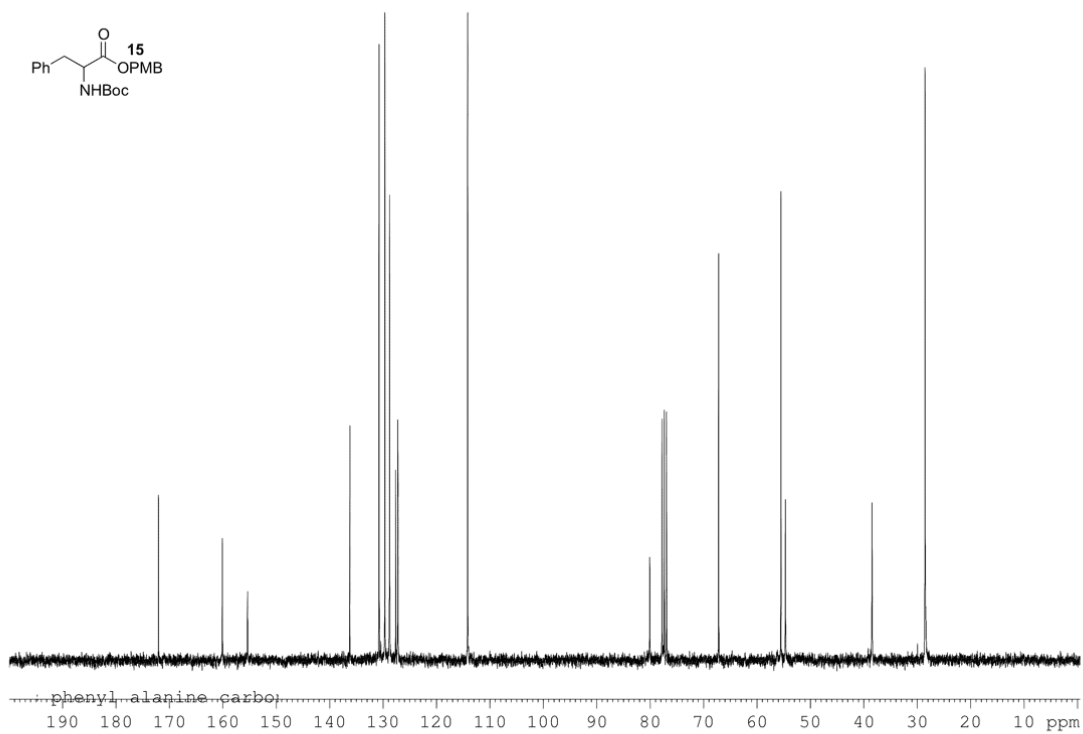
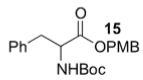


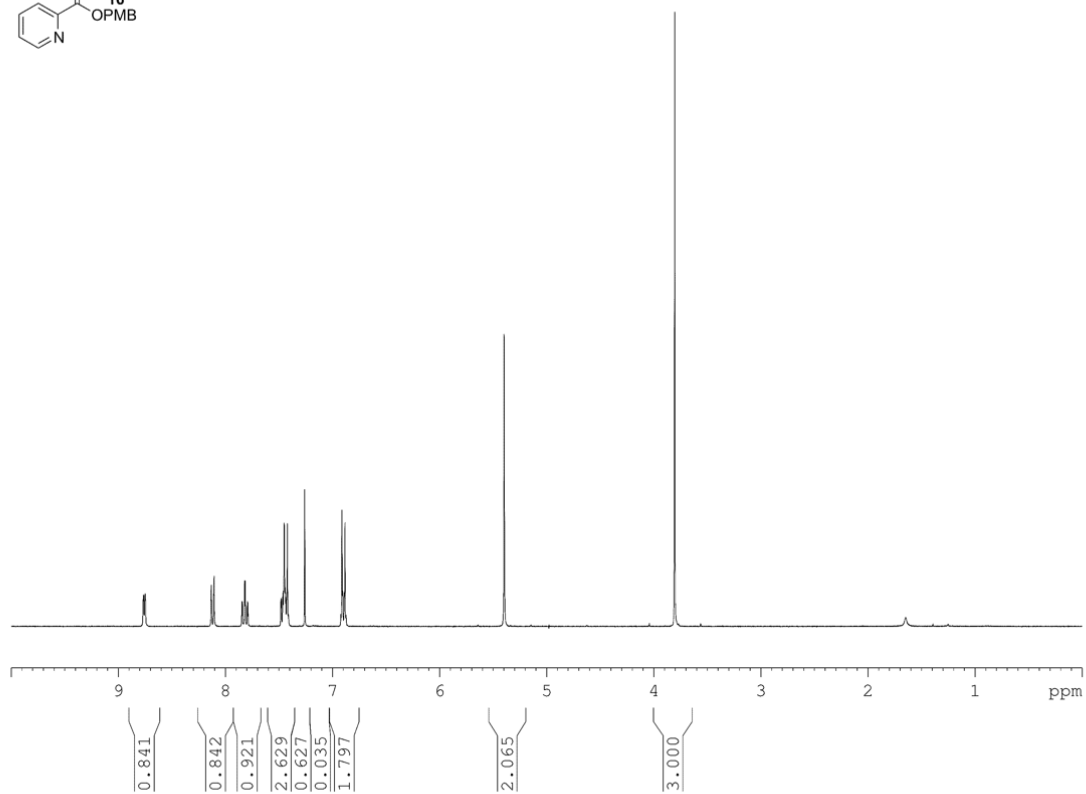
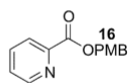


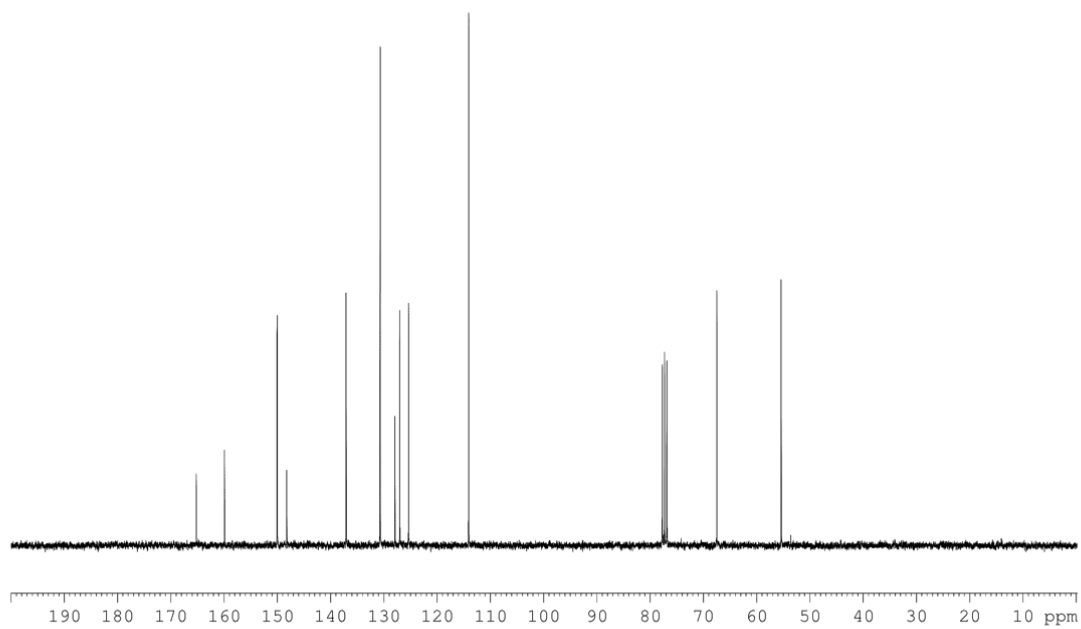
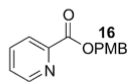


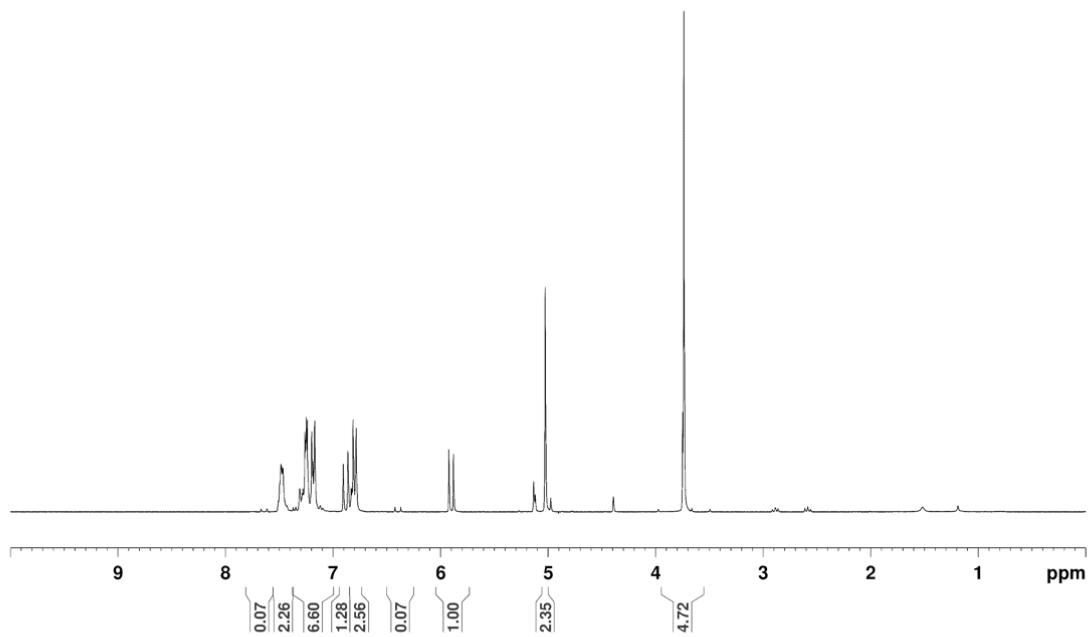
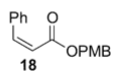


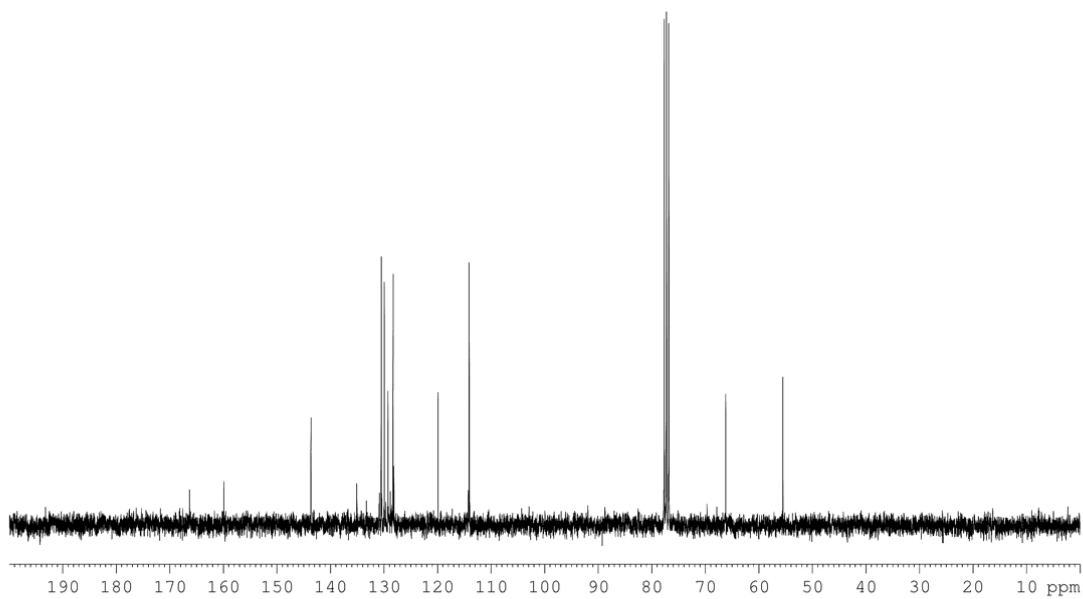
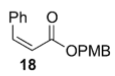


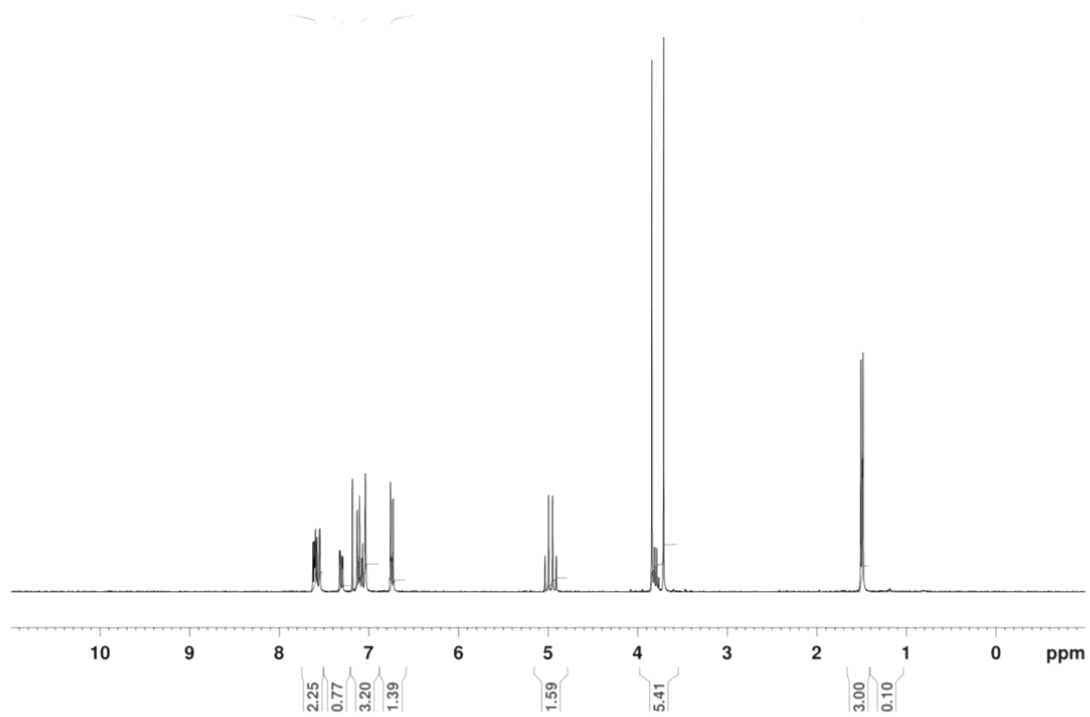
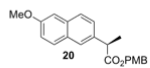


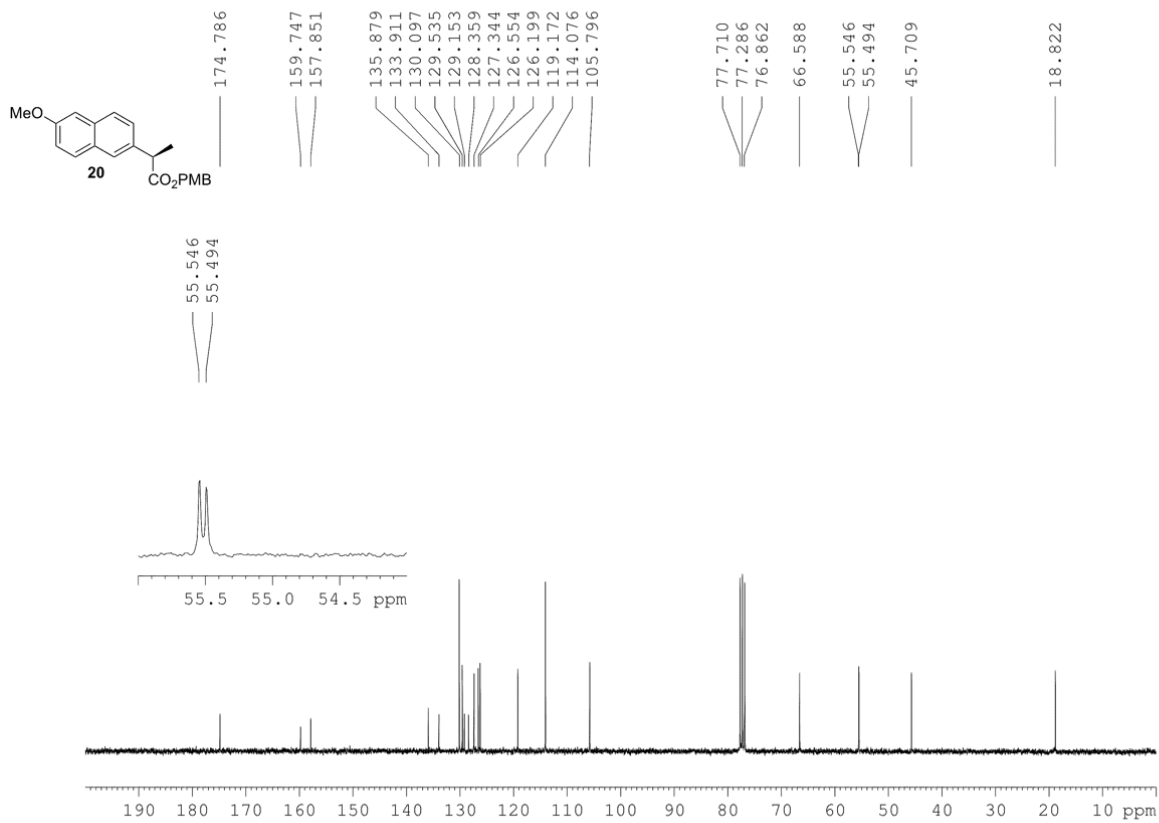












2.6. References

- (1) Greene, T. W.; Wuts, P. G. M. *Protective Groups in Organic Synthesis*. 4th Ed. Wiley, 2006; pp 610-611.
- (2) Kocienski, P. J. *Protecting Groups*. 3rd Ed. Thieme, 2005; pp 409-417.
- (3) Howard, K. T.; Chisholm, J. D. Preparation and Applications of 4-Methoxybenzyl Esters in Organic Synthesis. *Org. Prep. Proced. Int.* **2016**, *48*, 1-36.
- (4) Shoji, M.; Uno, T.; Hayashi, Y. Stereoselective Total Synthesis of ent-EI-1941-2 and Epi-ent-EI-1941-2. *Org. Lett.* **2004**, *6*, 4535-4538.
- (5) Shoji, M.; Uno, T.; Kakeya, H.; Onose, R.; Shiina, I.; Osada, H.; Hayashi, Y. Enantio- and Diastereoselective Total Synthesis of EI-1941-1, -2, and -3, Inhibitors of Interleukin-1 β Converting Enzyme, and Biological Properties of Their Derivatives. *J. Org. Chem.* **2005**, *70*, 9905-9915.
- (6) Sharma, G. V. M.; Reddy, C. G.; Krishna, P. R. Zirconium(IV) Chloride Catalyzed New and Efficient Protocol for the Selective Cleavage of p-Methoxybenzyl Ethers. *J. Org. Chem.* **2003**, *68*, 4574-4575.
- (7) Kern, N.; Dombay, T.; Blanc, A.; Weibel, J.-M.; Pale, P. Silver(I)-Catalyzed Deprotection of p-Methoxybenzyl Ethers: A Mild and Chemoselective Method. *J. Org. Chem.* **2012**, *77*, 9227-9235.
- (8) Ilangovan, A.; Saravanakumar, S.; Malayappasamy, S.; Manickam, G. A convenient approach for the deprotection and scavenging of the PMB group using POCl₃. *RSC Adv.* **2013**, *3*, 14814-14828.
- (9) Stelakatos, G. C.; Argyropoulos, N. Amino acid 4-methoxybenzyl esters. *J. Chem. Soc., C* **1970**, 964-967.

- (10) Feldman, K. S.; Eastman, K. J.; Lessene, G. Diazonamide Synthesis Studies: Use of Negishi Coupling to Fashion Diazonamide-Related Biaryls with Defined Axial Chirality. *Org. Lett.* **2002**, *4*, 3525-3528.
- (11) Hoye, T. R.; Wang, J. Alkyne haloallylation [with Pd(II)] as a core strategy for macrocycle synthesis: a total synthesis of (-)-haterumalide NA/(-)-oocydin A. *J. Am. Chem. Soc.* **2005**, *127*, 6950-6951.
- (12) Trost, B. M.; McDougall, P. J. Access to a Welwitindolinone Core Using Sequential Cycloadditions. *Org. Lett.* **2009**, *11*, 3782-3785.
- (13) Madduri, A. V. R.; Minnaard, A. J. Formal synthesis of the anti-angiogenic polyketide (-)-borrelidin under asymmetric catalytic control. *Chem. - Eur. J.* **2010**, *16*, 11726-11731, S11726/11721-S11726/11753.
- (14) Cosner, C. C.; Helquist, P. Concise, Convergent Syntheses of (\pm)-Trichostatin A Utilizing a Pd-Catalyzed Ketone Enolate α -Alkenylation Reaction. *Org. Lett.* **2011**, *13*, 3564-3567.
- (15) Kobayakawa, Y.; Mori, Y.; Okajima, H.; Terada, Y.; Nakada, M. Asymmetric and highly stereoselective synthesis of the DEF-ring moiety of (-)-FR182877 and its derivative inducing mitotic arrest. *Org. Lett.* **2012**, *14*, 2086-2089.
- (16) Cosner, C. C.; Bhaskara Reddy Iska, V.; Chatterjee, A.; Markiewicz, J. T.; Corden, S. J.; Loefstedt, J.; Ankner, T.; Richer, J.; Hulett, T.; Schauer, D. J.; et al. Evolution of Concise and Flexible Synthetic Strategies for Trichostatin Acid and the Potent Histone Deacetylase Inhibitor Trichostatin A. *Eur. J. Org. Chem.* **2013**, *2013*, 162-172.
- (17) Waddell, S. T.; Santorelli, G. M. Mild preparation of cephalosporin allyl and p-methoxybenzyl esters using diazoalkanes. *Tetrahedron Lett.* **1996**, *37*, 1971-1974.

- (18) Wang, M. F.; Golding, B. T.; Potter, G. A. A Convenient Preparation of p-Methoxybenzyl Esters. *Synth. Commun.* **2000**, *30*, 4197-4204.
- (19) Bernat, V.; Andre-Barres, C.; Baltas, M.; Saffon, N.; Vial, H. Synthesis of antimalarial G-factors endoperoxides: relevant evidence of the formation of a biradical during the autoxidation step. *Tetrahedron* **2008**, *64*, 9216-9224.
- (20) Adhikari, A. A.; Shah, J. P.; Howard, K. T.; Russo, C. M.; Wallach, D. R.; Linaburg, M. R.; Chisholm, J. D. Convenient Formation of Diphenylmethyl Esters Using Diphenylmethyl Trichloroacetimidate. *Synlett* **2014**, 283-287.
- (21) Armstrong, A.; Brackenridge, I.; Jackson, R. F. W.; Kirk, J. M. A new method for the preparation of tertiary butyl ethers and esters. *Tetrahedron Lett.* **1988**, *29*, 2483-2486.
- (22) Kokotos, G.; Chiou, A. Convenient synthesis of benzyl and allyl esters using benzyl and allyl 2,2,2-trichloroacetimidate. *Synthesis* **1997**, 168-170.
- (23) Thierry, J.; Yue, C.; Potier, P. 2-Phenylisopropyl and t-butyl trichloroacetimidates: Useful reagents for ester preparation of N-protected amino acids under neutral conditions. *Tetrahedron Lett.* **1998**, *39*, 1557-1560.
- (24) Respondek, T.; Cueny, E.; Kodanko, J. J. Cumyl Ester as the C-Terminal Protecting Group in the Enantioselective Alkylation of Glycine Benzophenone Imine. *Org. Lett.* **2012**, *14*, 150-153.
- (25) Schmidt, R. R.; Michel, J. Simple syntheses of α - and β -O-glycosyl imidates; preparation of glycosides and disaccharides. *Angew. Chem.* **1980**, *92*, 763-764.
- (26) Schmidt, R. R.; Michel, J. O-(α -D-Glucopyranosyl)trichloroacetimidate as a glucosyl donor. *J. Carbohydr. Chem.* **1985**, *4*, 141-169.

- (27) Schmidt, R. R.; Stumpp, M. Glycosyl imidates, 10. Glycosyl phosphates from glycosyl trichloroacetimidates. *Liebigs Ann. Chem.* **1984**, 680-691.
- (28) Schmidt, R. R. New methods of glycoside and oligosaccharide syntheses - are there alternatives to the Koenigs-Knorr method? *Angew. Chem.* **1986**, 98, 213-236.
- (29) Ueda, S.; Okada, T.; Nagasawa, H. Oxindole synthesis by palladium-catalyzed aromatic C-H alkenylation. *Chem. Commun.* **2010**, 46, 2462-2464.
- (30) Keck, G. E.; Boden, E. P.; Mabury, S. A. A useful Wittig reagent for the stereoselective synthesis of trans- α,β -unsaturated thiol esters. *J. Org. Chem.* **1985**, 50, 709-710.
- (31) Evans, D. A.; Black, W. C. Total synthesis of (+)-A83543A [(+)-lepicidin A]. *J. Am. Chem. Soc.* **1993**, 115, 4497-4513.
- (32) Könning, D.; Hiller, W.; Christmann, M. One-Pot Oxidation/Isomerization of Z-Allylic Alcohols with Oxygen as Stoichiometric Oxidant. *Org. Lett.* **2012**, 14, 5258-5261.
- (33) Pangborn, A. B.; Giardello, M. A.; Grubbs, R. H.; Rosen, R. K.; Timmers, F. J. Safe and Convenient Procedure for Solvent Purification. *Organometallics* **1996**, 15, 1518-1520.
- (34) Rolfe, A.; Loh, J. K.; Maity, P. K.; Hanson, P. R. High-load, hybrid Si-ROMP reagents. *Org. Lett.* **2011**, 13, 4-7.
- (35) Feng, X.; Sun, A.; Zhang, S.; Yu, X.; Bao, M. Palladium-catalyzed carboxylative coupling of benzyl chlorides with allyltributylstannane: remarkable effect of palladium nanoparticles. *Org. Lett.* **2013**, 15, 108-111.
- (36) Zeggaf, C.; Poncet, J.; Jouin, P.; Dufour, M. N.; Castro, B. Isopropenyl chlorocarbonate (IPCC) in amino acid and peptide chemistry: esterification of N-protected amino acids; application to the synthesis of the depsipeptide valinomycin. *Tetrahedron* **1989**, 45, 5039-5050.

Chapter 3. Rhodium-Catalyzed Tandem Alkyne Dimerization/1,4-Addition Reaction

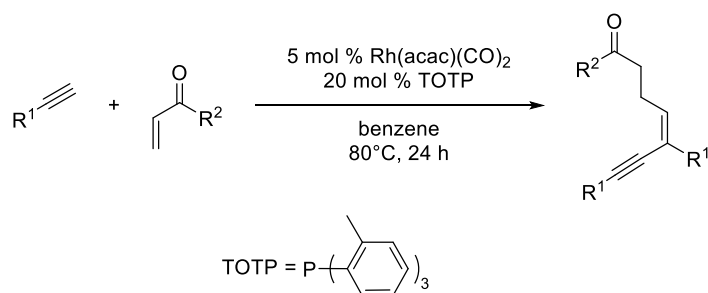
3.1. Introduction

One of the most challenging goals of synthetic chemistry is the development of methods to elaborate simple and readily available starting materials into significantly more complex products in a single step. Pursuant to this goal much effort has been devoted to the development of multicomponent reactions.¹ Interest in this area has been spurred in recent years by the use of such transformations in the synthesis of diverse chemical libraries, which are often used in screening efforts to develop new pharmaceuticals and small molecule probes of biological systems.²

Transition metals have also been shown to catalyze multicomponent reactions.³ During the course of our studies on the rhodium-catalyzed 1,4-addition of alkynes to α,β -unsaturated ketones,⁴ we serendipitously isolated a distinct π -conjugated enyne adduct that was comprised of two alkyne units and one equivalent of methyl vinyl ketone (MVK) (**3.3a**, **Scheme 3.1**). The dimerization of alkynes is a well precedented reaction,⁵ often used in organic synthesis.⁶ The use of the alkyne dimerization reaction as a starting point for a multicomponent coupling, however, is far more rare.⁷ Recently Tanaka highlighted a similar process⁸ where triisopropylsilyl acetylene was added to an alkynyl ester using rhodium catalysis, with the resultant vinylrhodium species being trapped by an electron-deficient alkene to form complex enyne products similar to **3.3a**. Also relevant are reports by Sato and Ikeda on the use of a nickel-catalyzed tandem coupling reaction of alkynyl-stannanes, alkynes and enones to form similar enynes.⁹ A distinguishing feature of the nickel-catalyzed process is the requirement for activation of an alkyne as an alkynyl stannane, which is not necessary for the rhodium-catalyzed reactions. As enynes similar to **3.3a** have found uses in transition metal catalyzed cycloadditions¹⁰ and in

materials science,¹¹ the reaction was further examined to optimize for the dimerization/addition product and determine the substrate scope.

Scheme 3.1. Isolation of an enyne side product in the Rh-catalyzed 1,4-addition reaction.

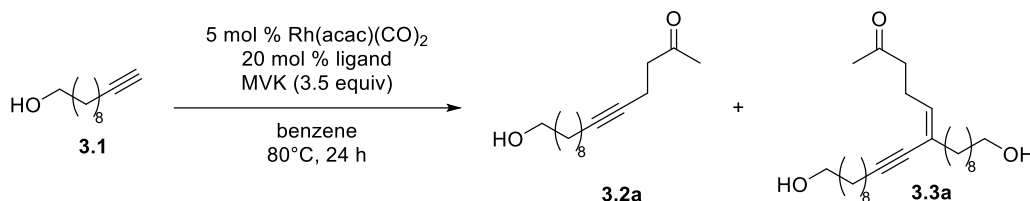


3.2. Results and Discussion

Initial attempts to influence the product distribution of the reaction focused on varying the phosphine ligand (Table 3.1). The use of tris(*o*-tolyl)phosphine (*TOTP*) significantly increased the yield of the dimerization/addition product while suppressing the formation of the 1,4-addition product (entry 2). The alkyne starting material could be completely accounted for in the two products when using the ligand *TOTP*. No apparent trends as a result of the phosphine's nature (electron rich, electron deficient, size of cone-angle, mono- or bidentate) could be identified. Additional experiments suggest that the active catalyst was generated *in situ* from both the rhodium complex Rh(acac)(CO)₂ and the phosphine. A control experiment with only the rhodium pre-catalyst present gave both 1,4-addition and dimerization/addition products in 17% and 5% yields, respectively (entry 11). When no rhodium precatalyst was applied and just the phosphine was used, the alkyne starting material **1** was isolated quantitatively. Other rhodium sources (such as Rh(acac)(ethylene)₂, [Rh(COD)Cl]₂ and [Rh(Cl)(CO)₂]₂) were less effective.

Based on this study, both the rhodium pre-catalyst and *TOTP* are required for the reaction to perform efficiently.

Table 3.1. Phosphine Ligand Screen.



Entry	Ligand	3.2a ^a	3.3a ^a
1	tris(<i>o</i> -methoxyphenyl)phosphine (TOMP)	72	11
2	<i>tris(o-tolyl)phosphine (TOTP)</i>	24	76
3	tris(<i>p</i> -methoxyphenyl)phosphine ^b	14	23
4	tris(2,4,6-trimethoxyphenyl) phosphine ^b	19	0
5	triphenylphosphine	26	16
6	tris(2,4,6-trimethylphenyl)phosphine	8	7
7	tris(pentafluorophenyl)phosphine	16	10
8	tris(<i>p</i> -trifluoromethylphenyl) phosphine	28	17
9	tris(<i>p</i> -fluorophenyl)phosphine	15	44
10	1,2-bis(diphenylphosphino)benzene ^c	0	0
11	none	17	5
12	tris(<i>o</i> -tolyl)phosphine (TOTP) ^d	23	36
13	tris(<i>o</i> -tolyl)phosphine (TOTP) ^e	34	8
14	tris(<i>o</i> -tolyl)phosphine (TOTP) ^f	8	trace

^a) isolated yields (%) ^b) Baylis-Hillman product **3.4** was also isolated ^c) Ether **3.5** was isolated ^d) Rh(acac)(ethylene) was used as catalyst ^e) [Rh(COD)Cl]₂ (2.5 mol %) was used as catalyst ^f) [Rh(Cl)(CO)₂]₂ (2.5 mol %) was used as catalyst

In some cases products other than alkyne **3.2** and enyne **3.3** were detected during the phosphine screening. The use of the electron-rich phosphines tris(*p*-methoxyphenyl)phosphine (Table 3.1, entry 2) and tris(2,4,6-trimethoxyphenyl)phosphine (entry 3) lead to a competing reaction, dimerizing the MVK to form the Baylis-Hillman product **3.4**. Both rhodium complexes¹² and phosphines¹³ have been reported to dimerize enones, forming 1,5-diketones like **3.4**, so either the phosphine or the rhodium complex formed with these phosphines may be responsible for this mode of reactivity. The use of 1,2-bis(diphenylphosphino)benzene as a

ligand (entry 10) failed to give either alkyne **3.2** or enyne **3.3** but instead gave *O*-Michael addition product **3.5**. This reaction is preceded from the work of Louie,¹⁴ but the ligand dependence is notable as in her report rhodium salts (including Rh(acac)(CO)₂) were used as catalysts in the presence of added Na₂CO₃ without added phosphine ligands.

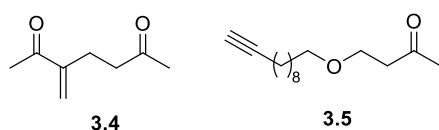
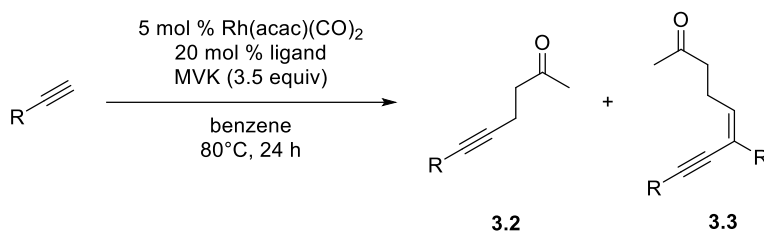


Figure 3.1. Side products observed during the phosphine screening.

Having optimized the phosphine ligand to favor the dimerization/addition product, the substrate scope of the reaction was investigated. Outlined in Table 3.2 are the comparative yields of the 1,4-addition adduct **3.2** versus the enyne product **3.3** using various alkynes. Alkynes containing primary alcohols, esters, and phthalamide-protected amines were found to participate in the dimerization/addition reaction (Table 3.2). These substrates afforded modest to satisfactory yields of dimerization/addition product **3.3**. Propargyl alcohol itself was a poor substrate (entry 4), perhaps ionizing to an inert rhodium allenylidene complex by dehydration. Similar organometallic structures have been isolated by Werner.¹⁵ Phenyl acetylene (entry 9) yielded only an inseparable mixture of products that did not appear to contain either alkyne **3.2** or enyne **3.3**. The use of triisopropylsilyl acetylene lead only to the 1,4-addition adduct (entry 10). This selectivity is dictated by the presence of the bulky TIPS group, which inhibits the dimerization reaction. Hayashi observed a similar reactivity pattern in the 1,4-addition reactions of alkynes.¹⁶

Table 3.2. Variation of alkynes in the dimerization/addition reaction.

Entry	R Group	2^a	3^a
1	(CH ₂) ₉ OH	24 (3.2a)	76 (3.3a)
2	(CH ₂) ₃ OH	30 (3.2b)	51 (3.3b)
3	(CH ₂) ₂ OH	30 (3.2c)	63 (3.3c)
4	CH ₂ OH	0 (3.2d)	21 (3.3d)
5	CH ₂ OTBDPS	3 (3.2e)	29 (3.3e)
6	(CH ₂) ₃ OBz	20 (3.2f)	67 (3.3f)
7	(CH ₂) ₉ NPhth	29 (3.2g)	38 (3.3g)
8	(CH ₂) ₅ CH ₃	24 (3.2h)	47 (3.3h)
9	Ph	0 (3.2i)	0 (3.3i)
10	TIPS	75 (3.2j)	0 (3.3j)

While the gross structure of the dimerization/addition product was clear, the stereochemistry of the trisubstituted alkene was as yet undetermined. NMR studies were therefore undertaken with enyne **3.3e** to determine the alkene stereochemistry. After the assignment of all protons and carbons of **3.3e** using COSY and HSQC experiments, an HMBC was performed which confirmed the connectivity of the structure. Specifically, the HMBC spectrum confirmed the dimerization of the alkyne component to form a sp-sp² bond, as indicated by correlations of H10 to C5, C6, C7 and C9 and of H5 to C3, C4, C7 and C10 (Figure 3.2). The Z stereochemistry of the alkene was also established by NMR, using a NOESY experiment, which showed a significant correlation between H5 and H10. The stereochemistry of the other enyne products was assigned in analogy to these findings.

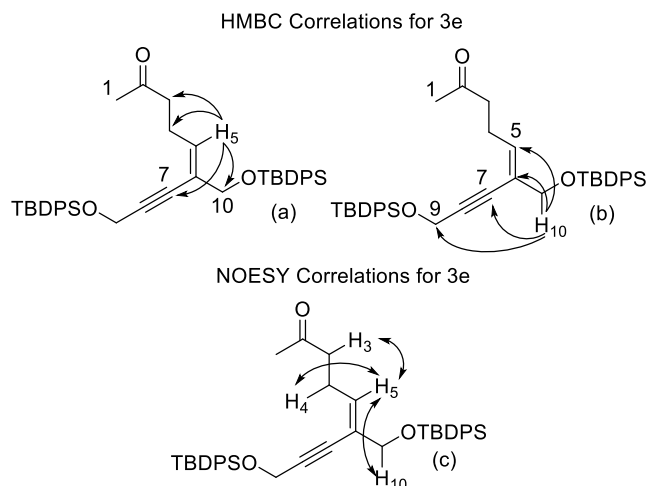
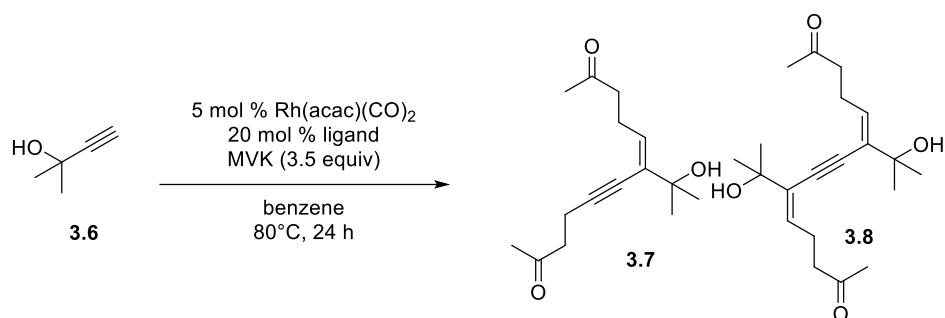


Figure 3.2. HMBC correlations (a) and (b) and NOESY correlations (c) on enyne **3.3e**.

In contrast to other alkynes, the reaction of 2-methyl-3-butyn-2-ol **3.6** with methyl vinyl ketone afforded two different alkyne products, **3.7** and **3.8** (Table 3.3). Alkyne **3.7** appeared to be the result of an alkyne dimerization/addition reaction that was followed by loss of acetone and 1,4-addition of the resulting alkyne to a second equivalent of MVK. Alkyne **3.8** was identified as a symmetrical alkyne adduct of 2-methyl-3-butyn-2-ol **3.6** and MVK. Attempts were made to determine if the yields of the alkyne products **3.7** and **3.8** were dependent on the ratio of alkyne to MVK (Table 3.3). Since both the alkyne and the MVK must compete for a coordination site on the transition metal catalyst, increasing the amount of MVK was expected to provide an improved ratio favoring product **3.7**. When equal ratios of both starting materials were used, a small amount of (17%) product **3.7** was isolated along with product **3.8** in 54% yield (entry 1). Using 2.5 equiv of MVK gave 50% of **7** and 41% of **3.8** (entry 2, a 55:45 ratio of **3.7:3.8**). Use of a large excess of MVK resulted in a further improvement in the ratio of **3.7:3.8** (71:29), although the yield of product **3.7** was only 53% compared to 22% of product **3.8** (entry 3). The requirement for a large excess of enone is likely due to the MVK being an inferior ligand for the rhodium relative to the alkyne.

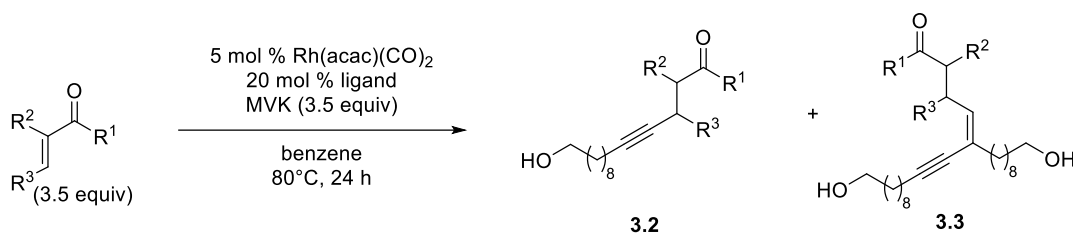
Table 3.3. Reaction of 2-methyl-3-butyn-2-ol **3.6**.

Entry	Equiv MVK	3.7 ^a	3.8 ^a	Ratio 3.7 : 3.8
1	1	17	54	24:76
2	3.5	50	41	55:45
3	10	53	22	71:29

Studies were also performed to determine the compatibility of other electron deficient alkenes with the reaction conditions (Table 4). Reactions with ethyl vinyl ketone, phenyl vinyl ketone and acryloyloxazolidinone^[17] proceeded to give the respective dimer addition products in more modest yields when compared to MVK. The greater amount of the 1,4-addition products **3.2k**, **3.2l** and **3.2m** formed may be due to the lower volatility of the alkenes in these cases. With MVK some loss by evaporation may occur, leading to more dimerization/addition, but with less volatile substrates a greater concentration of alkene may compete more effectively for the rhodium with the alkyne, leading to a more significant amount of the alkyne product **3.2**. Attempts were made to probe this hypothesis using a smaller excess of acryloyloxazolidinone, as in this case volatility should not be an issue (acryloyloxazolidinone is a solid with a melting point of 80-81 °C). Using a smaller excess of alkene did provide a product ratio favoring product **3.3**, but the conversion was significantly lower, with ~25% starting alkyne being recovered in both entries 5 and 6 (Table 3.4). Ethyl acrylate and dimethylacrylamide proved to be inert under these conditions. Any substitution on the alkene also caused the reaction to shut down, and provided no dimerization/addition or 1,4-addition product.

Taking into account the stereochemistry of the dimerization/addition product (Figure 3.2) and the need for a phosphine ligand to promote the reaction we propose the following reaction mechanism for the dimerization/addition reaction (Figure 3.3). Rhodium complex **3.15** is generated *in situ* by the displacement of the CO ligands with a phosphine and chelation of the alkyne. Oxidative addition of the alkyne C-H bond and protonation of the acetylacetonate ligand then provides complex **3.17**.

Table 3.4. Variation of electron deficient alkenes in the dimerization/addition reaction.



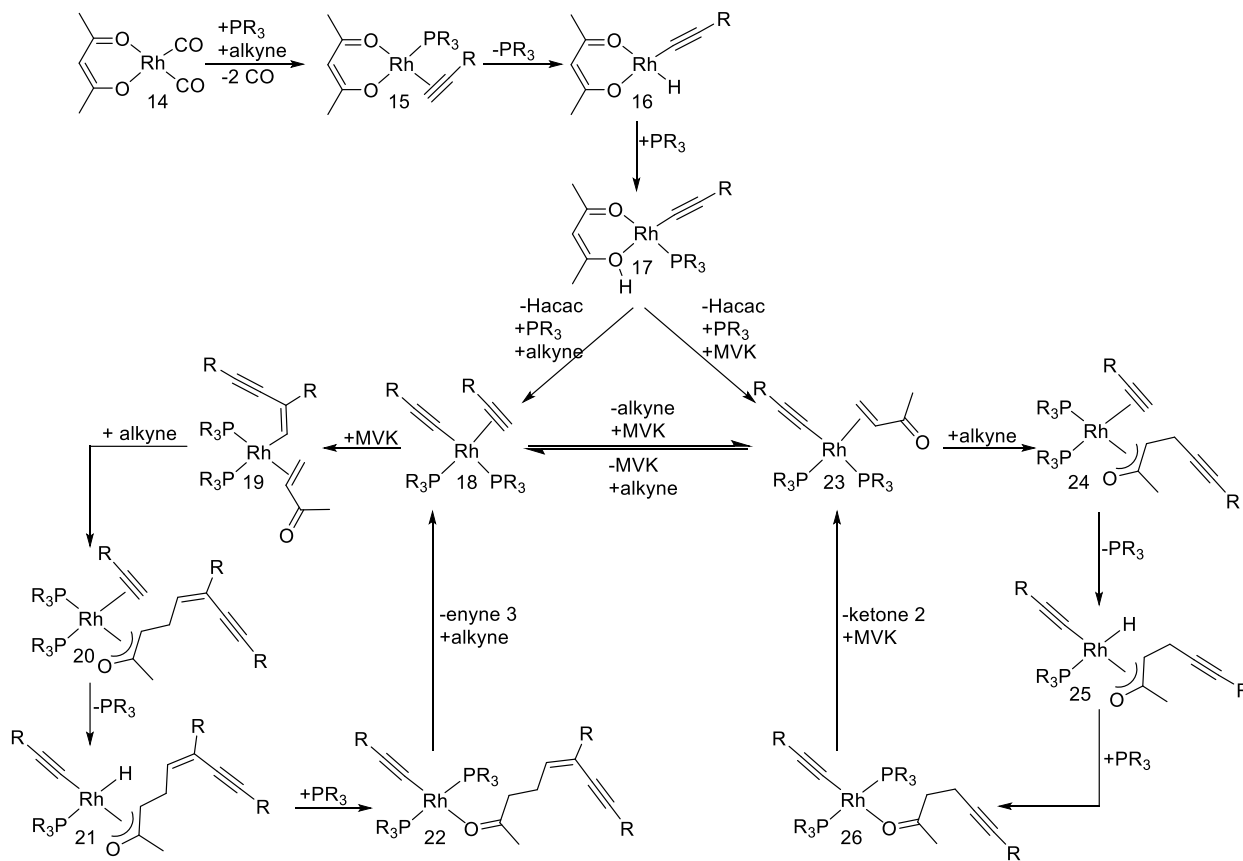
Entry	R ₁	R ₂	R ₃	2 ^a	3 ^a
1	Me	H	H	24 (3.2a)	76 (3.3a)
2	Et	H	H	34 (3.2k)	46 (3.3k)
3	Ph	H	H	36 (3.2l)	45 (3.3l)
4		H	H	44 (3.2m)	45 (3.3m)
5^b		H	H	18 (3.2m)	23 (3.3m)
6^c		H	H	8 (3.2m)	16 (3.3m)
5	OEt	H	H	0 (3.2n)	0 (3.3n)
6	NMe ₂	H	H	0 (3.2o)	0 (3.3o)
7	Ph	Me	H	0 (3.2p)	0 (3.3p)
8	Me	H	Bu	0 (3.2q)	0 (3.3q)

^a) isolated yields (%) ^b) 2.2 equiv of alkene was used ^c) 1.1 equiv of alkene was used

Loss of the acetylacetonate ligand from **3.17** and coordination of a second equivalent of alkyne and a phosphine provides intermediate **3.18**, which then undergoes a regio-selective head-to-tail dimerization of the alkynes to provide vinylrhodium **3.19**. A selective syn addition across the alkyne to generate **3.19** accounts for the observed alkene geometry in product **3.3**. The

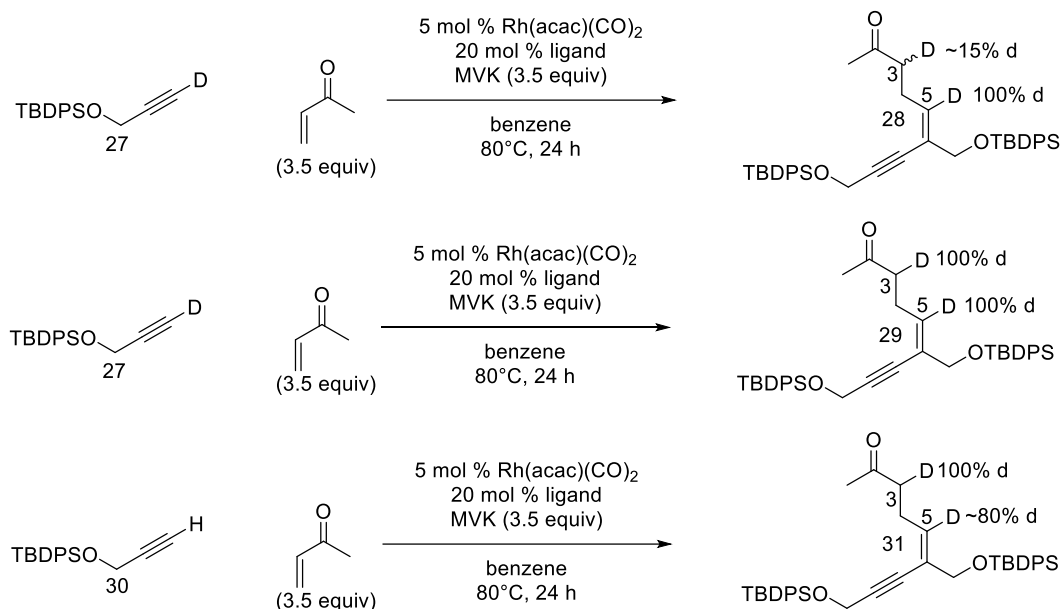
vinylrhodium then adds to MVK forming the oxa- π -allyl rhodium complex **3.20**. Coordination of another equivalent of alkyne and insertion into the alkyne C-H bond then provides complex **3.21**, which through reductive elimination releases the enyne product **3.3** and returns rhodium complex **3.18** to initiate another catalytic cycle. The formation of 1,4-addition product **3.2** can be explained by addition of MVK to complex **3.17** instead of the alkyne. The alkyne could then add directly to the MVK, providing the oxa- π -allyl rhodium complex **3.24**. Insertion of the rhodium into the alkyne C-H bond followed by protonation of the rhodium enolate leads to complex **3.26**, which can release ketone **3.2**, regenerating complex **3.23** and beginning another cycle. Complexes **3.23** and **3.18** may also equilibrate through ligand exchange, so the initial formation of **3.23** or **3.18** may not determine the dominant pathway.

Figure 3.3. Proposed Mechanism.



Deuterium-labeled terminal alkyne **27** was subjected to the dimerization/addition reaction conditions to gain additional insight into the mechanism of the reaction (Scheme 2). With alkyne **27** minimal deuterium incorporation (15%) was observed at C3 while 100% incorporation was observed at C5. The low incorporation of deuterium at C3 was initially puzzling, but we hypothesized that the deuterium on the alkyne may exchange with adventitious water or the free acetylacetonate ligand leading to lowered deuterium incorporation in the product. When the reaction was repeated with the addition of D₂O (10 equiv. with respect to alkyne) the ¹H NMR indicated quantitative inclusion of a single deuterium at the C3 position. Given that the deuterium could be incorporated from a reductive elimination or a protonation of a rhodium allyl intermediate, alkyne **30** was also subjected to the above experiment with excess of D₂O. The enyne product was obtained with 100% *d*-incorporation (relative to one proton) at C3 and with 80% *d*-incorporation at the olefinic position (C5). Deuterium incorporated at the olefinic position when using alkyne **30** suggests that the C-H insertion of the rhodium complex into the terminal alkyne is reversible and that this proton exchanges rapidly with the excess D₂O.

Scheme 3.2. Deuterium labeling studies.

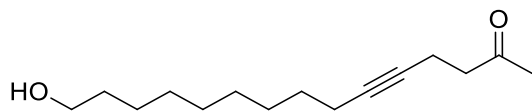


3.3. Conclusion.

In summary, a tandem rhodium-catalyzed dimerization/1,4-addition of terminal alkynes and enones is reported. This methodology provides a convenient entry into highly functionalized enyne systems. Two carbon-carbon bonds are formed in a single step in this tandem reaction, which is selective for a *Z* trisubstituted alkene. A number of alkynes (including some with unprotected alcohols) and electron deficient alkenes were compatible with the reaction conditions. This multicomponent reaction provides rapid access to π -conjugated alkynes, which are important intermediates in transition metal catalyzed cycloadditions and are also useful in molecular electronics.

General Procedure for the Dimerization/1,4-Addition Reaction of Alkynes and Electron Deficient Alkenes.

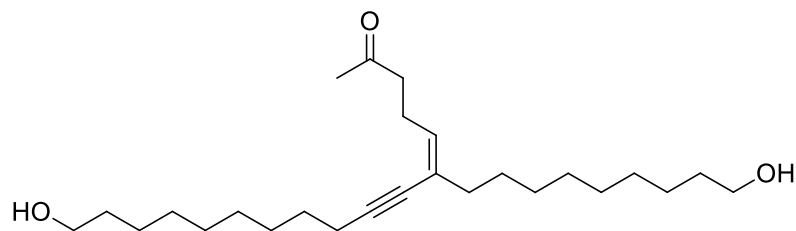
To the dicarbonylacetylacetonato rhodium (I) (0.021 mmol, 5.4 mg) and the tris(*o*-tolylphosphine) (0.08 mmol, 26 mg) in benzene (1.1 mL) was added a solution of 10-undecyn-1-ol (0.42 mmol, 73 mg) and methyl vinyl ketone (1.47 mmol, 121 μ L) dissolved in benzene (1.0 mL). The reaction was stirred for 24 h at 80°C then pre-absorbed onto silica gel and purified by silica gel flash chromatography (gradient elution with 40%, 50%, 70%, 80% ethyl acetate: hexanes) to give alkyne 1,4- product **2.2a** (24 mg, 24%) and dimerization-addition product **2.3a** (64 mg, 76%).



15-Hydroxypentadec-5-yn-2-one, **2.2a**.

Purified by flash chromatography on silica gel (gradient elution with 40%, 50%, 70%, 80% ethyl acetate: hexanes) to afford pure product (24 mg, 24%) as clear yellow oil.

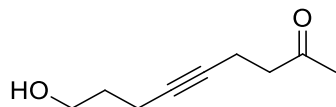
TLC R_f = 0.28 (40% ethyl acetate: hexanes). IR (film): 3289, 2920, 2848, 1703, 1458 cm^{-1} . ^1H NMR (300 MHz, CDCl_3) δ 3.55 (t, J = 6.6 Hz, 2H), 2.56 (t, J = 6.9 Hz, 2H), 2.36-2.26 (m, 2H), 2.10 (s, 3H), 2.08 -2.00 (m, 2H), 1.95 (s, 1H), 1.49 (p, J = 7.2 Hz, 2H), 1.40-1.33 (m, 2H), 1.22 (bs, 10H). ^{13}C NMR (75 MHz, CDCl_3) δ 207.4, 81.0, 78.5, 63.0, 43.1, 32.4, 30.0, 29.6, 29.5, 29.1, 29.0, 28.9, 25.8, 18.8, 13.6. Anal calcd for $\text{C}_{15}\text{H}_{26}\text{O}_2$: C, 75.58; H, 10.99. Found: C, 75.49; H, 10.97.



(Z)-17-Hydroxy-6-(9-hydroxynonyl)heptadec-5-en-7-yn-2-one, 2.3a.

Purified by flash chromatography on silica gel (gradient elution with 40%, 50%, 70%, 80% ethyl acetate: hexanes) to afford pure product (64 mg, 76%) as a yellow oil.

TLC R_f = 0.39 (80% ethyl acetate: hexanes). IR (film): 3431, 2925, 2851, 2215, 1703 cm^{-1} . ^1H NMR (300 MHz, CDCl_3) δ 5.53 (t, J = 6.8 Hz, 1H), 3.62 (t, J = 6.6 Hz, 4H), 2.49-2.48 (m, 4H), 2.33 (t, J = 6.8 Hz, 2H), 2.13 (s, 3H), 2.03 (t, J = 6.4 Hz, 2H), 1.57-1.45 (m, 10H), 1.35-1.23 (m, 20H). ^{13}C NMR (75 MHz, CDCl_3) δ 209.0, 133.4, 125.0, 95.2, 78.8, 62.8, 62.8, 43.3, 37.5, 32.8, 29.8, 29.6, 29.5, 29.5, 29.2, 30.0, 29.9, 28.9, 28.5, 27.2, 25.9, 24.9, 19.5. Anal calcd for $\text{C}_{26}\text{H}_{46}\text{O}_3$: C, 76.79; H, 11.40. Found: C, 76.81; H, 11.59.

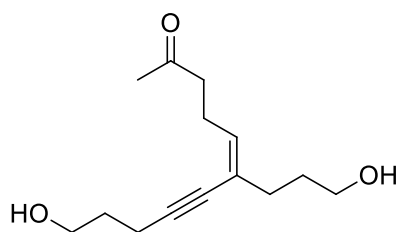


9-Hydroxynon-5-yn-2-one, 2.2b.

Purified by flash chromatography on silica gel (gradient elution with 40%, 60%, 90%, 100% ethyl acetate: hexanes) to afford pure product (78 mg, 30%) as clear yellow oil.

TLC R_f = 0.20 (50% ethyl acetate: hexanes). IR (film): 3419, 2924, 1716, 1362 cm^{-1} . ^1H NMR (300 MHz, CDCl_3) δ 3.67 (t, J = 6.2 Hz, 2H), 2.59 (t, J = 7.2 Hz, 2H), 2.39-2.32 (m, 2H), 2.24-

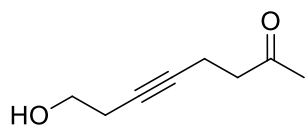
2.18 (m, 2H) 2.13 (s, 3H), 1.67 (p, $J = 6.2$ Hz, 2H). ^{13}C NMR (75 MHz, CDCl_3) δ 207.4, 80.12, 79.3, 61.8, 43.0, 31.6, 30.0, 15.4, 13.5. HRMS (EI): m/z calcd for $\text{C}_9\text{H}_{14}\text{O}_2\text{Na}$ ($\text{M}+\text{Na}$): 177.0885. Found: 177.0883.



(Z)-11-Hydroxy-6-(3-hydroxypropyl)undec-5-en-7-yn-2-one, 2.3b.

Purified by flash chromatography on silica gel (gradient elution with 40%, 60%, 90% ethyl acetate: hexanes then 100% ethyl acetate) to afford pure product (101 mg, 51%) as clear yellow oil.

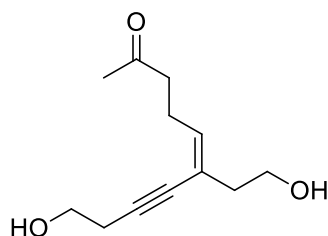
TLC $R_f = 0.26$ (100% ethyl acetate). IR (film): 3397, 2940, 1709, 1055 cm^{-1} . ^1H NMR (300 MHz, C_6D_6) δ 5.52 (t, $J = 6.7$ Hz, 1H), 3.67 (t, $J = 6.2$ Hz, 2H), 3.52 (t, $J = 6.5$ Hz, 2H), 3.12 (s, 1H), 2.85 (s, 1H), 2.45-2.36 (m, 6H), 2.07 (s, 5H) 1.75-1.62 (m, 4H). ^{13}C NMR (75 MHz, CDCl_3) δ 209.1, 134.2, 124.1, 94.7, 78.9, 61.8, 61.2, 43.1, 33.6, 31.5, 31.4, 29.8, 24.8, 16.0. Anal calcd for $\text{C}_{14}\text{H}_{22}\text{O}_3$: C, 70.56; H, 9.30. Found: C, 70.19; H, 9.25.



8-Hydroxyoct-5-yn-2-one, 2.2c.

Purified by flash chromatography on silica gel (gradient elution with 3%, 10%, 50%, 80% ethyl acetate: hexanes) to afford pure product (81 mg, 30%) as clear yellow oil.

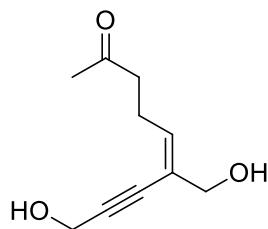
TLC $R_f = 0.18$ (30% ethyl acetate: hexanes). IR (film): 3410, 2918, 1714, 1367, 1046 cm^{-1} . ^1H NMR (300 MHz, CDCl_3) δ 3.66 (t, $J = 6.1$ Hz, 2H), 2.65 (t, $J = 7.2$ Hz, 2H), 2.45-2.36 (m, 4H), 2.17 (s, 3H) \square ^{13}C NMR (75 MHz, CDCl_3) δ 207.6, 80.4, 77.4, 61.1, 42.7, 29.9, 23.0, 13.3. Anal calcd for $\text{C}_8\text{H}_{12}\text{O}_2$: C, 68.54; H, 8.63. Found: C, 68.24; H, 8.57.



(Z)-10-hydroxy-6-(2-hydroxyethyl)dec-5-en-7-yn-2-one, 2.3c.

Purified by flash chromatography on silica gel (gradient elution with 3%, 10%, 50%, 80% ethyl acetate: hexanes) to afford pure product (125 mg, 63%) as clear yellow oil.

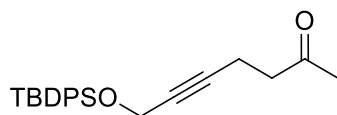
TLC $R_f = 0.25$ (90% ethyl acetate: hexanes). IR (film): 3394, 2924, 2218, 1708 cm^{-1} . ^1H NMR (300 MHz, CDCl_3) δ 5.60 (t, $J = 6.9$ Hz, 1H), 3.66 (t, $J = 6.3$ Hz, 4H), 3.46 (s, 1H), 2.83 (s, 1H), 2.52 (t, $J = 6.3$ Hz, 2H), 2.49-2.43 (m, 4H), 2.24 (t, $J = 6.0$ Hz, 2H), 2.08 (s, 3H). ^{13}C NMR (75 MHz, CDCl_3) δ 209.2, 136.8, 121.1, 92.5, 79.7, 61.1, 61.0, 42.8, 40.4, 30.0, 24.9, 23.9. HRMS (ES⁺): m/z calcd for $\text{C}_{12}\text{H}_{18}\text{O}_3\text{Na}$ (M+Na): 233.1153. Found: 233.1445.



(E)-9-Hydroxy-6-(hydroxymethyl)non-5-en-7-yn-2-one, 2.3d.

Purified by flash chromatography on silica gel (gradient elution with 20%, 40%, 60%, 80% ethyl acetate: hexanes then 100% ethyl acetate: hexanes) to afford pure product (42 mg, 21%) as clear yellow oil.

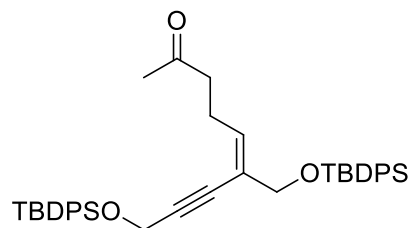
TLC R_f = 0.25 (80% ethyl acetate: hexanes). IR (film): 3445, 2922, 2863, 2213, 1707 cm^{-1} . ^1H NMR (300 MHz, C_6D_6) δ 5.88 (t, J = 6.7 Hz, 1H), 4.38 (s, 2H), 4.05 (s, 2H), 3.47 (s, 2H), 2.56-2.47 (m, 4H), 2.14 (s, 3H). ^{13}C NMR (75 MHz, CDCl_3) δ 208.9, 136.6, 123.9, 93.9, 81.8, 65.9, 51.4, 42.7, 30.1, 24.6. Anal calcd for $\text{C}_{10}\text{H}_{14}\text{O}_3$: C, 65.91; H, 7.74. Found: C, 65.76; H, 7.72.



7-((tert-Butyldiphenylsilyl)oxy)hept-5-yn-2-one, 2.2e.

Purified by flash chromatography on silica gel (gradient elution with 2, 5, 10, 15% ethyl acetate: hexanes) to afford pure product (22 mg, 3%) as yellow oil.

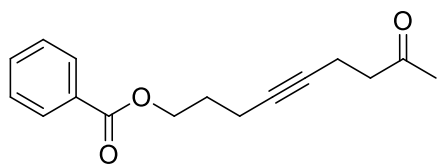
TLC R_f = 0.46 (10% dichloromethane: hexanes). IR (film): 2931, 2857, 1720, 1427, 1111, 1072 cm^{-1} . ^1H NMR (300 MHz, CDCl_3) δ 7.73-7.69 (m, 4H), 7.47-7.35 (m, 6H), 4.29 (t, J = 2.1 Hz, 2H), 2.58-2.53 (m, 2H), 2.43-2.36 (m, 2H), 2.14 (s, 3H), 1.05 (s, 9H). ^{13}C NMR (75 MHz, CDCl_3) δ 206.9, 135.8, 133.5, 129.9, 127.8, 84.3, 79.1, 53.1, 42.4, 30.1, 26.9, 19.3, 13.5. Anal. Calcd for $\text{C}_{23}\text{H}_{28}\text{O}_2\text{Si}$: C, 75.78; H, 7.74. Found: C, 75.56; H, 7.62.



(E)-9-((tert-Butyldiphenylsilyl)oxy)-6-(((tert-butyl-diphenylsilyl)oxy)methyl)non-5-en-7-yn-2-one, 2.3e.

Purified by flash chromatography on silica gel (gradient elution with 2%, 5%, 10%, 15% ethyl acetate: hexanes) to afford pure product (216 mg, 29%) as clear yellow oil.

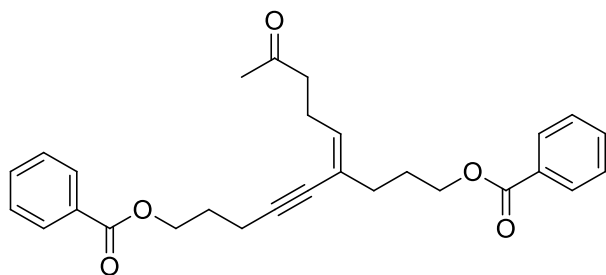
TLC R_f = 0.40 (10% ethyl acetate: hexanes). IR (film): 2931, 2857, 1717, 1428, 1112 cm^{-1} . ^1H NMR (300 MHz, C_6D_6) δ 7.74 -7.72 (m, 8H), 7.22-7.16 (m, 12H), 6.09 (t, J = 7.5 Hz, 1H), 4.36 (s, 2H), 4.20 (s, 2H), 2.53 (q, J = 7.4 Hz, 2H), 2.01 (t, J = 7.4 Hz, 2H), 1.62 (s, 3H), 1.14 (s, 9H), 1.08 (s, 9H). ^{13}C NMR (75 MHz, C_6D_6) δ 205.9, 136.2, 135.7, 130.4, 128.6, 128.0, 123.6, 93.9, 82.2, 66.6, 53.7, 42.8, 27.4, 27.2, 25.0, 19.8. Anal calcd for $\text{C}_{42}\text{H}_{50}\text{O}_3\text{Si}_2$: C, 76.55; H, 7.65. Found: C, 76.59; H, 7.49.



8-Oxonon-4-yn-1-yl benzoate, 2.2f.

Purified by flash chromatography on silica gel (gradient elution with 6%, 10%, 20% ethyl acetate: hexanes) to afford pure product (10 mg, 20%) as clear yellow oil.

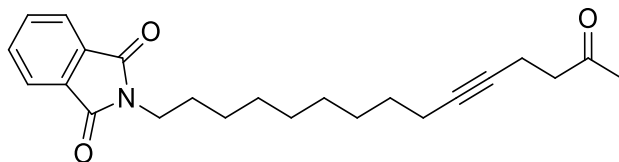
TLC R_f = 0.36 (20% ethyl acetate: hexanes). IR (film): 2921, 1717, 1274, 1116 cm^{-1} . ^1H NMR (300 MHz, CDCl_3) δ 8.06-8.01 (m, 2H), 7.55 (tt, J = 7.3, 1.4 Hz, 1H), 7.43 (tt, J = 7.2, 1.5 Hz, 2H), 4.39 (t, J = 6.3 Hz, 2H), 2.61 (t, J = 6.9 Hz, 2H), 2.42-2.29 (m, 4H), 2.15 (s, 3H), 1.93 (p, J = 6.4 Hz, 2H). ^{13}C NMR (75 MHz, CDCl_3) δ 207.1, 166.7, 133.1, 130.5, 129.8, 128.5, 79.7, 79.4, 63.9, 43.0, 30.1, 28.3, 15.8, 13.5. HRMS (EI): m/z calcd for $\text{C}_{16}\text{H}_{18}\text{O}_3\text{Na}$ (M+Na): 281.1148. Found: 281.1151.



(Z)-6-(4-Oxopentylidene)non-4-yne-1,9-diyl dibenzoate, 2.3f.

Purified by flash chromatography on silica gel (gradient elution with 6%, 10%, 20% ethyl acetate: hexanes) to afford pure product (30 mg, 67%) as clear yellow oil.

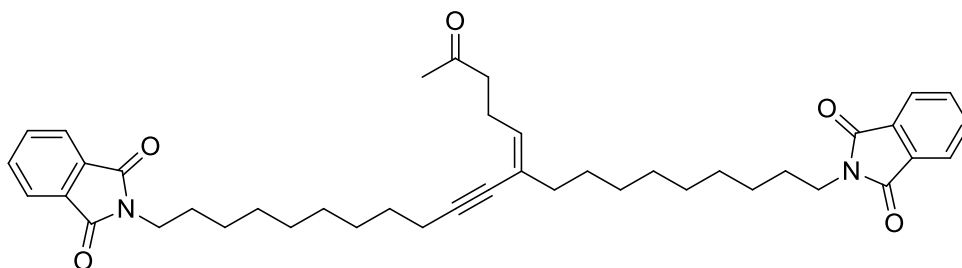
TLC R_f = 0.32 (20% ethyl acetate: hexanes). IR (film): 1717, 1274, 1116 cm^{-1} . ^1H NMR (300 MHz, CDCl_3) δ 8.05-8.01 (m, 4H), 7.56-7.51 (m, 2H), 7.46-7.40 (m, 4H), 5.64 (t, J = 3.3 Hz, 1H), 4.42 (t, J = 6.3 Hz, 2H), 4.30, (t, J = 6.4 Hz, 2H), 2.54 (t, J = 7.2 Hz, 2H), 2.48 (d, J = 3.4 Hz, 4H), 2.23 (t, J = 7.3 Hz, 2H), 2.11 (s, 3H), 2.04-1.97 (m, 4H). ^{13}C NMR (75 MHz, CDCl_3) δ 208.4, 135.3, 133.1, 133.0, 129.8, 128.5, 123.3, 94.0, 79.2, 64.3, 63.8, 43.2, 34.0, 28.3, 27.6, 24.9, 16.6. HRMS (EI): m/z calcd for $\text{C}_{28}\text{H}_{30}\text{O}_5\text{Na}$ (M+Na): 469.1990. Found: 469.1988.



2-(14-Oxopentadec-10-yn-1-yl)isoindoline-1,3-dione, 3.2g.

Purified by flash chromatography on silica gel (gradient elution with 10, 15, 20, 25% ethyl acetate: hexanes) to afford pure product (47 mg, 26%) as a tan solid. mp = 37-40 °C.

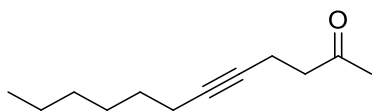
TLC R_f = 0.40 (30% ethyl acetate: hexanes). IR (KBr): 2931, 2851, 1771, 1710, 1614, 1398, 1062 cm^{-1} . ^1H NMR (300 MHz, CDCl_3) δ 7.86-7.81 (m, 2H), 7.74-7.67 (m, 2H), 3.67 (t, J = 7.4 H, 2H), 2.66-2.60 (m, 2H), 2.44-2.37 (m, 2H), 2.16 (s, 3H), 2.13-2.06 (m, 2H), 1.71-1.61 (m, 2H), 1.49-1.22 (m, 12H). ^{13}C NMR (75 MHz, CDCl_3) δ 207.3, 168.6, 134.0, 132.3, 123.3, 81.1, 78.6, 43.2, 38.2, 30.1, 29.5, 29.3, 29.2, 29.1, 28.9, 28.7, 27.0, 18.8, 13.6. Anal. Calcd for $\text{C}_{23}\text{H}_{29}\text{NO}_3$: C, 75.17; H, 7.95; N, 3.81. Found: C, 75.22; H, 8.22, N, 3.95.



(Z)-2,2'-(12-(4-Oxopentylidene)henicos-10-yne-1,21-diyl)bis(isoindoline-1,3-dione), 3.3g.

Purified by flash chromatography on silica gel (gradient elution with 10%, 15%, 20%, 25% ethyl acetate: hexanes) to afford pure product (49 mg, 30%) as a clear yellow oil. TLC R_f = 0.13 (30% ethyl acetate: hexanes). IR (film): 2929, 2854, 1772, 1713, 1639, 1396 cm^{-1} .

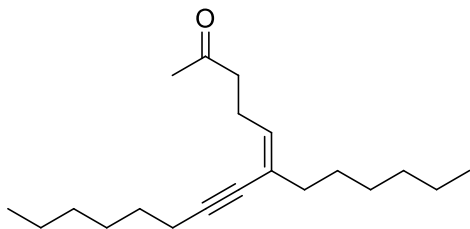
^1H NMR (300 MHz, CDCl_3) δ 7.86-7.80 (m, 4H), 7.73-7.67 (m, 4H), 5.56-5.50 (m, 1H), 3.67 (t, $J = 7.4$ Hz, 4H), 2.50-2.46 (m, 4H), 2.32 (t, $J = 7.1$ Hz, 2H), 2.13 (s, 3H), 2.02 (t, $J = 7.7$ Hz, 2H), 1.71-1.20 (m, 28H). ^{13}C NMR (75 MHz, CDCl_3) δ 208.8, 168.6, 134.0, 133.5, 132.3, 125.1, 123.3, 95.2, 78.8, 43.4, 38.2, 37.5, 29.9, 29.6, 29.5, 29.5, 29.3, 29.3, 29.2, 29.1, 29.0, 28.8, 28.5, 27.0, 27.0, 25.0, 19.6. Anal. Calcd for $\text{C}_{42}\text{H}_{52}\text{N}_2\text{O}_5$: C, 75.87; H, 7.88; N, 4.21. Found: C, 75.86; H, 7.69, N, 4.59.



Dodec-5-yn-2-one, 3.2h.

Purified by flash chromatography on silica gel (gradient elution with 20%, 30%, 40%, 50% dichloromethane:hexanes) to afford pure product (32 mg, 24%) as clear yellow oil.

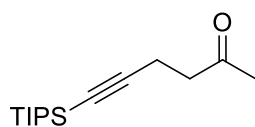
TLC $R_f = 0.27$ (10% ethyl acetate: hexanes). IR (film): 2956, 2930, 1720 cm^{-1} . ^1H NMR (300 MHz, CDCl_3) δ 2.57 (t, $J = 7.1$ Hz, 2H), 2.35-2.29 (m, 2H), 2.08 (s, 3H), 2.05-2.00 (m, 2H), 1.42-1.16 (m, 8H), 0.80 (t, $J = 7.1$ Hz, 3H). ^{13}C NMR (75 MHz, CDCl_3) δ 207.0, 80.9, 78.5, 43.0, 31.4, 29.9, 29.0, 28.6, 22.6, 18.7, 14.1, 13.5. Anal calcd for $\text{C}_{12}\text{H}_{20}\text{O}$: C, 74.84; H, 9.96. Found: C, 74.69; 10.25.



(Z)-6-Hexyltetradec-5-en-7-yn-2-one, 3.3h.

Purified by flash chromatography on silica gel (gradient elution with 20%, 30%, 40%, 50% dichloromethane: hexanes) to afford pure product (47 mg, 47%) as clear yellow oil.

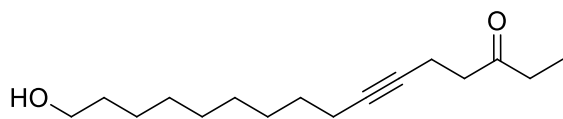
TLC R_f = 0.38 (40% dichloromethane: hexanes). IR (film): 2956, 2929, 2858, 1719 cm^{-1} . ^1H NMR (300 MHz, CDCl_3) δ 5.53 (t, J = 7.8 Hz, 1H), 2.48-2.47 (m, 4H), 2.32 (t, J = 6.9 Hz, 2H), 2.13 (s, 3H), 2.03 (t, J = 6.3 Hz, 2H), 1.57-1.24 (m, 16H), 0.90-0.84 (m, 6H). ^{13}C NMR (75 MHz, CDCl_3) δ 208.8, 133.5, 125.2, 95.3, 78.9, 43.5, 37.6, 31.9, 31.6, 29.9, 29.1, 28.8, 28.7, 28.6, 25.0, 22.8, 22.8, 19.7, 14.3, 14.3. HRMS (ES⁺): m/z calcd for $\text{C}_{20}\text{H}_{34}\text{ONa}$ (M+Na): 313.2507. Found: 313.2497.



6-(Triisopropylsilyl)hex-5-yn-2-one, 3.2j.

Purified by flash chromatography on silica gel (elution 6%, 10% ethyl acetate: hexanes) to afford pure product (80 mg, 75%) as clear yellow oil.

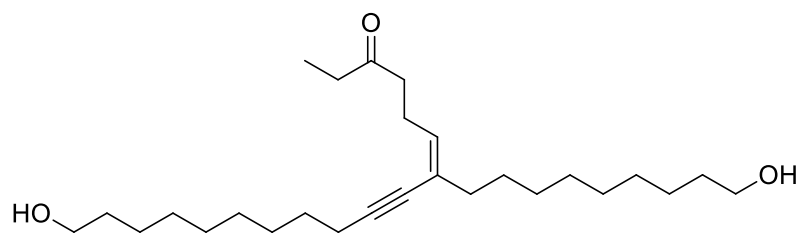
TLC R_f = 0.29 (10% ethyl acetate: hexanes). IR (film): 2942, 2865, 2173, 1721 cm^{-1} . ^1H NMR (300 MHz, CDCl_3) δ 2.63 (t, J = 7.6 Hz, 2H), 2.46 (t, J = 7.4 Hz, 2H), 2.13 (s, 3H), 0.93-1.04 (m, 21H). ^{13}C NMR (75 MHz, CDCl_3) δ 206.6, 107.4, 81.0, 42.9, 30.0, 18.7, 14.8, 11.4. Anal calcd for $\text{C}_{15}\text{H}_{28}\text{OSi}$: C, 71.36; H, 11.18. Found: C, 71.19; H, 11.40.



16-Hydroxyhexadec-6-yn-3-one, 3.2k.

Purified by flash chromatography on silica gel (gradient elution with 25%, 50% ethyl acetate: hexanes) to afford pure product (43 mg, 34%) as a tan solid. mp = 45-47 °C.

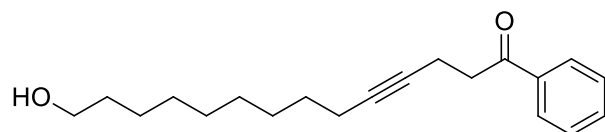
TLC R_f = 0.47 (50% ethyl acetate: hexanes). IR (KBr): 3416, 2929, 2853, 1715, 1364, 1223 cm^{-1} . ^1H NMR (300 MHz, CDCl_3) δ 3.64 (t, J = 6.6 Hz, 2H), 2.63-2.57 (m, 2H), 2.49-2.38 (m, 4H), 2.15-2.07 (m, 2H), 1.62-1.21 (m, 15H), 1.06 (t, J = 7.4 Hz, 3H). ^{13}C NMR (75 MHz, CDCl_3) δ 210.1, 81.1, 78.8, 63.3, 41.9, 36.2, 33.0, 29.9, 29.7, 29.6, 29.3, 29.2, 29.0, 25.9, 18.9, 13.8, 7.9. Anal. Calcd for $\text{C}_{16}\text{H}_{28}\text{O}_2$: C, 76.14; H, 11.18. Found: C, 76.24; H, 11.31.



(Z)-18-Hydroxy-7-(9-hydroxynonyl)octadec-6-en-8-yn-3-one, 3.3k.

Purified by flash chromatography on silica gel (gradient elution with 25%, 50% ethyl acetate: hexanes) to afford pure product (48 mg, 46%) as a tan solid. mp = 39-42 °C.

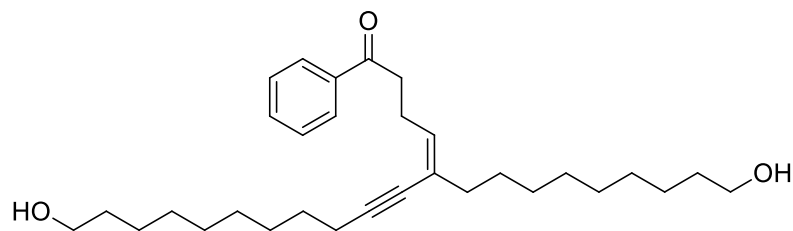
TLC R_f = 0.14 (50% ethyl acetate: hexanes). IR (KBr): 3361, 2925, 2850, 1704, 1465, 1063 cm^{-1} . ^1H NMR (300 MHz, CDCl_3) δ 5.57-5.51 (m, 1H), 3.64 (t, J = 6.5 Hz, 4H), 2.50-2.39 (m, 6H), 2.34 (t, J = 6.89 Hz, 2H), 2.04 (t, J = 7.6 Hz, 2H), 1.62-1.22 (m, 30H), 1.05 (t, J = 7.4 Hz, 3H). ^{13}C NMR (75 MHz, CDCl_3) δ 211.5, 133.7, 125.0, 95.2, 78.9, 63.1, 42.1, 37.6, 35.9, 32.9, 29.9, 29.7, 29.7, 29.6, 29.6, 29.3, 29.1, 29.1, 29.0, 28.6, 25.9, 25.0, 19.7, 8.0. Anal. Calcd for $\text{C}_{27}\text{H}_{48}\text{O}_3$: C, 77.09; H, 11.50; N. Found: C, 77.03; H, 11.59.



14-Hydroxy-1-phenyltetradec-4-yn-1-one, 3.2l.

Purified by flash chromatography on silica gel (gradient elution with 30, 40, 60, 70% ethyl acetate: hexanes) to afford pure product (47 mg, 36%) as a tan solid.

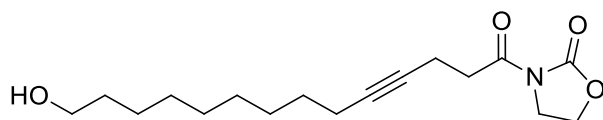
mp = 45-48 °C. TLC R_f = 0.64 (30% ethyl acetate: hexanes). IR (KBr): 3392, 2927, 2848, 1678, 1447, 1061 cm^{-1} . ^1H NMR (300 MHz, CDCl_3) δ 8.00-7.95 (m, 2H), 7.60-7.53 (m, 1H), 7.50-7.43 (m, 2H), 3.64 (t, J = 6.6 Hz, 2H), 3.22-3.17 (m, 2H), 2.63-2.55 (m, 2H), 2.16-2.07 (m, 2H), 1.62-1.24 (m, 15H). ^{13}C NMR (75 MHz, CDCl_3) δ 198.6, 136.8, 133.3, 128.7, 128.2, 81.1, 78.9, 63.1, 38.4, 32.9, 29.6, 29.5, 29.2, 29.1, 28.9, 25.9, 18.8, 13.9. Anal. Calcd for $\text{C}_{20}\text{H}_{28}\text{O}_2$: C, 79.96; H, 9.39. Found: C, 79.94; H, 9.55.



(Z)-16-Hydroxy-5-(9-hydroxynonyl)-1-phenylhexadec-4-en-6-yn-1-one, 3.l.

Purified by flash chromatography on silica gel (gradient elution with 30%, 40%, 60%, 70% ethyl acetate: hexanes) to afford pure product (45 mg, 45%) as clear yellow oil.

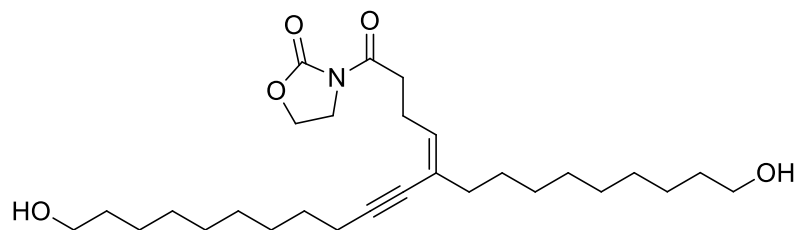
TLC R_f = 0.36 (70% ethyl acetate: hexanes). IR (film): 3307, 2926, 2852, 1684 cm^{-1} . ^1H NMR (300 MHz, C_6D_6) δ 7.98-7.95(dt, J = 7.2, 1.5 Hz, 2H), 7.54 (tt, J = 7.2, 1.3 Hz, 1H), 7.45 (tt, J = 6.9, 1.6 Hz, 2H), 5.66 (t, J = 7.4 Hz, 1H), 3.62 (td, J = 6.6, 1.8 Hz, 4H), 3.05 (t, J = 7.2 Hz, 2H), 2.65(q, J = 7.4 Hz, 2H), 2.32 (t, J = 6.8 Hz, 2H), 2.06 (t, J = 7.3 Hz, 2H), 1.60-1.41 (m, 10H), 1.27 (bs, 20H). ^{13}C NMR (75 MHz, CDCl_3) δ 200.0, 137.1, 133.9, 133.1, 128.7, 128.3, 125.2, 95.3, 63.2, 38.5, 37.6, 33.0, 29.72, 29.68, 29.61, 29.58, 29.57, 29.2, 29.1, 29.0, 20.0, 28.6, 25.9, 25.4, 19.7. Anal calcd for $\text{C}_{31}\text{H}_{48}\text{O}_3$: C, 79.44; H, 10.32. Found: C, 79.33; H, 10.30.



3-(14-Hydroxytetradec-4-ynoyl)oxazolidin-2-one, 3.2m.

Purified by flash chromatography on silica gel (gradient elution with 40%, 60%, 80%, 95% ethyl acetate: hexanes then 100% ethyl acetate) to afford pure product (57 mg, 44%) as clear yellow oil.

TLC R_f = 0.59 (90% ethyl acetate: hexanes). IR (film): 3213, 2929, 1781, 1702 cm^{-1} . ^1H NMR (300 MHz, CDCl_3) δ 4.40 (t, J = 7.5 Hz, 2H), 4.00 (t, J = 8.4 Hz, 2H), 3.60 (t, J = 6.6 Hz, 2H), 3.10 (t, J = 7.2 Hz, 2H), 2.48 (tt, J = 7.8, 2.4 Hz, 2H), 2.08 (tt, J = 6.9, 2.4 Hz, 2H), 1.55-1.48 (m, 2H), 1.45-1.36 (m, 2H), 1.27 (s, 10H). ^{13}C NMR (75 MHz, CDCl_3) δ 172.0, 153.7, 81.3, 78.2, 63.2, 62.3, 42.6, 35.2, 32.9, 29.6, 29.5, 29.2, 29.1, 28.9, 25.8, 18.9, 14.1. Anal calcd for $\text{C}_{17}\text{H}_{27}\text{NO}_4$: C, 65.99; H, 8.80. Found: C, 65.87; H, 8.91.

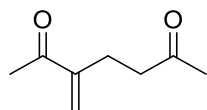


(Z)-3-(16-Hydroxy-5-(9-hydroxynonyl)hexadec-4-en-6-ynoyl)oxazolidin-2-one, 3.3m.

Purified by flash chromatography on silica gel (gradient elution with 40%, 60%, 80%, 95% ethyl acetate: hexanes then 100% ethyl acetate) to afford pure product (45 mg, 45%) as clear yellow oil. TLC $R_f = 0.49$ (90% ethyl acetate: hexanes). IR (film): 3338, 2926, 2852, 1783, 1687 cm^{-1} .

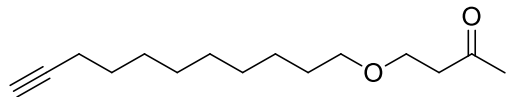
^1H NMR (300 MHz, CDCl_3) δ 5.57 (t, $J = 6.9$ Hz, 1H), 4.37 (t, $J = 7.5$ Hz, 2H), 4.37 (t, $J = 7.5$ Hz, 2H), 3.98 (t, $J = 7.8$ Hz, 2H), 3.59 (t, $J = 6.6$ Hz, 4H), 2.96 (t, $J = 6.9$ Hz, 2H), 2.56 (t, $J = 7.2$ Hz, 2H), 2.30 (t, $J = 6.6$ Hz, 2H), 2.01 (t, $J = 7.8$ Hz, 2H), 1.80 (s, 2H), 1.52-1.27 (m, 14H).

^{13}C NMR (75 MHz, CDCl_3) δ 173.1, 153.7, 133.2, 125.4, 95.2, 78.9, 63.1, 62.23, 60.6, 43.0, 42.7, 37.6, 35.1, 32.9, 31.7, 29.68, 29.65, 29.6, 29.5, 29.2, 29.1, 29.0, 28.9, 28.78, 28.6, 25.9, 25.2, 22.8. Anal calcd for $\text{C}_{28}\text{H}_{47}\text{NO}_5$: C, 70.40; H, 9.92. Found: C, 70.39; H, 10.04.



3-Methyleneheptane-2,6-dione, 3.4.

Purified by flash chromatography on silica gel (gradient elution with 3%, 6% ethyl acetate: hexanes) to afford pure product as clear yellow oil. ^1H NMR (300 MHz, CDCl_3) δ 5.98 (s, 1H), 5.78 (t, $J = 1.1$ Hz, 1H), 2.55-2.44 (m, 4H), 2.27 (s, 3H), 2.06 (s, 3H). ^{13}C NMR (75 MHz, CDCl_3) δ 207.9, 199.6, 147.7, 126.4, 42.5, 29.9, 25.9, 25.3. Anal calcd for $\text{C}_8\text{H}_{12}\text{O}_2$: C, 68.54; H, 8.63. Found: C, 68.18; H, 8.77.

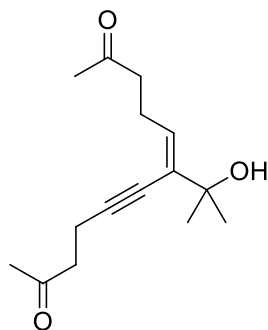


4-(Undec-10-yn-1-yloxy)butan-2-one, 3.5.

Purified by flash chromatography on silica gel (gradient elution with 40%, 50%, 70%, 80% ethyl acetate: hexanes) to afford pure product (47 mg, 41%) as clear yellow oil.

TLC R_f = 0.51 (30% ethyl acetate: hexanes). IR (film): 3292, 2929, 2856, 2116, 1717, 1115 cm^{-1} .

^1H NMR (300 MHz, C_6D_6) δ 3.49 (t, J = 6.3 Hz, 2H), 3.23 (t, J = 6.3 Hz, 2H), 2.25 (t, J = 6.3 Hz, 2H), 1.97 (tt, J = 6.6, 2.7 Hz, 2H), 1.82 (t, J = 2.4 Hz, 1H), 1.71 (s, 3H), 1.49 (p, J = 6.6 Hz, 2H), 1.40-1.17 (m, 6H), 1.15 (s, 6H). ^{13}C NMR (75 MHz, C_6D_6) δ 205.4, 84.9, 71.7, 69.2, 66.5, 44.0, 30.5, 30.3, 30.2, 30.1, 29.7, 29.4, 29.2, 26.9, 19.0. Anal calcd for $\text{C}_{15}\text{H}_{26}\text{O}_2$: C, 75.58; H, 10.99. Found: C, 75.27; H, 10.94.



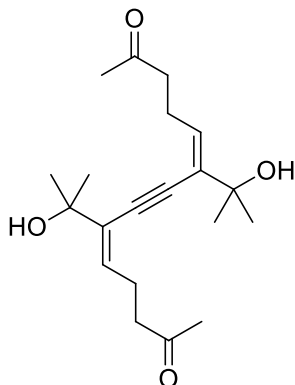
(E)-6-(2-Hydroxypropan-2-yl)dodec-5-en-7-yne-2,11-dione, 3.7.

Purified by flash chromatography on silica gel (gradient elution with 20%, 60%, 70% ethyl acetate: hexanes) to afford pure product (73 mg, 53%) as clear yellow oil.

TLC R_f = 0.44 (80% ethyl acetate: hexanes). IR (film): 3444, 2975, 2928, 1997, 1715, 1364,

1165 cm^{-1} . ^1H NMR (300 MHz, C_6D_6) δ 5.88 (t, J = 6.6 Hz, 1H), 2.70-2.65 (t, J = 6.3 Hz, 2H),

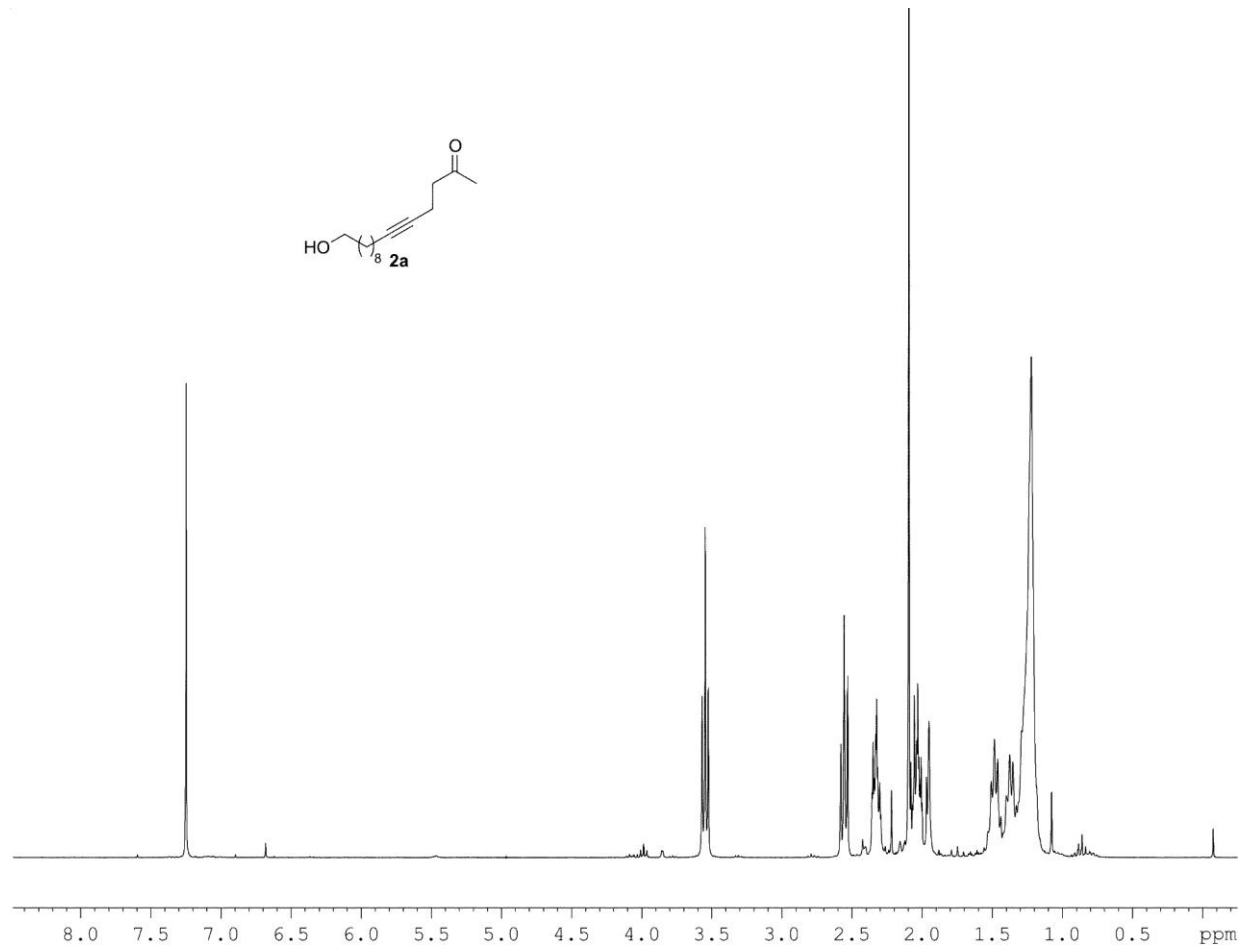
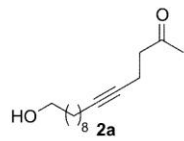
2.60-2.55 (t, $J = 6.2$ Hz, 2H), 2.46 (t, $J = 6.3$ Hz, 4H), 2.14 (s, 3H), 2.10 (s, 3H), 2.08 (s, 1H), 1.31 (s, 6H). ^{13}C NMR (75 MHz, CDCl_3) δ 208.5, 206.7, 132.6, 131.2, 95.7, 72.4, 43.0, 42.6, 30.0, 29.9, 29.3, 24.8, 24.7, 14.3. HRMS (ES⁺): m/z calcd for $\text{C}_{15}\text{H}_{22}\text{O}_3\text{Na}$ (M+Na): 273.1466. Found: 273.1456.

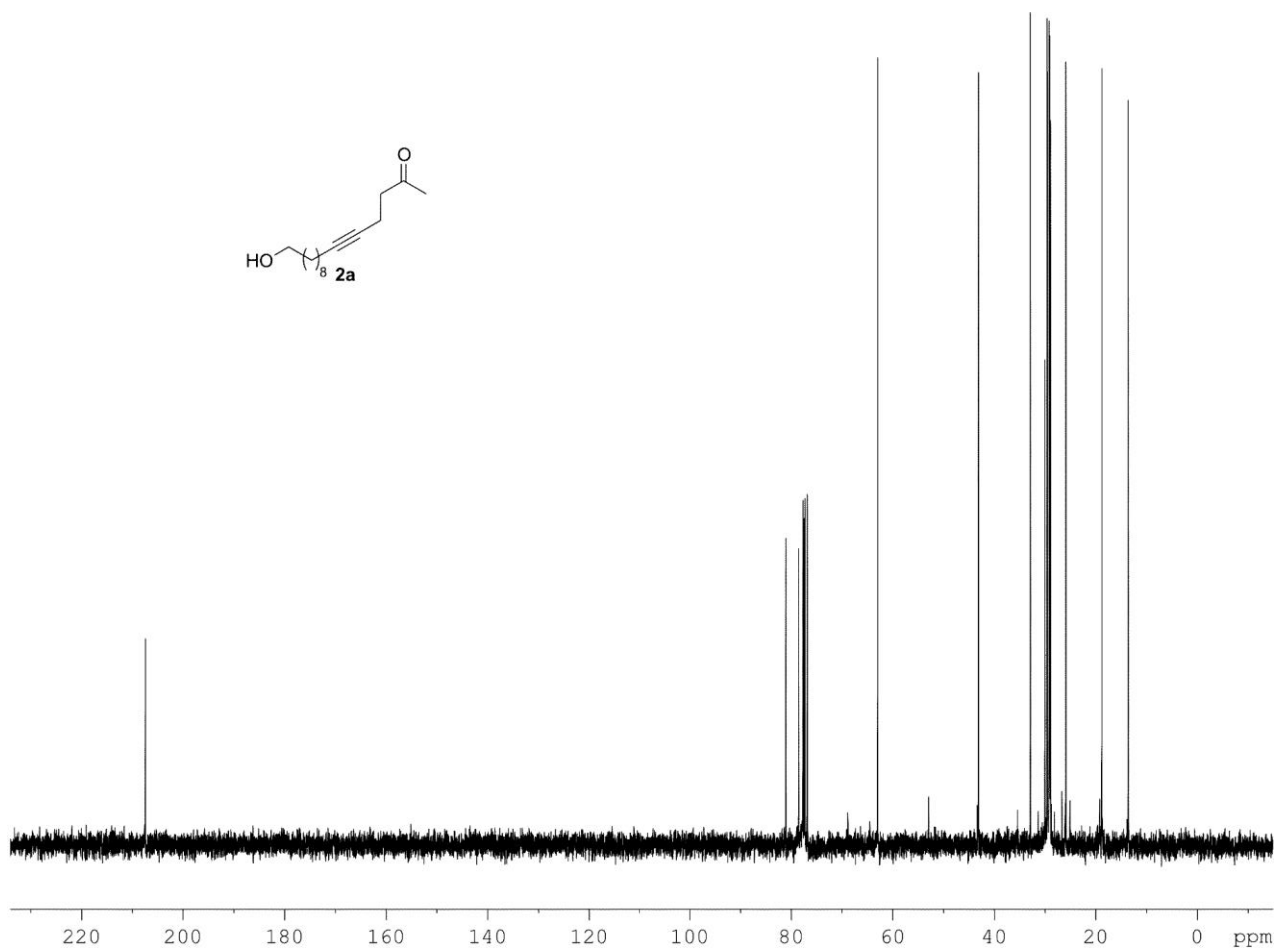
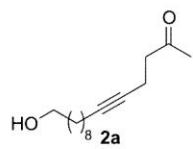


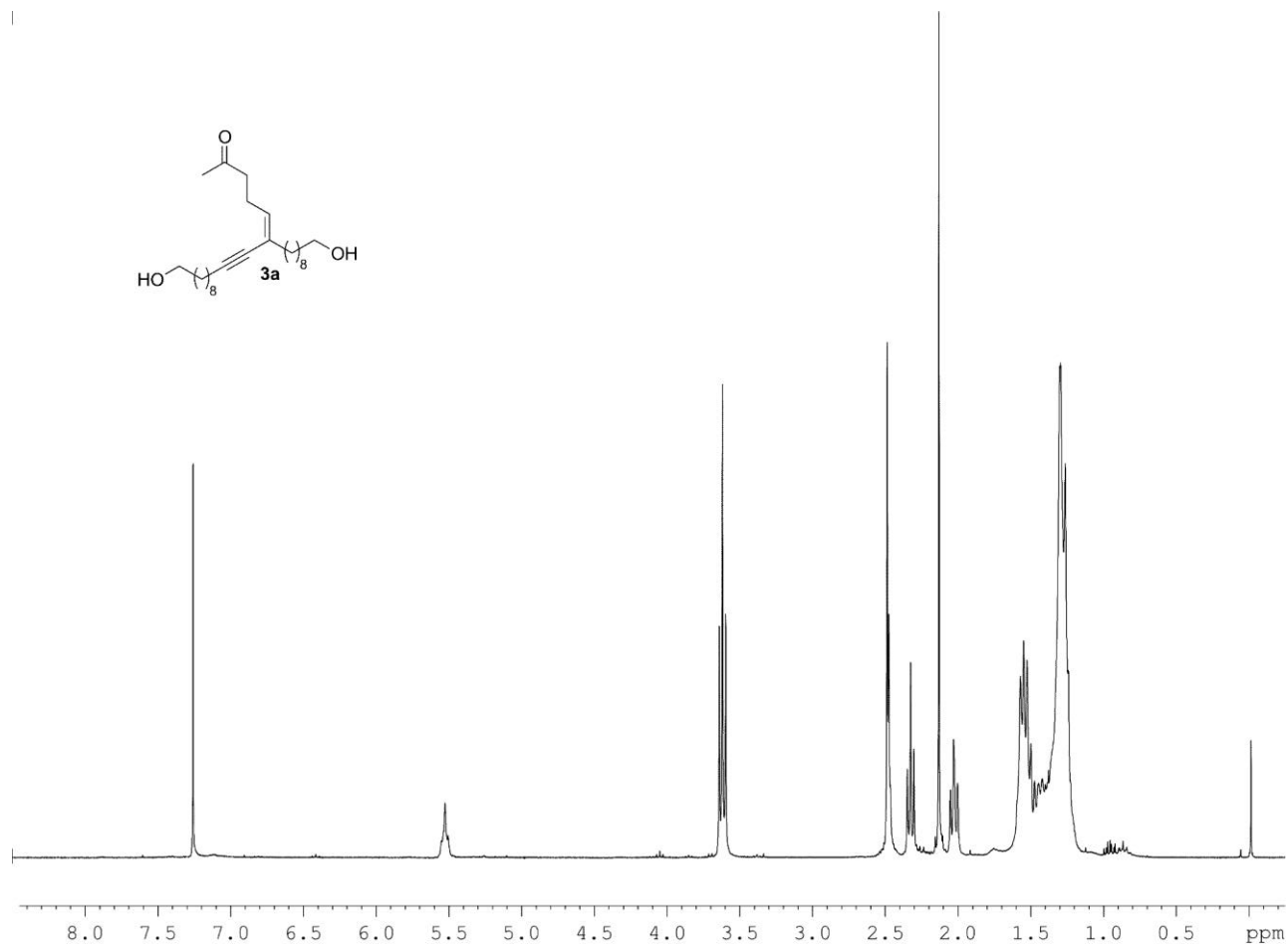
(5E,9E)-6,9-bis(2-Hydroxypropan-2-yl)tetradeca-5,9-dien-7-yne-2,13-dione, 3.8.

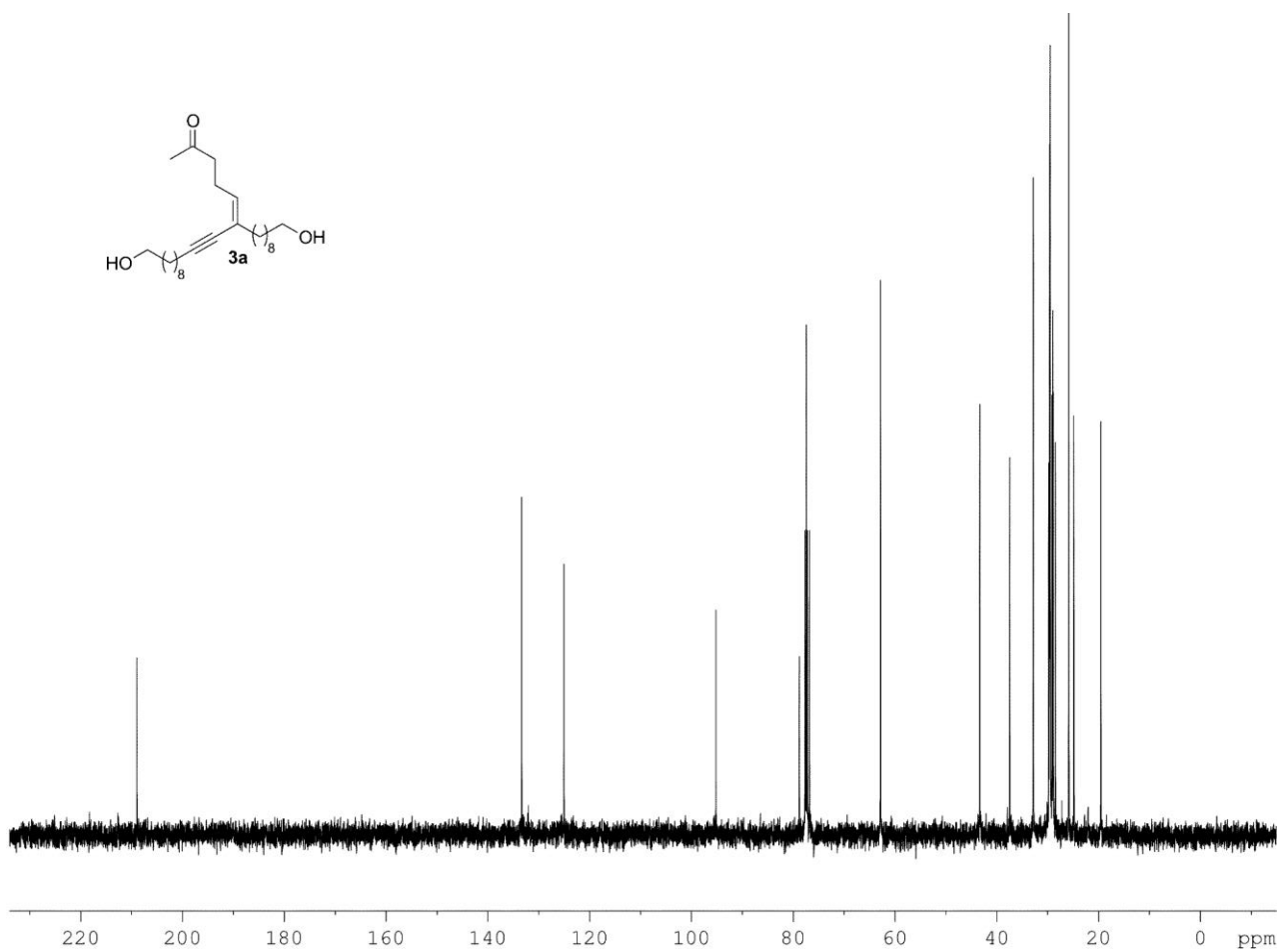
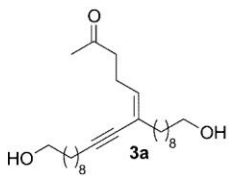
Purified by flash chromatography on silica gel (gradient elution with 20%, 60%, 70% ethyl acetate: hexanes) to afford pure product (67 mg, 54%) as clear yellow oil.

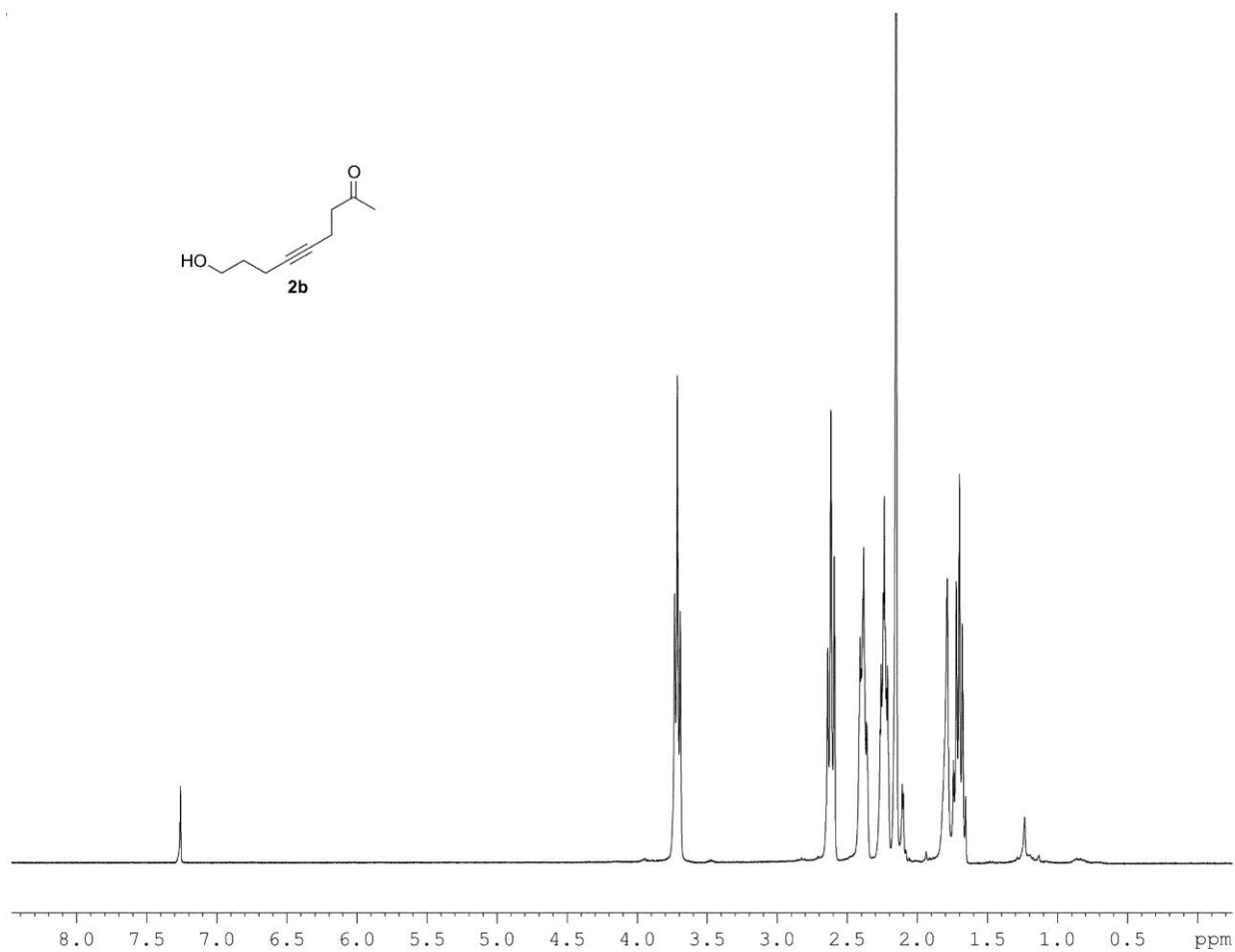
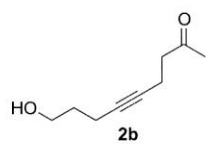
TLC $R_f = 0.21$ (80% ethyl acetate: hexanes). mp = 78-80 °C. IR (film): 3425, 2968, 2926, 1707 cm^{-1} . ^1H NMR (300 MHz, CDCl_3) δ 6.03-5.98 (m, 2H), 2.54-2.52 (m, 8H), 2.44 (s, 2H), 2.11 (s, 6H), 1.39 (s, 12H). ^{13}C NMR (75 MHz, CDCl_3) δ 208.2, 132.8, 132.2, 92.9, 72.6, 42.9, 30.0, 29.7, 25.0. HRMS (ES⁺): m/z calcd for $\text{C}_{20}\text{H}_{30}\text{O}_4\text{Na}$ (M+Na): 357.2041. Found: 357.2028.

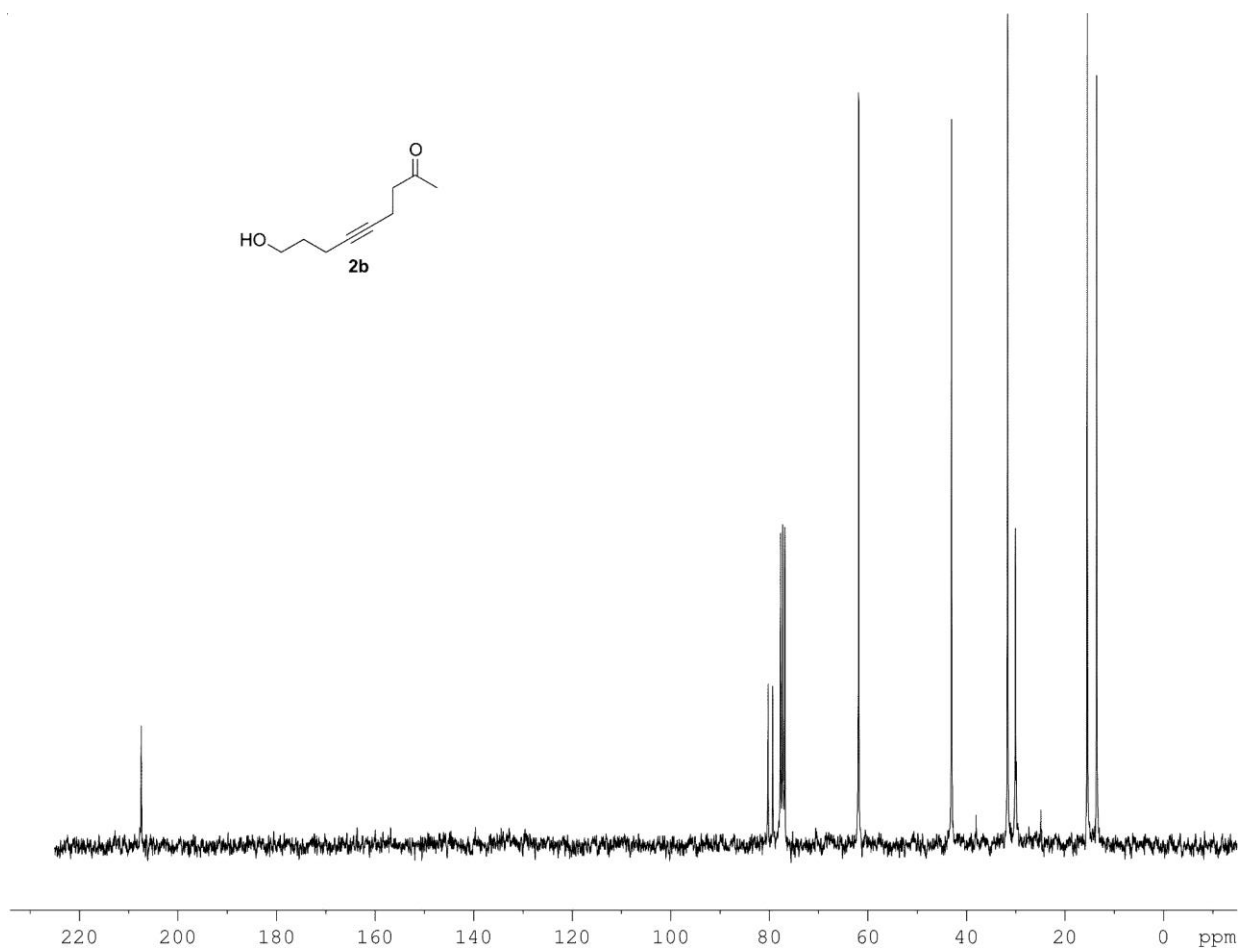
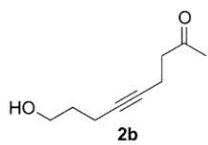


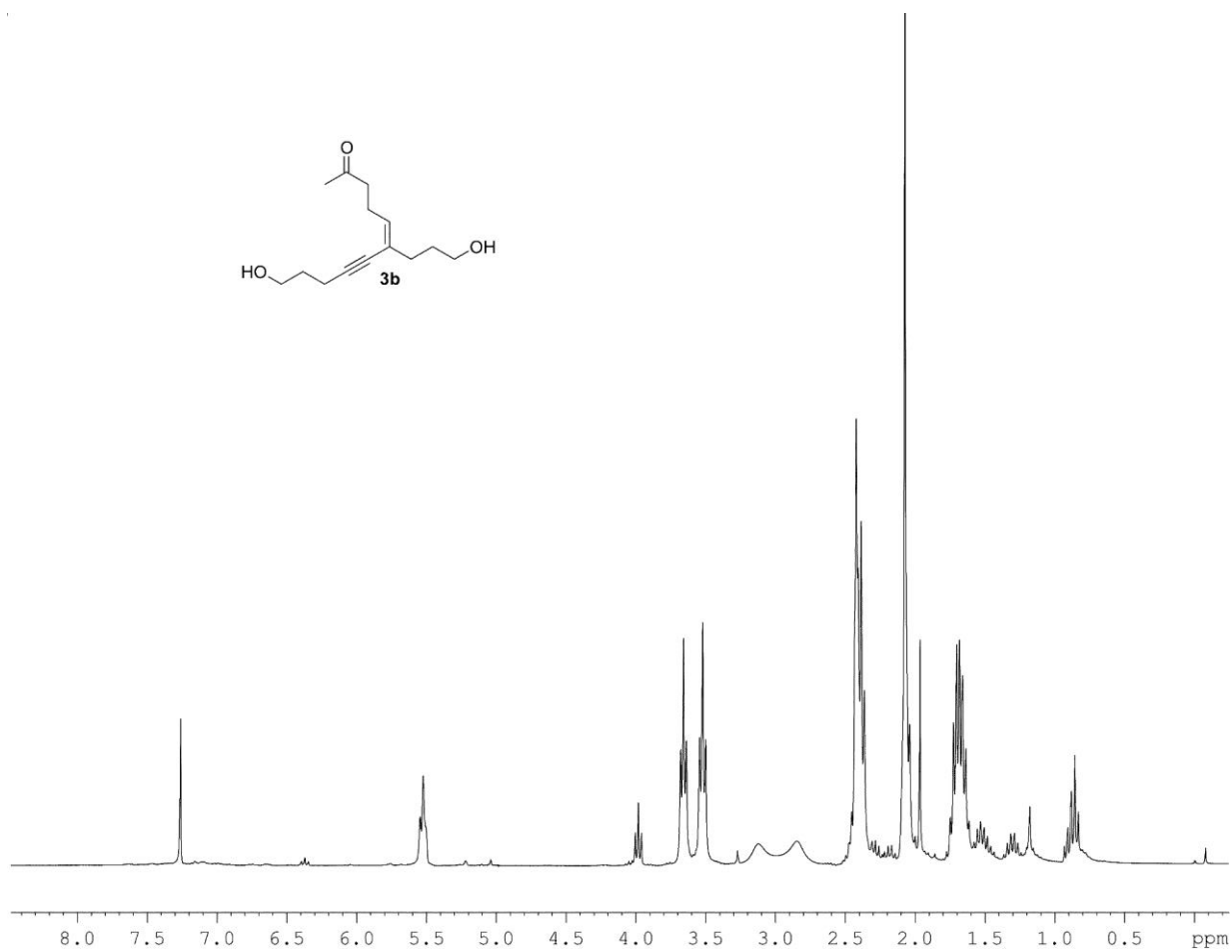
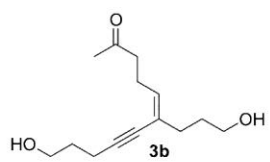


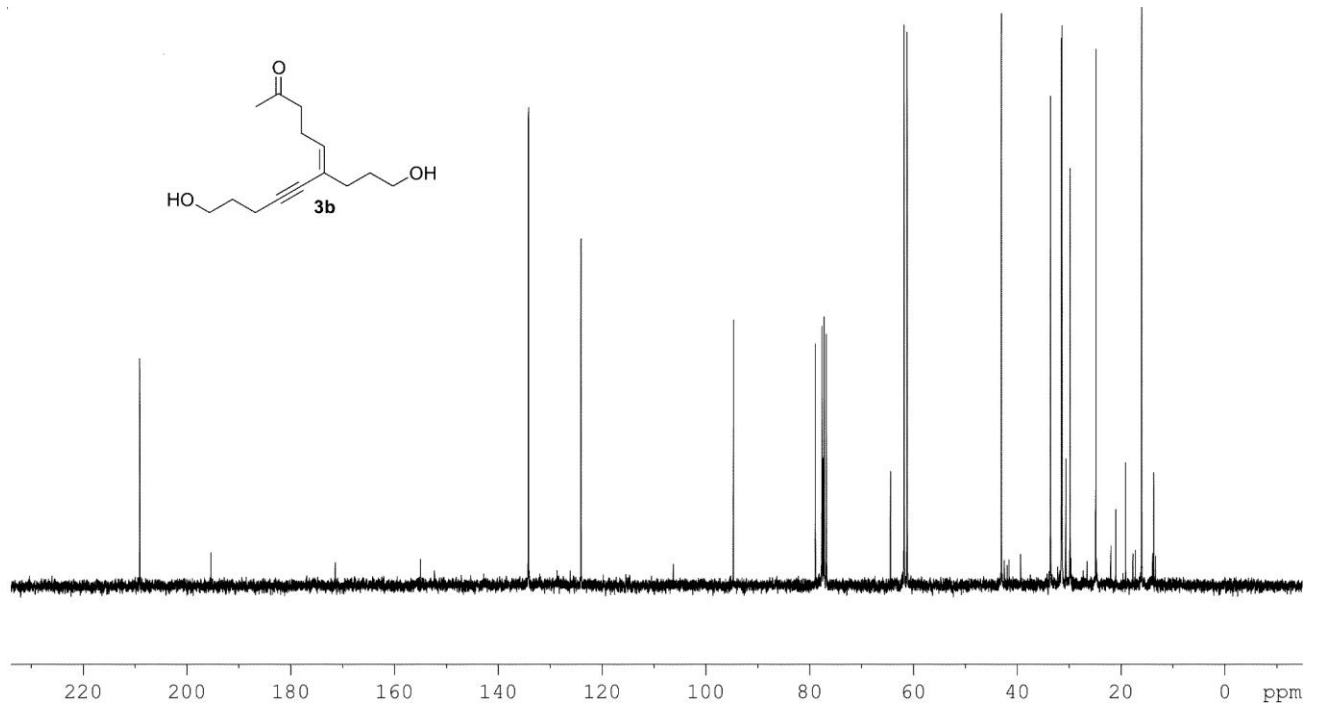


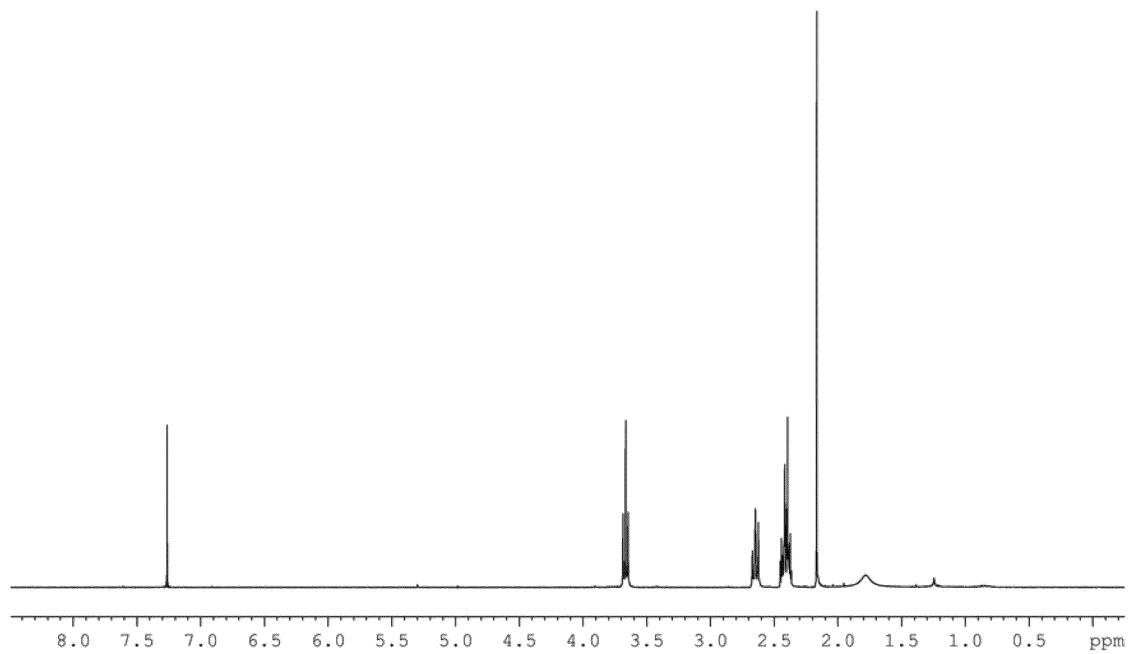
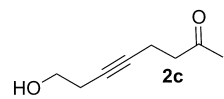


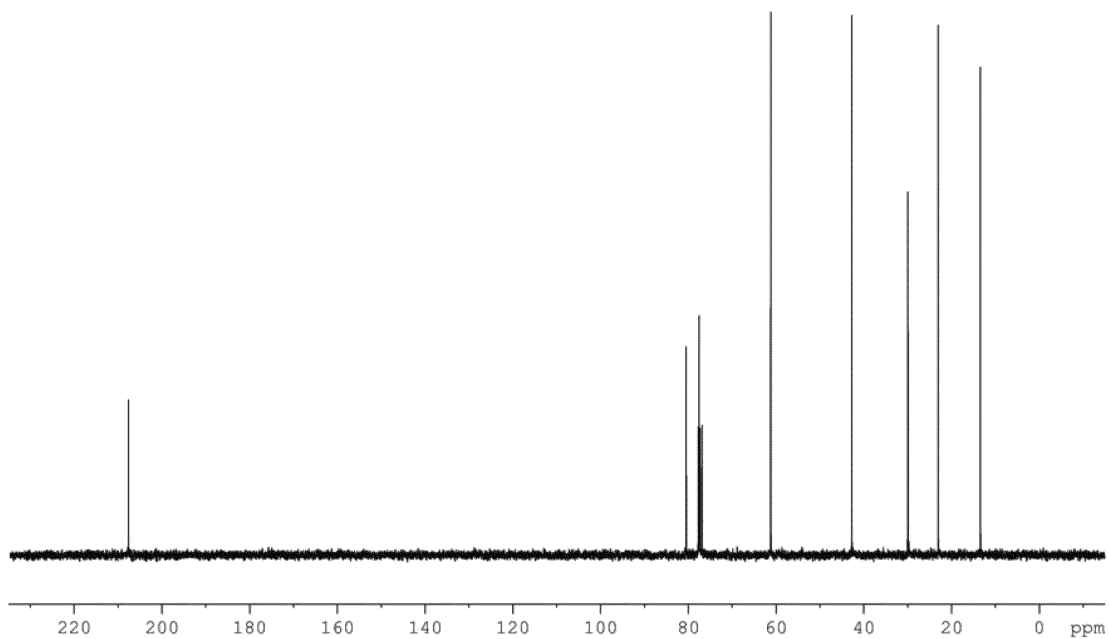
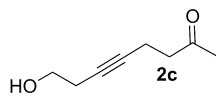


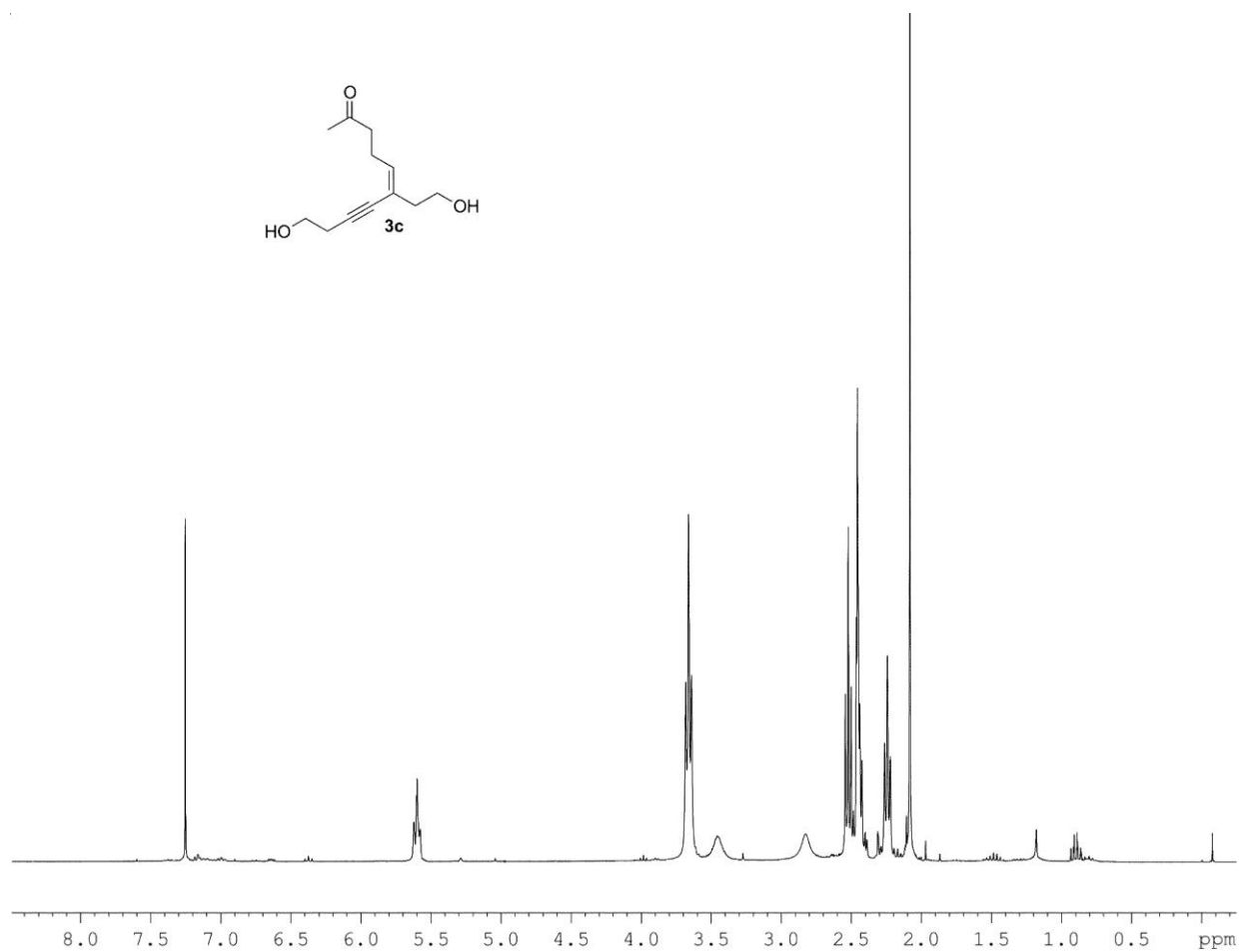
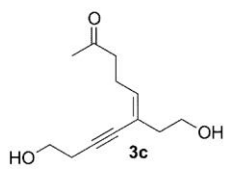


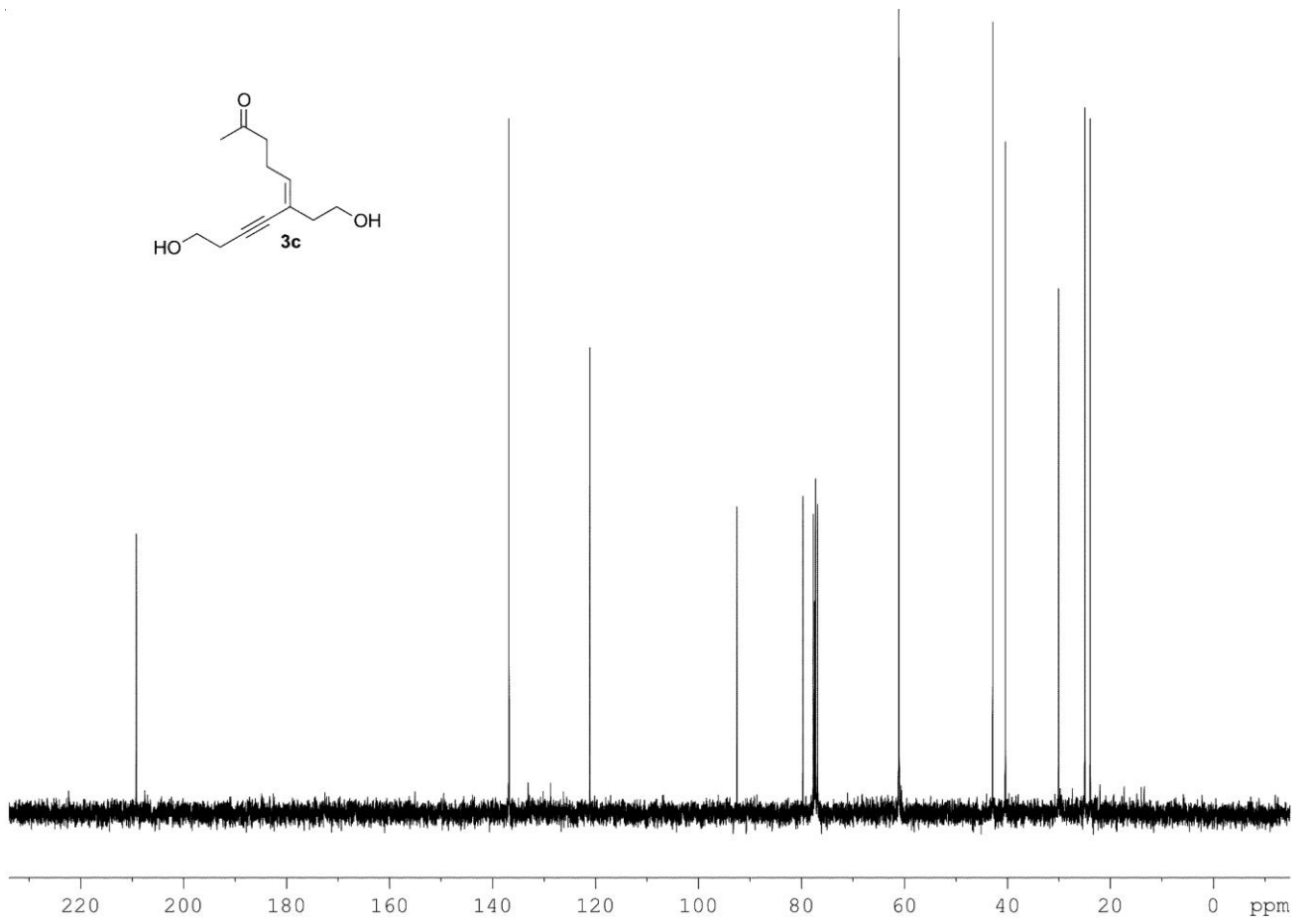
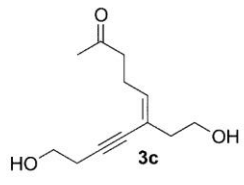


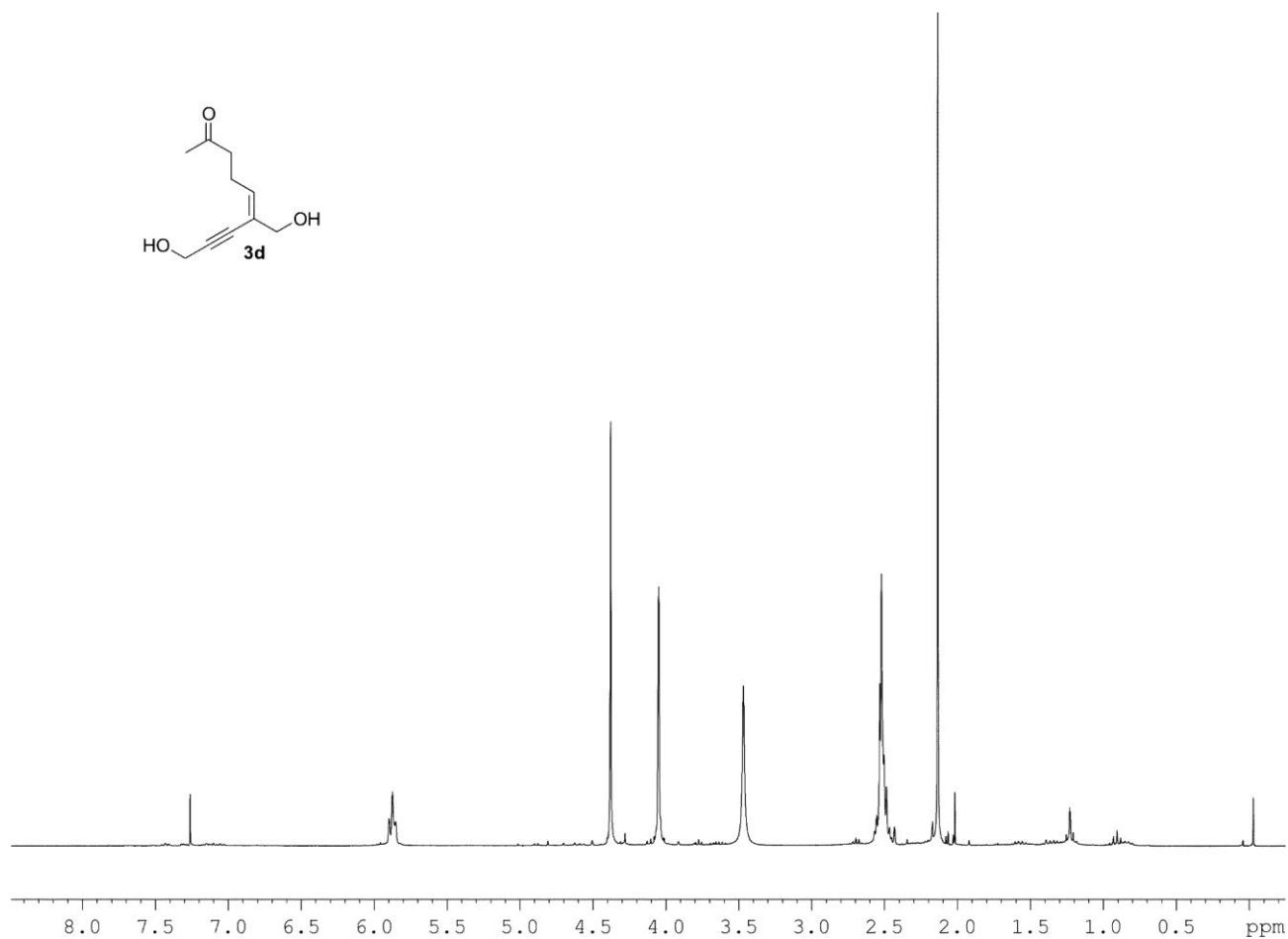
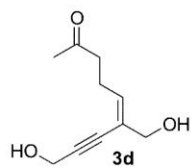


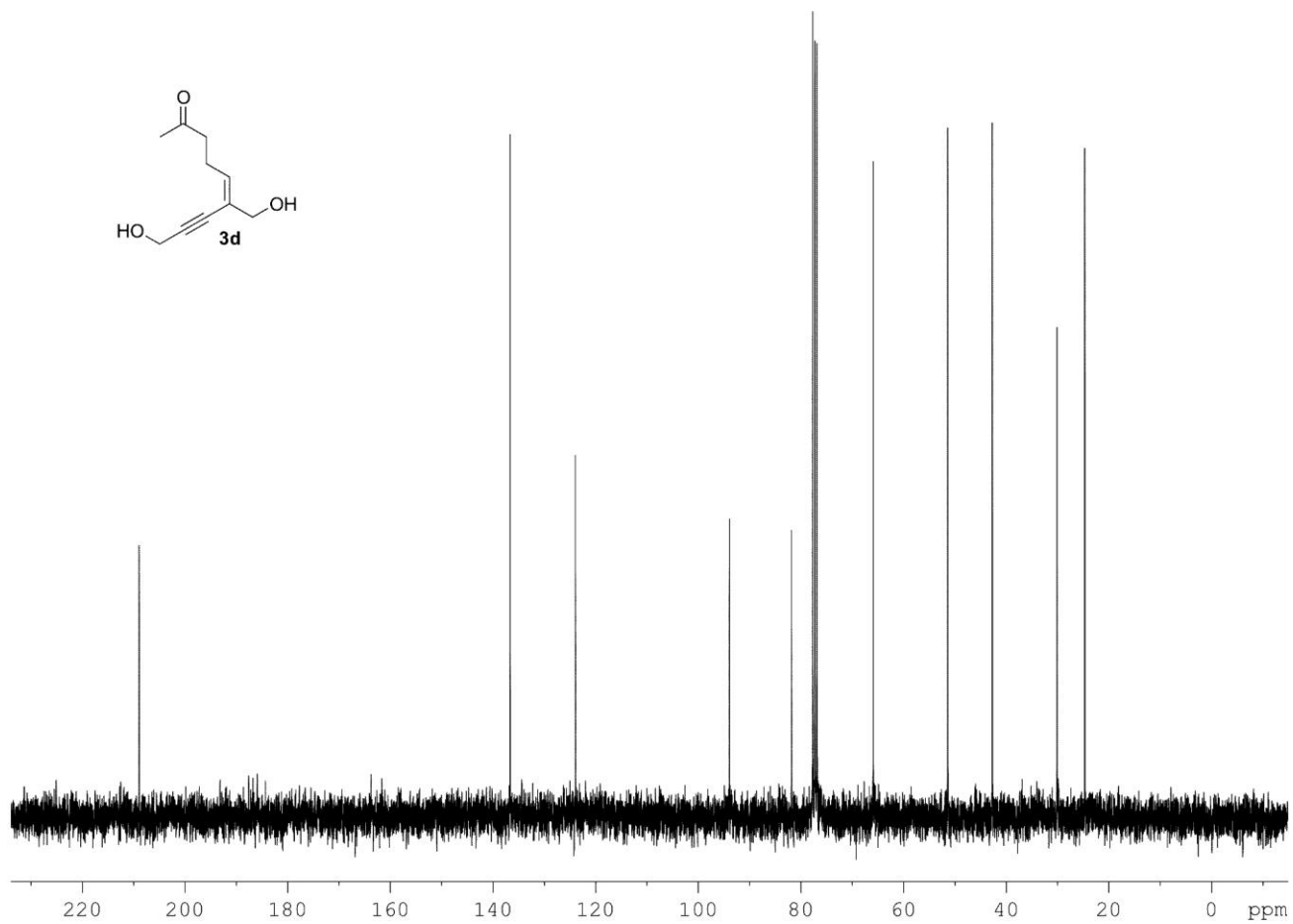
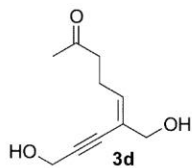


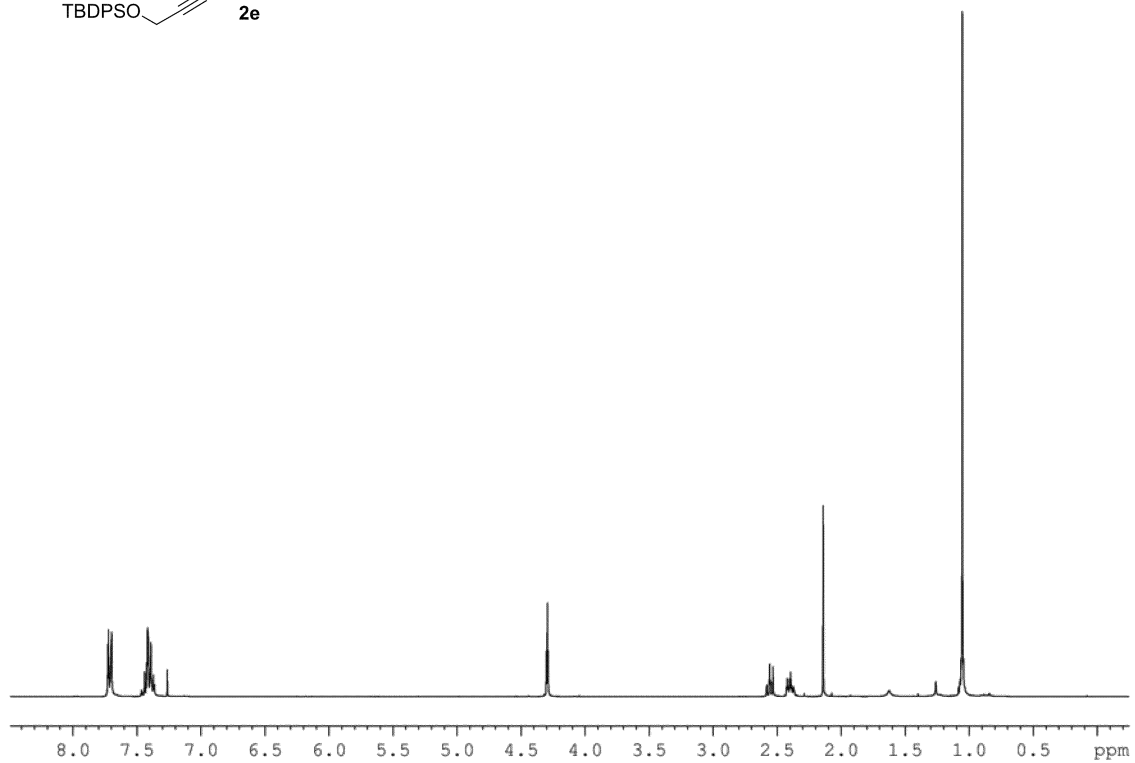
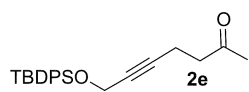


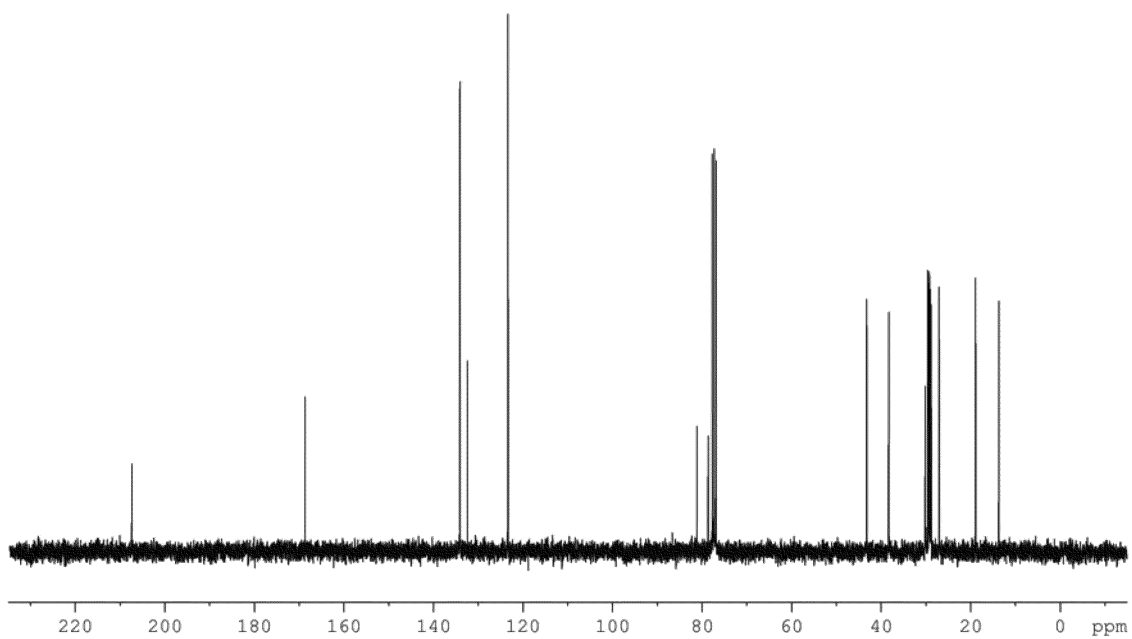
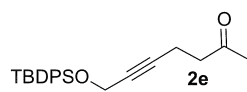


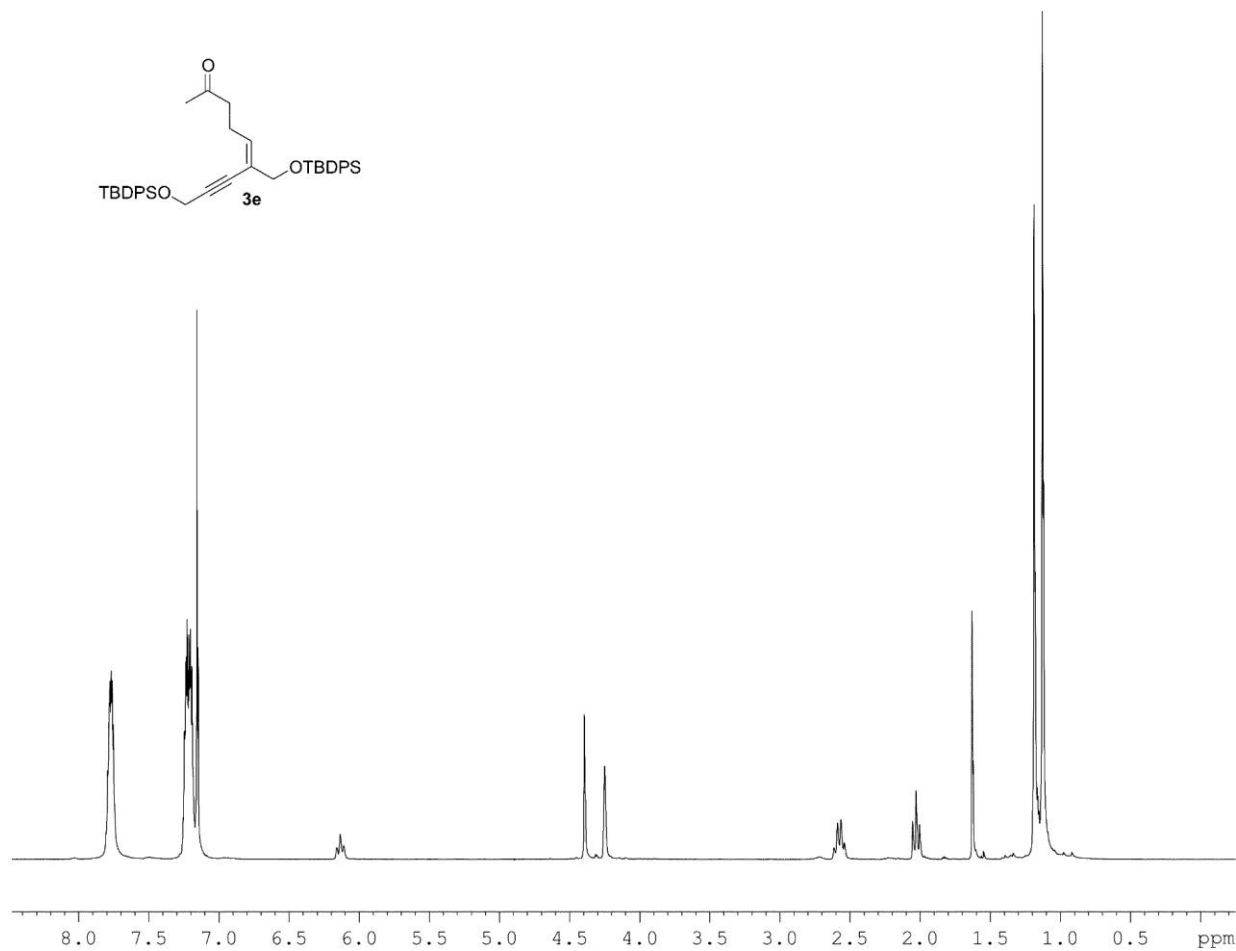
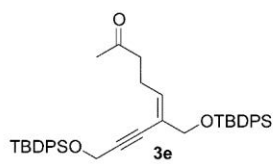


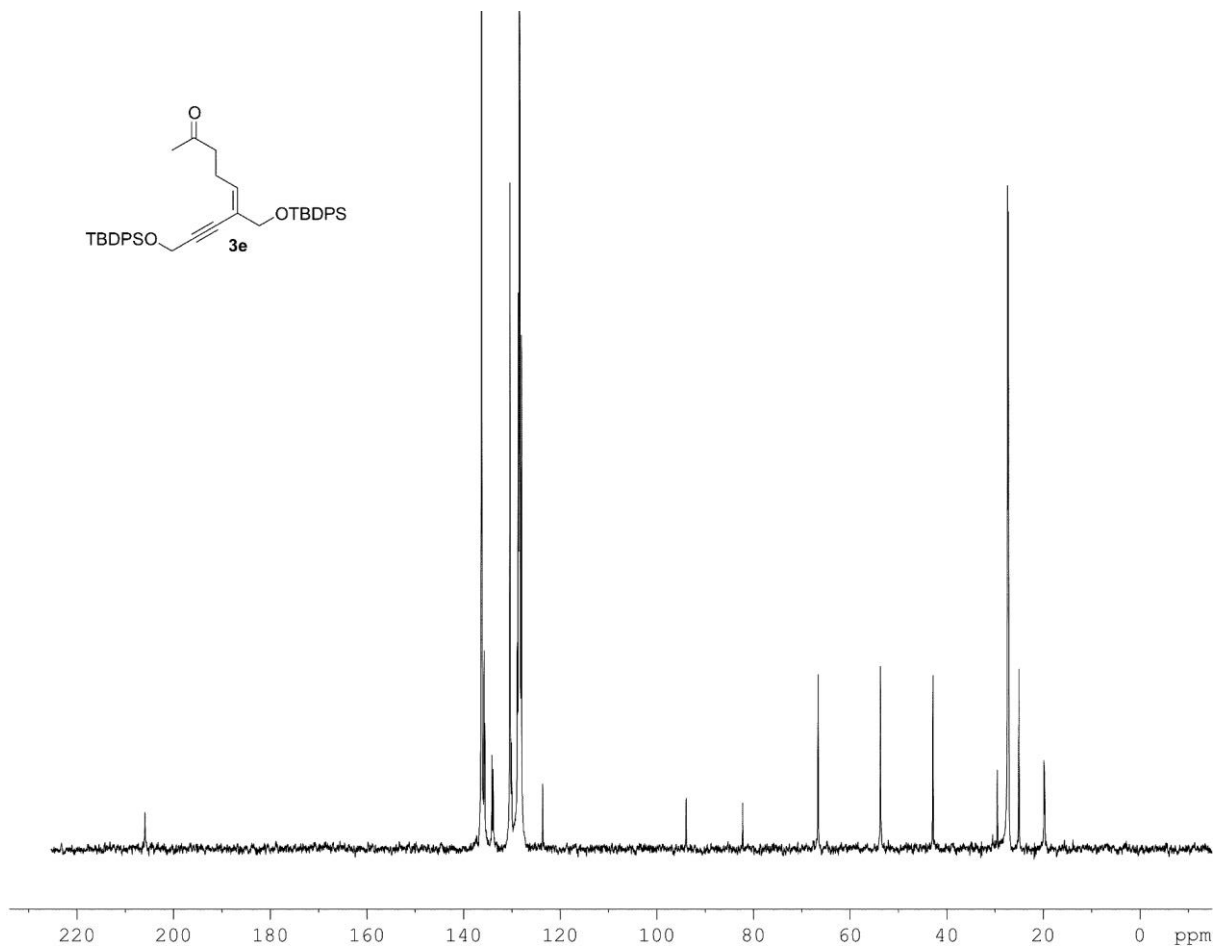
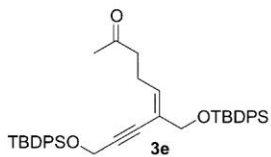


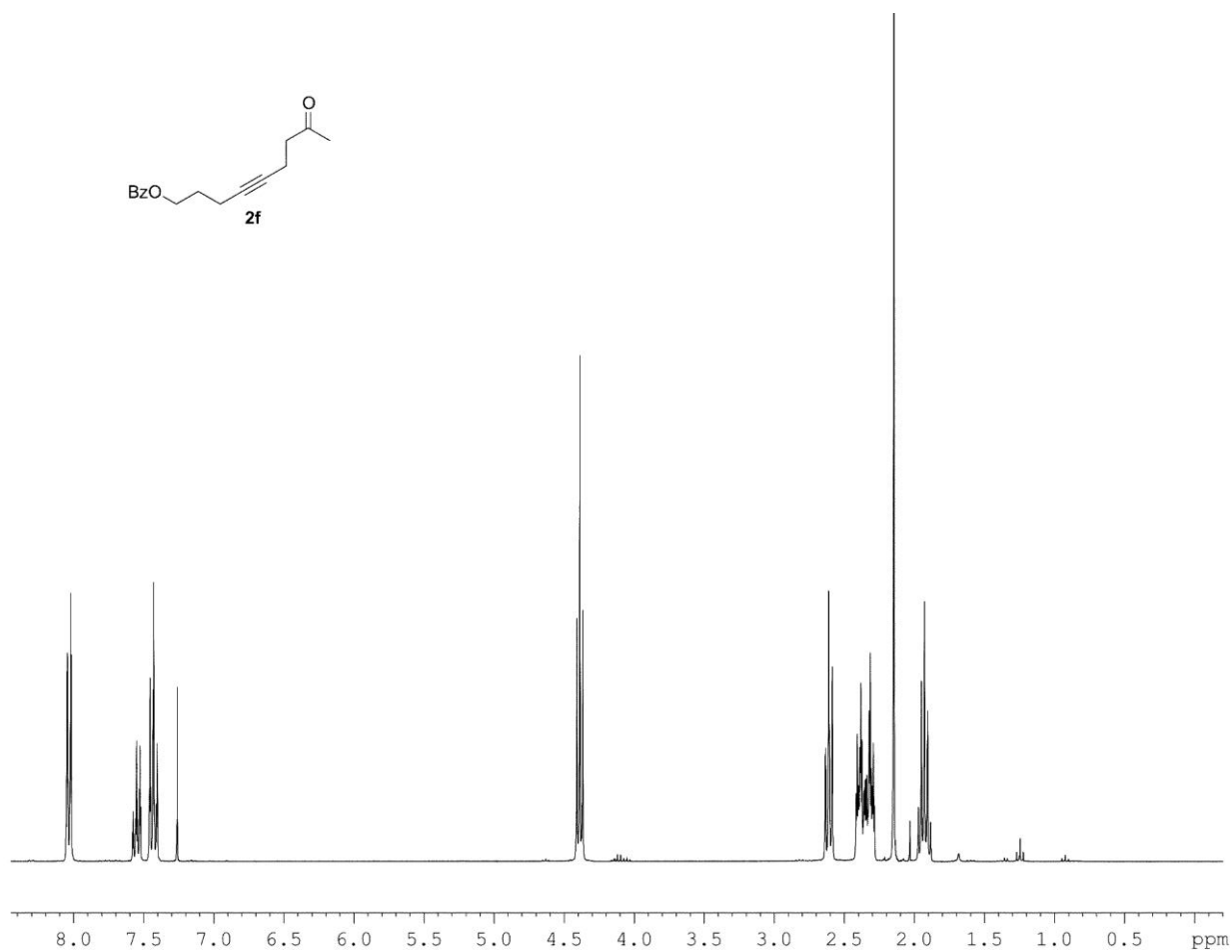
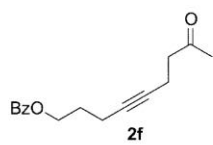


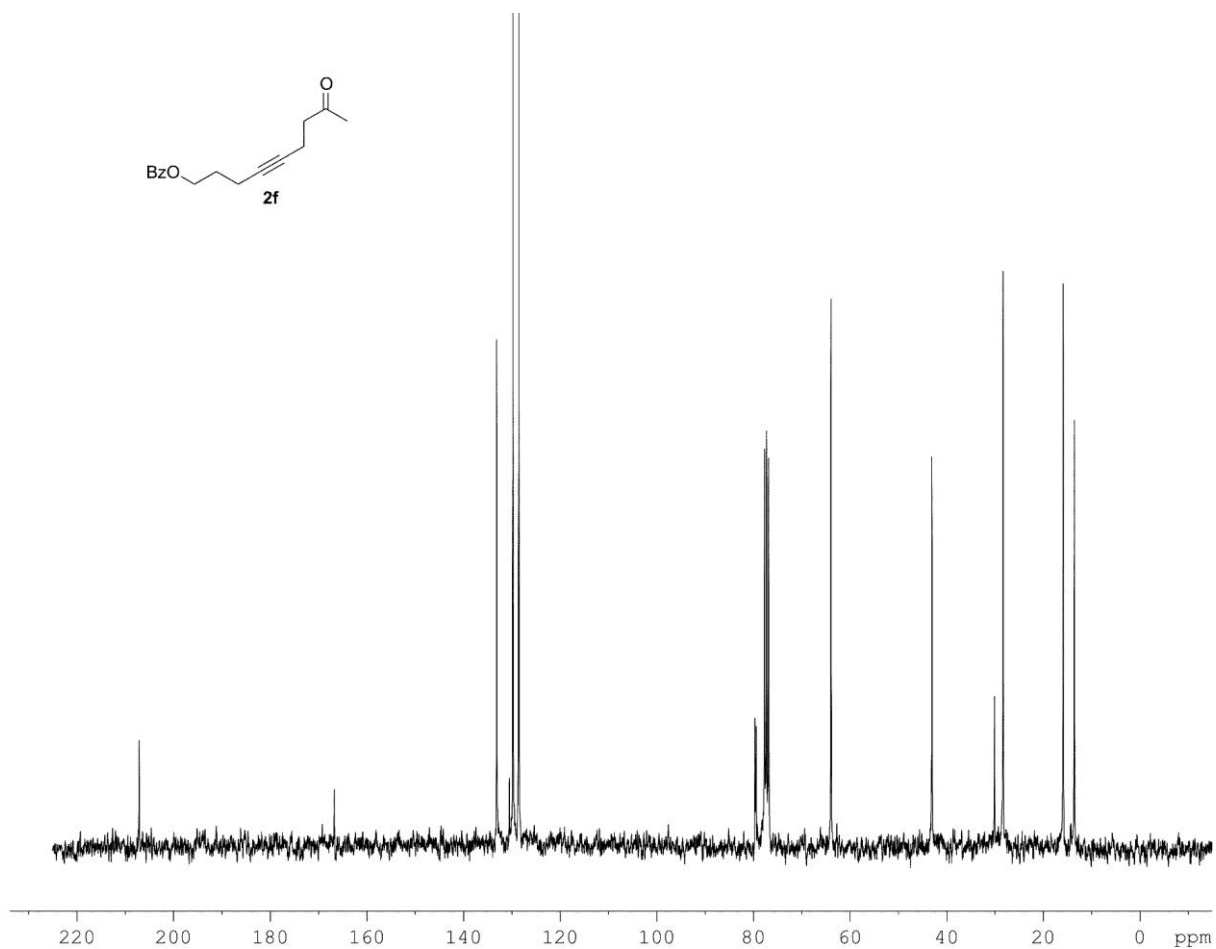
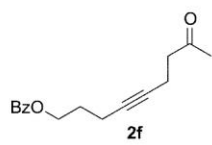


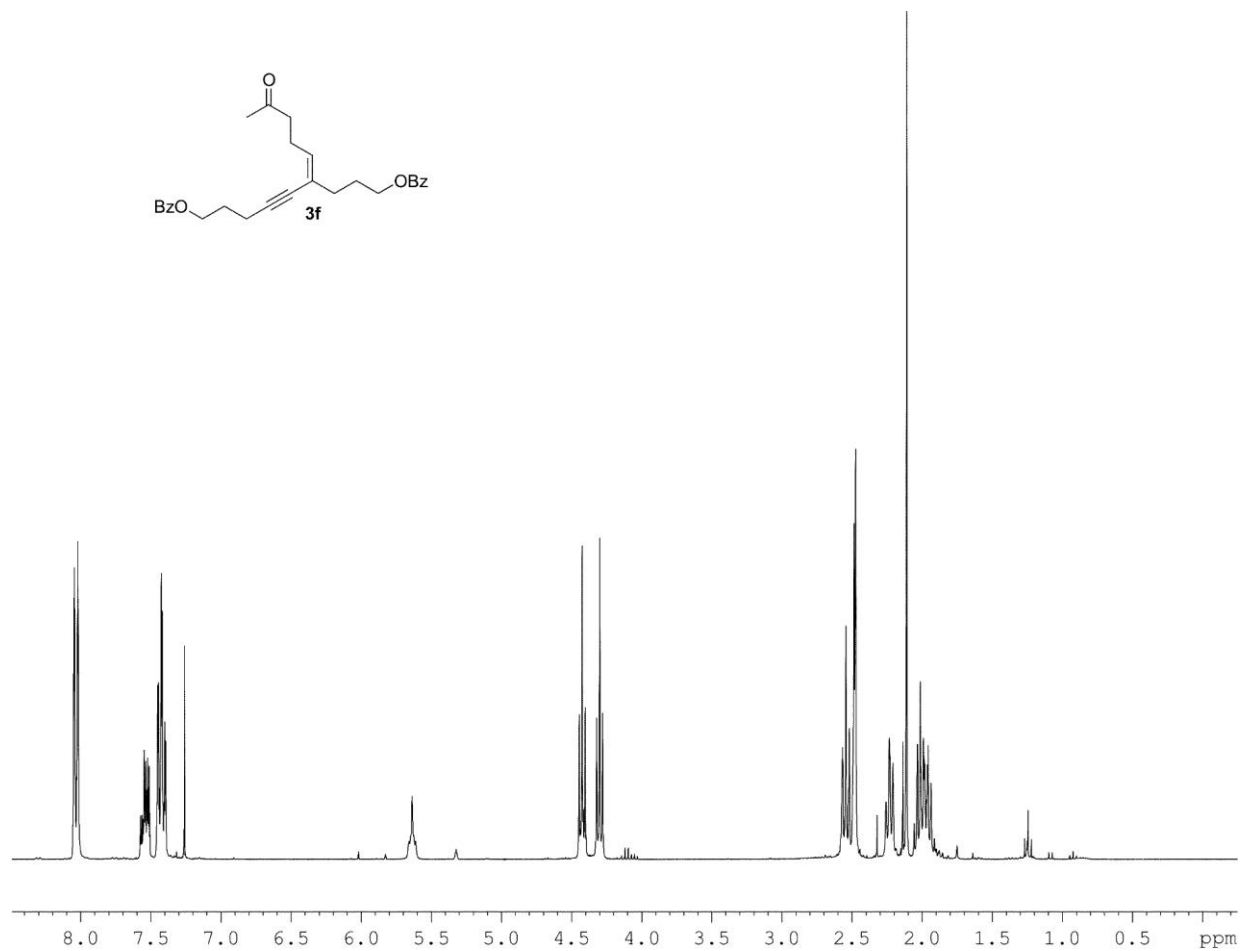
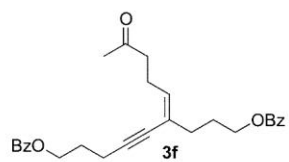


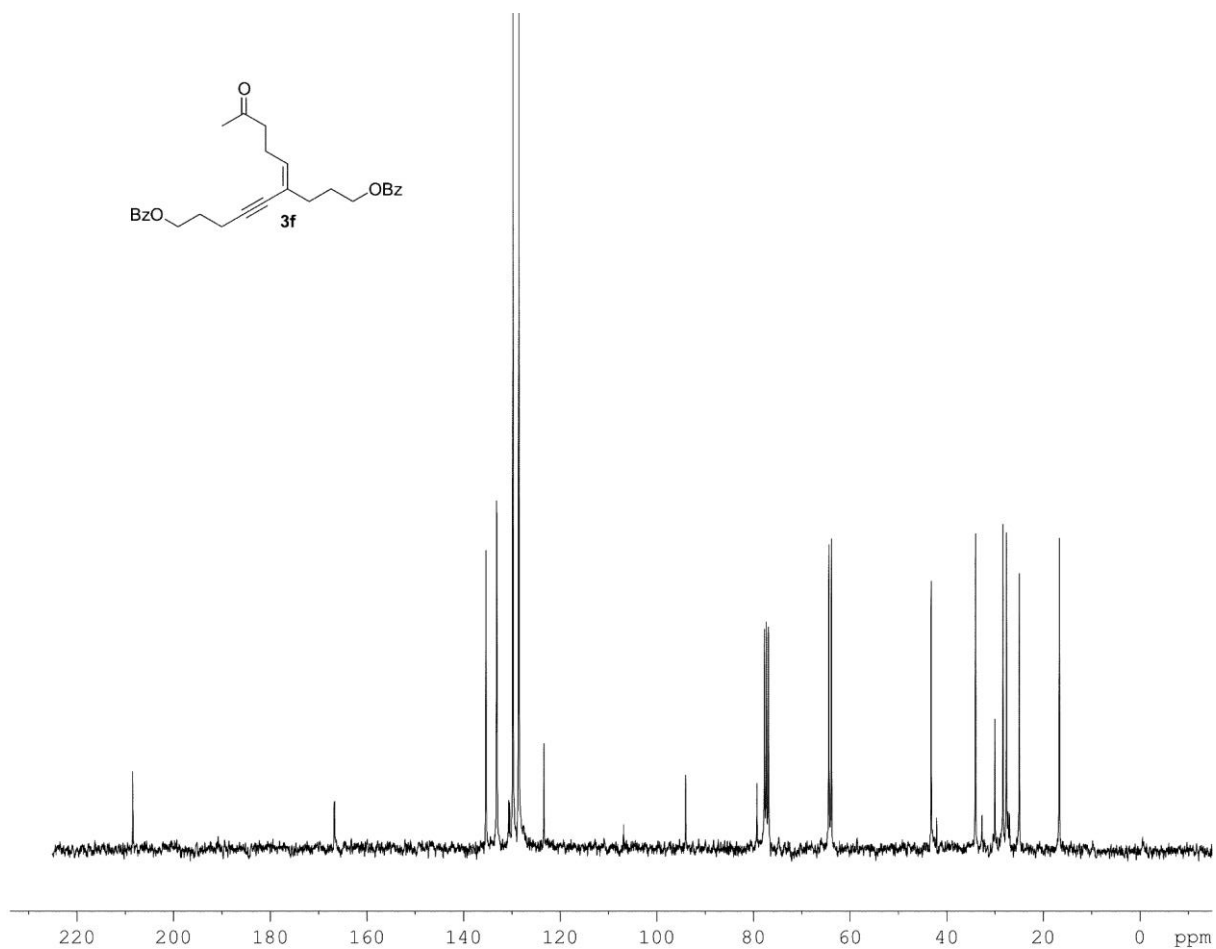
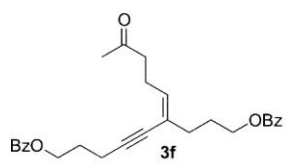


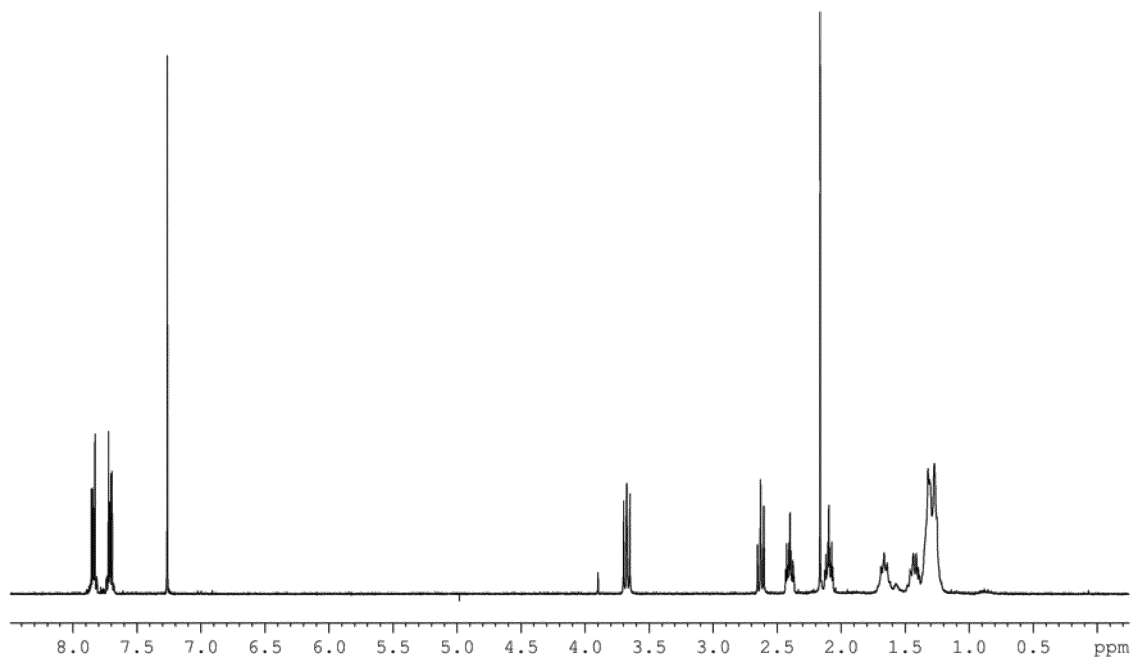
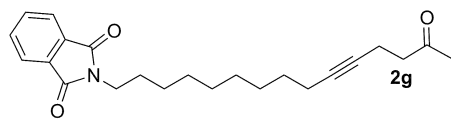


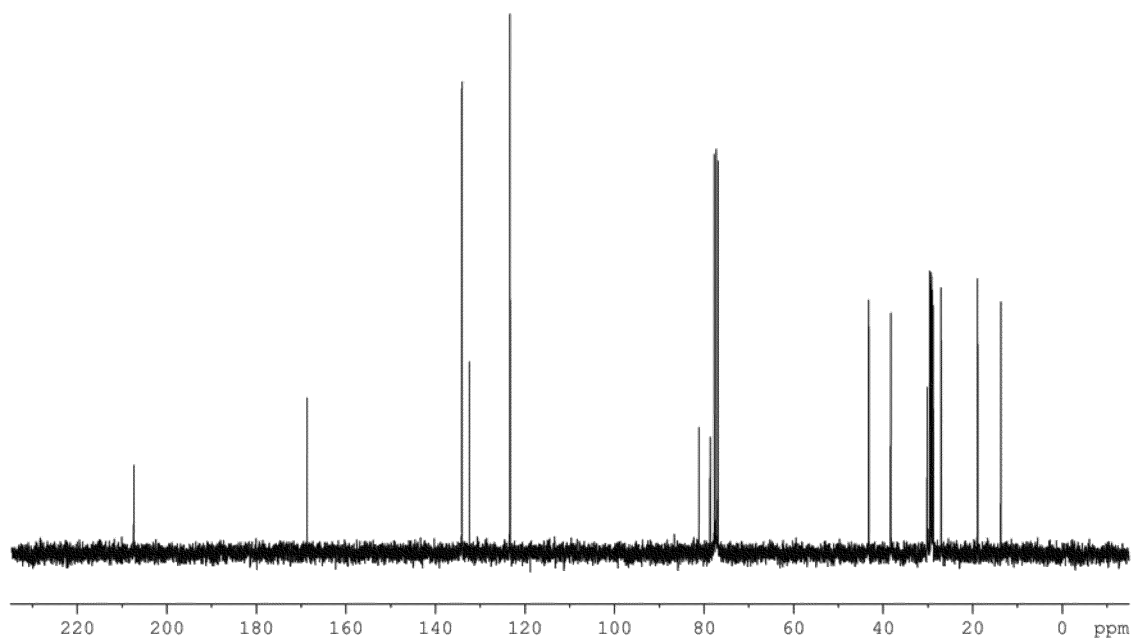
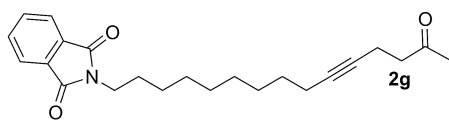


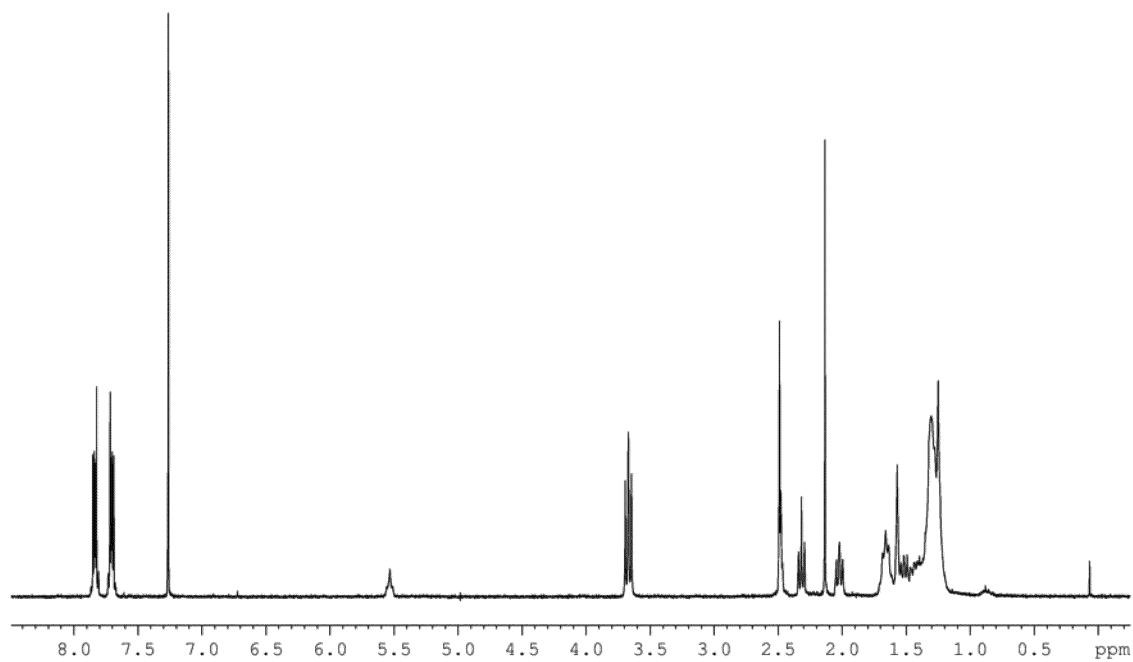
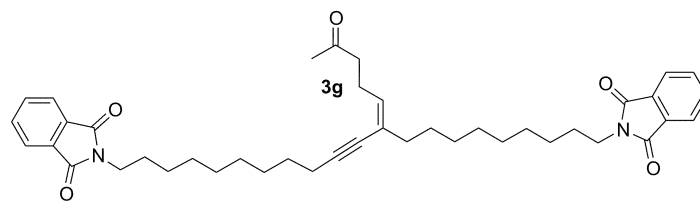


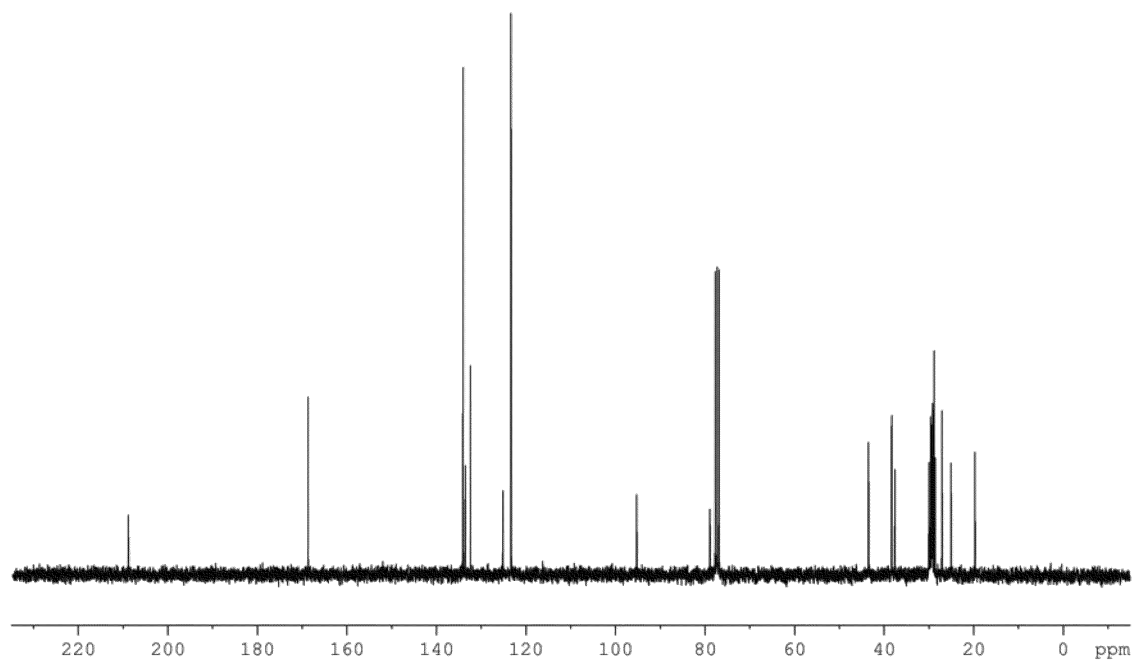
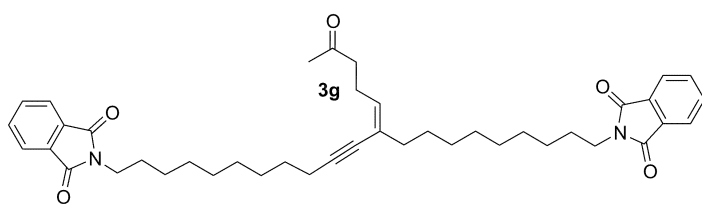


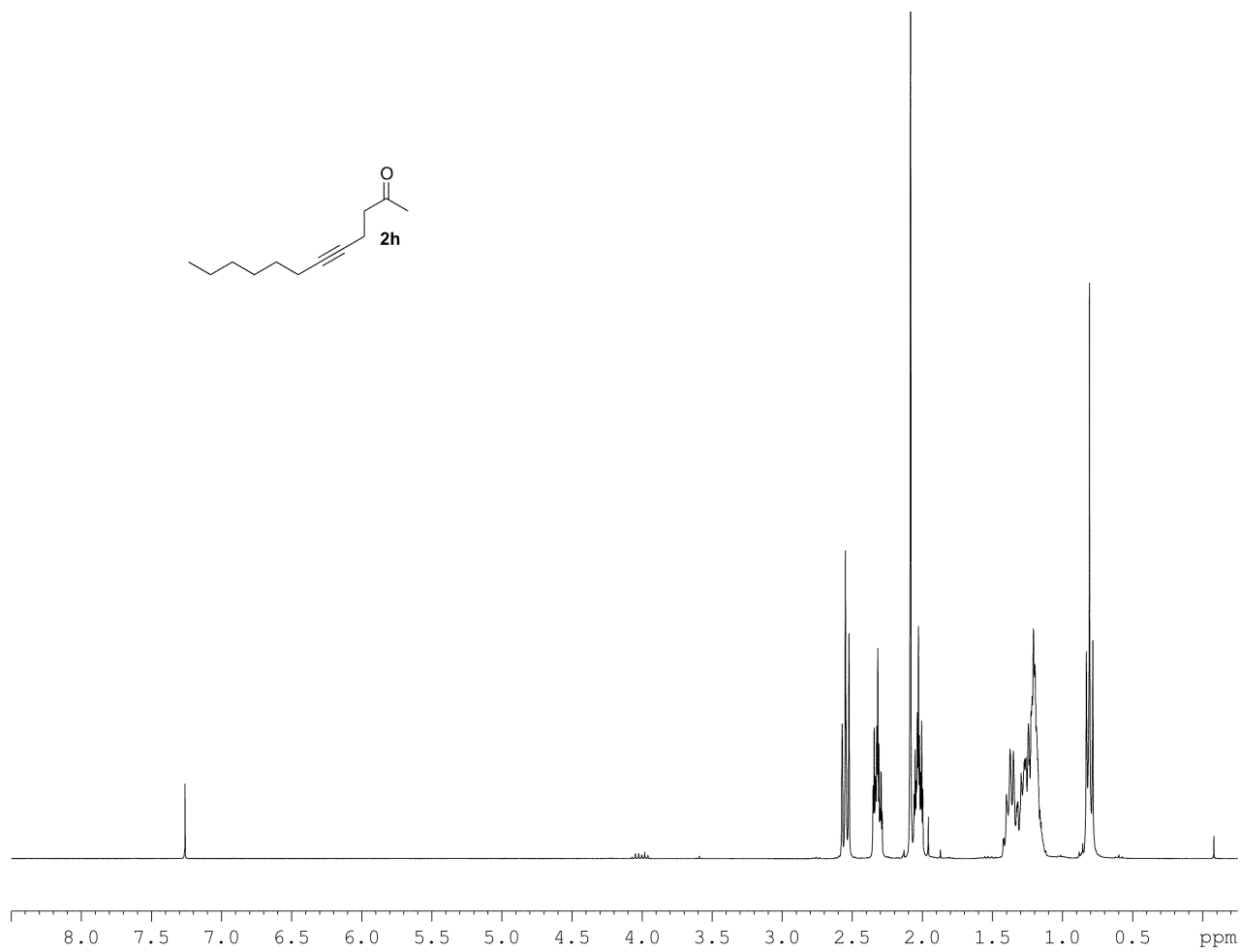
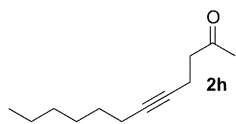


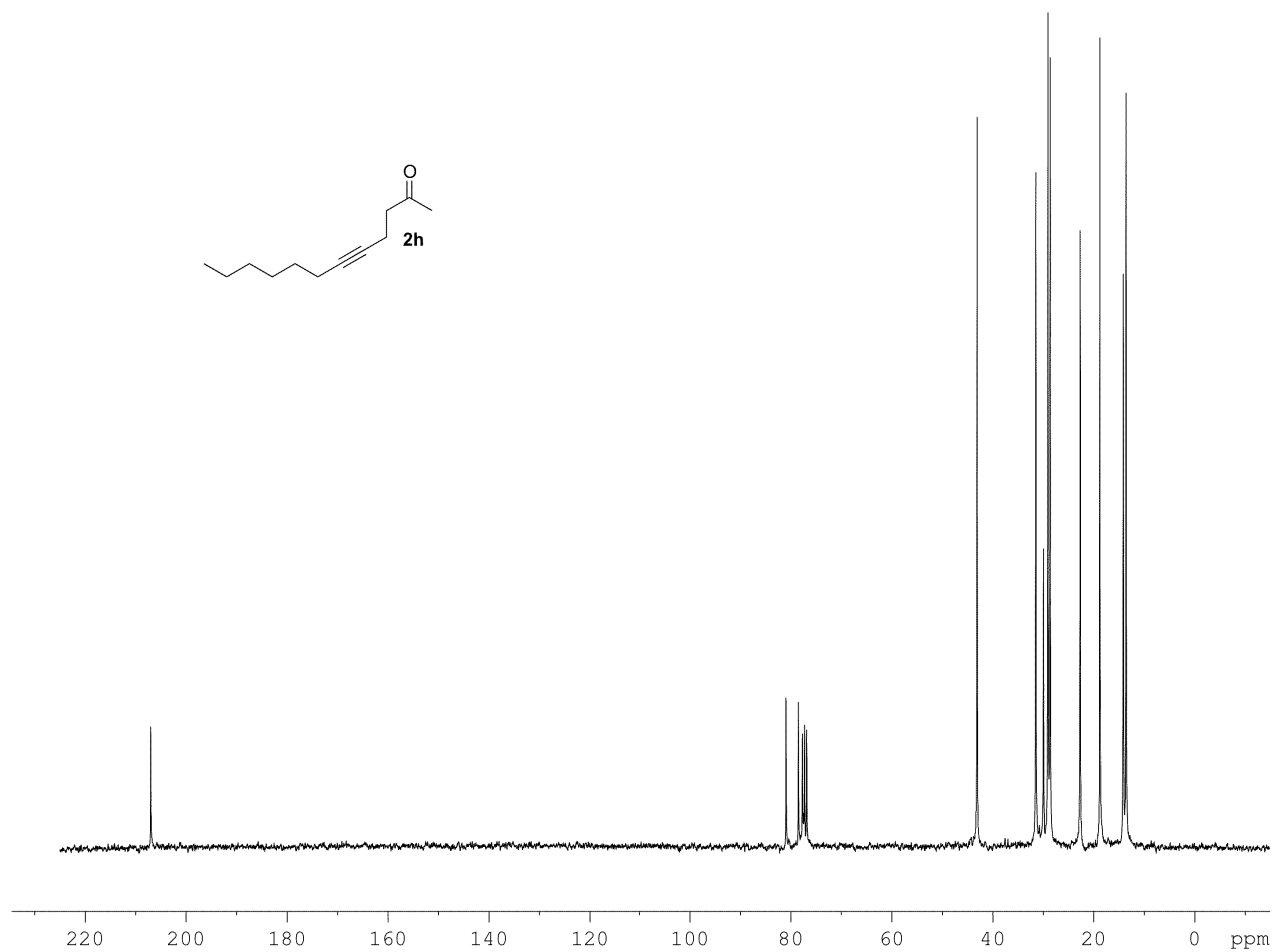
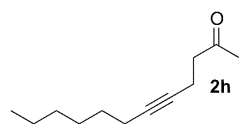


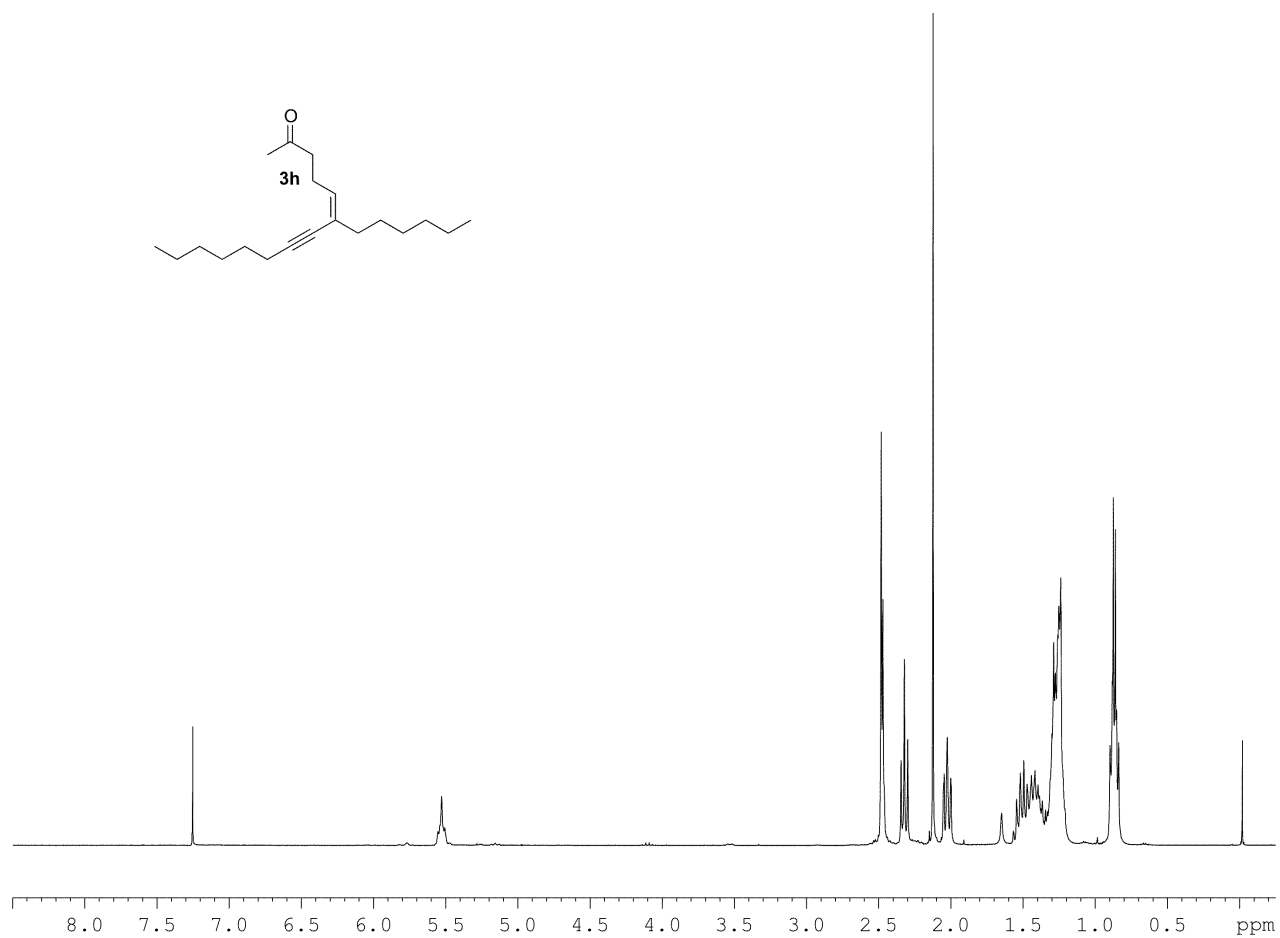
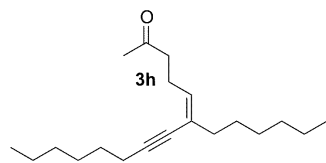


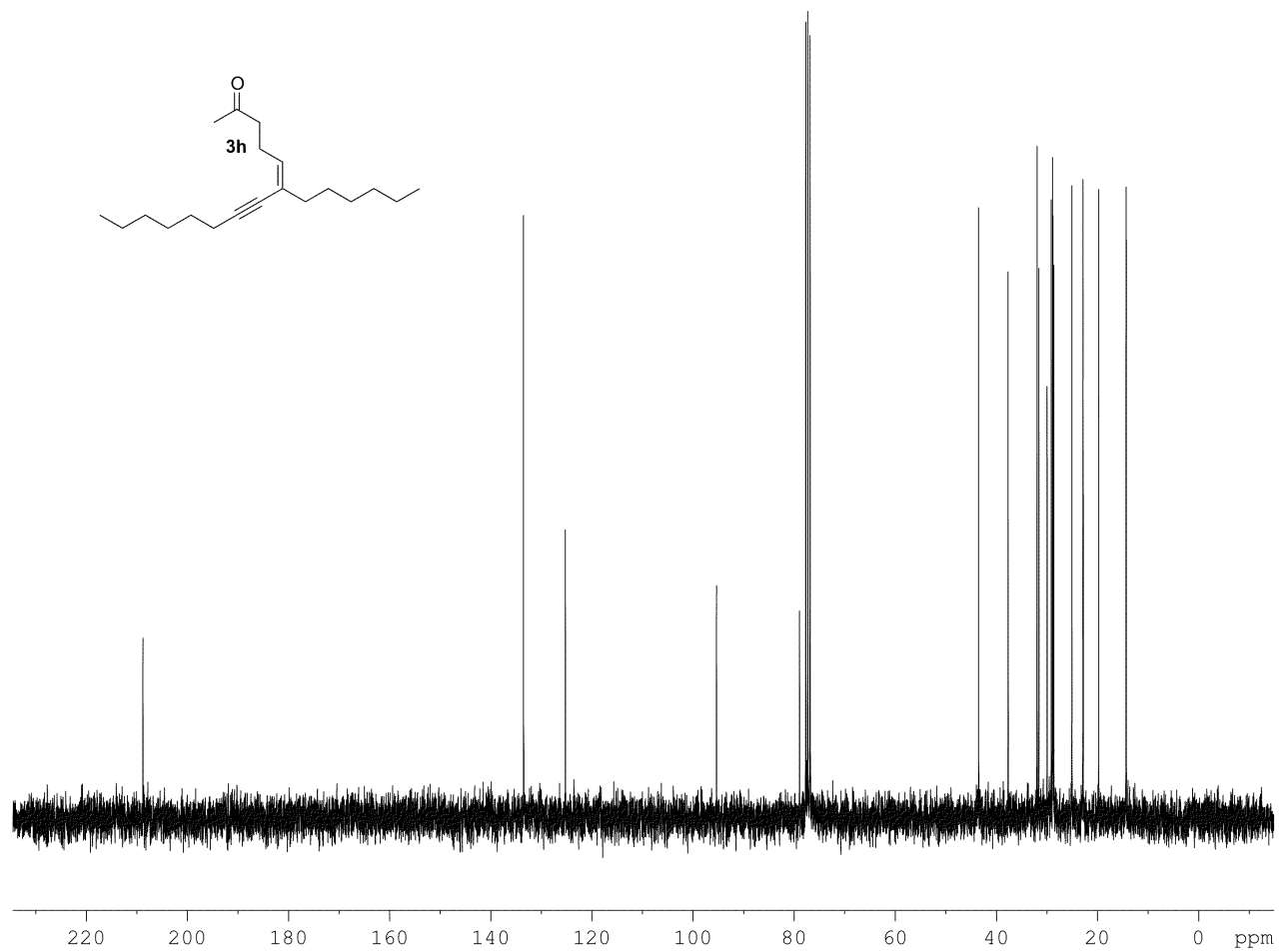


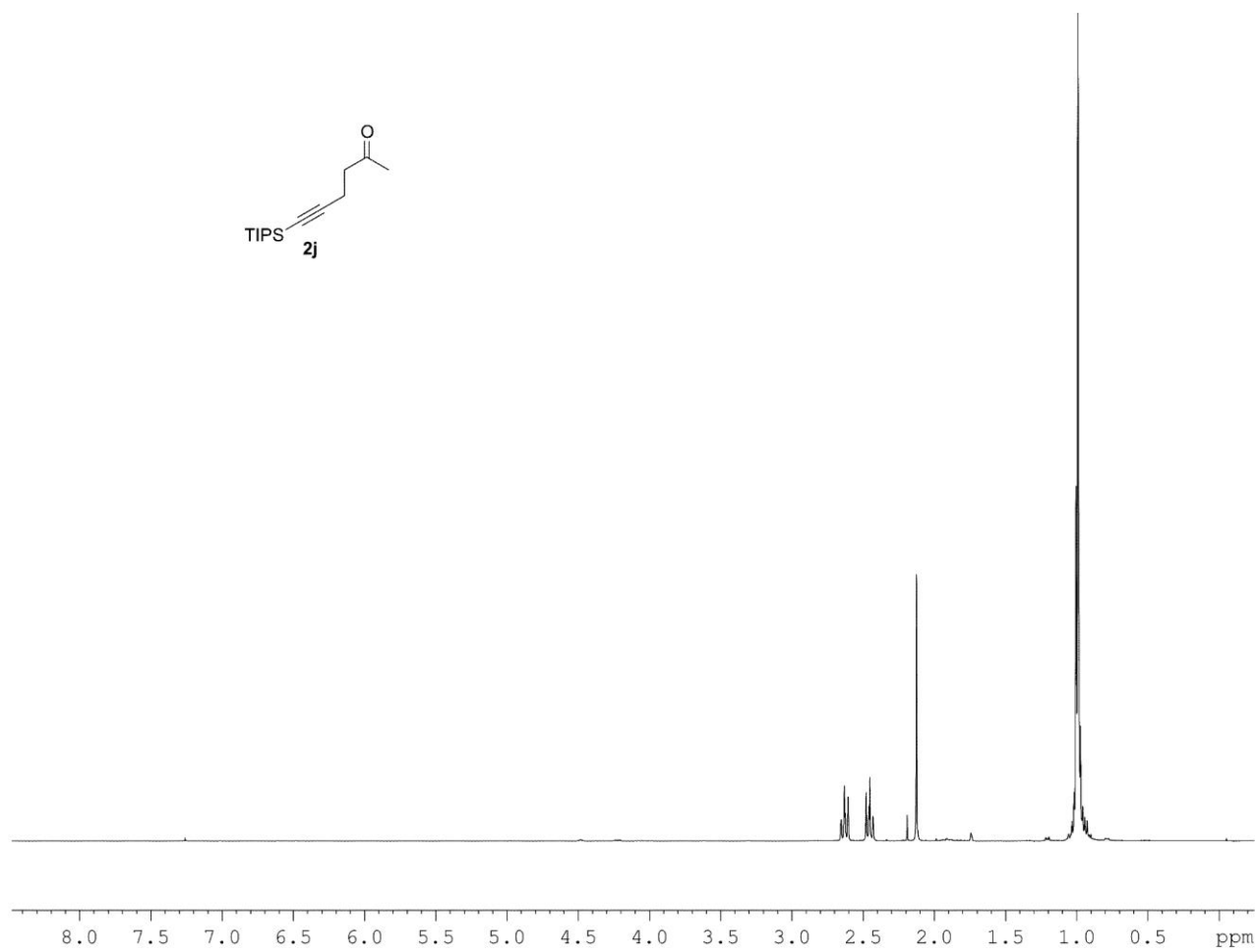
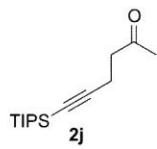


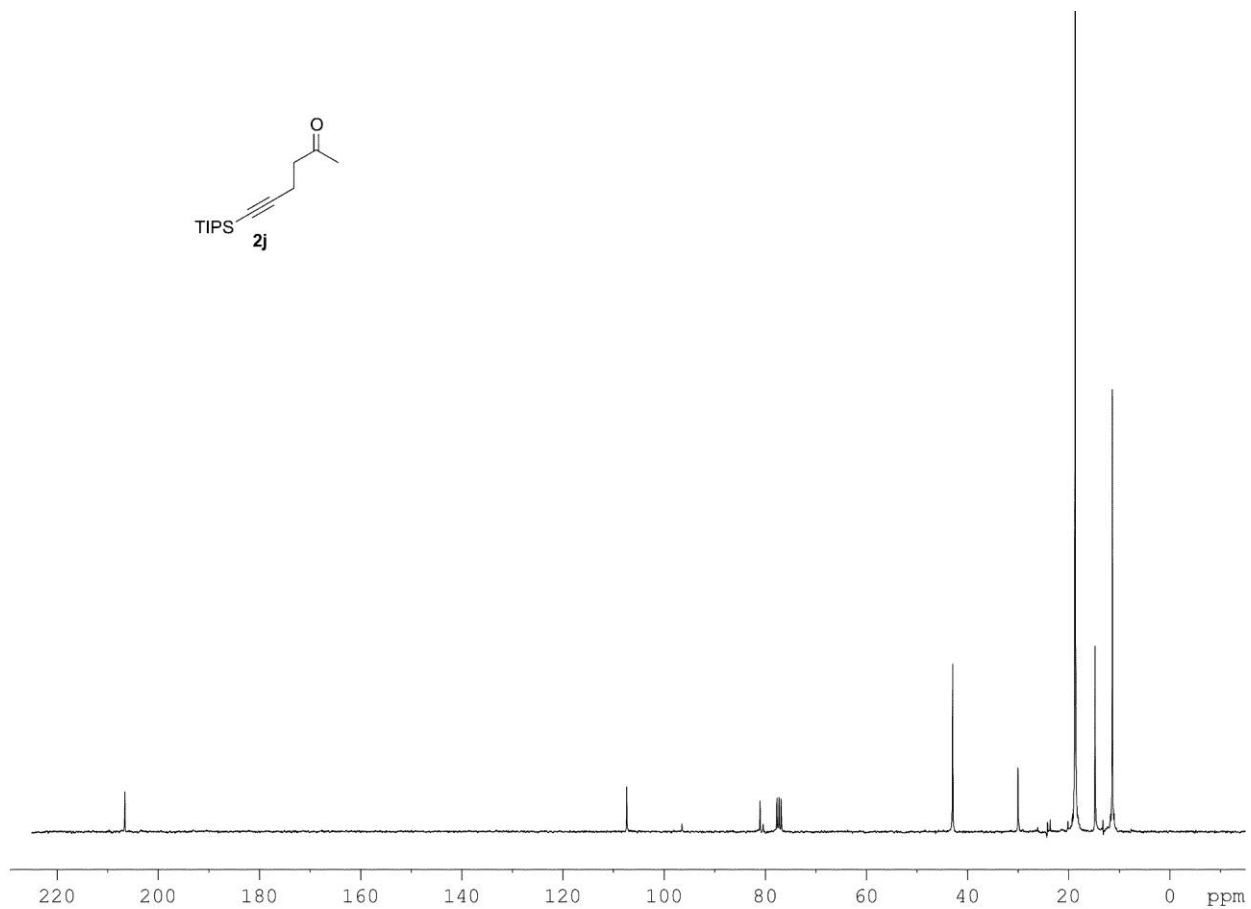
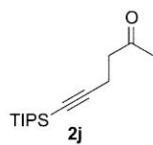


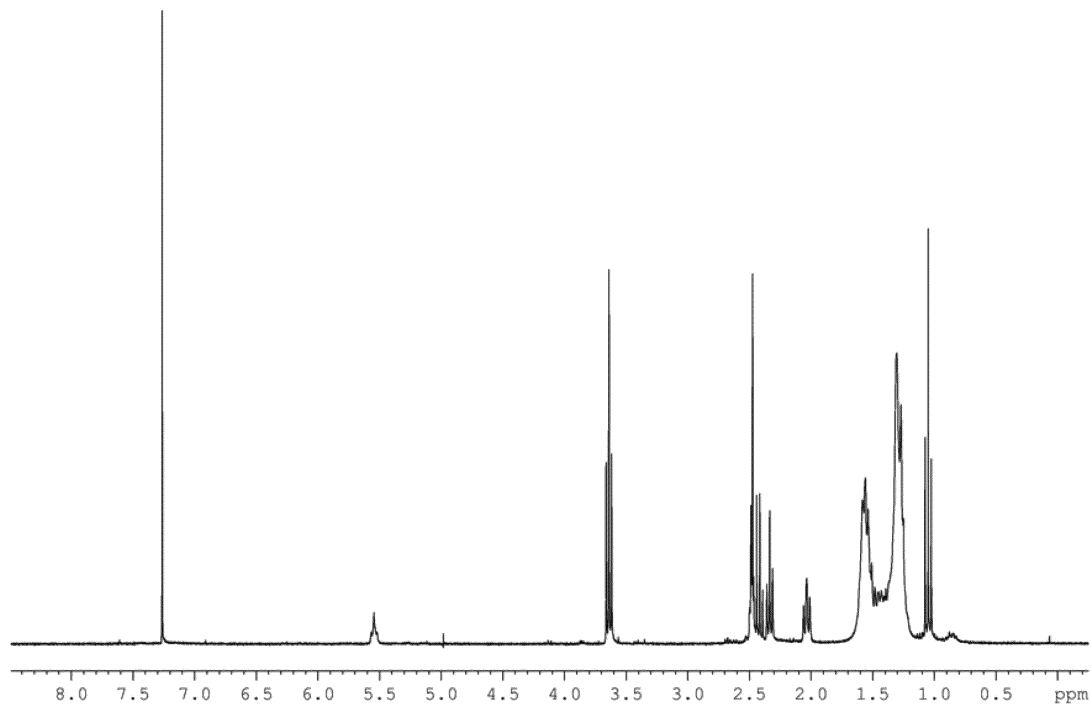
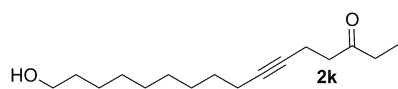


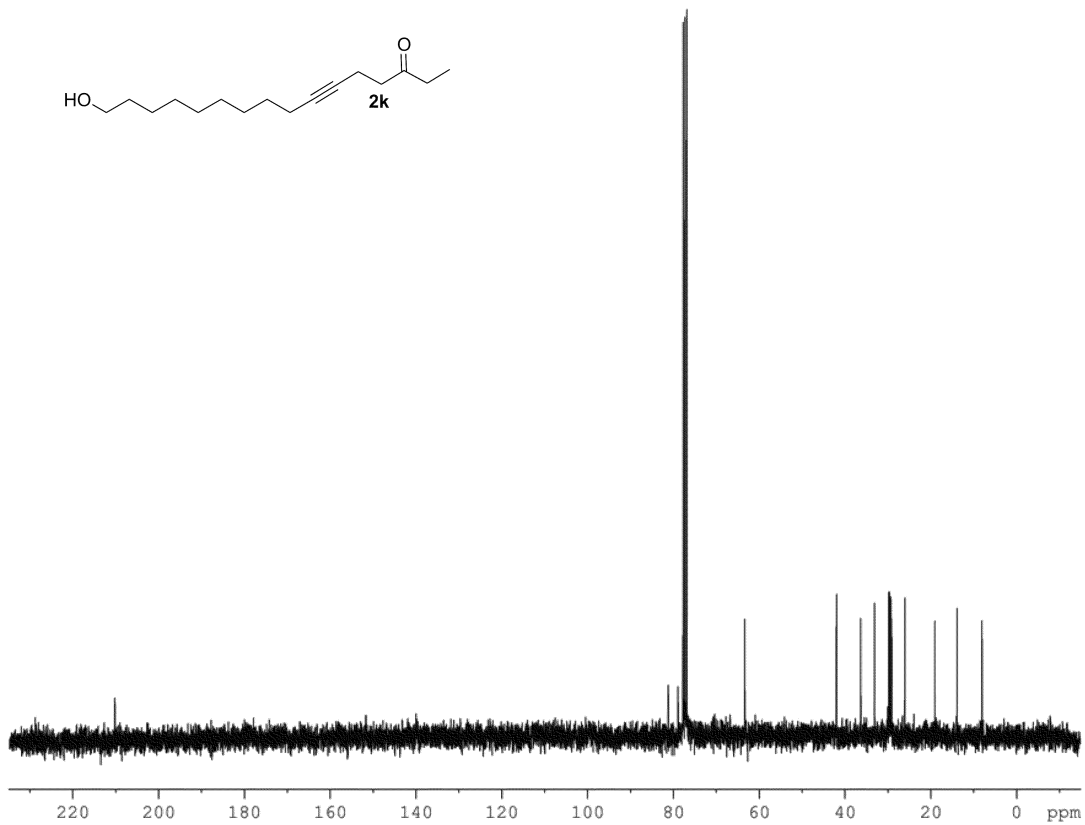
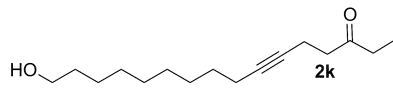


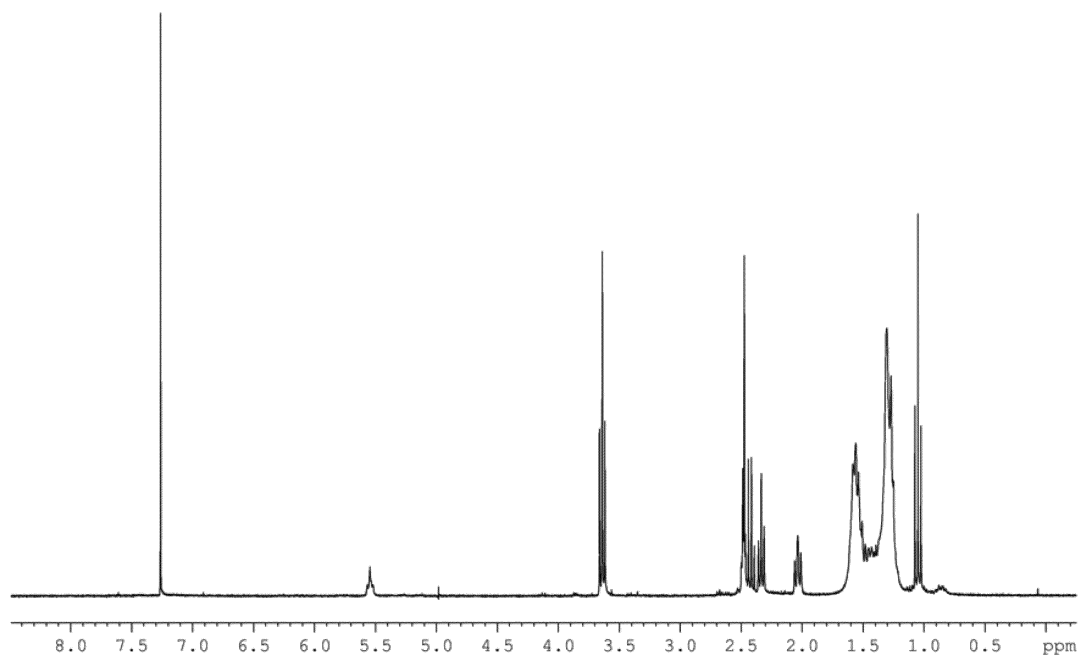
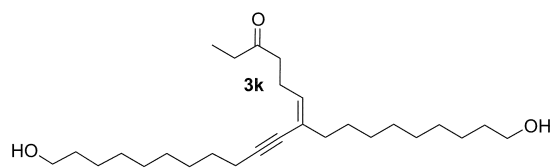


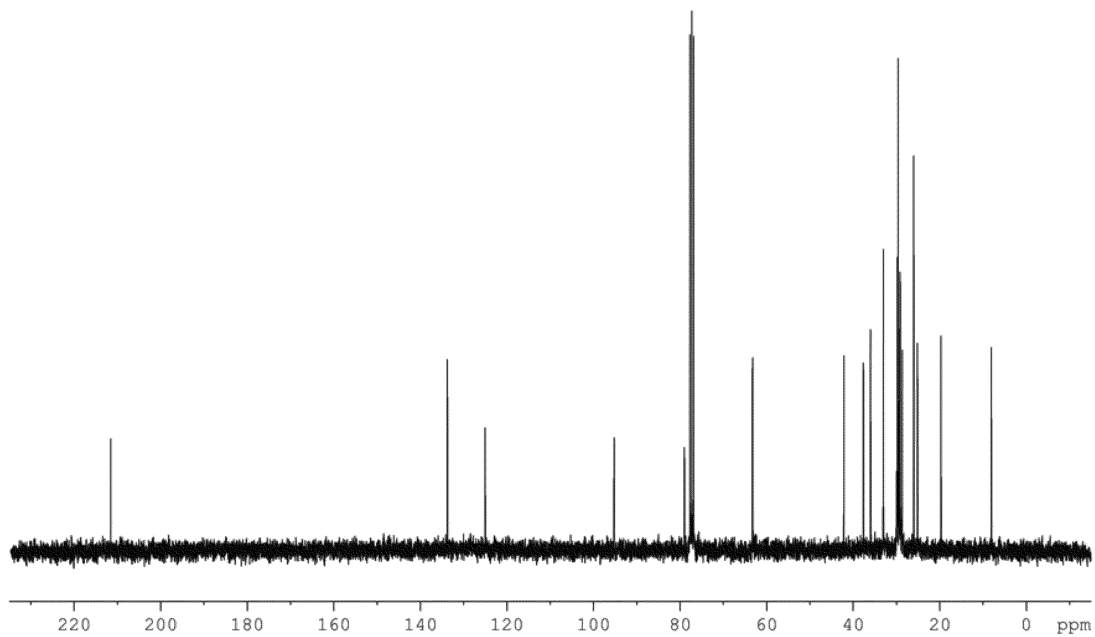
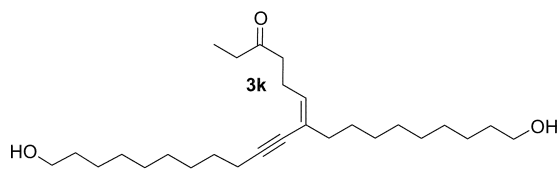


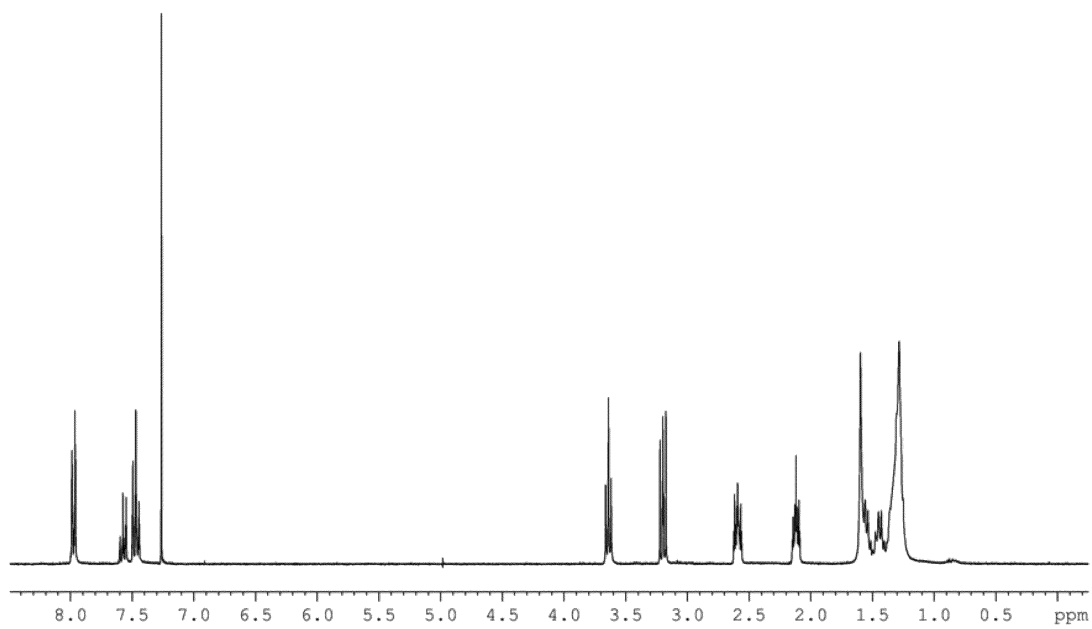
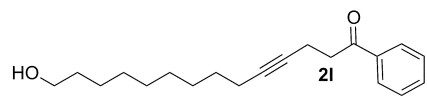


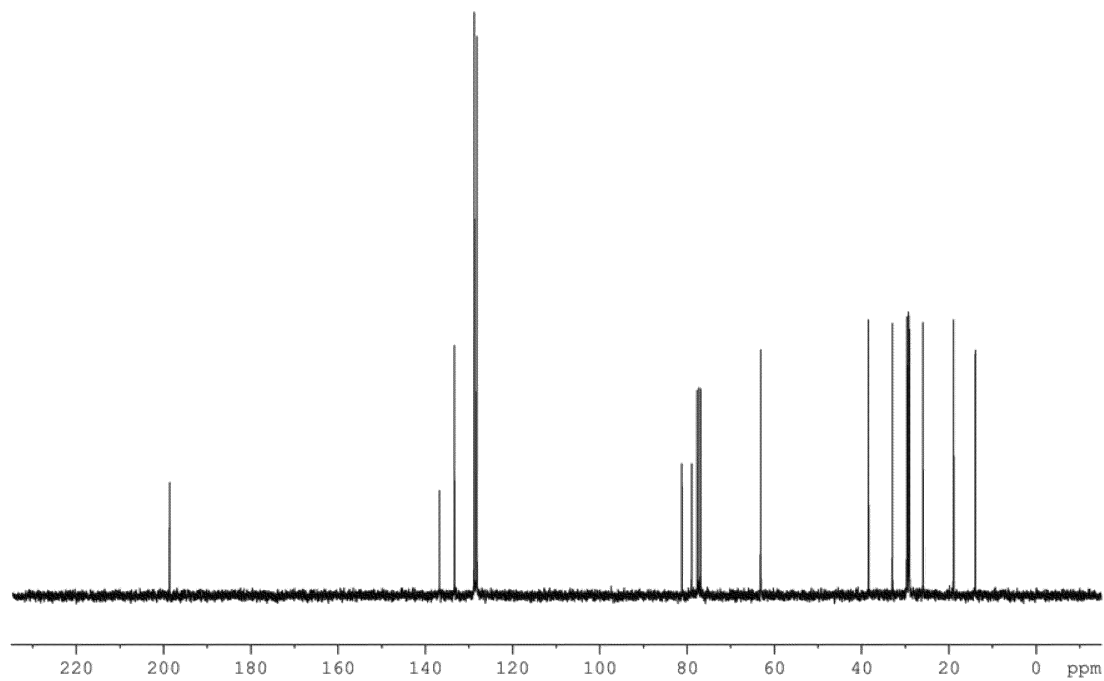
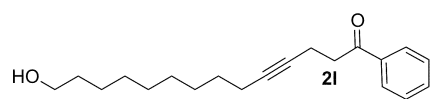


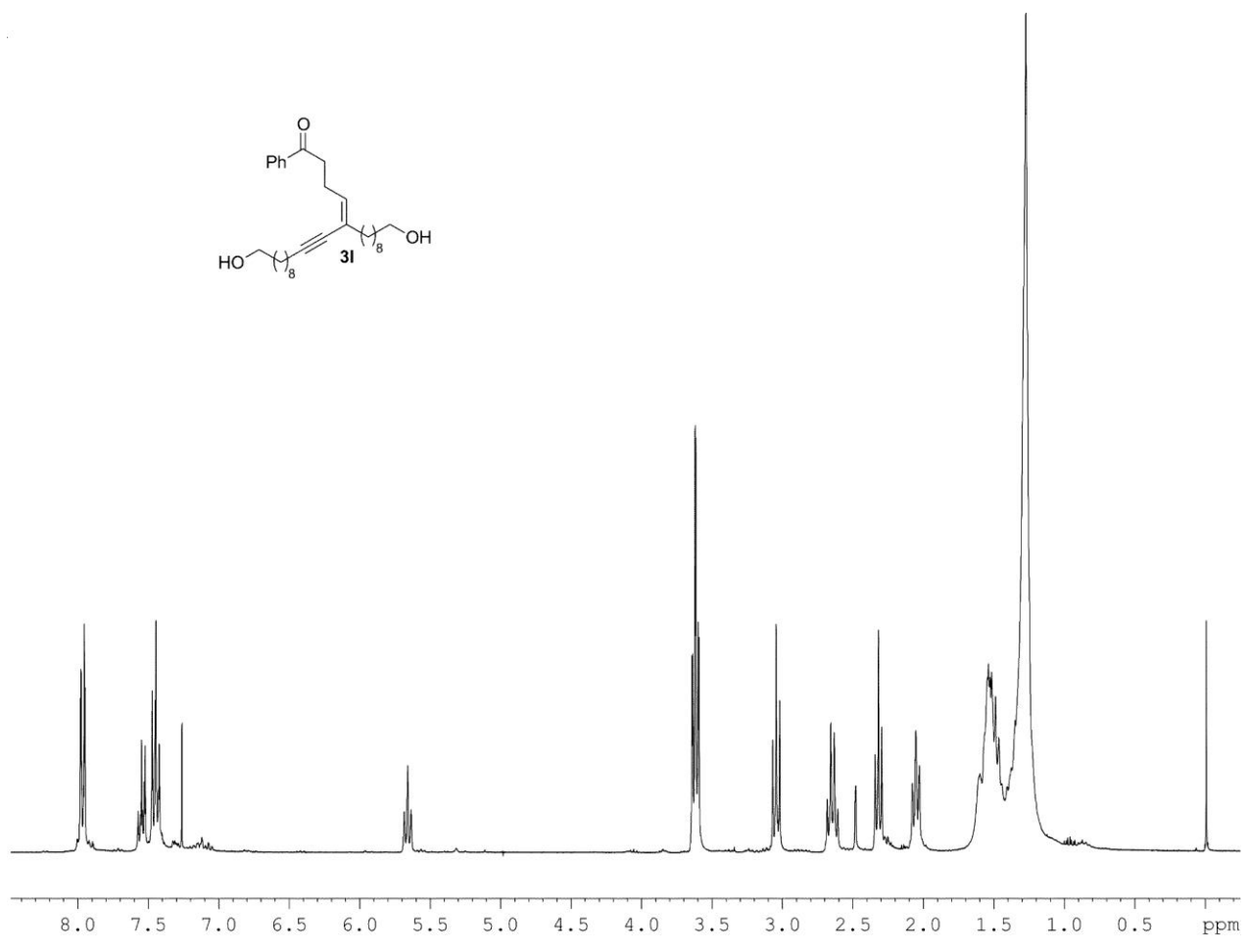
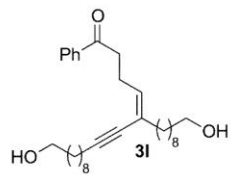


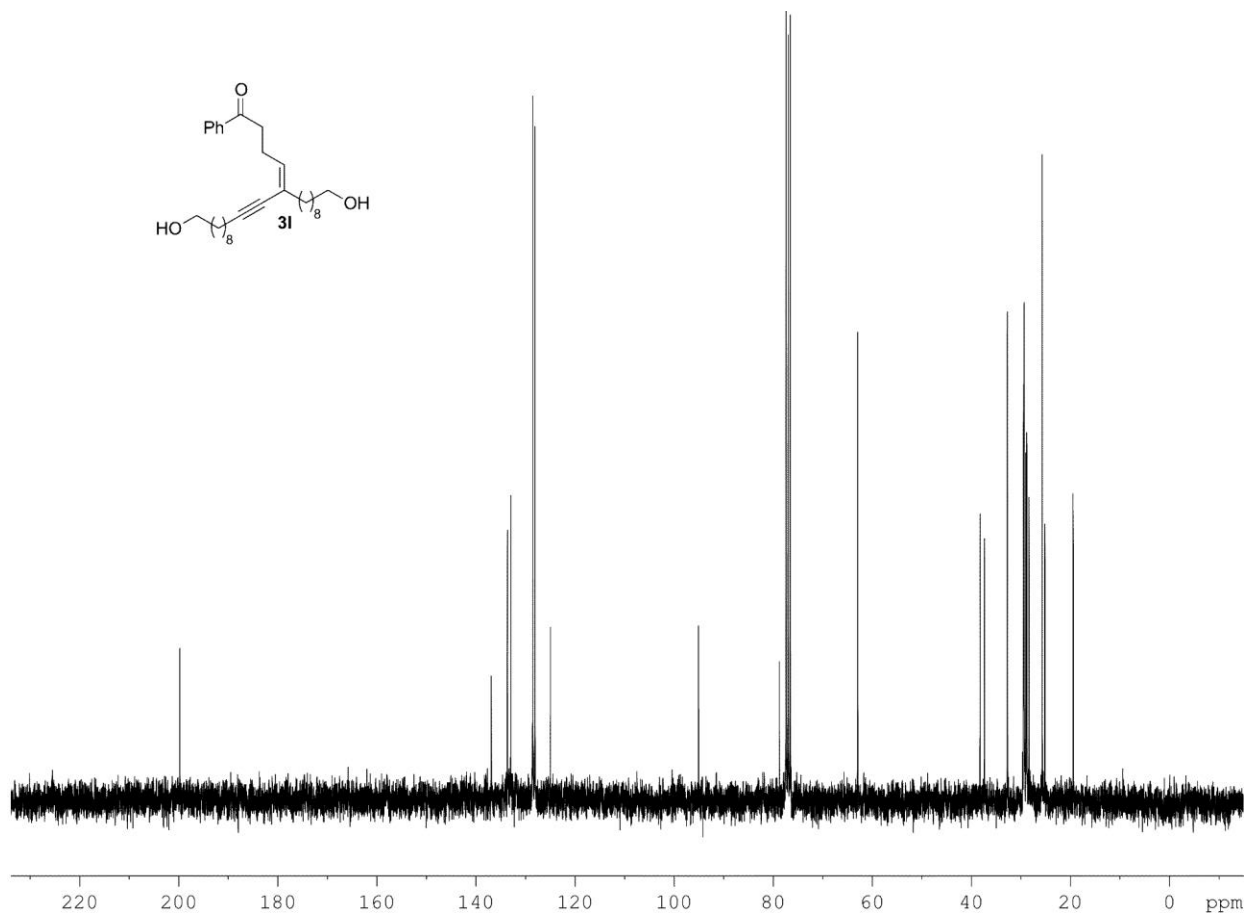
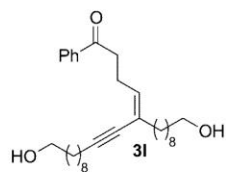


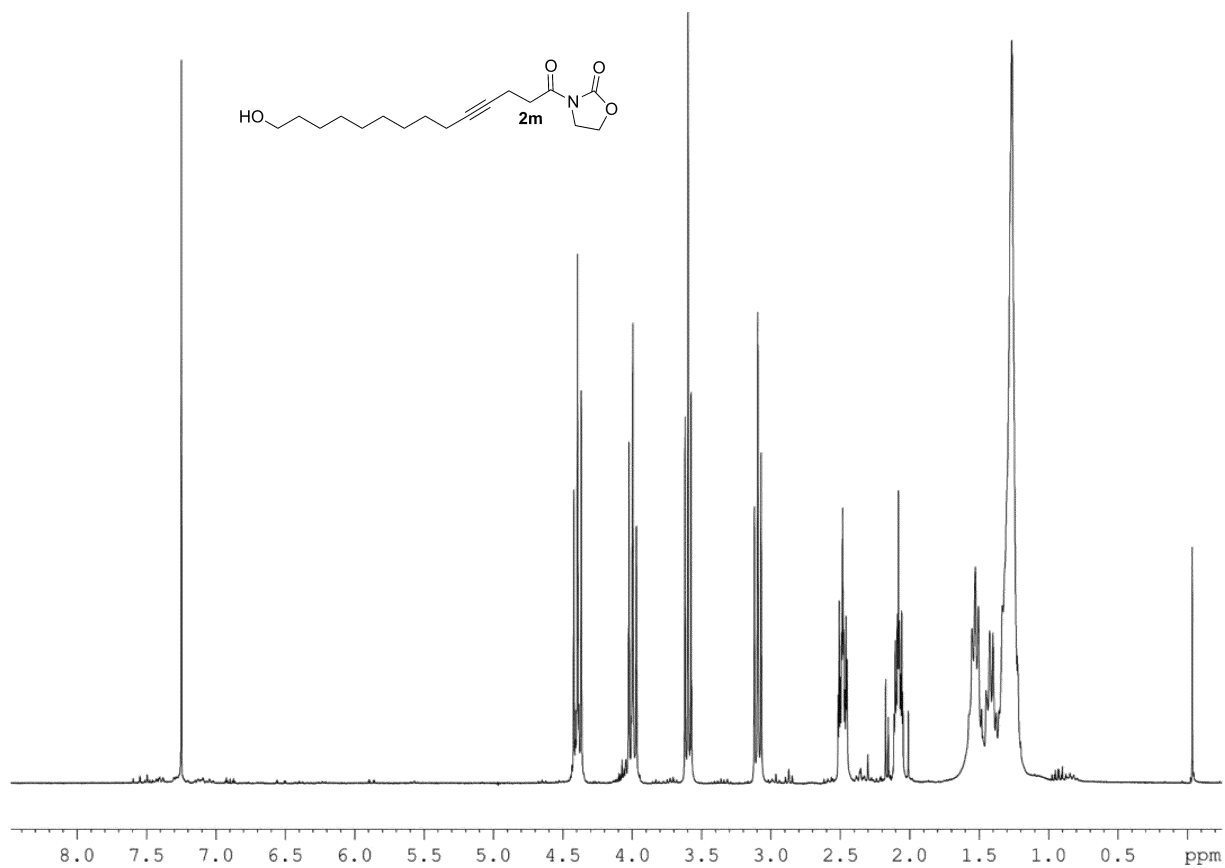


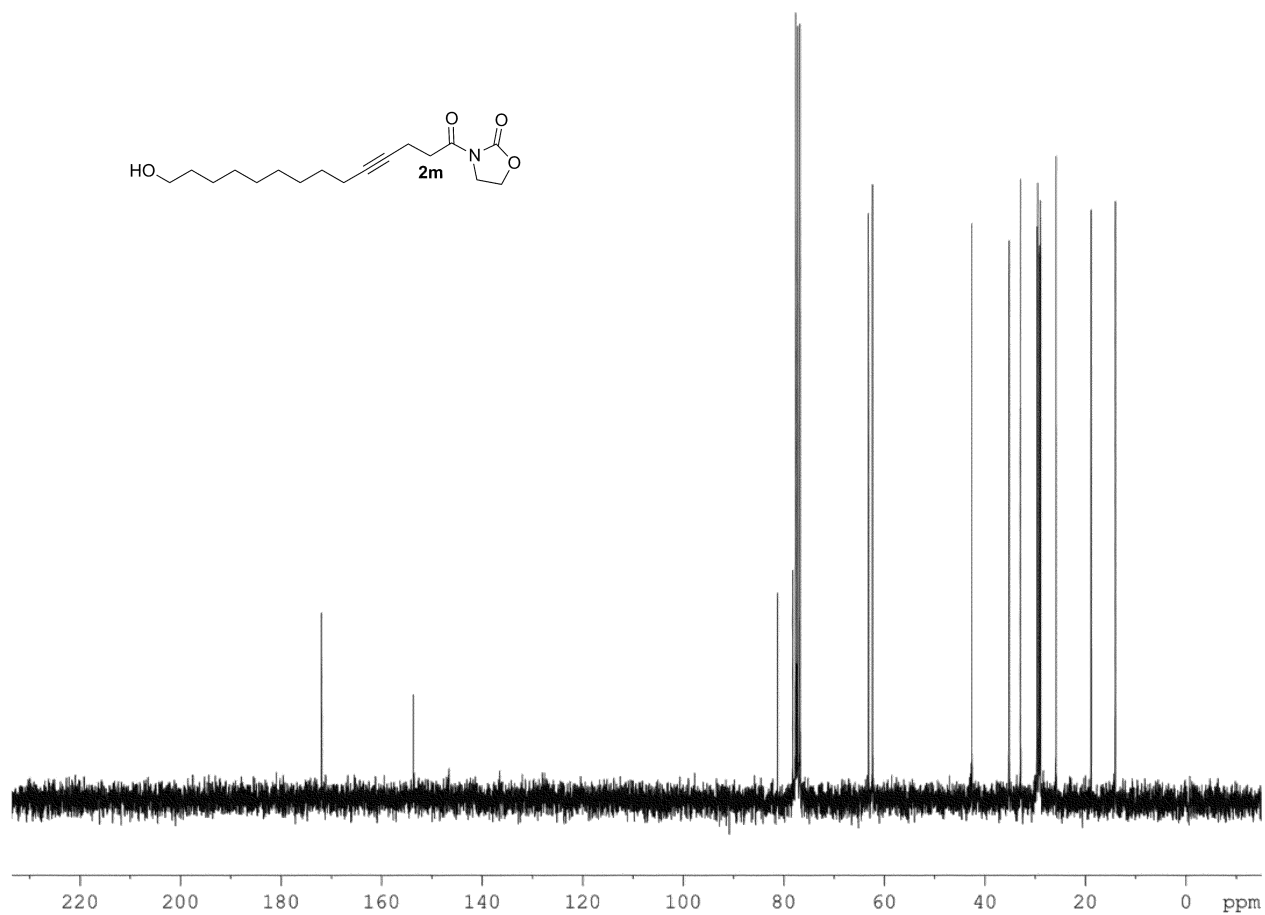
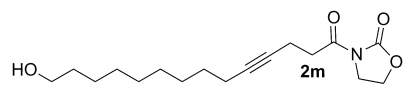


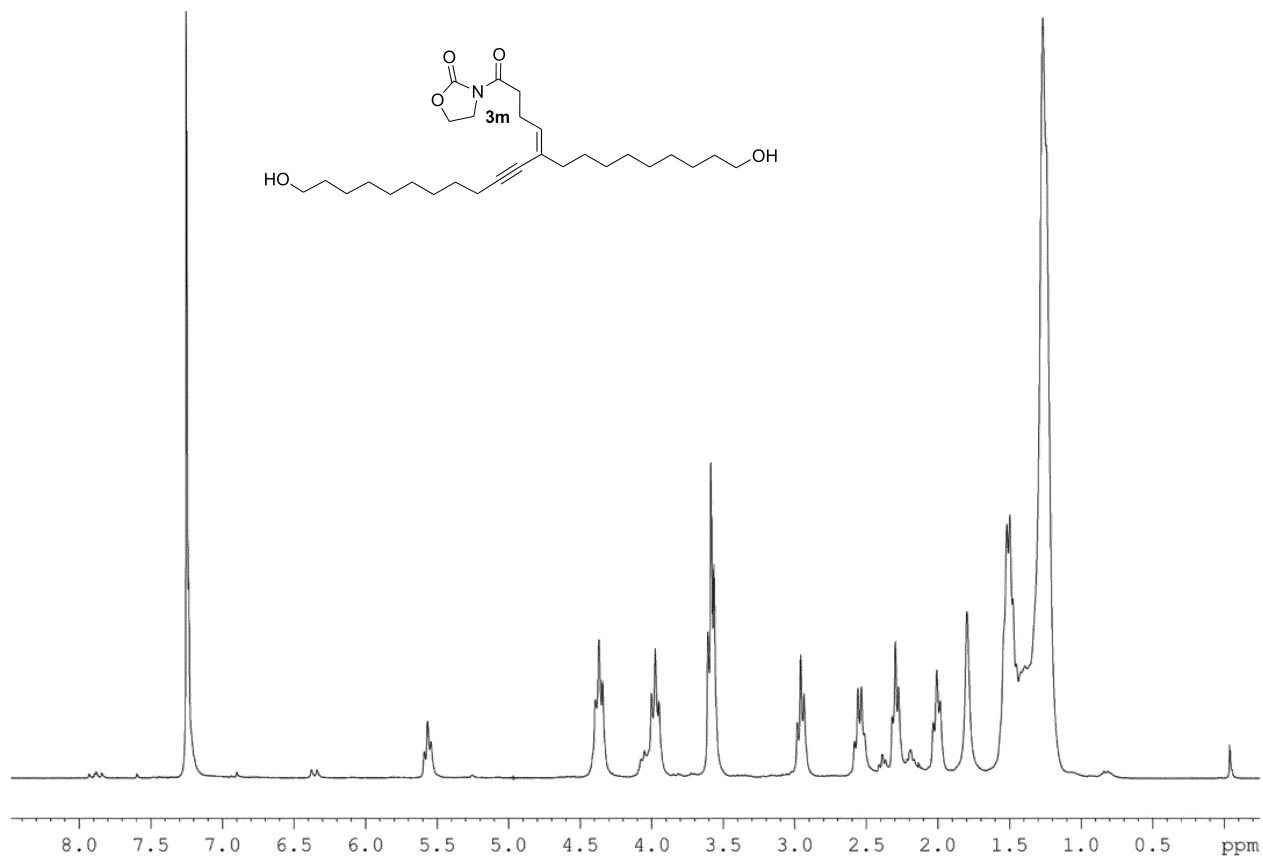


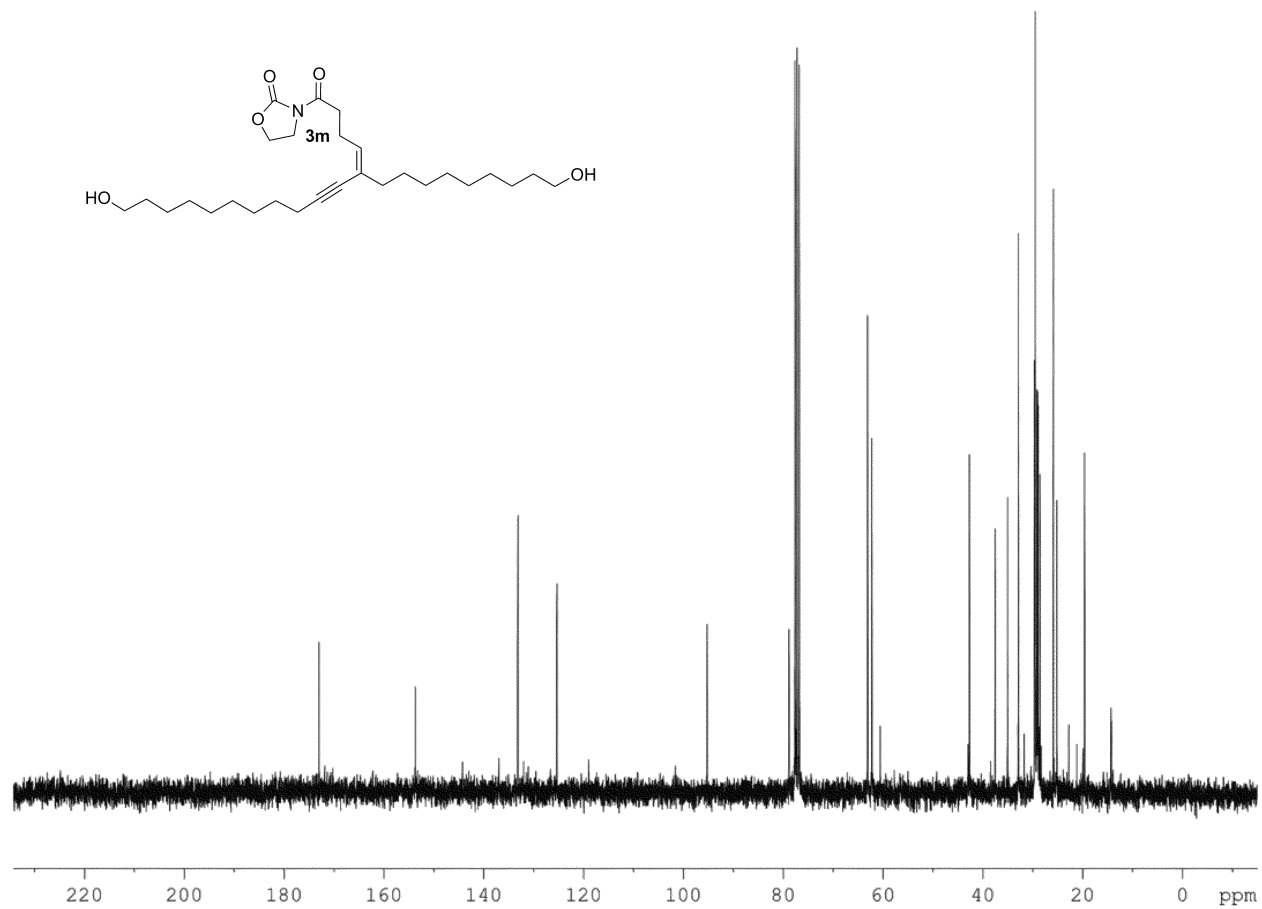


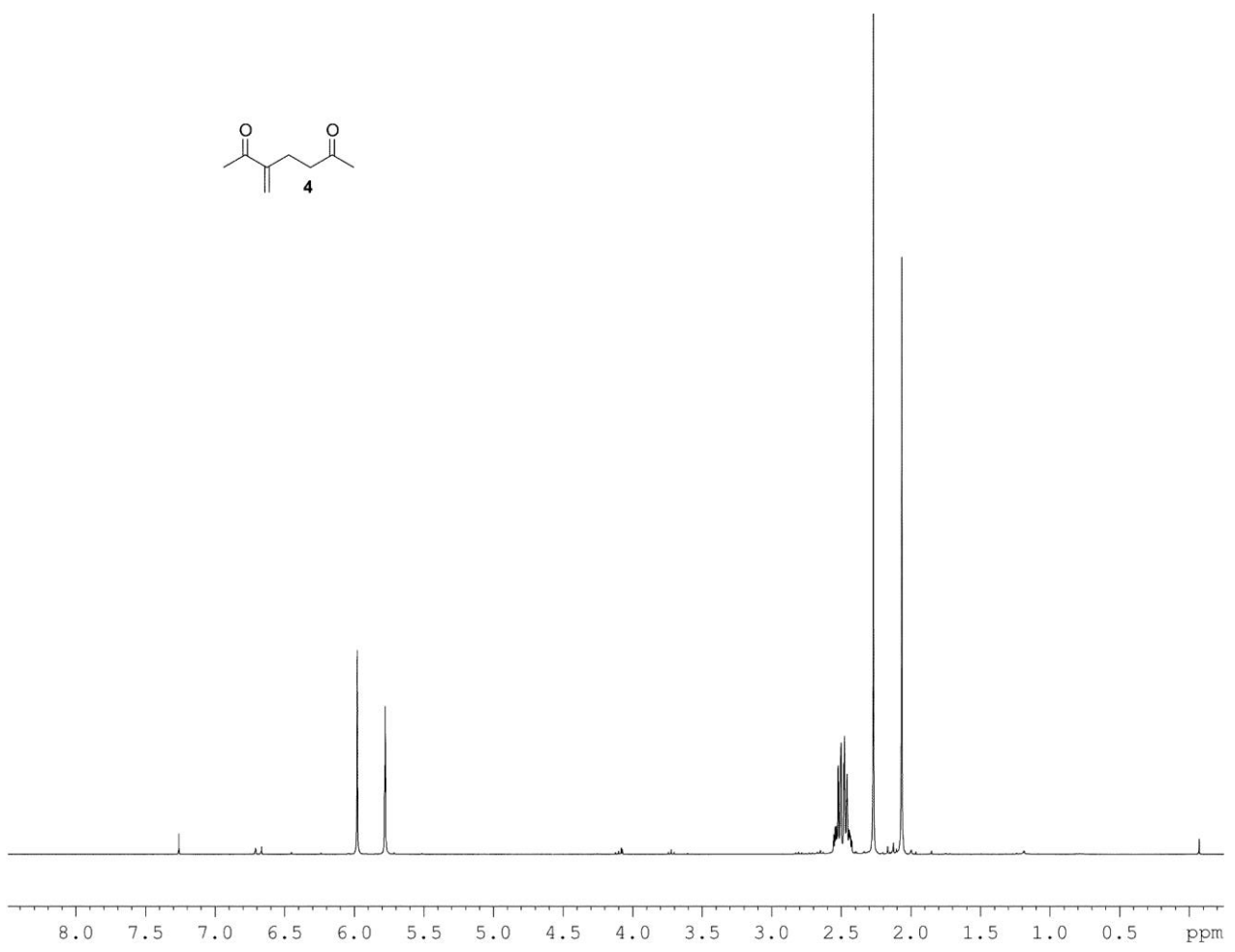
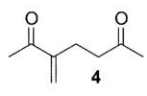


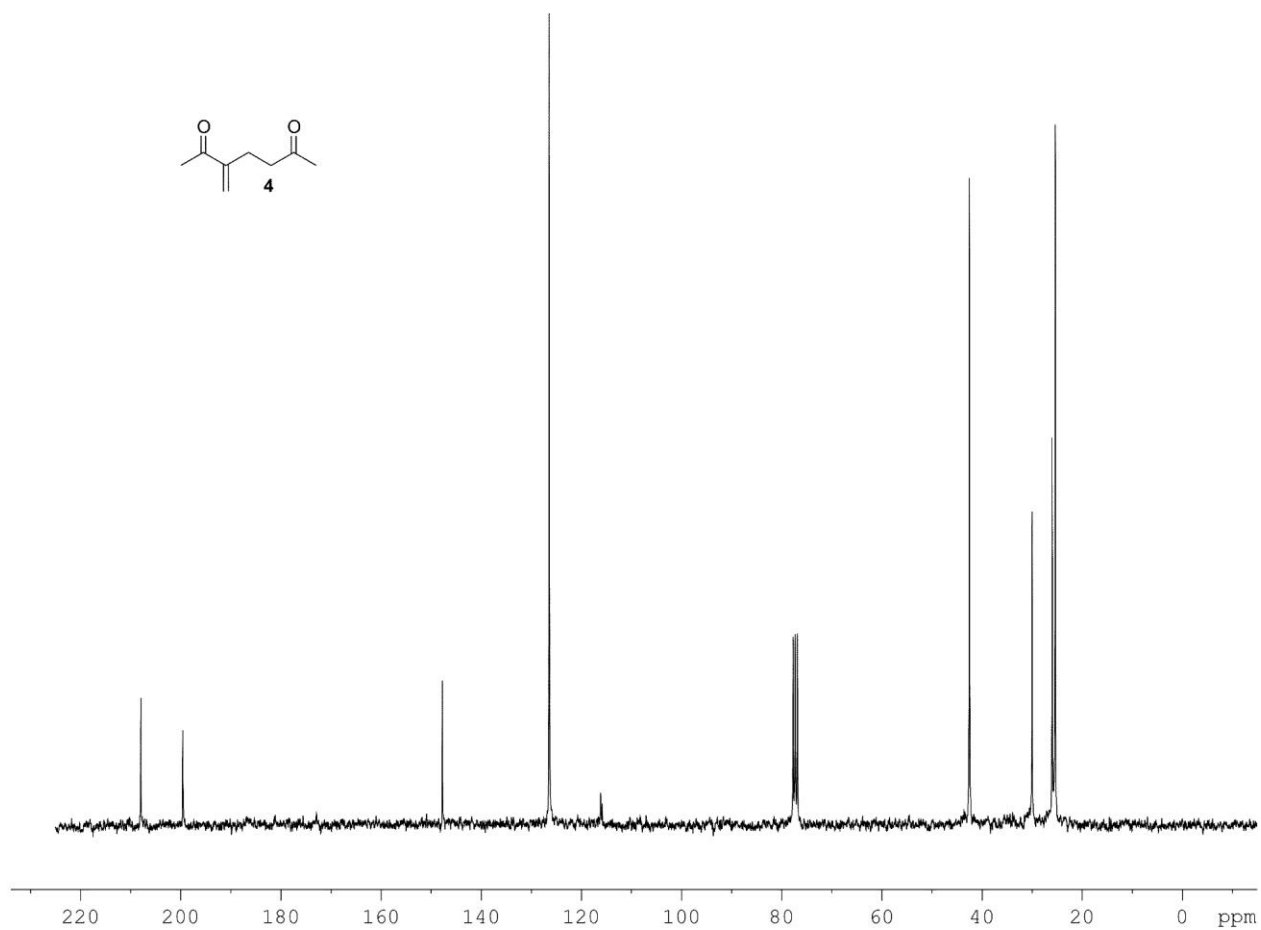
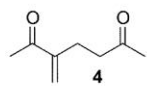


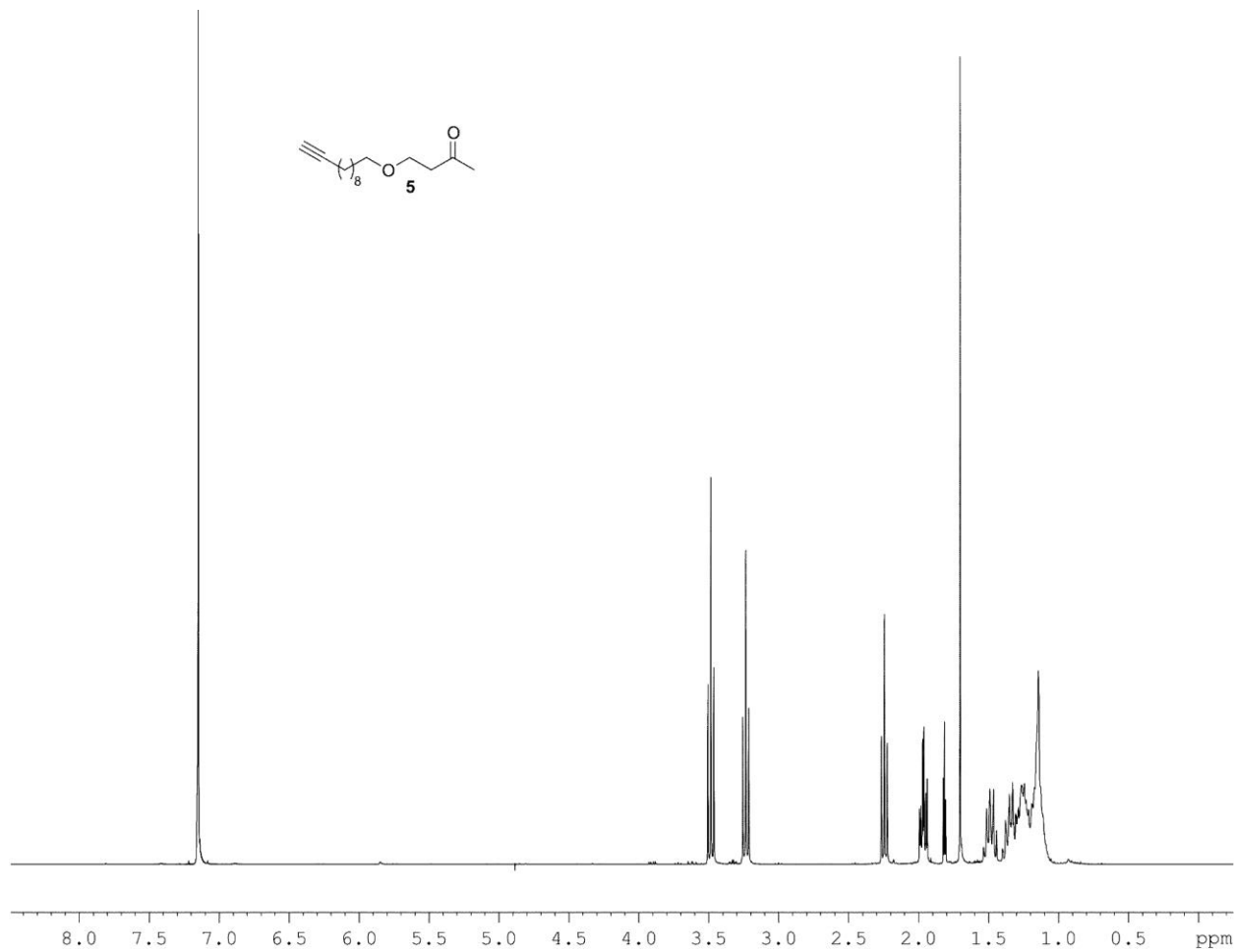
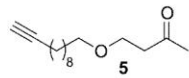


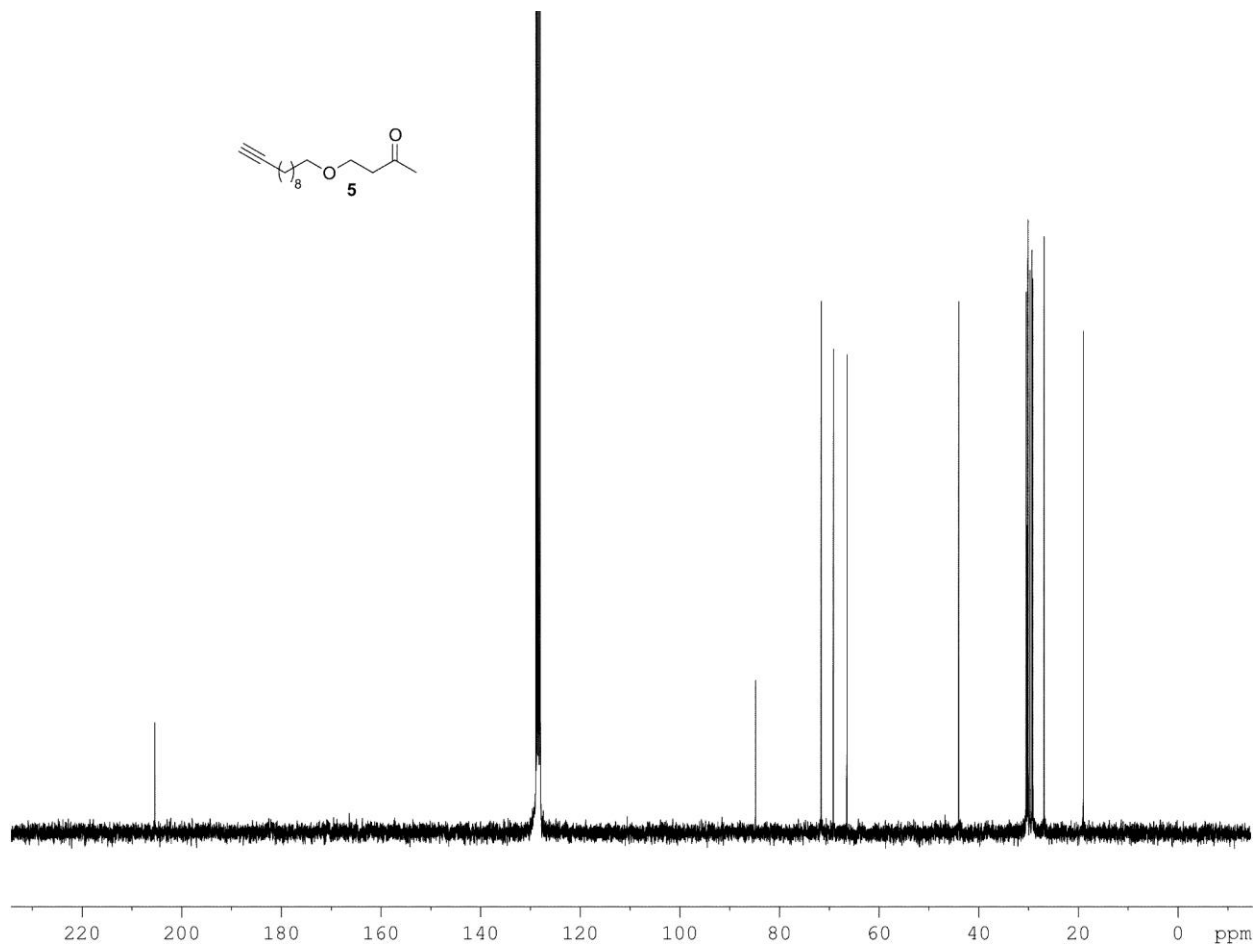
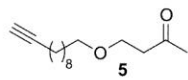


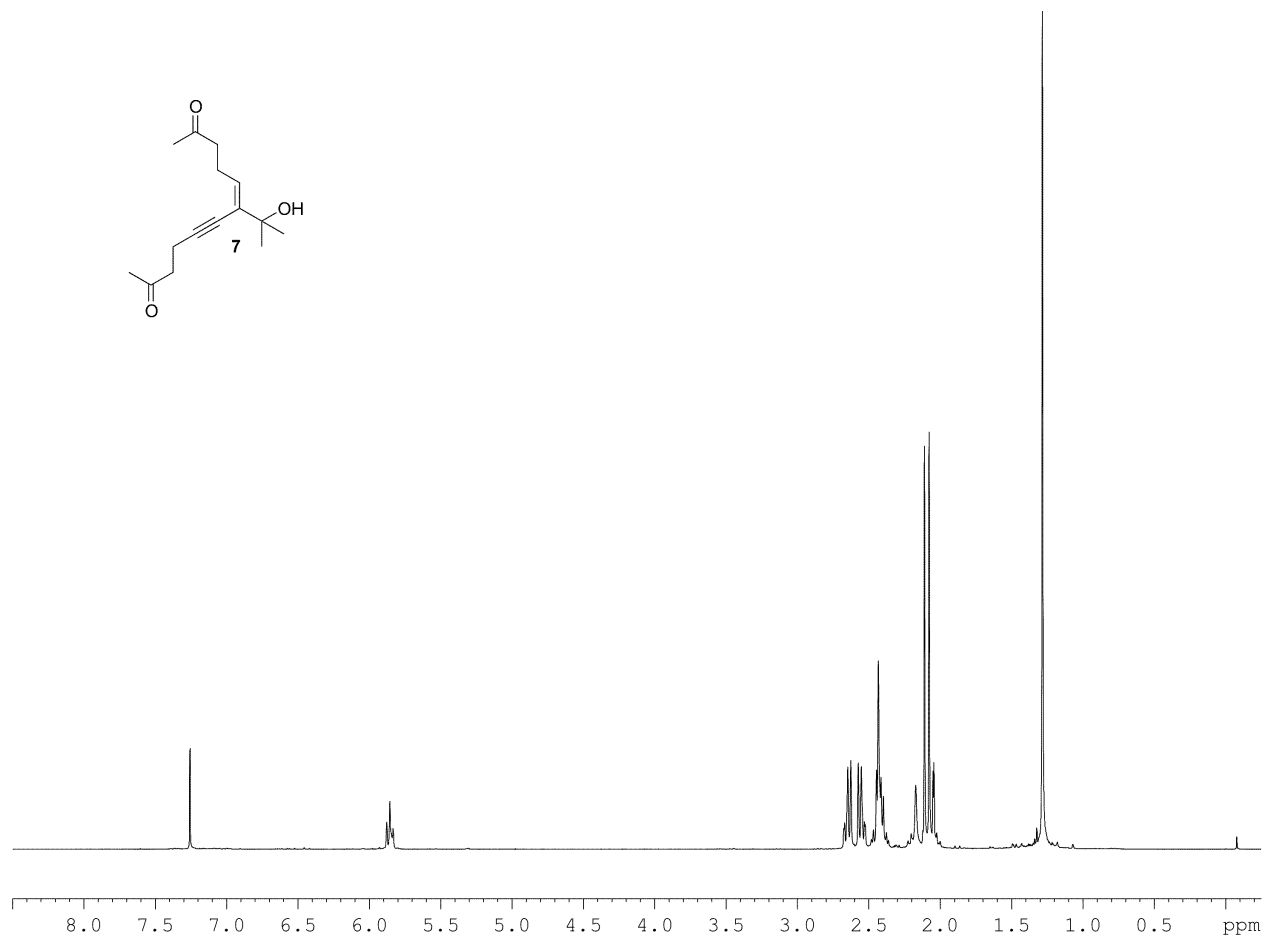
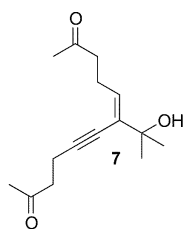


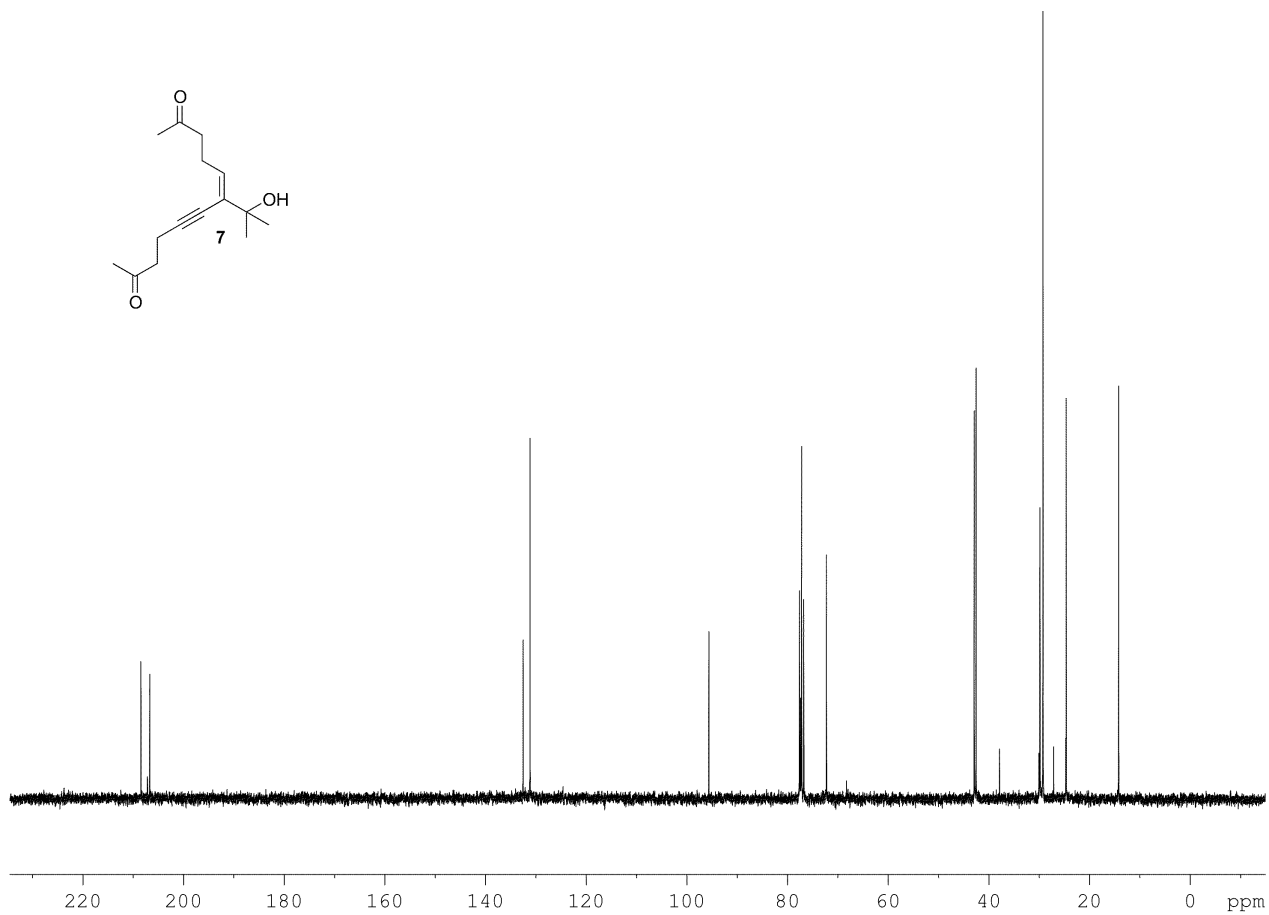
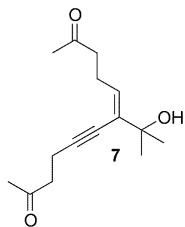


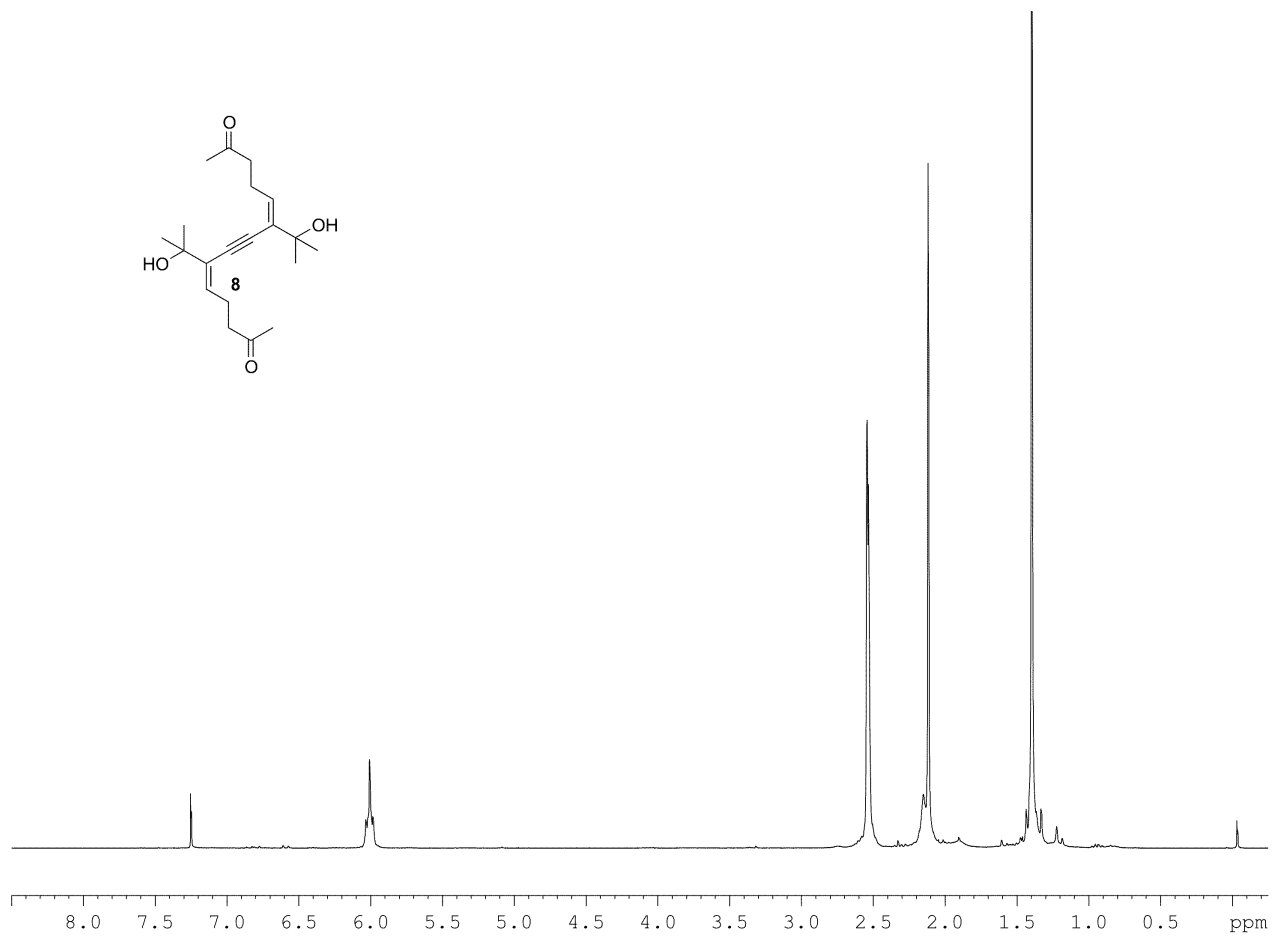
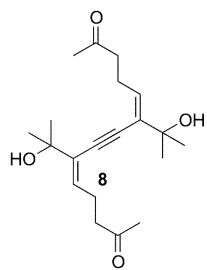


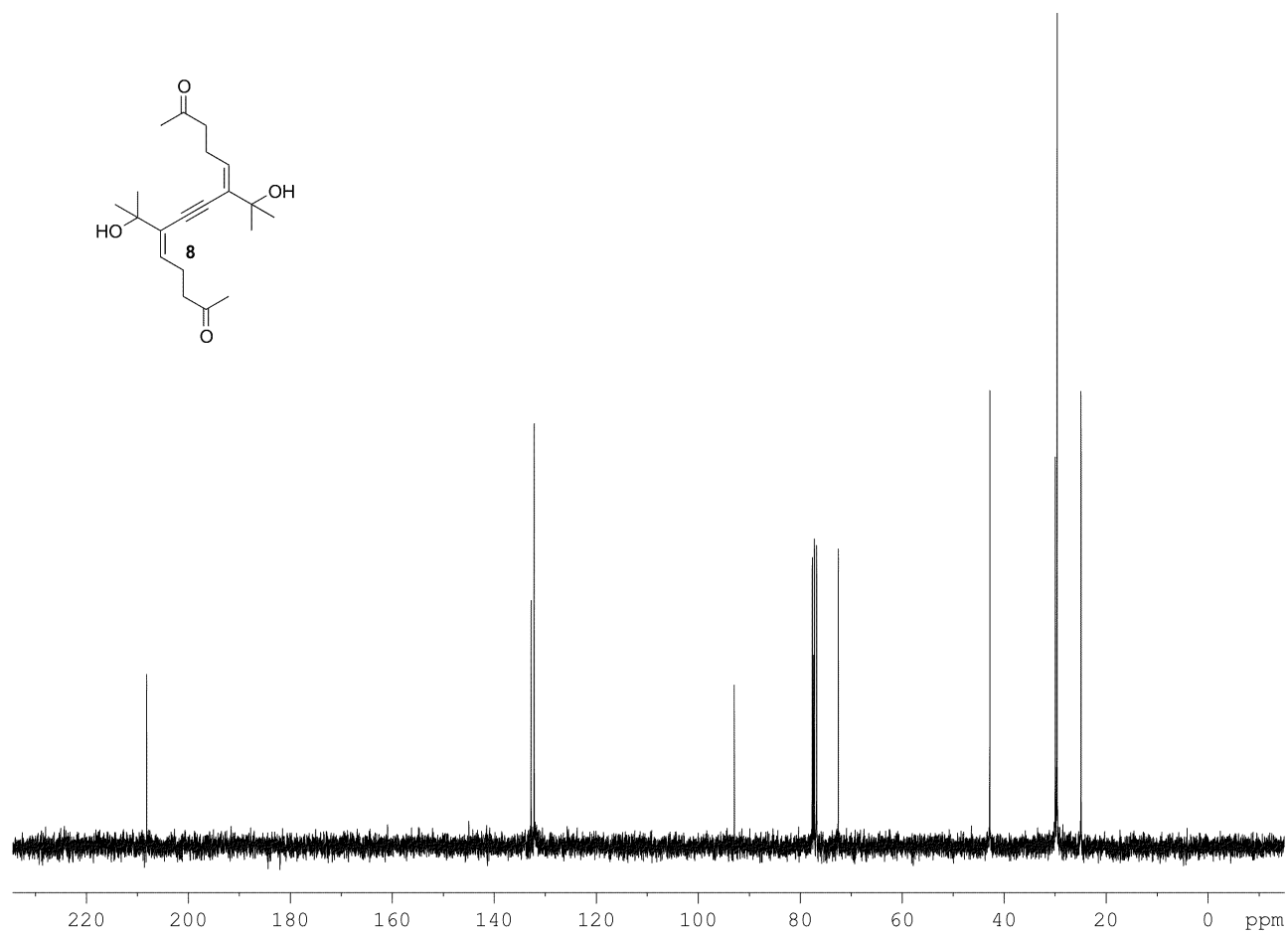
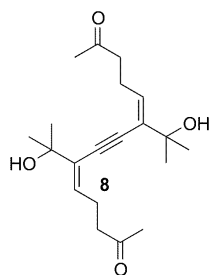




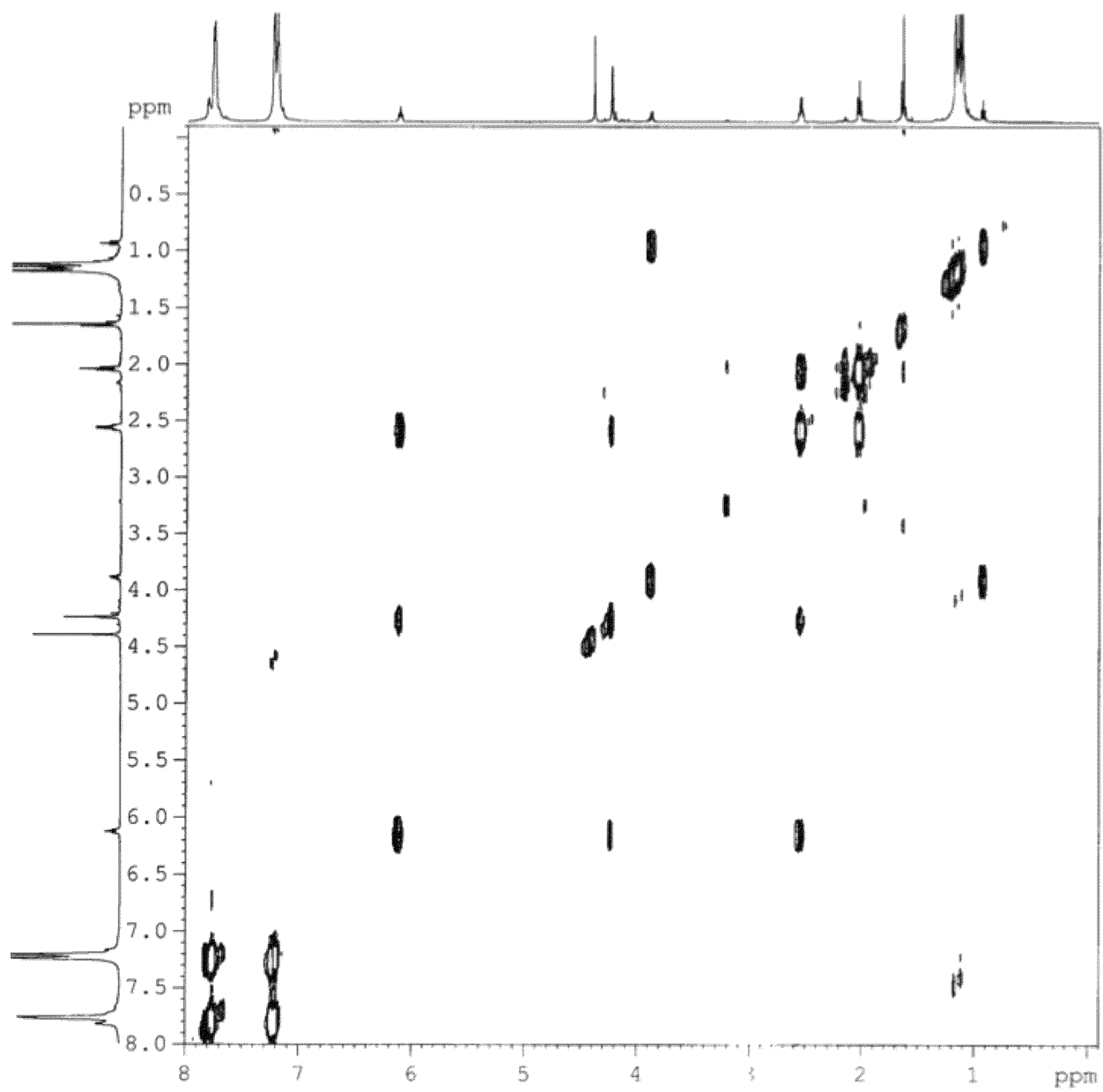
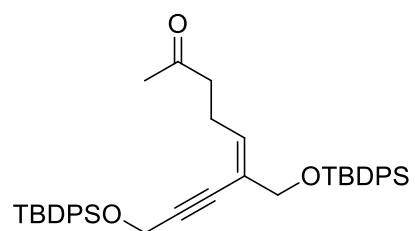




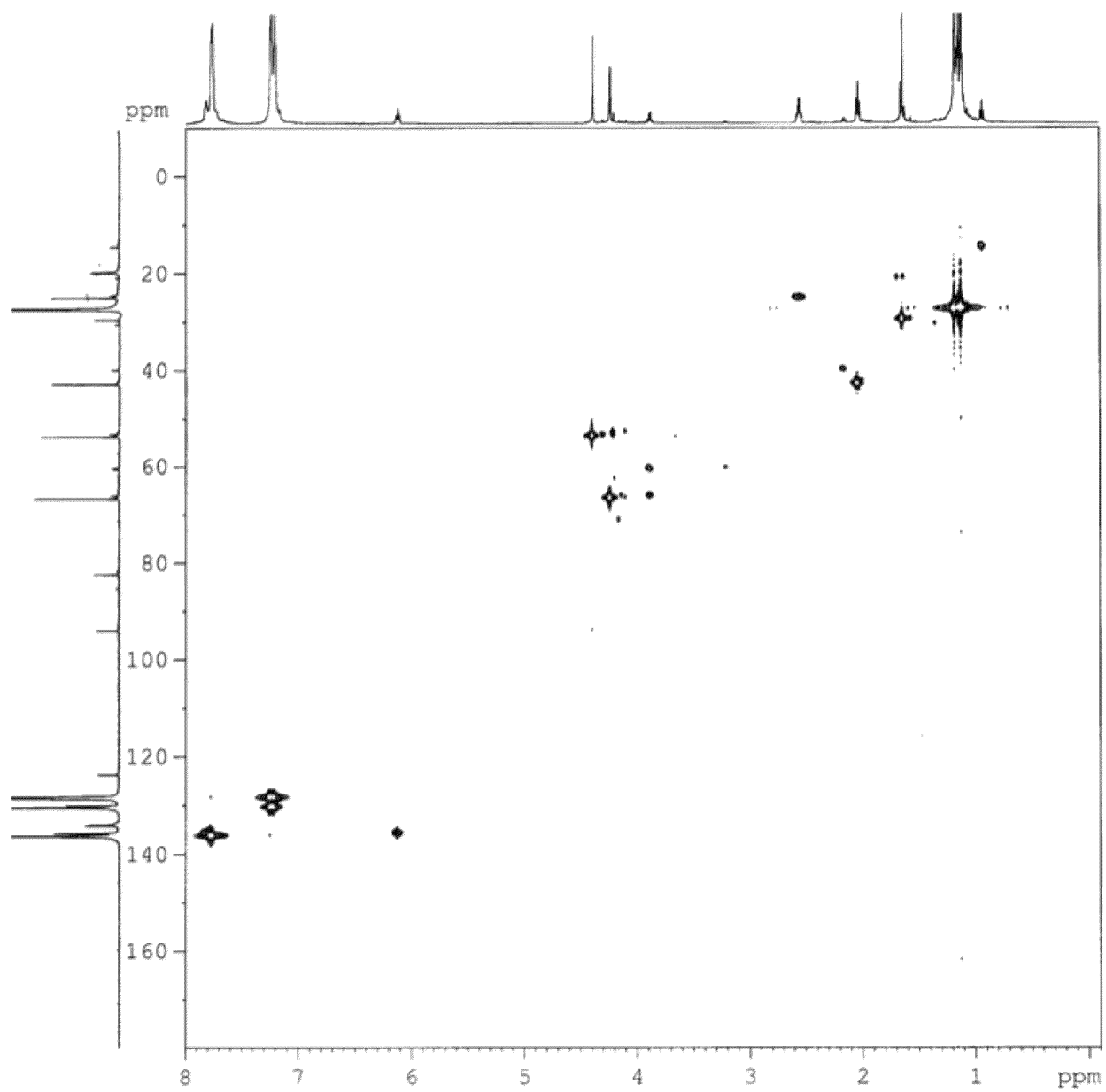
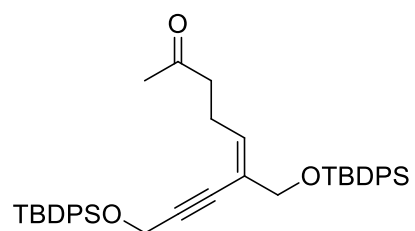




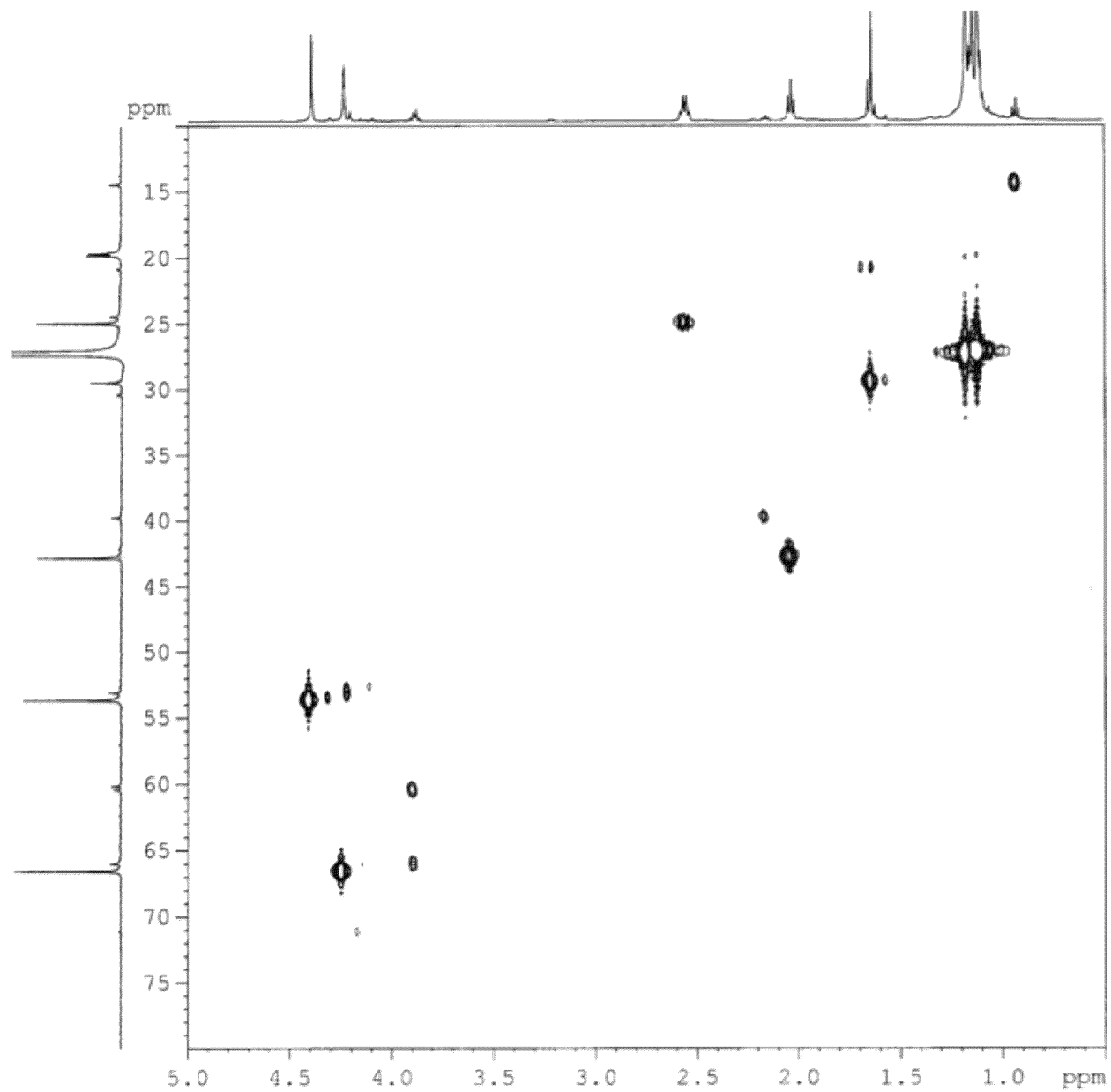
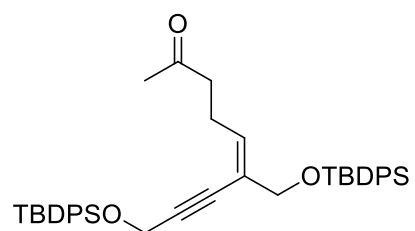
COSY for **3.3e**



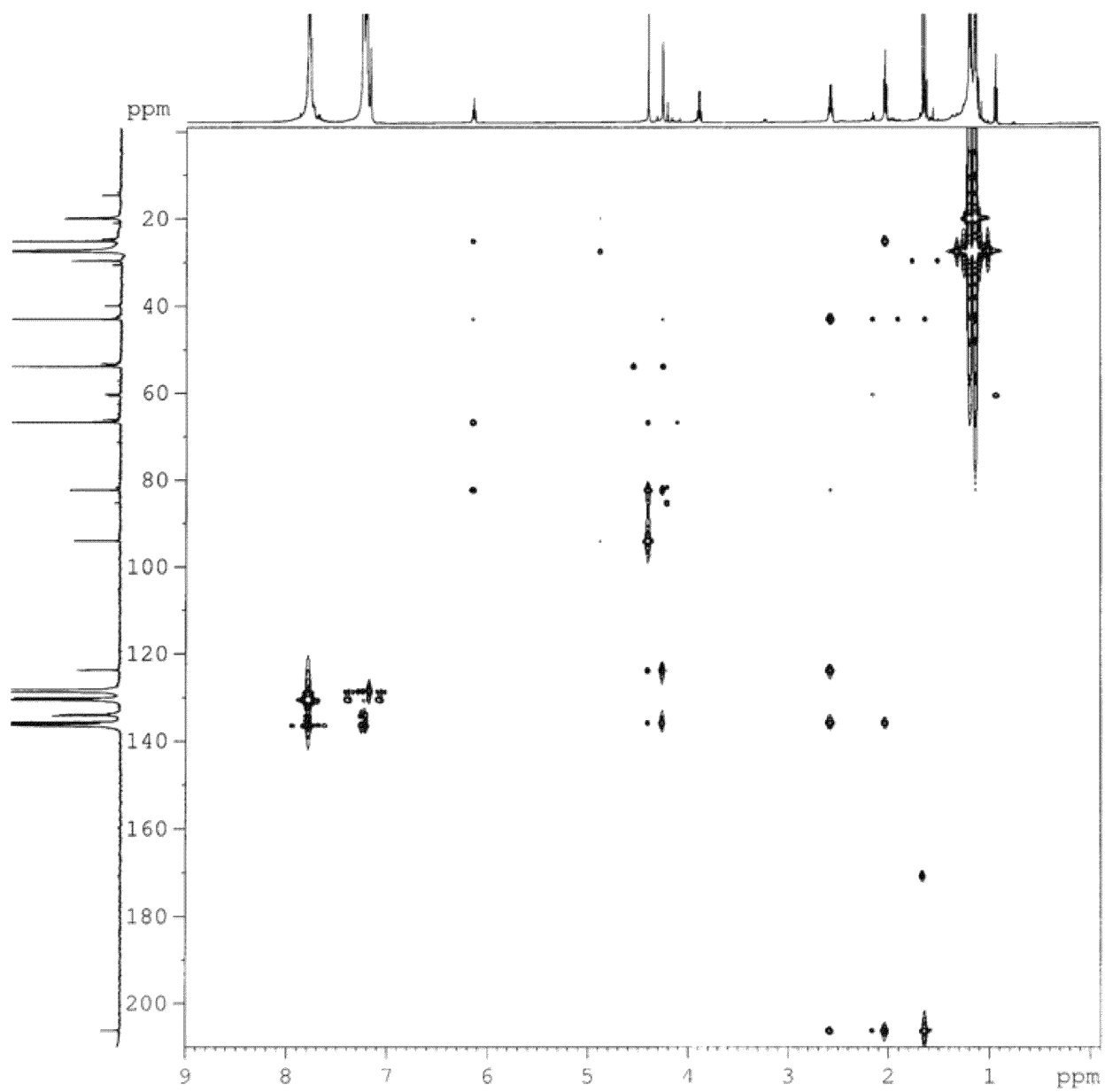
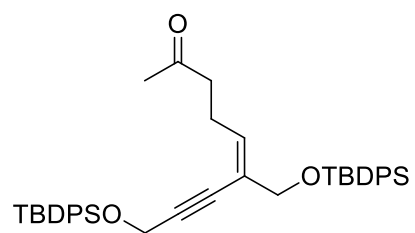
HSQC for **3.3e**



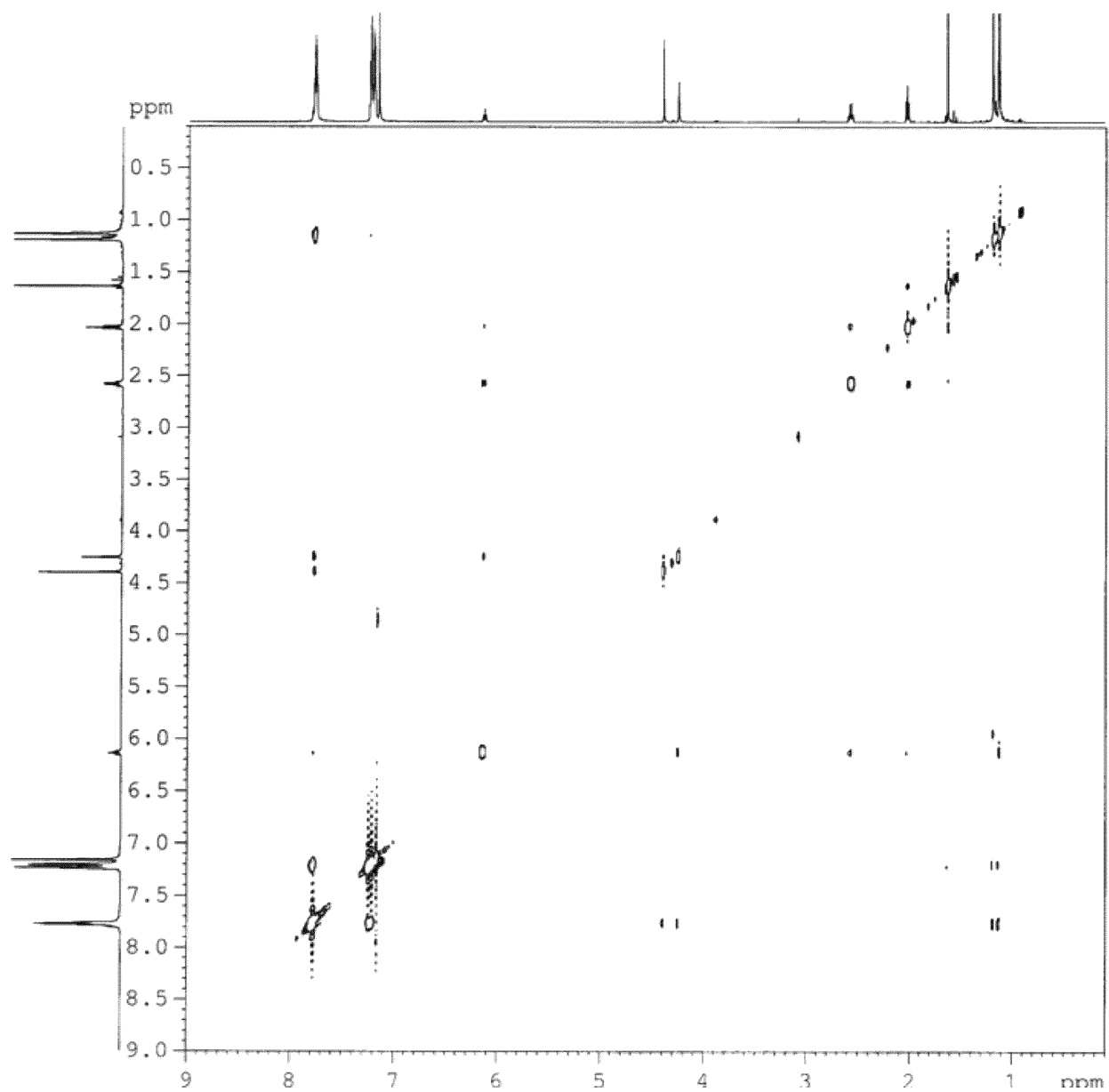
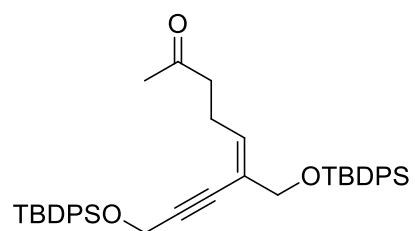
HSQC (expanded) for **3.3e**



HMBC for **3.3e**



NOESY for **3.3e**



3.6. References

- [1]a) M. Gonzalez-Lopez, J. T. Shaw, *Chem. Rev.* **2009**, *109*, 164-189; b) B. B. Toure, D. G. Hall, *Chem. Rev.* **2009**, *109*, 4439-4486; c) B. Jiang, T. Rajale, W. Wever, S.-J. Tu, G. Li, *Chem. Asian J.* **2010**, *5*, 2318-2335; d) J. G. Hernandez, E. Juaristi, *Chem. Commun.* **2012**, *48*, 5396-5409.
- [2]a) A. Ulaczyk-Lesanko, D. G. Hall, *Curr. Opin. Chem. Biol.* **2005**, *9*, 266-276; b) J. E. Biggs-Houck, A. Younai, J. T. Shaw, *Curr. Opin. Chem. Biol.* **2010**, *14*, 371-382; c) E. Ruijter, R. Scheffelaar, V. A. Orru Romano, *Angew. Chem. Int. Ed. Engl.* **2011**, *50*, 6234-6246; d) A. Domling, W. Wang, K. Wang, *Chem. Rev.* **2012**, *112*, 3083-3135.
- [3]a) G. Balme, D. Bouyssi, N. Monteiro, in: *Multicomponent Reactions* (Eds.: J. Zhu, H. Bienaymé), Wiley-VCH, Weinheim, **2005**, pp. 224-276; b) D. M. D'Souza, T. J. J. Müller, *Chem. Soc. Rev.* **2007**, *36*, 1095-1108; c) B. A. Arndtsen, *Chem. Eur. J.* **2009**, *15*, 302-313; d) M. Zhang, *Adv. Synth. Catal.* **2009**, *351*, 2243-2270; e) M. J. Climent, A. Corma, S. Iborra, *RSC Adv.* **2012**, *2*, 16-58; f) H. Clavier, H. Pellissier, *Adv. Synth. Catal.* **2012**, *354*, 3347-3403; g) H. Pellissier, *Chem. Rev.* **2013**, *113*, 442-524; h) J. S. Quesnel, B. A. Arndtsen, *Pure Appl. Chem.* **2013**, *85*, 377-384; i) M. A. Fernandez-Rodriguez, P. Garcia-Garcia, E. Aguilar, *Chem. Commun.* **2010**, *46*, 7670-7687.
- [4]R. V. Lerum, J. D. Chisholm, *Tetrahedron Lett.* **2004**, *45*, 6591-6594.
- [5]a) B. M. Trost, C. Chan, G. Ruhter, *J. Am. Chem. Soc.* **1987**, *109*, 3486-3487; b) H.-D. Xu, R.-W. Zhang, X. Li, S. Huang, W. Tang, W.-H. Hu, *Org. Lett.* **2013**, *15*, 840-843; c) C. Jahier, O. V. Zatolochnaya, N. V. Zvyagintsev, V. P. Ananikov, V. Gevorgyan, *Org. Lett.* **2012**, *14*, 2846-2849.

- [6]a) M. Charpenay, A. Boudhar, G. Blond, J. Suffert, *Angew. Chem., Int. Ed.* **2012**, *51*, 4379-4382; b) B. M. Trost, A. J. Frontier, *J. Am. Chem. Soc.* **2000**, *122*, 11727-11728; c) C. J. Brennan, J. M. Campagne, *Tetrahedron Lett.* **2001**, *42*, 5195-5197; d) X.-Y. Wu, X. She, Y. Shi, *J. Am. Chem. Soc.* **2002**, *124*, 8792-8793; e) J. R. Hanson, C. Uyanik, *J. Chem. Res., Synop.* **2003**, 426-427; f) A. Gopalarathnam, S. G. Nelson, *Org. Lett.* **2006**, *8*, 7-10; g) S. Lopez, J. Montenegro, C. Saa, *J. Org. Chem.* **2007**, *72*, 9572-9581; h) B. M. Trost, G. Dong, *J. Am. Chem. Soc.* **2010**, *132*, 16403-16416; i) B. M. Trost, J.-P. Lumb, J. M. Azzarelli, *J. Am. Chem. Soc.* **2011**, *133*, 740-743; j) B. M. Trost, B. R. Taft, J. T. Masters, J.-P. Lumb, *J. Am. Chem. Soc.* **2011**, *133*, 8502-8505; k) L. M. Geary, S. K. Woo, J. C. Leung, M. J. Krische, *Angew. Chem., Int. Ed.* **2012**, *51*, 2972-2976.
- [7]L. Zhao, X. Lu, *Org. Lett.* **2002**, *4*, 3903-3906.
- [8]Y. Hoshino, Y. Shibata, K. Tanaka, *Angew. Chem., Int. Ed.* **2012**, *51*, 9407-9411.
- [9]a) S. Ikeda, K. Kondo, Y. Sato, *J. Org. Chem.* **1996**, *61*, 8248-8255; b) S. Ikeda, Y. Sato, *J. Am. Chem. Soc.* **1994**, *116*, 5975-5976.
- [10] a) M. Rubina, M. Conley, V. Gevorgyan, *J. Am. Chem. Soc.* **2006**, *128*, 5818-5827; b) H. Kusama, Y. Onizawa, N. Iwasawa, *J. Am. Chem. Soc.* **2006**, *128*, 16500-16501; c) R. L. Danheiser, A. E. Gould, R. F. de la Pradilla, A. L. Helgason, *J. Org. Chem.* **1994**, *59*, 5514-5515; d) J. M. Robinson, S. F. Tlais, J. Fong, R. L. Danheiser, *Tetrahedron* **2011**, *67*, 9890-9898.
- [11] a) Y. Liu, M. Nishiura, Y. Wang, Z. Hou, *J. Am. Chem. Soc.* **2006**, *128*, 5592-5593; b) N. K. Pahadi, D. H. Camacho, I. Nakamura, Y. Yamamoto, *J. Org. Chem.* **2006**, *71*, 1152-1155; c) K. Campbell, C. J. Kuehl, M. J. Ferguson, P. J. Stang, R. R. Tykwinski, *J. Am. Chem. Soc.*

- 2002**, *124*, 7266-7267; d) N. N. P. Moonen, C. Boudon, J.-P. Gisselbrecht, P. Seiler, M. Gross, F. Diederich, *Angew. Chem., Int. Ed.* **2002**, *41*, 3044-3047.
- [12] I. P. Kovalev, Y. N. Kolmogorov, Y. A. Strelenko, A. V. Ignatenko, M. G. Vinogradov, G. I. Nikishin, *J. Organomet. Chem* **1991**, *420*, 125-133.
- [13] J. D. McClure, *J. Org. Chem.* **1970**, *35*, 3045-3048.
- [14] M. V. Farnworth, M. J. Cross, J. Louie, *Tetrahedron Lett.* **2004**, *45*, 7441-7443.
- [15] H. Werner, *J. Chem. Soc., Chem. Commun.* **1997**, 903-910.
- [16] T. Nishimura, X.-X. Guo, N. Uchiyama, T. Katoh, T. Hayashi, *J. Am. Chem. Soc.* **2008**, *130*, 1576-1577.
- [17] a) G.-J. Ho, D. J. Mathre, *J. Org. Chem.* **1995**, *60*, 2271-2273; b) M. P. Sibi, H. Miyabe, *Org. Lett.* **2002**, *4*, 3435-3438.

Christopher M. Russo

Email: christoher.russo@villanova.edu
Phone: 732-614-7725

Education

Ph.D. in Organic Chemistry

Syracuse University; Syracuse, NY
June 2023

B.S. in Chemistry with a minor concentration in Mathematics

The University of Scranton; Scranton, PA
May 2009

Teaching Experience

Villanova University

Department of Chemistry
Post-Doctoral Instructor

- CHE 1103 – General Chemistry Laboratory – Fall 2022

Hamilton College

Chemistry Department
Adjunct Lecturer

- CHE 190 – Organic Chemistry Laboratory – Spring 2016, Spring 2017

Syracuse University

Department of Chemistry
Graduate Teaching Assistant

- CHE 106 – General Chemistry I Recitation – Fall 2009
- CHE 275 – Organic Chemistry I Recitation – Fall 2010, Fall 2012, Fall 2013
- CHE 276 – Organic Chemistry I Laboratory – Fall 2015
- CHE 325 – Organic Chemistry II Recitation – Spring 2011
- CHE 326 – Organic Chemistry II Laboratory – Spring 2010

The University of Scranton

Center for Teaching and Learning Excellence
Student Tutor

- Group tutoring sessions for Organic Chemistry I & II – 2007 to 2009

Research Experience

Villanova University, Department of Chemistry

Post-Doctoral Fellow, Advisor: Matthew C. O'Reilly

Developed a new protocol for synthesizing and testing Phenylalanine Arginine β -Naphthylamide, an efflux pump inhibitor, using peptide coupling chemistry. PA β N and analogues were made from readily available starting materials without chromatography and standard protocols for their use in potentiating antibiotics in wild-type strains were established.

Syracuse University, Department of Chemistry
Graduate Research Assistant, Advisor: John D. Chisholm

Synthesized small organic molecules for the inhibition of SH2-containing inositol phosphatase (SHIP) in the PI3K signaling pathway. Molecules included aminoalcohol-containing quinolines and aminosteroids. Focused on developing and implementing successful milligram-scale syntheses for these compounds followed by the expansion to gram-scale syntheses. Through a collaborative effort, these compounds and some analogues underwent *in vitro* and *in vivo* testing for their SHIP inhibition potential and immunological effects.

Investigated acid-catalyzed alkylation reactions using trichloroacetimidates as electrophiles. Focused on the alkylation of carbon- and hetero-nucleophiles under acidic conditions, the use of imidates as reagents for catalyst-free alkylations, studies investigating the mechanism of imidate alkylations, and the synthesis of some new fluorinated C2-symmetrical BINOL-based catalysts for asymmetric alkylation reactions.

The University of Scranton, Department of Chemistry
Undergraduate Research Assistant, Advisor: Jennifer A. Tripp

Developed a method for preparing molluscan shells for radiocarbon dating. Focused on maximizing the homogeneity of shell samples by using a cryogenic mechanical grinding procedure and isolating their constituent minerals, mostly calcite and aragonite, by using a density fractionation method. Samples were analyzed using infrared spectroscopy prior to further processing and eventual radiocarbon dating via accelerator mass spectrometry at the University of Oxford Radiocarbon Accelerator Unit.

Publications

Russo, C. M.; Howey, K. G.; O'Reilly, M. C. Scalable and Chromatography-Free Synthesis of Efflux Pump Inhibitor Phenylalanine Arginine β -Naphthylamide for Its Validation in Wild-Type Bacterial Strains. *ChemMedChem*, **2023**, early view.

Kessler, H.; Russo, C. M.; Fumo, V.; O'Reilly, M. C. What's in a Tablet? Extraction and Spectroscopic Identification of Pharmaceutical Unknowns. *J. Chem. Ed.*, **2022**, *99*, 3024.

Mahajani, N. S.; Meador, R. I. L.; Smith, T. J.; Canarelli, S. E.; Adhikari, A. A.; Shah, J. P.; Russo, C. M.; Wallach, D. R.; Howard, K. T.; Millimaci, A. M.; Chisholm, J. D. Ester Formation via Symbiotic Activation Utilizing Trichloroacetimidate Electrophiles. *J. Org. Chem.* **2019**, *84*, 7871.

Fellows, R.; Russo, C. M.; Silva, C. S.; Lee, S. G.; Jez, J. M.; Chisholm, J. D.; Zubieta, C.; Nanao, M. H. A multisubstrate reductase from *Plantago* major: structure-function in the short chain reductase superfamily. *Sci. Rep.* **2018**, *8*, 14796.

Gumbleton, M.; Sudan, R.; Fernandes, S.; Engelman, R. W.; Russo, C. M.; Chisholm, J. D.; Kerr, W. G. Dual enhancement of T and NK cell function by pulsatile inhibition of SHIP1 improves antitumor immunity and survival. *Sci. Signal.* **2017**, *10*, 5353.

Itkin, T.; Kumari, A.; Gur-Cohen, S.; Ludwig, C.; Brooks, R.; Golan, K.; Khatib, E.; Hornstein, E.; Russo, C. M.; Chisholm, J. D.; Kerr, W. G.; Kuchenbauer, F.; Lapidot, T. "MicroRNA-155 promotes G-CSF-induced mobilization of murine hematopoietic stem and progenitor cells via propagation of CXCL12 signaling." *Leukemia*, **2017**, *31*, 1247-1250.

Srivastava, N.; Iyer, S.; Sudan, R.; Youngs, C.; Engelman R. W.; Howard, K. T.; Russo, C. M.; Chisholm, J. D.; Kerr, W. G. A small-molecule inhibitor of SHIP1 reverses age- and diet-associated obesity and metabolic syndrome. *JCI Insight*, **2016**, *1*, 2379.

Russo, C. M.; Adhikari, A. A.; Wallach, D. R.; Fernandes, S.; Balch, A. N.; Kerr, W. G.; Chisholm, J. D. Synthesis and Initial Evaluation Quinoline-Based Inhibitors of SHIP. *Bioorg. Med. Chem. Lett.* **2015**, *25*, 5344.

Fernandes, S.; Brooks, R.; Gumbleton, M.; Park, M-Y.; Russo, C. M.; Howard, K. T.; Chisholm, J. D.; Kerr, W. G. SHIPi Enhances Autologous and Allogeneic Hematopoietic Stem Cell Transplantation. *EBioMedicine*, **2015**, *2*, 205.

Brooks, R.; Iyer, S.; Akada, H.; Russo, C. M.; Chisholm, J. D.; Kerr W. G. Coordinate Expansion of the Hematopoietic and Mesenchymal Stem Cell Compartments by SHIPi. *Stem Cells*, **2014**, *33*, 848-858.

Shah, J. P.; Russo, C. M.; Howard, K. T.; Chisholm, J. D. Spontaneous Formation of PMB Esters Using 4-Methoxybenzyl-2,2,2-trichloroacetimidate. *Tetrahedron Lett.* **2014**, *55*, 1740.

Adhikari, A. A.; Shah, J. P.; Howard, K. T.; Russo, C. M.; Wallach, D. R.; Linaburg, M. R.; Chisholm, J. D. Convenient Formation of Diphenylmethyl Esters Using Diphenylmethyl Trichloroacetimidate. *Synlett* **2014**, *25*, 283.

Lerum, R. V.; Russo, C. M.; Marquez, J. E.; Chisholm, J. D. A Rhodium-Catalyzed Tandem Alkyne Dimerization/1,4-Addition Reaction. *Adv. Synth. Catal.* **2013**, *355*, 3485.

Russo, C. M.; Tripp, J. A.; Douka, K.; Higham, T. F. G. A New Radiocarbon Pretreatment Method for Molluscan Shell Using Density Fractionation of Carbonates in Bromoform. *Radiocarbon* **2010**, *52*, 1301.

Presentations

Russo, C. M.; Howey, K. G.; O'Reilly, M. C. Development of a General, Efficient, and Chromatography-Free Synthesis of Phenylalanine-Arginine β -Naphthylamide Toward Evaluation of its Efflux Pump Inhibition Structure Activity Relationships. ACS Mid-Atlantic Regional Meeting, The College of New Jersey, Ewing, NJ, 2022.

Russo, C. M.; Chisholm, J. D. New Brønsted Acid Catalyzed Alkylations Using Trichloroacetimidates. 247th ACS National Meeting & Exposition, Dallas, TX, 2014.

Russo, C. M.; Tripp, J. A. Density Fractionation of Molluscan Carbonates for Radiocarbon Dating. 237th ACS National Meeting & Exposition, Salt Lake City, UT, 2009.

Donnelly, P. E.; Churilla, T. M.; Russo, C. M.; Vinson, J. Comparison of polyphenol antioxidants in vitamin enhanced waters, raw fruits and their juices. 237th ACS National Meeting & Exposition, Salt Lake City, UT, 2009.

Research Grants

Syracuse University Summer Fellowship, 2013

Stipend granted to select Syracuse University graduate students working full-time on study or research towards their degree during summer months.

University of Scranton President's Fellowship for Summer Research, 2008

Stipend and travel funds granted to select University of Scranton undergraduate students doing research during summer months.

University Service

Villanova University

Department of Chemistry Committee for Safety and Sustainability
Sept 2022 – current

Affiliations

American Chemical Society

Since 2009

Phi Lambda Upsilon National Chemistry Honor Society

Since 2009

Phi Kappa Phi National Honor Society

Since 2010

Golden Key International Honor Society

Since 2013